CHARACTERIZATION AND MODELLING OF THE MIXING IN THE ATHABASCA RIVER DOWNSTREAM OF A PULP MILL

A Thesis Submitted to the College of Graduate Studies and Research
in Partial Fulfillment of the Requirements
for the Degree of Master of Science
in the Division of Environmental Engineering
University of Saskatchewan
Saskatoon

By
Ifeanyi S. Odigboh
Spring 1999

PERMISSION TO USE

Whereas this thesis is submitted in partial fulfillment of the requirements for the degree of Master of Science from the University of Saskatchewan, the author has agreed that the libraries of this University may make it freely available for inspection. Further, the author has agreed that permission for copying of this thesis for scholarly purposes may be granted by the professor who supervised the thesis work reported herein or, in his absence by the Head of the Department or the Dean of the College in which the thesis work was carried out. It is understood that any copying or publication or use of this thesis or parts thereof for financial gain shall not be allowed without the author's written permission. Furthermore, it is understood that due recognition shall be given to the author and to the University of Saskatchewan in any scholarly use which may be made of any material in this thesis.

Requests for permission to copy or make use of material in this thesis in whole or part should be addressed to:

Head of the Division of Environmental Engineering
University of Saskatchewan
Saskatoon, Canada S7N 0W0

ABSTRACT

Methods for predicting the transverse mixing coefficient, E_z in rivers based solely upon estimates or measurements of the channel geometry, channel slope and flow parameters are not completely reliable. Therefore, it is generally necessary to perform field tracer tests in order to determine E_z for a particular river reach at a given stage and flow.

Characterizations of the transverse mixing in the Athabasca River downstream of a pulp mill located near Boyle, Alberta are described herein. The characterization of the mixing is based upon analysis of four tracer tests conducted on the river (three continuous input tests and one slug test). The tracer tests were conducted on different dates and cover a range of flow conditions (October 1994, 270 m^3/s; February 1995, 84 m^3/s, and August 1997, 960 m^3/s and 876 m^3/s). The February test was conducted under ice-covered conditions. Beak Consultants Ltd. conducted the October 1994 and February 1995 tests.

The tracer input for each field test consisted of injection of Rhodamine WT fluorescent dye at the mill outfall location. In the continuous input tests, the tracer was injected into the mill effluent stream at a constant rate and entered the river via the effluent diffuser structure. The diffuser is 52 m long, oriented perpendicular to the flow, and located close to the left bank of the river. In the slug input, test a known mass of tracer was instantaneously dumped directly into the river at approximately the mid-point along the length of the diffuser. For each test the dye plume was sampled across transects oriented perpendicular to the river flow at a number of downstream locations stretching over a 32-km reach of the river. Hydrographic surveys were conducted at each sampled transect and at several other transects to determine channel geometry and flow parameters. The hydrographic survey information and the tracer input conditions were required for numerical modelling of the mixing in the river reach.

The implementation of the two-dimensional river mixing modelling procedure used in the present study was written by Putz (1996), based upon the descriptions given by Beltaos and Arora (1988). The numerical model utilizes a streamtube approach and a

numerical procedure employing an advection optimized grid to limit numerical errors. The model is capable of simulating continuous input and unsteady input conditions. The modelling package includes two preprocessing programs for generating the calculation grid based upon channel characteristics, a two-dimensional, transient mass input mixing program, and a post-processing program for output of data at selected locations.

The transverse mixing coefficient was determined for each field test using the model fit of predicted tracer concentrations compared to the concentration of the samples collected in the field. The mixing simulations provide a very good representation of the measured concentration distributions. The four field verification studies demonstrate that the Advection Optimized Grid method can be applied to two-dimensional, steady and unsteady source mixing problems in natural streams satisfactorily. Non-dimensionalized transverse mixing coefficients determined from the modelling procedure are compared to the range of values reported in other locations. These comparisons show that the values of β which characterize the transverse mixing in the reach of the Athabasca River studied fall well within the range of reported β values from other studies. Reach-averaged dimensionless mixing coefficient, β, is fairly consistent (in the range of 0.34 to 0.48) for the range of flow conditions represented by the four tests. The overall weighted average of β for the different ranges of flow was found to be 0.41. The results demonstrate that the dimensionless mixing coefficient measured at one flow condition may be used with the appropriate flow parameters to estimate mixing for other flow conditions for the same reach. The results of the modelling procedure are also used to assess the variation in mixing with discharge and due to the presence of an ice cover.

ACKNOWLEDGMENTS

First, I would like to thank the Lord Almighty for his blessings and guidance.

I would like to express my sincere thanks to my supervisor, Dr. Gordon Putz, for his support and patience throughout my program. His guidance and encouragement were instrumental in the achievement of my goals.

The following agencies kindly provided field data and information from their files: Alberta Environmental Protection, Beaks Consultants Limited and Alberta Pacific Forest Industries Inc.

The efforts and assistance of these individuals in the field and laboratory studies is greatly appreciated.
Daniel Smith, Kevin McCullum, Nick Chernuka, Michael Lapoint, Ian Baker, Mohammed Gamal El-Din, Ahmed Gamal El-Din, Garry Solonynko, Renato Chiarella, Christine Brodie, Xiuguo Yang, Maria Demeter and the graduate students and staff of the Environmental Engineering group, University of Alberta who participated in the 1997 field studies.

I would like to thank the following people for financial support during my studies:
Frederick W. Hill and Dr. G. Putz, (Operating Grant); and the following organizations for supporting the project: Sustainable Forest Management Network of Centres of Excellence, Minimum Impact Technologies Theme for supporting the studies financially. Alberta Pacific Forest Industries Inc. (Mr. Keith White and Mr. Mark Spafford) for supporting these studies by providing field equipment, access to mill locations and storage facilities, and copies of reports of previous tracer and water quality studies.

Finally, I would like to thank my parents, brothers, sisters and friends for their continuous support, patience and encouragement.

TABLE OF CONTENTS

LIST OF TABLES

LIST OF FIGURES

LIST OF SYMBOLS

A	cross sectional area
A^n	amplitude at time step n
c	concentration
C_d	depth-averaged concentration
Cr	Courant No.
D	dosage
e_x, e_y, e_z	dispersion coefficients
E_x, E_y, E_z,	mixing coefficients
g	gravitational constant
h	water depth
H	mean sectional depth
M	total mass of tracer
M^*	mass of tracer injected per unit time
M_{in}	mass of tracer injected
M_r	mass recovery ratio
ns	number of streamtubes
N	number of nodes per wavelength
NS	number of sections
NT	number of transects
q	cumulative flow
Q	total channel flow
r	local hydraulic radius
r_r	ratio = $E_z\Delta t/\Delta z^2$
rbd	right boundary depth
R_h	channel hydraulic radius
S	channel slope
sw	streamtube width
t	time
u,v,w	velocities in the x, y, z directions

u_*	local shear velocity
U_*	mean channel shear velocity
V	volume
W	section width
x	longitudinal distance downstream
y	vertical distance
z	transverse distance
β	dimensionless mixing coefficient
γ	amplification factor
θ	phase angle error
Δt	time step
ε_x, ε_y, ε_z	turbulent diffusion coefficients

1. INTRODUCTION

1.1 Problem Overview

The rivers of the world have, for a long time, been used for the disposal of agricultural, domestic and industrial wastes. Therefore the possibility of a contaminant being accidentally or intentionally discharged upstream of a water intake is an ever-present danger and a constant concern to those diverting and using water from rivers. More recently, increased environmental awareness has demonstrated that, without careful planning, such discharges may result in serious and long lasting ecological damage. In order to regulate effluent sources, it is necessary to relate the spread of effluent components to measurable flow characteristics. Travel time and mixing of water within a river are basic streamflow characteristics that should be understood in order to predict the rate of movement and dilution of effluent that may be introduced into rivers.

Prediction of effluent concentration as a function of time and location is a complex problem. The basic tool that is available for quantitative descriptions of the mixing process is a differential equation that expresses the principle of conservation of mass within the fluid. For neutrally buoyant tracers, analytical solution of this equation for natural rivers is only possible under certain simplifying circumstances. In general, it is necessary to resort to numerical computations. Although many numerical models are available to make the calculations needed to estimate travel time and dispersion, none can be used with confidence without calibration and verification to the particular river reach.

In general, there are no completely reliable methods of predicting mixing coefficients for rivers from commonly available hydraulic information. Also, very detailed channel geometry data needed to predict river velocities are seldom available. The availability of reliable flow velocities and mixing rates is, almost always, the weakest link in the chain of information needed to predict the rate of movement and mixing of pollutants in rivers.

1.2 Physical Processes

In order to provide a better understanding of mixing processes in rivers, the processes that governs the rates and patterns of spread are reviewed. The behavior of a dissolved neutrally buoyant, mass conservative substance (i.e., has the same density as the ambient river water and it neither decays nor undergoes chemical reaction) passively discharged to a river is governed by processes that can be characterized as river-specific or substance-specific. Passive meaning there is negligible difference in momentum of the river flow and the discharged effluent. River specific processes are entirely attributable to the nature of river flow and act regardless of the nature of the substance (or tracer) discharged. River specific processes are diffusion and advection.

Diffusion is the process by which a substance suspended or dissolved in a fluid is transferred from regions of high concentrations to those of low concentrations due to random motions of fluid particles. The random motion may be molecular, a property of the fluid, or turbulent, a property of fluid flow. In most natural flow situations turbulent diffusion is the dominant mechanism.

Advection is transport by the mean motion of the fluid. Natural streams never exhibit uniform velocity distributions. In most cases they are characterized by significant velocity gradients in both the vertical and transverse directions as shown in Figure 1.1. Non-uniform velocity distributions cause differential advection and it is this process that significantly contributes to mixing in rivers. Mixing by differential advection occurs in conjunction with diffusion as shown in Figure 1.2.

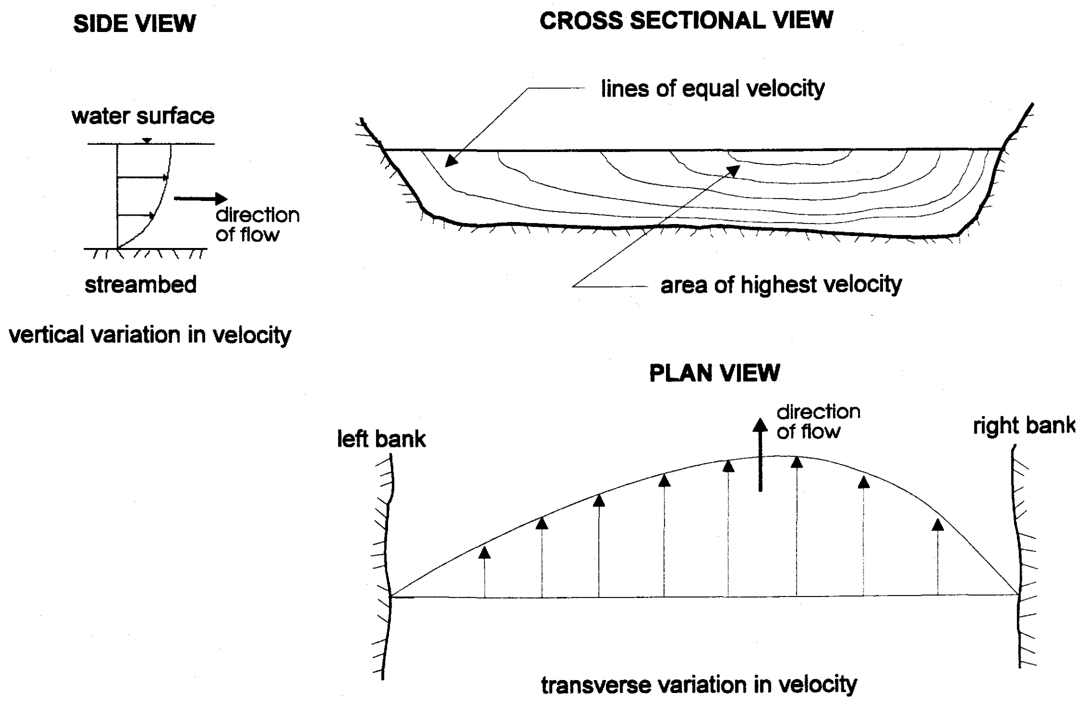

Figure 1.1 Typical velocity gradients in a natural stream (from Putz 1996).

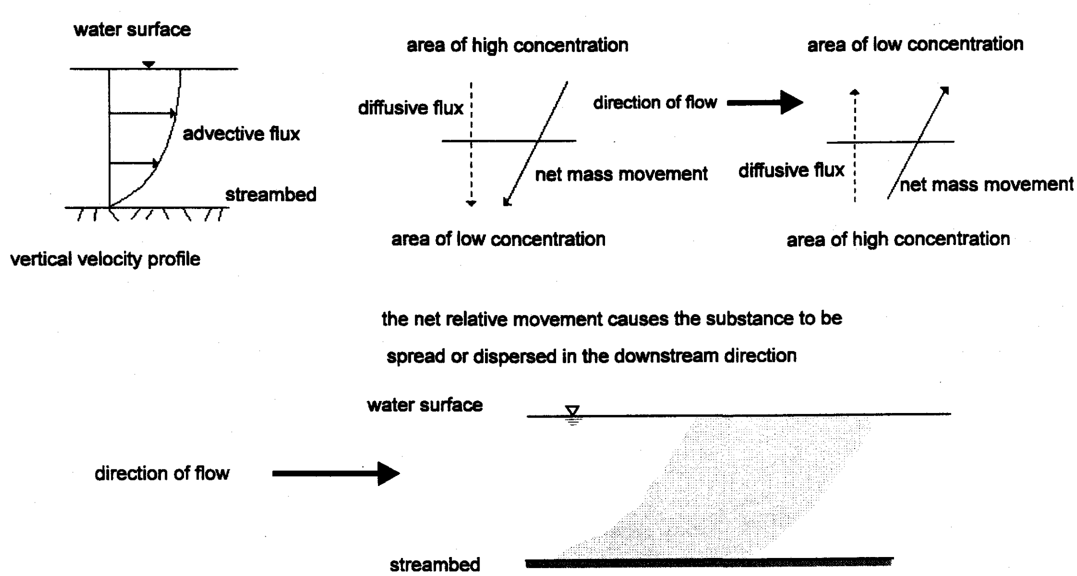

Figure 1.2 Mixing due to differential advection (from Putz 1996).

The velocity profile of the main fluid flow cause substances moving upward, due to random motion, to increase in velocity, while substances moving downward will decrease in velocity. The end result is the spreading of the substance in the streamwise (longitudinal) direction. Similarly longitudinal spreading is also caused by the transverse velocity gradients. The differential advection process is often called `longitudinal dispersion'.

In natural river flows, secondary currents are known to exist. These circulating velocities, which are in the plane perpendicular to the mean flow direction, are caused by the fact that the turbulence is not identical in all directions, resulting in an imbalance in the normal Reynolds stresses. The most well known mechanism that generates secondary currents in open channels is the imbalance between the centrifugal force and the lateral pressure gradient in bends (Elhadi *et al.* 1984). Bend induced secondary currents enhance lateral mixing. Normally, there is a flow at the surface toward the outside of the bend and a return flow near the bottom. This type of secondary circulation increases with channel curvature. In fairly straight channels, wind and turbulence generate secondary currents. In straight channels the effect of secondary circulation is usually small but can become significant if the width-to-depth ratio becomes smaller than say 10 (Elhadi *et al.* 1984).

Most rivers and open channel flows are characterized by high Reynolds numbers (about $1*10^5$) and are turbulent. In rivers, turbulence is generated by velocity shear (Rutherford 1994) and hence originates in regions where there are strong velocity gradients, notably near the bed, banks and obstacles within the flow. Figure 1.3 shows a typical secondary circulation and transverse velocity profile.

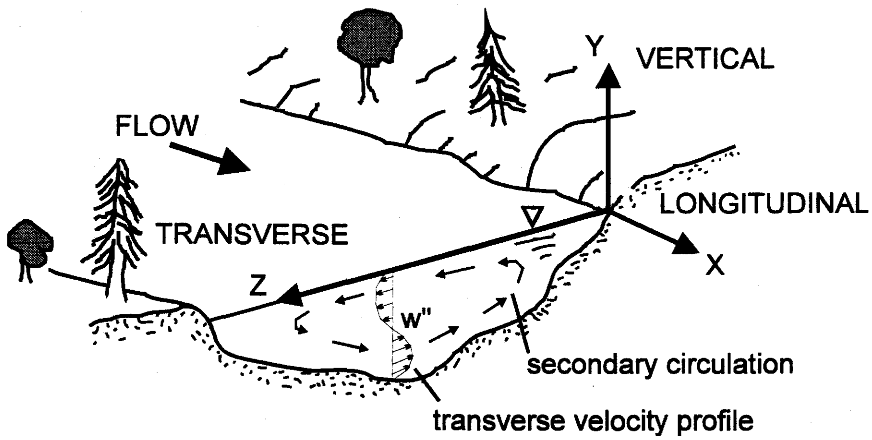

Figure 1.3 Typical secondary circulation and transverse velocity profile (from Putz 1996).

1.2.1 Mixing Zones

The interaction of diffusion, differential advection and channel geometry creates several characteristic mixing regions in a river. From a hydraulic viewpoint, the river downstream from an injection source may be divided into three zones, each corresponding to a different stage in the mixing process. Putz (1996) and Beltaos (1979) described these interactions with the aid of Figures 1.4 and 1.5, respectively.

Suppose a slug of tracer is dumped at point x_o at time t_o as shown in Figures 1.4 and 1.5. It will be transported downstream by the local flow velocity and, at the same time, will expand in all directions due to diffusion. The first zone extends from the source downstream to a section where the distribution of effluent concentration becomes reasonably uniform over the depth. At this point, the main body of the substance cloud has become uniformly mixed in the vertical due to the 'no flux' boundary conditions of the streambed and the water surface. Generally in this region the substance is well mixed in the vertical some 50 to 100 river depths (i.e., 50 to 100 times the depth of that portion of the river into which the effluent is discharged) downstream of the substance source. This region is called the three-dimensional mixing zone because concentration gradients exist in every direction.

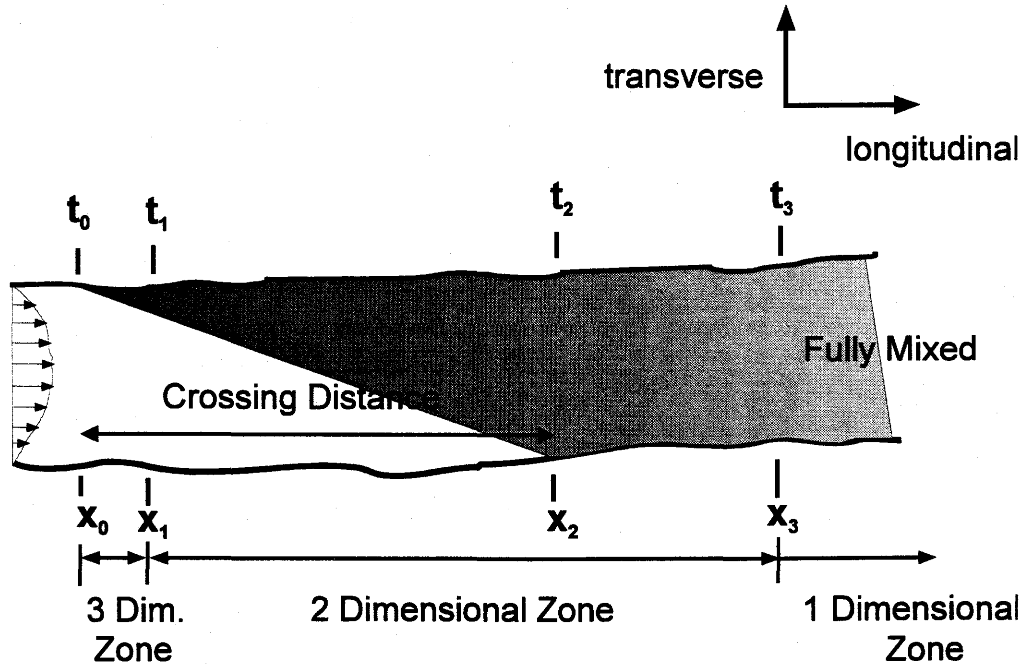

Figure 1.4 Typical spread of substance mass in each of the characteristic mixing regions for steady state flow condition – plan view (from Putz 1996).

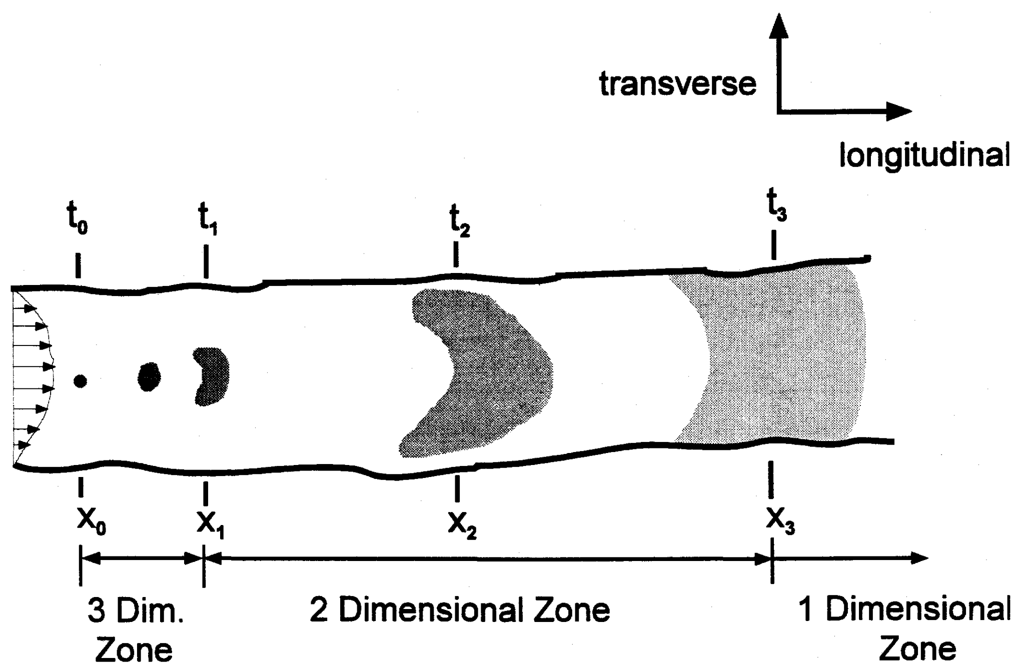

Figure 1.5 Typical spread of substance mass in each of the characteristic mixing regions for unsteady state flow condition – plan view (adapted from Beltaos 1979).

The second zone extends farther downstream from x_1 to a section x_3 where the concentration distribution becomes reasonably uniform over the channel width. So it can be said that the two-dimensional or transverse mixing zone is located downstream of a river outfall beyond the distance required for complete vertical mixing. A common rule of thumb is that the two-dimensional mixing zone will extend for approximately 100 to 300 river widths downstream of an outfall. In this region, transverse (lateral) spreading of the substance mass occurs and continues until the edge of the plume encounters the river banks and eventually near uniform concentrations are established across the river. This is known as the two-dimensional or the transverse (lateral) mixing zone because transverse gradients are dominant. Transverse mixing includes all processes that may change the lateral concentration distribution of a neutrally buoyant tracer.

The third zone begins at x_3 and extends downstream for as far as the effluent concentration is detectable. In this region, the dominant concentration gradients exist in the longitudinal direction and the region is called the one-dimensional or longitudinal mixing zone. This longitudinal direction stage is of limited significance for a continuous, stationary discharge into a steady flow. In other (non-steady) input circumstances, longitudinal dispersion may be of importance, but the effluent will travel a long distance downstream before the one-dimensional dispersion theory is valid (Fischer, 1973). The concentration levels will by then have decreased considerably which makes this phase less interesting in many instances. In most cases it is the second stage, that of lateral mixing, which is of greatest practical importance (Engmann and Kellerhals, 1974). A similar opinion was expressed by Nokes and Wood (1988).

1.2.2 Nature of Inputs

A factor that influences the solution approach used in mixing analysis is the nature of the inputs. When a tracer is injected into a river at a constant rate over an extended period of time (continuous input), a steady state condition of varying duration will be established downstream of the injection point. The duration of the steady state period will decrease with distance downstream. For such situations, analytical predictions are possible. However, if injection is more-or-less instantaneous or of limited duration (slug input), the concentration at any given point downstream will vary with time (unsteady state). These situations results in transient mixing since the injections are time-dependent and so involve a complex process that requires use of numerical computation techniques.

1.2.3 Other Processes

The physical processes, diffusion and advection are attributed to the nature of river flow (river-specific processes). Here, the substance is assumed to be a "neutral tracer", meaning that its properties are similar to those of water. In nature, however, there are several additional processes, associated with the physical and chemical properties of the tracer (substance-specific processes). These include buoyant or settling tendencies, chemical reaction and decay, degradation, adsorption etc. Analysis of the mixing of non-neutral tracers requires identification and quantification of substance-specific processes. Additional terms must therefore be added to the differential equations, and these increase the complexity of the problem.

1.2.4 Model Considerations

Many of the conditions and assumptions taken into consideration for the modelling work described in this thesis are in accordance with past work and literature. The river mixing and transport model used has been developed using the principles of fluid mechanics, mass transport and numerical procedures. This model like most river mixing models is derived for a depth-averaged concentration, which reduces the complexity of the overall problem. In addition, the mixing model used is derived for steady river flow. The model used has the capability to handle time varying input conditions. This is a very important feature of the mixing model. The Cartesian coordinate system is used in the model. This would be very convenient for channels that have consistent width. However it can also be used in natural rivers where the plan form of the river and the river width vary along the length in addition to the variation of flow depth along and across the river.

1.3 Research Objectives

The work reported herein is concerned with the transverse mixing process under steady and unsteady state input conditions. Attention is focused on the mixing of substances that are neutral and conservative. The specific objectives of the work are:

1. To determine the dimensionless transverse mixing coefficient, β, of the Athabasca River over a 32 km reach using a microcomputer-based set of computer programs for modelling two-dimensional, steady and unsteady effluent source river mixing based upon the explicit method first conceptualized by Fisher (1968) and further developed by Beltaos (1978);
2. To assess the variation in the dimensionless transverse mixing coefficient, β, with discharge over a range of flow conditions;
3. To assess the variation of the dimensionless transverse mixing coefficient, β, due to the presence of an ice cover; and
4. To verify the Advection Optimized Grid (AOG) modelling approach, using field data from three continuous input tests and one slug input test.

1.4 Scope of the Investigation

Much of the work described herein was completed as part of a continuing program to develop a comprehensive water quality modelling method applicable to the two-dimensional mixing zone in rivers. The modelling method has the capability to predict the combined effects of time-dependent input and in-stream reaction of substances. However, this work is focused on neutrally buoyant, mass conservative, passively discharged substances.

Field verification of the modelling method was originally to be done using two tracer tests conducted in August 1997 on the Athabasca River downstream of the Alberta Pacific Forest Industries Inc. mill site near Boyle, Alberta. While compiling background information in order to plan the field work, it was discovered that two previous tracer tests had been conducted at this same location for Alberta Pacific Forest Industries Inc. by Beak Consultants Limited. However, neither of these earlier tests had ever been analyzed to characterize the transverse mixing of the reach. This is quite unique and gives the rare opportunity of having four tests at the same location. The scope of the thesis work was therefore expanded to these four tests which cover a range of flow and input conditions as outlined below:

- 84 m^3/s, ice cover, February 1995, continuous tracer input,
- 270 m^3/s, open water, October 1994, continuous tracer input,
- 960 m^3/s, open water, August 1997, continuous tracer input,
- 876 m^3/s, open water, August 1997, slug input of tracer.

The February 1995 and October 1994 continuous input tests were carried out by Beak Consultants Ltd.

2. REVIEW OF TWO-DIMENSIONAL RIVER MIXING THEORY

2.1 Mass Balance Equation

When a tracer or substance is injected into a river, its concentration will generally vary with respect to both time and space. Prediction of the concentration or mixing of a mass conservative, neutrally buoyant substance in a river is governed by the principle of conservation of mass. The conservation principle is expressed by:

$$\frac{\partial c}{\partial t}+u\frac{\partial c}{\partial x}+v\frac{\partial c}{\partial y}+w\frac{\partial c}{\partial z}=\frac{\partial}{\partial x}\left(\varepsilon_x\frac{\partial c}{\partial x}\right)+\frac{\partial}{\partial y}\left(\varepsilon_y\frac{\partial c}{\partial y}\right)+\frac{\partial}{\partial z}\left(\varepsilon_z\frac{\partial}{\partial z}\right) \quad . \quad . \quad . (2.1)$$

where c is the local tracer concentration; t is time; u, v, w are the time-averaged local velocity components in the x, y, and z directions, respectively, as can be seen in Figure 2.1; and ε_x, ε_y, and ε_z are coefficients of diffusion in the indicated coordinate directions. A derivation of equation 2.1 is given in Elhadi *et al.* (1984). The terms on the left are the advective terms (with the exception of the time differential), which represent transport of the tracer by the components of mean local velocity, while the terms on the right are the diffusive terms, which represent transport due to turbulent diffusion.

Strictly speaking, the diffusion coefficients appearing in equation (2.1) should be a sum of turbulent and molecular diffusivities. However, in open channel flows turbulent diffusion is several orders of magnitude higher than molecular, therefore the molecular diffusivity is often neglected (Beltaos, 1979).

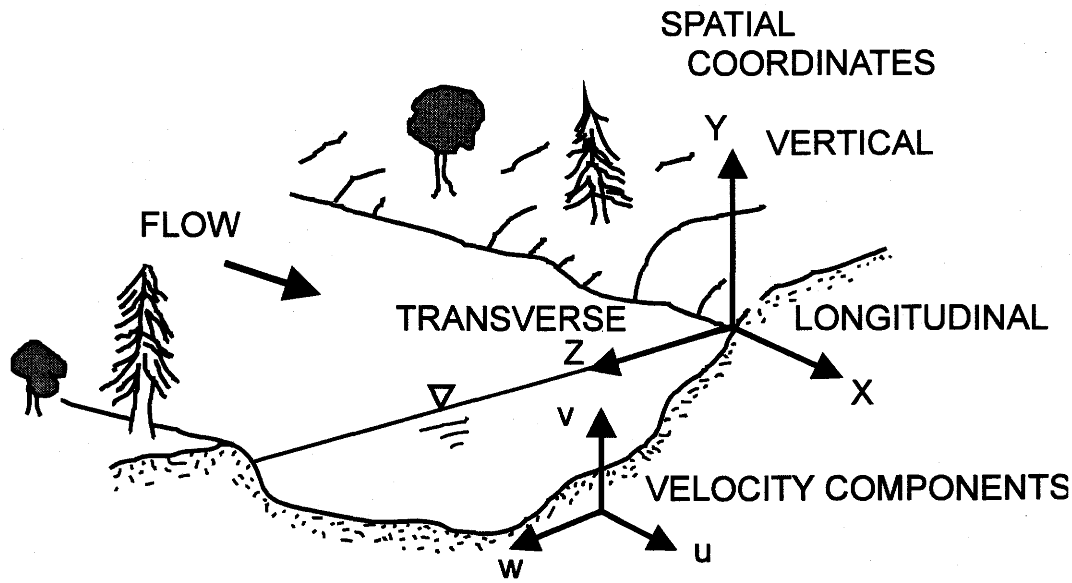

Figure 2.1 Coordinate system for spatial and velocity components (from Putz 1996).

In most rivers, channel geometry varies spatially; so that the application of equation (2.1) requires knowledge of all three local velocity components as shown in Figure 2.1. Solving equation (2.1) presents difficulties. An attempt to do this, even using numerical solutions, is often impractical for extended lengths of the river. To circumvent this problem, various simplifications are made.

2.2 Two-dimensional Mixing

Natural rivers are very wide in comparison with their depth. When a neutral substance is released in a flow field that has a large width-to-depth ratio, the concentration distribution of the substance (tracer) becomes nearly uniform over the depth much sooner (i.e., within a distance of 50 to 100 river depths downstream of the injection point) than it becomes nearly uniform over the entire cross section. The two-dimensional or transverse mixing zone is located downstream of a river outfall beyond the distance required for complete mixing in the vertical direction. For two-dimensional mixing zones, neutral substances become well mixed in the vertical in comparison to the longitudinal and transverse directions. It then becomes advantageous to work with a depth-averaged equation beyond this point. Because of this, the mass conservation equation can be simplified by integrating it over depth so that the terms representing the advective and diffusive transports in the vertical disappear. The resulting equation is given below (Elhadi *et al.* 1984).

$$\frac{\partial}{\partial t}(hc)+\frac{\partial}{\partial x}(huc)+\frac{\partial}{\partial z}(hwc)=\frac{\partial}{\partial x}\left(hE_x\frac{\partial c}{\partial x}\right)+\frac{\partial}{\partial z}\left(hE_z\frac{\partial c}{\partial z}\right) \quad . \quad . \quad .(2.2)$$

Where, E_x and E_z are mixing coefficients which include the effects of turbulent diffusion and differential advection; c is the tracer concentration; t is time; u, v, and w are the time-averaged velocity components in the x, y, and z directions, respectively. The terms on the left of equation (2.2) represents the local rate of concentration change, and advective flux in the longitudinal and transverse directions. The terms on the right represents diffusive flux in the longitudinal and transverse directions.

Equation (2.2) is a simpler equation than the full three-dimensional mass balance equation and, as a result it is comparatively easier to solve. However it is still difficult to get an analytical solution since quantities such as u, w, h, E_x, and E_z in general, vary with x and z. Hence, the only alternative is to solve it numerically.

For the case of a continuous release of a tracer at a steady rate in a river flow that is steady or that only fluctuates mildly about a certain mean value, equation (2.2) can be further simplified. For such a case, the term representing the dispersive transport in the longitudinal direction becomes small compared with its counterpart representing the advective transport, since advection is much more effective in spreading the tracer in the x-direction than diffusion (Beltaos, 1979). Therefore as a first approximation, the first term on the right hand side of equation (2.2) is neglected. In addition, the advective transport in the z direction is generally negligible, i.e. $wc \approx 0$. And so the last term on the left-hand side of the equation drops out also. As a result the mixing and transport in the transverse mixing zone can be described by the following equation (Holly, 1975, Beltaos, 1978):

$$\frac{\partial}{\partial t}(hc)+\frac{\partial}{\partial x}(huc)=\frac{\partial}{\partial z}\left(hE_z\frac{\partial c}{\partial z}\right) \quad . \quad . \quad . \quad . \quad . \quad . \quad . \quad (2.3)$$

in which x is the longitudinal direction, z is the transverse (across stream) direction, c is depth-averaged concentration, u is depth-averaged velocity in the longitudinal direction, h is the local depth and E_z is the transverse mixing coefficient. The first term on the left of equation (2.3) represents the local rate of concentration change. The second term on the left of equation (2.3) represents advective mass transport in the longitudinal direction. The term on the right represents diffusive transport across the stream. If the substance mass flux of the source is steady state then a time independent concentration distribution will be established downstream of the source. In such a case equation (2.3) may further be simplified by omitting the time differential.

2.2.1 Transverse Coordinate Transformation

The transverse changes in local stream depth, streamwise velocity and the presence of transverse advective flux considered within the moment analysis of Holley *et al.* (1972) and Fischer (1967), can be accounted for by using a transverse coordinate transformation. Equation (2.3) is in the form of an advection-diffusion equation. This can be transformed into a simpler form of advection-diffusion equation by introducing the cumulative discharge, q, in place of z.

$$q=\int_0^z hudz \quad . \quad . \quad . \quad . \quad . \quad . \quad . \quad . \quad . \quad (2.4)$$

Where $z = 0$ represents the left bank as shown in Figure 2.2 and u is the mean velocity in the direction of flow. At the right bank $z = W$, the total stream width and $q = Q$, the total stream discharge. The cumulative discharge q represents the discharge that passes between the bank and a distance z out from the bank. Equation (2.4) indicates that a line of constant q represents a depth-averaged streamline and hence two adjacent lines of constant q define a streamtube. This adaptation of a streamtube approach for representation of the river flow was introduced by Yotsukura and Cobb (1972). Some important features of the 'q' transformation are:

a) there is no average flow across a line of constant q and therefore no transverse advection, and

b) the plan view of the natural stream of variable width is transformed into a simple rectilinear form of constant width.

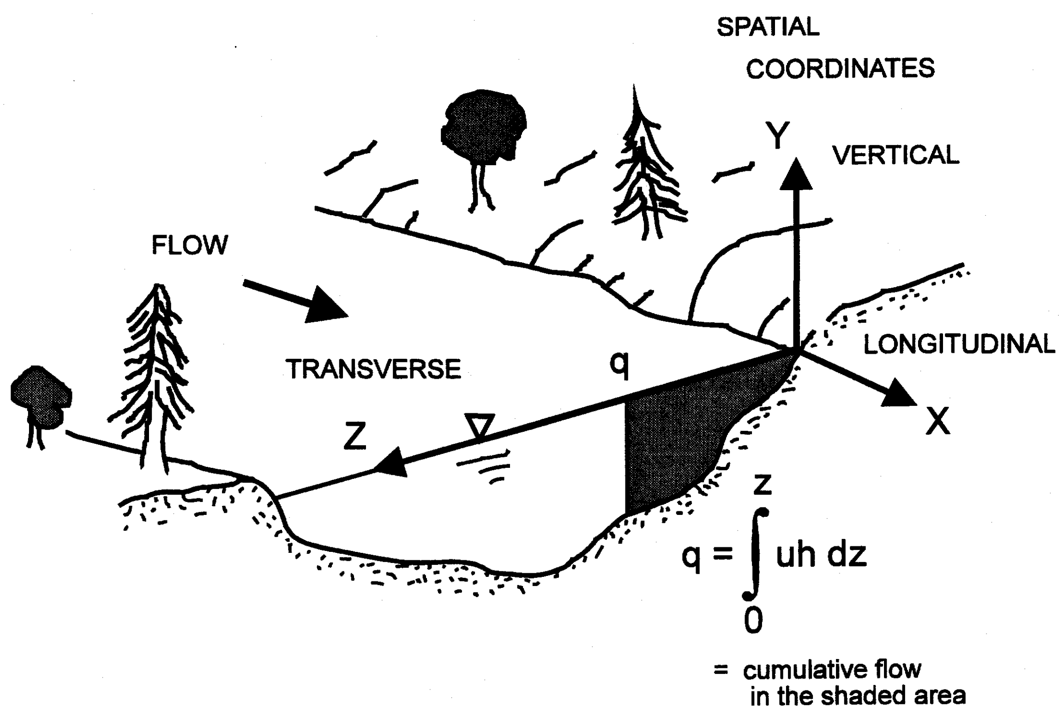

Figure 2.2 Transverse coordinate transformation (From Putz, 1996).

The use of this concept in the numerical solution of equation (2.3) further justifies not including a transverse advective term in equation (2.3). Yotsukura and Sayre (1976) introduced the 'q' transformation into the steady-state version of equation (2.3) and obtained the following equation:

$$\frac{\partial c}{\partial x} = \frac{\partial}{\partial q}\left(uh^2 E_z \frac{\partial c}{\partial q} \right) \quad . \quad . \quad . \quad . \quad . \quad . \quad . \quad . \quad . \qquad (2.5)$$

The product (uh^2E_z) is analogous to a diffusion coefficient. Equation (2.5) has the same transport mechanisms as equation (2.3).

2.2.2 Analytical Solutions

For most natural rivers, the diffusion factor will vary across the channel and the variations can be very large where there are bends. Therefore equation (2.5) can only be solved numerically. However, it is possible to obtain rough estimates by solving equation (2.5) analytically assuming the diffusion factor to be a constant equal to its cross-stream average. Yotsukura and Cobb (1972) give one such solution of equation (2.5) for a steady state point source of conservative substance in dimensionless form as:

$$\frac{c_{(x,\eta)}}{c_\infty} = \frac{1}{\sqrt{4\pi\chi}} \sum_{m=-\infty}^{+\infty} \left\{ \exp\left[-\frac{(\eta - 2m - \eta_o)^2}{4\chi} \right] + \exp\left[-\frac{(\eta - 2m + \eta_o)^2}{4\chi} \right] \right\} \qquad (2.6)$$

Where: $\chi = xE_z/(uW^2)$, a dimensionless longitudinal distance,

- η_o is the transverse location of the source, expressed in terms of cumulative flow,
- η is the solution location, expressed in terms of cumulative flow ($\eta = q/Q$),
- m is an integer,
- $C_{(x,\eta)}$ is the depth averaged concentration,

C_∞ is the fully mixed concentration of the tracer mass within the river flow ($C_\infty = M^*/Q$). M^* is the mass of tracer injected per unit time; Q is the total discharge of the river.

Yotsukura and Cobb (1972) also presented the following solution to equation (2.5) for a horizontal line source of substance:

$$\frac{c_{(x,\eta)}}{c_\infty} = \frac{1}{2(\eta_2 - \eta_1)} \sum_{m=-\infty}^{+\infty} \left\{ \begin{array}{l} \operatorname{erf}\left[\dfrac{(\eta_2 + 2m - \eta)}{2\sqrt{\chi}}\right] - \operatorname{erf}\left[\dfrac{(\eta_1 + 2m - \eta)}{2\sqrt{\chi}}\right] + \\ \operatorname{erf}\left[\dfrac{(\eta_2 + 2m + \eta)}{2\sqrt{\chi}}\right] + \operatorname{erf}\left[\dfrac{(\eta_1 + 2m + \eta)}{2\sqrt{\chi}}\right] \end{array} \right\} \tag{2.7}$$

Where: η_1 is the left side of the line source in terms of q/Q,

η_2 is the right side of the line source in terms of q/Q, and

erf is the error function

For accurate predictions of concentration distributions, the variations of velocity and depth across the river have to be taken into account, therefore the diffusion factor cannot be assumed to be constant. Lau and Krishnappan (1981) have shown that the solutions using constant cross-stream averages of uh^2E_z can be inaccurate.

2.3 Transverse Mixing Coefficient

The transverse mixing characteristics of a river reach are quantified by determining E_z the transverse mixing coefficient, which occurs at a particular stage and discharge. Knowledge of the transverse mixing coefficient is a prerequisite in assessing the total dispersive capacity of a river. River-specific processes can be effectively accounted for by means of a transverse mixing coefficient, E_z. This coefficient has the dimensions of diffusivity (L^2/T) and expresses the combined effect of diffusion in the transverse direction, z, and secondary circulation.

Secondary circulation is weak in straight, prismatic channels, but is very significant in natural streams. Because knowledge of secondary circulation in open channel flows is quite incomplete, the effect of secondary circulation is incorporated in the transverse mixing coefficient. Therefore, a flow in a curved channel is expected to have a larger mixing coefficient than a flow in a straight channel with the same flow cross section. The transverse mixing coefficient E_z is generally given by an expression in the form:

$$E_z = \beta L V \qquad (2.8)$$

Here, L is a length scale representative of the mixing length (the distance from injection required for the cross-sectional distribution of concentration to become nearly uniform), V is a velocity scale representative of the level of turbulence, and β is the dimensionless transverse mixing coefficient. The length scale is generally taken to be the local depth, h, or the channel average stream depth, H. The velocity scale is generally taken to be the local shear velocity $u*$ or the channel average, $U*$ given by the expression:

$$u* = \sqrt{grS} \quad \text{or} \quad U* = \sqrt{gRS} \qquad (2.9)$$

Where, g is the gravitational constant, r is the local hydraulic radius, R is the channel average hydraulic radius, and S is the slope of the energy grade line (slope of the water surface for uniform flow).

Knowledge concerning the functional relationship between the transverse mixing coefficient and flow and channel geometry is still limited. At present, there is no reliable theoretical method for predicting the transverse mixing coefficient. For natural channels direct measurement of E_z is very tidious since it involves the transport due to turbulence fluctuations as well as that due to differential advection. Currently evaluations rely heavily on laboratory and field tracer experiments.

2.3.1 Laboratory Studies

Diffusive mixing processes have usually been interpreted by use of the Fickian theory of diffusion. Adolph Fick was one of the earliest investigators of the diffusion process. In 1855 Fick proposed an expression describing molecular diffusion. He stated that solute mass flux in a given direction is proportional to the gradient of the solute concentration in that direction, which is analogous to Fourier's law of heat flow. Solutions to Fickian theory results in Gaussian distribution of the solute downstream of a discharge point.

Random walk statistical theory was developed following Fick's hypothesis. This theory describes the probable distribution of solute resulting from random collisions of molecules (molecular diffusion). Random walk theory indicates that after the initial number of individual movements or time periods the distribution of solute molecules will closely approximate the Gaussian distribution, thus validating Fick's law (Fischer *et. al.* 1979).

G.I. Taylor (1954) extended diffusion theory to turbulent flows. Taylor's work suggested that after an initial time period the diffusion process might be described by a turbulent diffusion equation, in which turbulent diffusive flux is described by Fick's law with turbulent diffusion coefficients. Turbulent diffusion is analogous to molecular diffusion but is the result of a distinctly different physical process. Molecular diffusion, as noted in chapter one, is the result of molecular collisions, while turbulent diffusion results from the much larger scale random motion of "fluid packages" or "eddies" characteristic of turbulent flow. Taylor's work also showed that after an initial time period the turbulent diffusion coefficient is the product of a length scale and a velocity scale. The length scale is a measure of the size of eddies created by the turbulence and the velocity scale is a measure of the intensity of the turbulence.

Several investigators have carried out measurements of E_z in straight laboratory flumes. Elder (1959) was the first to conduct an experimental evaluation of E_z in a laboratory flume. While investigating longitudinal dispersion in a wide channel, Elder (1959) observed the transverse concentration distributions resulting from a point source slug injection of tracer. He noted that the distributions were Gaussian in shape implying a Fickian diffusion type process and proposed the empirical expression:

$$E_z = \beta H U^* \qquad (2.10)$$

Where H is the mean channel depth and β a constant. Elder estimated β to have a value of 0.23 on the basis of a best fit Gaussian curve to his experimental results. Several studies have been carried out since then. These have shown that generally E_z/U^*H varies between 0.1 and 0.3 (Beltaos 1978) and depends on the friction factor, f and the channel aspect ratio, W/H.

Fischer (1969) presented an analysis similar to that applied for longitudinal dispersion, to predict the transverse mixing coefficient. He reported several laboratory experiments in a curving wide flume and indicated that his analysis was capable of predicting the observed coefficients to within a factor of two.

Chang (1971) presented the results of laboratory experiments in meandering flumes. His findings suggested a strong dependence of the transverse diffusion coefficient on the helical motion induced by bends.

Engmann (1974) reported results of transverse mixing experiments in a meandering flume. The main goal of the study was the assessment of the effects of an ice cover on transverse mixing capacity. Engmann reached the conclusion that the presence of an ice cover reduced the mixing capacity significantly. Other investigators have also conducted flume studies of transverse diffusion. Yotsukura and Cobb (1972), in a brief review of the results of these studies, indicated the value of β for Elder's relationship may range from 0.11 to 0.26.

Webel and Schatzmann (1984) conducted a comprehensive laboratory study of the hydraulic and geometric parameters, which could influence β. They concluded E_z/HU^* was independent of all parameters except friction factor and that flow depth was the most appropriate length scale for non-dimensionalizing E_z. However Lau and Krishnappan (1977) had earlier suggested using the width as the length scale for non-dimensionalizing the mixing coefficient.

Nokes and Wood (1988) further studied the issue of non-dimensionalizing E_z and also concluded that the depth was the most appropriate length scale. They qualified their findings by stating investigators must define what processes E_z is intended to represent. If E_z is intended to represent transverse turbulent diffusion, with negligible secondary circulation, then depth is the correct parameter. A summary of laboratory results from several investigators is given in Table 2.1.

Table 2.1 Dimensionless transverse mixing coefficients in laboratory channels from several investigators (adapted from Beltaos, 1979, Rutherford 1994).

Description of channel	**Investigators**	**W (cm)**	**H (cm)**	**W/R**	**E_z (cm²/s)**	**E_z/RU_***
Long rectangular channel, open water	Fischer (1969)			27.3		1.51
Long rectangular channel, open water	Fischer (1969)			36.7		0.54
Meandering, rectangular flume, Open water	Chang (1971)			6.7		0.88
Meandering, larger flume, Open water	Chang (1971)			20.3		1.35
Meandering, rectangular flume, open water	Engmann (1974)			20		0.89
Meandering, rectangular flume, ice-covered	Engmann (1974)			25		0.88
Straight laboratory channel	Engmann (1974)	122	4 to 6.5		0.86 to 1.55	0.147 to 0.192

Table 2.1 *Contd.*

Description of channel	Investigators	W (cm)	H (cm)	W/R	E_z (cm^2/s)	E_z/RU_*
Meandering channel with equilibrium bed, sinusoidal, open water	Krishnappan and Lau (1977)			10.5		0.22
Meandering channel with equilibrium bed, sinusoidal, open water	Krishnappan and Lau (1977)			10		0.31
Straight laboratory channel	Krishnappan and Lau (1977)	45	1.3 to 4		0.67 to 1.16	
Straight laboratory channel	Krishnappan and Lau (1977)	60	3.9 to 5		0.74 to 1.4	0.16 to 0.20
Straight laboratory channel	Okoye (1970)	85	1.5 to 17.3		0.64 to 2.9	0.09 to 0.2
Straight laboratory channel	Okoye (1970)	110	1.7 to 22		0.79 to 3.3	0.11 to 0.24
Straight laboratory channel	Prych (1970)	110	4 to 11.1		1.1 to 3.6	0.14 to 0.16
Straight laboratory channel	Sayre and Chang (1968)	238	14.8 to 37.1		9.6 to 36.9	0.16 to 0.18
Straight laboratory channel	Sullivan (1968)	80	7.3 to 10.2		0.9 to 1.18	0.107 to 0.133
Straight laboratory channel	Miller and Richardson (1974)	60	12.7 to 13.2		3.7 to 36.3	0.10 to 0.18
Straight laboratory channel	Sayre and Chamberlin (1964)	244	17.4		15	
Straight laboratory channel	Engelund (1969)	220	5.5 to 17.3		4 to 6.5	
Straight laboratory channel	Nokes (1986)	56	5 to 6.5		0.92 to 1.24	
Straight laboratory channel	Webel and Schatzmann (1984)	49	9		2.22	
Straight laboratory channel	Webel and Schatzmann (1984)	132	9		2.22	

Table 2.1 *Contd.*

Description of channel	Investigators	W (cm)	H (cm)	W/R	E_z (cm^2/s)	E_z/RU_*
Straight laboratory channel	Elder (1959)	36	1.2		1.89	0.16
Straight laboratory channel	Holley and Abraham (1973)	220	9.7			0.36 to 0.49
Laboratory model of Ijssel River	Holley and Abraham (1973)	122	90			0.45 to 0.77
Straight laboratory channel	Holley and Abraham (1973)	120	9.7		0.92	
Straight laboratory channel	Kalinske and Pien (1944)	69	15.8		6.65	

2.3.2 Field Studies

While the mixing studies in rectangular channels with minimal secondary circulation are of academic interest they are not very useful for predicting mixing in natural channels. Extrapolation of the laboratory results to natural rivers is difficult, partly due to the uncertainty of the accuracy of scaling laws, and partly because the shape and irregularity of the river cross section may play a role (Fischer *et al.* 1979). Natural channels differ from uniform rectangular ones in three important respects: the depth varies irregularly, the channel is likely to curve, and there may be large sidewall irregularities such as points of land. At present, there is insufficient information for predicting E_z and thus heavy reliance on field tests is necessary.

Curvilinear flows cause transverse advection, which tends to enhance the value of the transverse mixing coefficient. Because meandering is inevitable in natural rivers, the transverse mixing coefficients in natural rivers will be larger than the values obtained in straight channels. One of the earliest field investigations regarding transverse mixing was done by Glover (1964), on the Columbia River. Glover reported a value for E_z/RU^* of 0.72.

Fischer (1967) conducted tracer studies along a straight portion of an earth canal. He reported a value for β of 0.24 for continuous point source discharges located at midstream and at the bank. He also calculated the variance of the transverse distribution of the tracer mass flux rather than concentration passing a measured section. This implicitly includes the effects of local depth and velocity in the calculation. He also adjusted the variance for minor changes in channel width. Fischer (1967), in commenting on the large magnitude of the transverse mixing in comparison to that in the vertical, had eluded to the fact that eddy size is partially dependent upon the proximity of normal boundaries. Hence eddy size is less restricted in the transverse than in the vertical direction. Fischer (1967) suggested larger eddies in the transverse direction may provide more effective mixing explaining the larger coefficients measured in the transverse compared to that which can be theoretically predicted for the vertical.

Yotsukura, *et al.* (1970) observed that transverse mixing in natural channels might be greatly enhanced due to the influence of secondary currents. Variable bed shear, channel irregularities or bends within the stream may create secondary currents. Yotsukura *et al.* (1970) conducted a steady-state transverse mixing investigation along a gently curved reach of the Missouri River downstream of a mid-channel tracer injection. A numerical simulation of the mixing was used to find the transverse mixing coefficient by fitting solution distributions to the measured tracer concentrations. The explicit finite difference scheme they used was based on a stream tube concept and accounted for varying channel depth and velocity. The mass transfer between stream tubes was assumed to be entirely diffusive, incorporating any secondary current effects into the diffusion term. The numerical solution gave an overall best fit to the measured distributions with a reach-averaged β of 0.6. However, a sensitivity analysis indicated the transverse mixing coefficient could vary as much as 100 percent along the reach without appreciably altering the solution. They concluded that β for large meandering channels would generally be larger and more variable than results obtained for small straight channels.

Holley *et al.* (1972) investigated the effects of secondary currents, channel geometry and local velocity, which are generally lumped into the diffusion coefficient, in an effort to distinguish which mechanisms should be represented by the coefficient. Specifically, they considered the effects of transverse variation of depth, streamwise velocity, the diffusion coefficient itself and the presence of transverse velocities. Holley *et al.* worked with an implicit finite difference model, which gave solutions to equation (2.3). They first looked at the influence of the local depth by considering a trapezoidal and rectangular channel with equivalent mean velocity and depth. They found that neglecting the variation of h (i.e. assuming a rectangular channel) produces significantly different calculated concentration distributions compared to those calculated for the trapezoidal channel. The solution obtained for a continuous bank injection of tracer indicated the equivalent rectangular section seriously underestimated the concentration along the injection bank. However, they also emphasized that this relates to a few examples and therefore could not draw a general conclusion on the basis of the calculations.

The effects of local stream geometry, variable streamwise velocity, and the presence of transverse velocity, considered in the analysis of Holley *et al.* (1972) and Fischer (1967), may more easily be accounted for using a transverse coordinate transformation introduced by Yotsukura and Cobb (1972) defined as the cumulative flow, q, as given by equation (2.4).

Beltaos (1979, 1980) presents an excellent review of transverse mixing theory, past investigations, applications, field procedures and results. The values of E_z/HU^* for the studies of natural streams reported in literature range from 0.18 to 7.20. Even though several field experiments have been carried out since Glover's study, these have hardly been sufficient to permit reasonable estimates of transverse mixing coefficients. Field values of E_z/HU_* range mostly between 0.1 and 1.3. A value of 3.3 given by Sayre and Yeh (1973) was observed along a continuous bend.

Although the transverse mixing coefficient may be determined from tracer tests, uncertainty remains as to the best method of predicting its magnitude from channel and flow characteristics. Take for instance the empirical expression defining the transverse mixing (diffusion) coefficient proposed by Elder as given in equation (2.10). There is still some dispute as to the most appropriate parameter to use as a length scale in the relationship. Most investigators have used a vertical length scale such as *H*, as proposed by Elder. Fischer recognized the length scale of turbulence is restricted by boundaries in the vertical direction, implying that the vertical scale may not be representative of the lateral scale of the eddies. Wide variations in the values of dimensionless mixing coefficients, even for straight channels, have been reported. Lau and Krishnappan in explaining these variations, used dimensional analysis to identify the functional relationship for the dimensionless mixing coefficient in a straight rectangular channel expressed as:

$$\frac{E_z}{\ell U_*} = func\left(\mathrm{f}, \frac{W}{H}\right) \qquad (2.11)$$

Here, *f* is the friction factor (bed shear), *l* is the length scale and *W/H* is the width to depth ratio (aspect ratio) of the channel. Lau and Krishnappan's analysis of straight rectangular flume experiments indicated the dominant mechanism involved in the transverse mixing is lateral secondary circulation (created by bed shear) which may be characterized by aspect ratio. Considering secondary circulation to be the dominant mechanism, the product *HU**, which characterizes the magnitude and vertical scale of turbulence, was found to be undesirable as a scaling factor for E_z. They felt *WU* or *WU**, which characterizes the magnitude and lateral scale of turbulence, was more appropriate. In a comparison of plots involving *Ez/WU** versus *W/H* and *Ez/HU** versus *W/H* it was observed that the former formed a near single curve, with only minor influence of friction factor as opposed to the later which had considerable scatter. Therefore they suggested non-dimensionalizing E_z with *WU**.

In a related study Lau and Krishnappan (1981) identified secondary circulation due to stream curvature as a major mechanism contributing to transverse mixing. Taking the variability of river bend occurrence, shape, and radius into consideration, Lau and Krishnappan felt channel sinuosity, *Sn*, a rough measure of channel curvature more appropriate than a rigid measure such as bend radius. Sinuosity is defined as the ratio of thalweg length and down valley distance, the thalweg being the line of peak flow intensity along the channel length. Lau and Krishnappan concluded that sinuosity is important in determining E_z for natural streams but felt more data is required before any empirical relationship may be formulated.

Smith and Gerald (1981) demonstrated similar dependence of E_z upon channel curvature by listing measured dimensionless mixing coefficients for natural streams ranked according to stream irregularity. The streams with higher channel irregularity consistently had higher values of E_z.

Putz and Smith (1998) reported verification studies on tracer tests conducted on the North Saskatchewan, Peace, and Slave Rivers. The magnitude of the E_z/HU^* values they obtained fell within the range of 0.06 to 5.1.

Although understanding of the transverse mixing process has improved substantially since Elder's first open channel experiments, extrapolation of field results from one location to another remains difficult. Numerical or analytical predictions based upon estimated coefficients may be adequate as first order approximations, however, uncertainty as to the actual value of transverse mixing coefficient requires tracer tests for accurate assessments of plume characteristics. Beltaos (1979) suggests at least two or three tests are required to define the variation of transverse mixing coefficient and mixing capacity over a range of flow conditions along the river reach of interest. A summary of field results from several investigators is given in Table 2.2.

Table 2.2 Dimensionless transverse mixing coefficients in natural streams from several investigators (adapted from Rutherford, 1994).

Stream Description	**Investigators**	**W/H**	**E_z/HU_***
Columbia River (meandering)	Glover (1964)	100	0.72
Missouri River (meandering)	Yotsukura *et al.* (1970)	67	0.60
Missouri River near Blair	Yotsukura and Cobb (1972)	66.7	0.50
Aristo feeder canal	Yotsukura and Cobb (1972)	27.3	0.22
South River	Yotsukura and Cobb (1972)	46.2	0.29
Athabasca River	Yotsukura and Cobb (1972)	169.5	0.76
Bernardo conveyance channel	Yotsukura and Cobb (1972)	28.7	0.30
South River	Fischer (1973)	41.6	0.26
Bernado River	Fischer (1973)	28.6	0.30
Atrisco River	Fischer (1973)	27.3	0.25
Mackenzie River (meandering)	Fischer *et al.* (1979)	185	0.66
Potomac River (meandering)	Fischer *et al.* (1979)	282	0.52 to 0.65
Mobile River	Meyer (1977)	87.2	7.2
Waal River (meandering)	Holley and Abraham (1973)	51	0.36
Ijssel River	Holley and Abraham (1973)	17	0.51
Isere River (bend)	Holly and Nerat (1984)	29	0.5 to 1.6
Slave River (meandering)	Engmann and Kellerhals (1974)	18.3	0.38
Slave River (ice-covered)	Engmann and Kellerhals (1974)	18	0.12
Mackenzie River, Ft Simpson to Norman Wells	Mackay (1970)	185	0.66
Athabasca River below Ft. McMurray (open water)	Beltaos (1978)	170	0.75
Athabasca River below Ft. McMurray (ice-covered)	Beltaos (1978)	131	0.58
Athabasca River below Athabasca (open water)	Beltaos (1978)	156	0.41
Athabasca River below Athabasca (ice-covered)	Beltaos (1978)	288	0.29
North Saskatchewan River below Edmonton	Beltaos (1978)	137	0.25
Bow River at Calgary	Beltaos (1978)	104	0.61
Beaver River near Cold Lake (open water)	Beltaos (1978)	45	1.03
Beaver River near Cold Lake (ice-covered)	Beltaos (1978)	64	1.27
Missouri River below Cooper Generation station	Sayre and Yeh (1975)	59	3.30

Table 2.2 *Contd.*

Stream Description	**Investigators**	**W/H**	**E_z/HU_***
Missouri river (bend)	Sayre (1979)	65.7	1.27
Missouri river (meandering)	Sayre (1979)	73	0.74
Grand River below Kitchener	Lau and Krishnappen (1981)	117	0.26
Saskatchewan River (meandering)	Lau and Krishnappen (1981)	137.4	0.25
Bow River (meandering)	Lau and Krishnappen (1981)	104	0.61
Kris-Raba River (meandering)	Somlyody (1977)	9.4	0.16
Danube River (meandering)	Somlyody (1977)	144	0.13
Danube River (meandering)	Somlyody (1982)	143	0.25
Rea River	Cotton and West (1980)	37.2	0.24
Waikato River (meandering)	Rutherford *et al.* (1980)	34	0.45
Waikato River (meandering)	Rutherford and Williams (1992)	176.5	0.31
Slave River below Ft. Smith (open water)	Putz (1983)	161	0.88
Slave River below Ft. Smith (ice-covered)	Putz (1983)	163	0.47
Mississippi River below Monticello generating plant	Demetracopoulous and Stefan (1983)	171	0.24 to 4.65

2.3.3 Determination of E_z

There are several methods available for the calculation or prediction of mixing coefficients. These include:

1. Change of moments analysis of measured concentration distributions:

This method requires measurement of the substance concentration, channel geometry and velocity distribution downstream of the source. The concentration distribution is often determined by means of a tracer test. It also uses the relationship between substance or tracer plume spreading and diffusion theory to obtain a reach-averaged value of mixing coefficient. The variance (second central moment) of the concentration distribution at each section is used as a measure of the plume spreading.

2. Simulation method:

This method involves the numerical or analytical solution of the governing differential equations, using trial and error values of mixing coefficients, to obtain an optimum fit to the measured concentration distributions. For use of the simulation method, it is also necessary to have data on velocities, depths, and concentrations at various locations along the river reach. Therefore field tests are necessary in order to obtain these data. When it is not feasible to conduct a field test and determine the value of E_z, then one can select a value based on one's knowledge of how E_z varies with river geometry and flow conditions.

3. ADVECTION OPTIMIZED GRID METHOD

3.1 Introduction

Analytical solutions have been developed for equation 2.3 for simplified cases in which the river channel is considered to have a consistent depth and velocity. But despite these approximate solutions, in order to adequately handle variable geometry and the transverse velocity gradients, which occur in a river, a numerical solution is required. Numerical solution procedures for equation 2.5 for steady state mass input are well established (for instance the model documented by Krishnappan and Lau, 1983) and have been tested and verified with numerous field tests. Several modelling procedures for two-dimensional river mixing with unsteady mass input have also been proposed and tested.

The 'Advection Optimized Grid' (AOG) method is a numerical concept first proposed by Fischer (1968) to simulate the two-dimensional river mixing of a mass conservative substance. The method uses the streamtube approach to represent the river and a numerical procedure employing an advection optimized grid to limit numerical errors associated with advective transport calculations. The major innovation of the AOG method is the selection of element lengths, which ensure complete advective mass exchange from element to element down each streamtube, during each time step of the simulation. Also a simple explicit forward finite difference expression can be used to represent longitudinal advection and each calculation will have a Courant number, C_r, of one.

Having a $C_r = 1$ ensures complete advective exchange of mass between nodal points or elements during a time step calculation. Hence, problems of numerical dispersion, dissipation and solution oscillations normally associated with numerical representations of the advective step are minimized (Putz and Smith 1998).

This modelling method has the capability to predict the combined effects of time-dependent input and in-stream reaction of substances. The AOG method is also able to directly handle the variations in cross section geometry (i.e., the u and h variations both transversely and longitudinally) and to indirectly handle the enhanced transverse mixing by means of the dimensionless transverse mixing coefficient.

3.2 Previous Investigations

The method for river modelling which involved the streamtube representation of the river was first proposed by Fischer (1968). The model optimized the longitudinal node spacing for the entire channel on the basis of the streamtube having the maximum velocity. As a result, advective transport calculations in the lower velocity regions of the river were still subject to numerical errors. Beltaos (1978) and Beltaos and Arora (1988) refined Fischer's method by extending the grid optimization procedure to each of the streamtubes comprising the overall channel flow.

The Beltaos model used the streamtube approach and separated each time step into two substeps for calculation of the advective and diffusive exchange between elements. In so doing, each element in the calculation grid was specifically sized to ensure the Courant number is equal to one ($C_r = 1$). The Courant number, C_r, is a function of the extent of mass exchange between elements. It is given by:

$$C_r = u\frac{\Delta t}{\Delta x} \qquad (3.1)$$

where Δt is the time step interval and Δx is the longitudinal grid interval. For $C_r \neq 1$, there is incomplete advective exchange of mass between elements, and this condition leads to the introduction of numerical errors. Beltaos used two one-dimensional and one two-dimensional unsteady substance source laboratory experiments reported by other investigators and a field slug injection test on the Athabasca River to verify the model.

Luk *et al.* (1990) further contributed to the development of the model and described laboratory verification studies of the modelling method. This work involved an explicit two-dimensional unsteady substance source model very similar to that developed by Beltoas. The model can be applied to steady flows in a sinuous, non-prismatic channel. Velocity and depths are represented on a curvilinear coordinate system (i.e., a coordinate system consisting of three mutually perpendicular coordinate surfaces). The Luk model can also account for differences in longitudinal distance due to stream curvature and has the added features of first-order reaction term and some source-sink terms. By dividing the streamtubes representing the river into varying length elements and thus maintaining a Courant number of one, numerical diffusion and dispersion in the computation of streamwise advection are avoided even though a simple explicit finite difference scheme is employed. The model was verified against analytical solutions of the one-dimensional advection equation and the two-dimensional advection-diffusion equation, and against two-dimensional unsteady tracer tests in a sinusoidally curved laboratory flume.

Verification studies of the method utilizing data from several field studies were recently completed by Putz and Smith (1998). Here the application of the modelling procedure to natural river systems is evaluated by comparing model output with the results of tracer studies conducted on the North Saskatchewan, Peace and Slave rivers. The Putz model was coded for use on microcomputers and incorporated the capability to handle "no flux" boundary conditions created by islands. Putz and Smith (1998) demonstrated that the advection optimized grid (AOG) method can be successfully applied to two-dimensional, transient mass input mixing problems in natural streams. The study results represent a far more extensive field verification of this modelling procedure than had been previously reported by other authors. A listing of previous studies, indicating the type of numerical method used and the type of verification test(s) conducted, is shown in Table 3.1. The methods have been placed in two groups, according to the strategy used to minimize errors associated with the advective transport term in equation (2.3).

Table 3.1 Two-dimensional, transient input, modelling studies (adapted from Putz and Smith, 1998).

Study	Method	Verification
Group 1: uniform grid		
Verboom (1973, 1975)	High order, explicit	2D, steady-state, laboratory test
Holly (1975),	High order, implicit/ explicit	2D, steady-state, laboratory test
Holly and Cunge (1975)		2D, steady-state, river test
		1D, unsteady-state, river test
Holly and Preissman (1977),	Explicit, nonlinear	2D, steady-state, river test
Holly and Nerat (1983)		
Harden and Shen (1979)	High order, implicit/ explicit	2D, steady-state, river test
Group 2: advection optimized grid		
Fischer (1968)	Explicit, partial optimization	1D, unsteady, river test
Beltaos (1978),	Explicit, full optimization	1D, unsteady, laboratory test
Beltaos and Arora (1988)		2D, unsteady, river test (one x-section)
Luk et al. (1990)	Explicit, full optimization, curvilinear coordinates	2D, unsteady, laboratory tests
Putz and Smith (1998)	Explicit, full optimization	2D, unsteady, river test

3.3 General Numerical Solution Considerations

Numerical solution procedures involve the following stages:

a) determine the governing partial differential equations and establish boundary conditions
b) discretization of the governing differential equations

c) assembly of a system of algebraic equations
d) equation solver
e) approximate solution for $c(x,z,t)$.

The simplest and most direct means of discretization is to replace the governing equation differentials with finite difference expressions and this can be done by approximation. In some discretization schemes the initial concentration distribution and the boundary conditions at the edges of the grid system must be known. Discretization schemes of this type are called 'explicit'. In other schemes the solution at each node is dependent on the adjacent nodes. Discretization schemes of this type are called 'implicit'.

The discretization stage consists of the following steps:

1) Establishment of a system of nodes called a grid, which represents temporal and spatial increments,
2) Approximation of the governing partial differential equations and any applicable boundary conditions at each node by replacing the differentials with approximate algebraic expressions, and,
3) Assemble of the complete system of algebraic equations representing each node in the grid system.

In the third stage of the numerical procedure, the system of algebraic equations is solved simultaneously using matrix elimination or iterative techniques if it is an implicit scheme. If it is explicit, like the Advection Optimized Grid (AOG), then each node value is solved directly. This produces an approximate solution to the governing mass balance equation at each grid node.

3.4 Description of Method

The governing mass balance equation (equation 2.3) is solved in fractional steps (Fischer, 1968) therefore, the two-dimensional equation is separated into advection and diffusion substeps as follows:

advective substep

$$\frac{\partial c}{\partial t} = -u \frac{\partial c}{\partial x} \qquad (3.2)$$

diffusion substep

$$\frac{\partial c}{\partial t} = \frac{\partial c}{\partial z}\left(Ez \frac{\partial c}{\partial z} \right) \qquad (3.3)$$

The two substeps are solved in succession using explicit finite difference representations of the above equations on a grid of points within the channel. The solution procedure utilizes a streamtube representation of the channel but calculations proceed using the cartesian z coordinate rather than the cumulative flow coordinate, q.

3.4.1 Representation of Streamtubes

The hydraulic and geometric parameters of the river reach to be modelled must be represented by a series of measured or synthesized cross sections. At each cross section the channel geometry and velocity distribution must be known for a particular flow, Q, as shown in Figure 3.1a. Integration of the h and u curves according to Equation (2.4) and division by Q produces a dimensionless cumulative flow curve as shown in Figure 3.1b. The channel is then divided into a series of adjacent streamtubes with boundaries at specified q/Q intervals. Sufficient stream tubes must be defined to obtain a good representation of the channel within the expected plume region. At each cross section the width of the streamtubes is determined by the subtraction of the z coordinate at the left and right q/Q boundaries of the tubes.

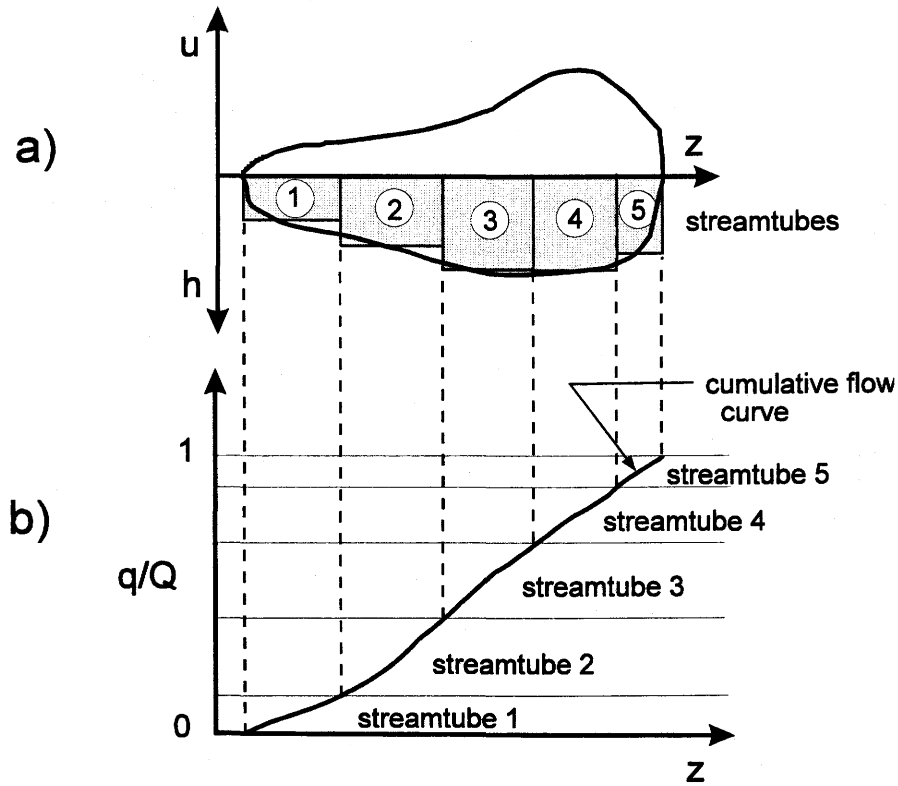

Figure 3.1 Streamtube representation of cross sections (from Putz, 1996).

3.4.2 Longitudinal Spacing of Streamtube Elements

The longitudinal spacing of the streamtube element boundaries is variable, and is selected in order to optimize the advection calculations. The balance between the magnitude of the advective transport and longitudinal grid interval is characterized by the Courant number, C_r. For $C_r \neq 1$, there is incomplete exchange of mass between elements during a particular time step. This results in numerical dispersion and dissipation errors.

For $C_r = 1$ there is complete exchange and numerical dispersion errors are eliminated. Therefore the basis of the AOG method is to select the upstream and downstream streamtube element boundaries to ensure $C_r = 1$ for each advective exchange between elements. Courant number, C_r can also be defined in terms of the volume and of the flow through each element as follows (Beltaos and Arora, 1988):

$$C_r = \frac{\Delta q_j \Delta t}{\Delta V_i} \qquad (3.4)$$

where Δq_j is the flow within streamtube j and ΔV_i is the volume of element i. The volume of each element is solely a function of the element length Δx because the element depth and width are linearly interpolated on the basis of longitudinal distance along the streamtube between defined sections. Therefore, the longitudinal length of each element must be carefully selected to ensure each element of a streamtube has the appropriate volume. Each element has a volume, which will ensure complete advective exchange with its upstream and downstream neighbors during a time step calculation. An example of streamtube elements and the grid structure are shown in Figures 3.2 and 3.3, respectively.

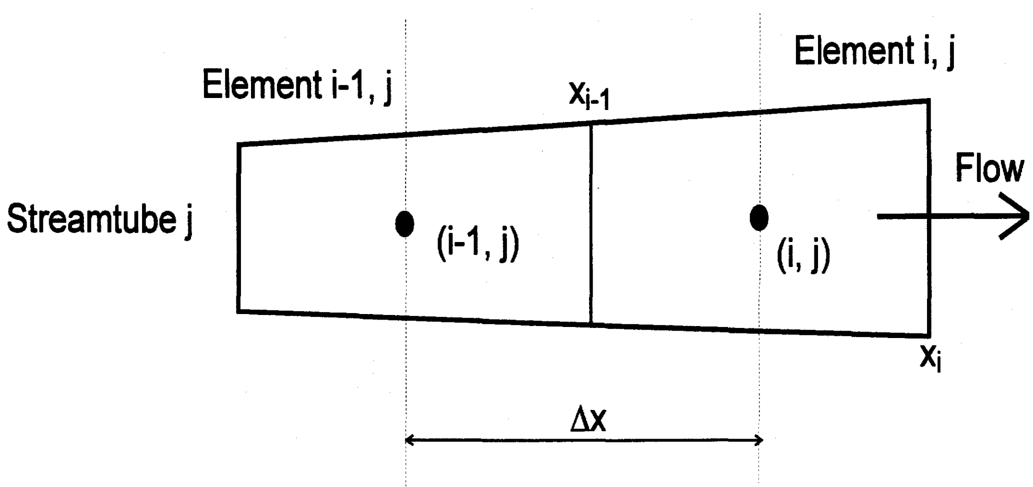

Figure 3.2 Successive streamtube elements (from Putz, 1996).

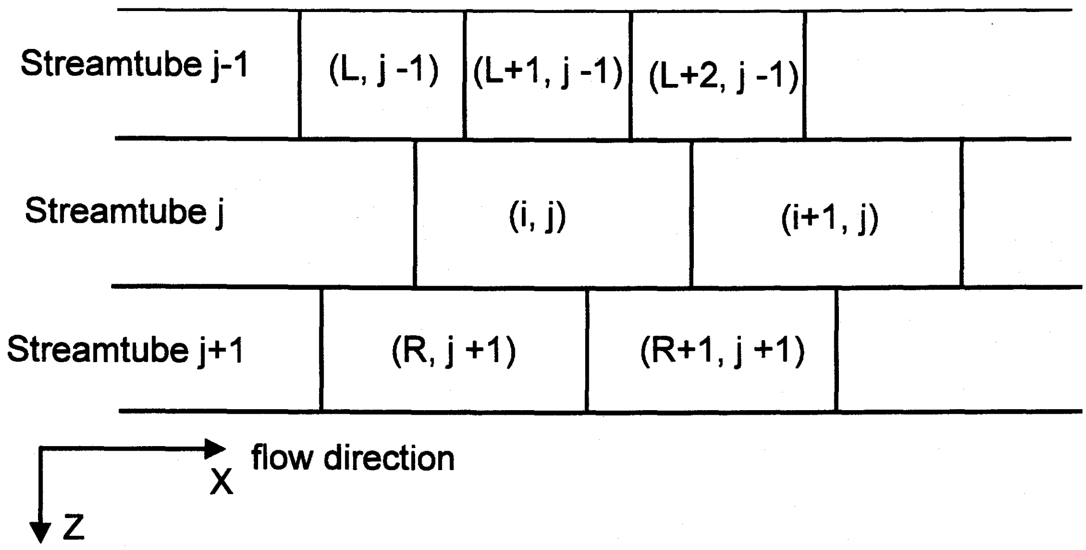

Figure 3.3 Discretization grid optimized for advection (from Putz, 1996).

3.5 Error and Stability Considerations

Error and stability considerations should be taken into consideration when handling numerical procedures. Discretization schemes are choosen so as to minimise factors influencing error generation. During discretization the governing equation differentials are replaced with finite difference expressions and this introduces certain types of errors. For example, the one dimensional equation:

$$\frac{\partial c}{\partial t} = E_z \frac{\partial^2 c}{\partial z^2} \qquad (3.5)$$

can be approximated as follows:

$$\frac{c_j^{n+1} - c_j^n}{\Delta t} = E_z \frac{(c_{j-1}^n - 2c_j^n + c_{j+1}^n)}{\Delta z^2} \qquad (3.6)$$

This type of discretization scheme is explicit since c_j^{n+1} is the only unknown in equation (3.6). The time and spatial steps and z and the grid notation scheme for Equation (3.6) are shown in Figure 3.4.

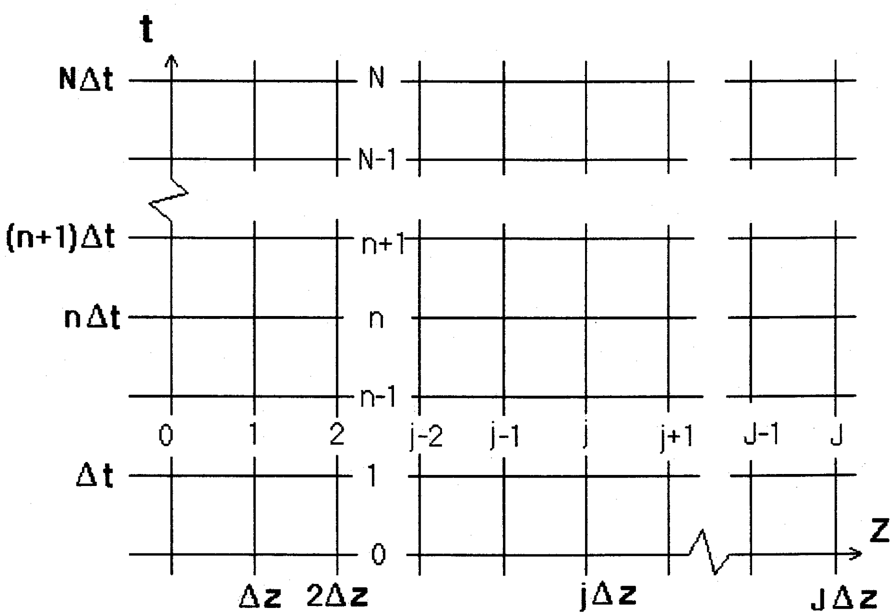

Figure 3.4 Discretization grid (from Putz, 1996)

Equation (3.5) can also be approximated as:

$$\frac{c_j^{\,n+1} - c_j^{\,n}}{\Delta t} = E_z \frac{(c_{j-1}^{n+1} - 2c_j^{n+1} + c_{j+1}^{n+1})}{\Delta z^2} \quad . \qquad (3.7)$$

This discretization scheme has three unknowns at the n + 1 time level and is implicit since the solution at each node is dependent upon the adjacent node. Since equation's (3.6) and (3.7) are only approximations of equation (3.5), certain errors associated with approximations are introduced. Discretization schemes should provide sufficient resolution, minimize the truncation error, and have properties of consistency and stability.

3.5.1 Truncation Error Analysis

One error introduced by approximating the governing differential equations is the truncation error. Approximation must have the property of consistency i.e. the approximation should be such that it satisfactorily represents the original equation. One method of assessing this error is to use a Taylor series expansion as follows:

$$c_j^n = c$$

$$c_j^{n+1} = c_j^n + \frac{\partial c}{\partial t}\Delta t + \frac{\partial^2 c}{\partial t^2}\frac{\Delta t^2}{2} + \frac{\partial^3 c}{\partial t^3}\frac{\Delta t^3}{6} + ...$$

$$c_{j-1}^n = c_j^n - \frac{\partial c}{\partial z}\Delta z + \frac{\partial^2 c}{\partial z^2}\frac{\Delta z^2}{2} - \frac{\partial^3 c}{\partial z^3}\frac{\Delta z^3}{6} + \frac{\partial^4 c}{\partial z^4}\frac{\Delta z^4}{12} - ....$$

$$c_{j+1}^n = c_j^n + \frac{\partial c}{\partial z}\Delta t + \frac{\partial^2 c}{\partial z^2}\frac{\Delta z^2}{2} + \frac{\partial^3 c}{\partial z^3}\frac{\Delta z^3}{6} + \frac{\partial^4 c}{\partial z^4}\frac{\Delta z^4}{12} + ... \quad . \quad . \quad . \quad .(3.8)$$

Substituting equation (3.8) equation (3.6) gives:

$$\frac{\partial c}{\partial t} = E_z\frac{\partial^2 c}{\partial z^2} - \left[\frac{\partial^2 c\Delta t}{\partial t^2 2} - E_z\frac{\partial^4 c\Delta z^2}{\partial z^4 6} + ...\right] \quad . \quad . \quad . \quad . \quad . \quad .(3.9)$$

from which it can be seen that the original differential equation is recovered and that the error of approximation is of the order Δt and Δz^2. The size of Δt and Δz can play a role in the size of the truncation error.

3.5.2 Stability Analysis

A discretization scheme must have stability. Stability means that small disturbances such as round off errors or spikes in the initial concentration distribution will not propagate and cause the solution to diverge. One method of stability analysis is the Fourier or Von Neumann approach. Grid size plays a major role in stability considerations. A general procedure for sizing the grid increments is to first select the transverse spatial increment to provide sufficient resolution, then choose Δt to minimize the truncation error and finally check for stability. If the chosen discretization scheme and increment sizes are consistent and stable, then convergence of the numerical solution is implied. The stability analysis for the forward time, central difference explicit representation of the one-dimensional diffusion equation (3.5) is given in Putz 1996. The results of the analysis indicate that $(E_z\Delta t/(\Delta z)^2$ must be less than 0.5 to ensure stability.

3.5.3 Numerical Diffusion, Dispersion and Dissipation

The discretization of advection-diffusion problems introduces an error term. This is often referred to as numerical or artificial diffusion. The artificial diffusion term will cause the solution distribution to either spread more or less rapidly depending on its sign. One way of reducing artificial diffusion is to keep Δx small or to use higher order discretization schemes involving a greater number of nodal points. Other errors associated with advection-diffusion problems are numerical dispersion and dissipation errors as shown in Figure 3.5. Numerical dispersion errors are lagging errors which cause oscillations and negative concentrations while numerical dissipation errors are characterized by attenuation in waveform peak.

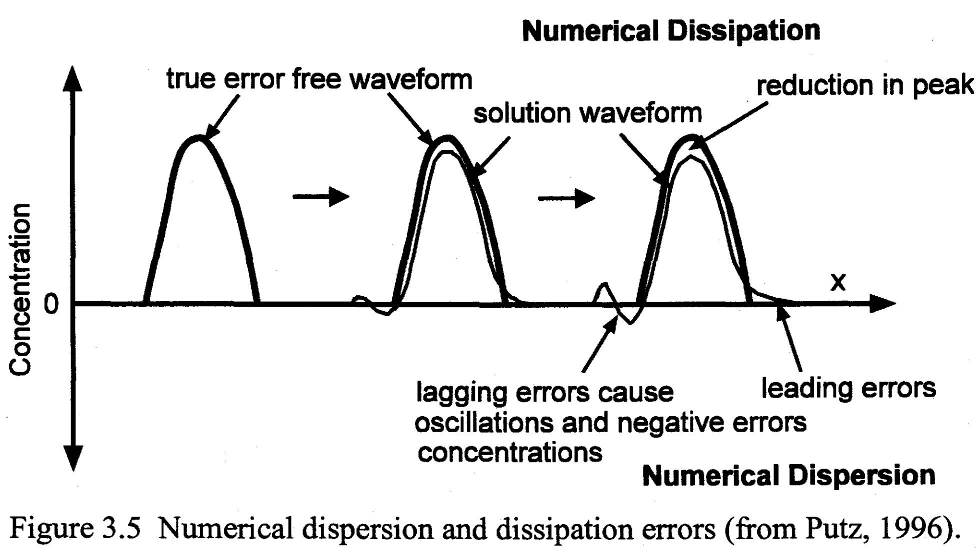

Figure 3.5 Numerical dispersion and dissipation errors (from Putz, 1996).

3.5.4 Secondary Error

Beltaos and Arora (1988) note that the diffusion substep can cause a numerical diffusion error in the longitudinal direction if $\Delta x/\Delta z$ ratio is too large (i.e. if the streamtube elements are too long and slender). When mass is exchanged between elements in the diffusion substep it is distributed uniformly over the element giving an average concentration. Depending on the alignment of the elements the mass can be artificially advanced in the longitudinal direction. The effect is shown schematically in Figure 3.6. They also found that this effect is minor in comparison to the longitudinal dispersion resulting from differential advection. However, in order to limit this effect, they recommend the element dimensions be limited to $\Delta x/\Delta z < 10$ for good results.

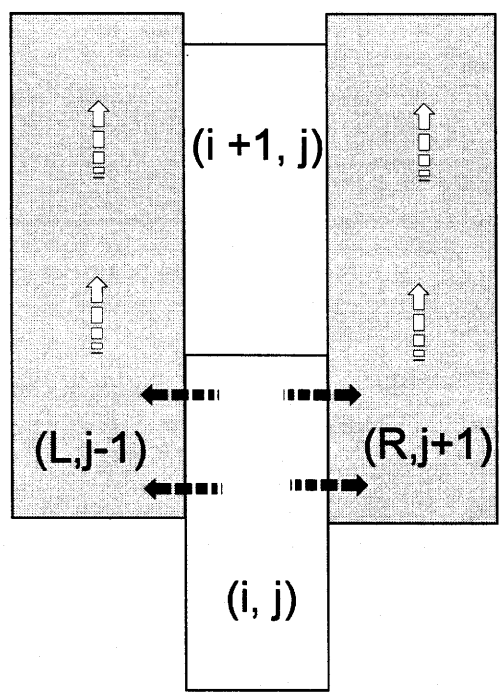

Diffusive flux from element (i,j) is artificially spread in the longitudinal direction due to concentration averaging in elements (L,j-1) and (R,j+1)

Figure 3.6 Secondary advective flux (from Putz, 1996).

3.5.5 Time Step and Transverse Grid Spacing Selection

The time step is the time (in seconds) for each step of the simulation. The number of time steps specifies how many time steps to run the simulation for. The maximum number of time steps represents the time required for an elemental volume of water to translate all the way down the reach in the streamtube with the slowest average velocity. The minimum number of time steps represents the time required for an element or volume of water to translate all the way down the reach in the stream tube with the fastest average velocity. In some cases one must run the simulation for longer than the maximum (for instance if you have an extended input). In others one can run for shorter than the maximum (for example with slug input) because the mass will advance a lot faster by advection and diffusion than by advection alone. A strategy for selecting the appropriate time step and transverse grid spacing for the modelling procedure can be summarized as follows:

1. Select the streamtube spacing across the channel in terms of q/Q and thus the Δz spacing in order to obtain a reasonable and above number of points (approximately 10 to 20) across the lateral extent of the effluent plume or slug release of interest. The spacing in terms of q/Q must be consistent at each section. The streamtube spacing should also take into consideration the location of mid channel bars and/ or islands if they are to be included in the simulation. This is done by choosing the tube boundaries to correspond to the location of mid channel bars and/ or islands within the reach. This would allow the "no flux" boundaries to be accounted for.

2. Select a proposed time step. Small time steps will mean that the simulation is more representative and that the process will take a longer time to complete while larger time steps will have the opposite effect. Then at each section using the mean velocity in each stream tube estimate Δx. Check that $\Delta x/\Delta z < 10$ for each streamtube at each section. If this condition is not met the time step should be shortened or the streamtube spacing revised.

3. Once the $\Delta x/\Delta z < 10$ criteria is satisfied check the transverse diffusion stability criteria i.e. $E_z\Delta t/\Delta z^2 < 0.5$ for each streamtube at each section. Again if this condition is not met the time step should be shortened or the streamtube spacing revised.

Beltaos and Arora (1988) demonstrated that the transverse diffusion stability requirement will generally be met if the $\Delta x/\Delta z < 10$ condition is satisfied. Therefore $\Delta x/\Delta z < 10$ is always checked first.

3.6 Implementation of the AOG Method

The implementation of the AOG method used in the present study was written by Putz (1996), based upon the descriptions given by Beltaos and Arora (1988). The model was coded for use on microcomputers and incorporated the capability to handle "no flux" boundary conditions created by islands. The overall AOG method is implemented using a series of four programs, which comprise of two preprocessing programs, one main program and one post processing program. The first preprocessing program divides the channel into streamtubes using input from measured or simulated data and the second generates the optimized grid for the river reach of interest with input from the output of the first preprocessing program. The main program then conducts the mixing calculations using input from the preprocessing programs. Finally, a post processing program is used to interpolate a series of concentrations vs. time readings for each streamtube at a specified x location using output from the main program. All the programs mentioned above have been developed for use with Microsoft Windows.

3.6.1 Preprocessing Program STRMTUBE

STRMTUBE is a utility program used in building input files for the next preprocessing program. The input includes depth (h), transverse distance (z), total flow (Q), time step

(Δt), streamtube boundaries (q/Q), downstream location (x), dimensionless mixing coefficient (β), and channel slope (S). The program takes a series of cross sections with defined z, q/Q, *and* h values at each section and interpolates between them at specified q/Q boundaries in order to determine streamtube widths and depths. STRMTUBE also checks whether the transverse grid spacing and the time step violate the stability criteria. The program results are output in two files. One file includes average streamtube depths, streamtube widths, streamtube right boundary depth, dimensionless mixing coefficient and channel slope. The other is a summary of the simulation results and the check for the stability criteria. The output of the first file is such that it is ready for input into the next preprocessing program. Input/ output summary of AOG programs and samples of data files are given in Appendix D and E respectively.

3.6.2 Preprocessing Program GRIDGEN

GRIDGEN is the preprocessing program used to generate the advection optimized grid through a series of cross sections. This is done using information from the previous preprocessing program. The required input file (PARM.DAT) contains information on streamtube boundaries, depths, widths at each section; the number of sections; section locations (x); and the dimensionless mixing coefficient (β) and slope at each streamtube within each section (this allows for variation in β and slope across the channel if required). The program generates a list of element parameters for use by the main mixing program.

The output is stored in two data files. SIMDIMS.OUT contains the grid information with an i, j designation of each element and a list of the element parameters. RCHCHAR.OUT contains reach information including the number of streamtubes, number of sections, maximum time step, minimum time step, time step, number of elements in each tube, volume of the elements in each tube and an index to the structure of the grid information file. A schematic representation of the function of the GRIDGEN preprocessing program is shown in Figure 3.7.

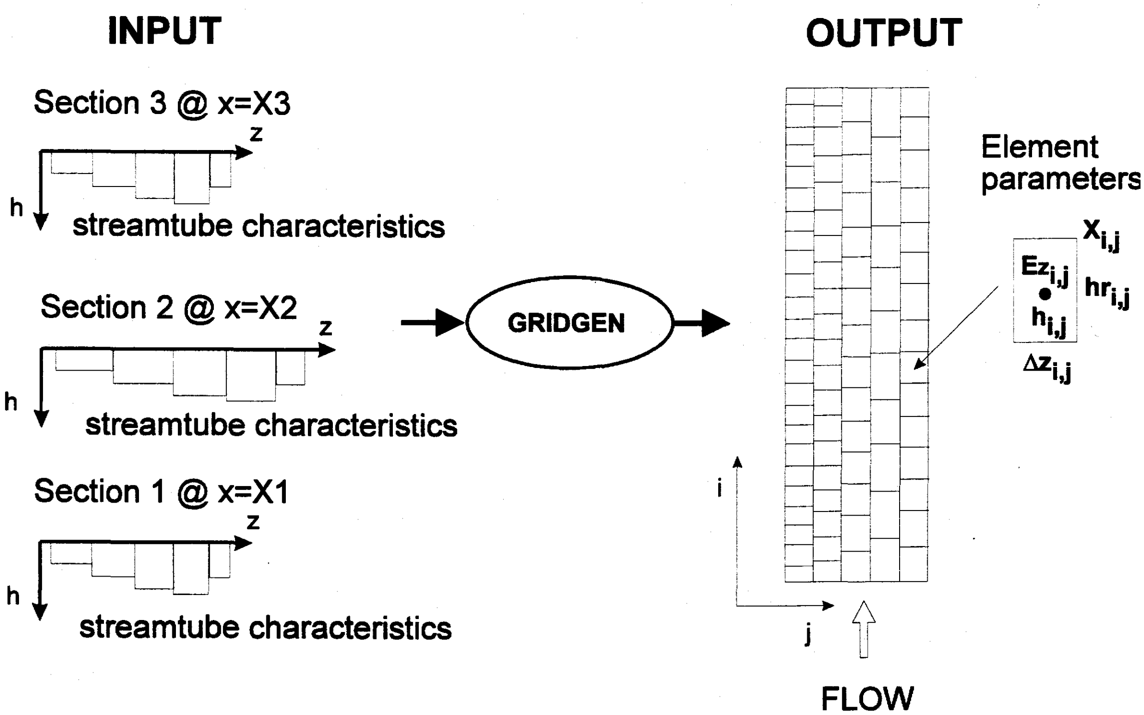

Figure 3.7 Representation of the GRIDGEN program (from Putz, 1996).

3.6.3 Main Program 2DMIX

2DMIX is the main mixing program. 2DMIX performs the entire fractional time step mixing calculations on the grid established by the preprocessing programs. It receives input data from three files SIMDIMS.OUT, RCHCHAR.OUT and CONC.TXT. The CONC.TXT file is a time series of input concentrations at specified elements in the grid.

The CONC.TXT file is the means by which mass is input into the model. It contains concentration values for the initial grid element in each streamtube for a series of time steps. This tells 2DMIX in which streamtubes the dye or tracer is injected and how the mass is released.

The RCHCHAR.OUT file cannot be used directly. It is first edited with a text editor in order to add two parameters, the number of time steps and the initial x location to the first line of the file that are needed for the simulation. The initial x location is required because the initial section may not be designated 0.0 metres in all cases. The tasks performed by 2DMIX consists of the following steps:

1. Read the information from RCHCHAR.OUT and SIMDIMS.OUT into memory.
2. Determine the shared area, mean E_z, Δz between streamtube centrelines, i, j coordinates of each element and store this information in an array in memory.
3. Determine the longitudinal extent to which mass has been advected down the channel.
4. The for each time step perform the following operations:

a) Read the upstream boundary concentratios.
b) Perform the advective exchange operation for each element to establish an intermediate concentration.
c) Perform a diffusion calculation for each element using the intermediate concentrations.
d) The results are then written to a data file TIMECONC.DAT that contains the concentrations at specified times (elapsed time) for each element.
e) Repeat steps a) to d) until the requested number of time steps have been completed.

The output to TIMECONC.DAT is arranged as one long vector or series of records, one record for each element in each time step (see Figure 3.8). This output file can be very large (dozens of MB's) depending on the size of the simulation being run.

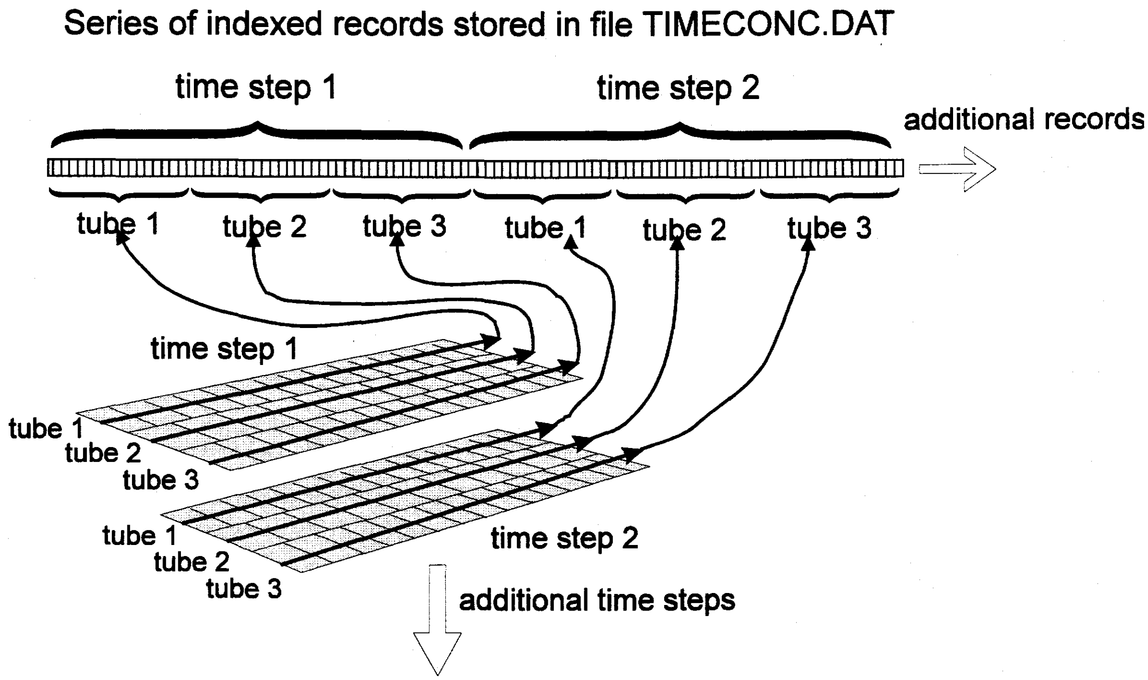

Figure 3.8 Organization of output from 2DMIX (from Putz 1996).

3.6.4 Post Processing Program XSLICE

XSLICE is a post processing program used to retrieve records from TIMECONC.DAT. It interpolate a series of concentrations versus time readings for each streamtube at a specified x location. The input files for XSLICE are SIMDIMS.OUT, RCHCHAR.OUT, and TIMECONC.DAT. Once again the RCHCHAR.OUT file cannot be used directly. It must be edited and like above an additional parameter, a time offset must be added to the first line of the file. The time offset is the time required to correct the elapsed time if the initial input does not occur at time zero. In most cases the time offset should be set to zero. One only has to worry about a non zero entry if the simulation has to be divided into several runs to keep the time of runs reasonable. The interpolated results from XSLICE are output to a text file called LSLICE.DAT, one line per time step in the format outlined in Appendix E. It can then be imported into a spreadsheet program in order to make plots and further analyze the data. A schematic representation of the function of the XSLICE program is shown in Figure 3.9.

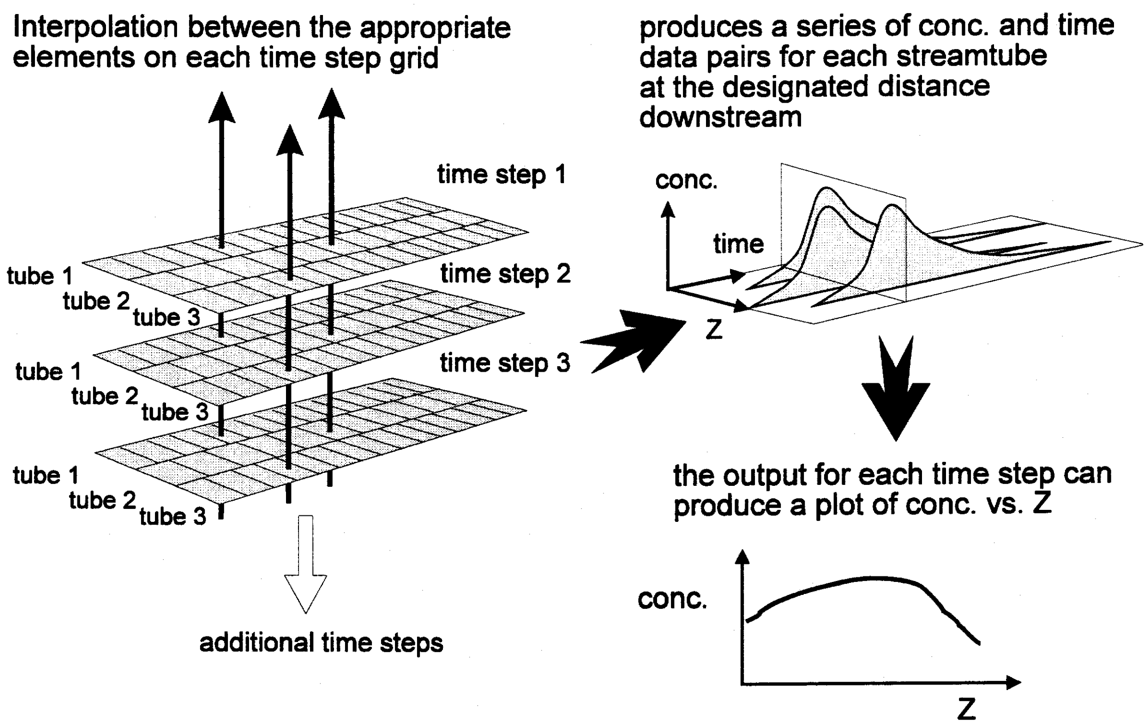

Figure 3.9 Post processing of 2DMIX output data (from Putz, 1996).

4. FIELD TRACER STUDIES

4.1 Background

Though there are different methods of predicting mixing rates, in many cases recourse to field tracer studies must be made, either because of uncertainty in estimation of mixing parameters or because of site-specific requirements demanding reliable mixing data. Also models cannot be used with confidence before calibration and verification to the particular river reach in question. The methodology of conducting tracer tests includes slug and continuous injection tests. For either the slug tests or continuous tests, hydrometric surveys are required, preferably at each sampling site.

4.1.1 Continuous Input Tests

In continuous injection tests, a tracer is continuously injected into a river at a constant rate so that a steady-state distribution of concentration is established some time after commencement of injection. When injecting a tracer to measure transverse mixing rates it is advantageous for the tracer source to be steady.

The three most commonly used devices for continuous injection of tracer are the marriotte vessel, the floating siphon and the peristaltic pump. A marriotte vessel is a sealed container with a vent tube exposed to the atmosphere. The elevation difference between the bottom of the vent tube and the outlet determines the head as long as the liquid in the vessel is above the bottom of the vent tube. The marriotte vessel is often troublesome to fill and seal. The floating siphon is a low cost device that works well, although it can be difficult to prime. A good quality peristaltic pump that is well maintained is required to achieve a reliable, steady rate of injection. A peristaltic pump was used for all continuous input tests described in this thesis.

4.1.2 Slug Input Tests

In the slug input test, a known quantity of fluorescent dye is dropped into the river. A review of the literature reveals that existing methods of analysis are mostly applicable to steady-state input experiments. Extensions to unsteady situations are theoretically possible but they introduce complexities in both the calculation and the design of the field sampling program. Despite these, in some instances it is preferable to perform a slug test. Some of the advantages include:

1. Economy in material: The amount of tracer needed to perform a slug test is much less than that required for a continuous test.
2. Feasibility: Injection of a slug is rather simple whereas constant injection requires special equipment and may be problematic in rivers with poor accessibility.
3. Scientific value: A slug test provides information not only with respect to lateral mixing but also regarding longitudinal and time spread characteristics. This type of information cannot be obtained from a continuous test, since time variations vanish.
4. Environmental aspects: Aquatic life can be adversely affected, not only by high concentrations, but also by long times of exposure to moderate concentrations of the tracer. The time during which a certain concentration level is equaled or exceeded can be minimized with a slug test.

4.1.3 Choice of Dye

Many tracers have been used in field experiments. The most commonly used tracers are fluorescent dyes, which are characterized as blue, green, or orange. Blue dyes, for example Photine *CU*, are barely visible at very high concentrations. They are generally unsuitable for qualitative work due to their high photochemical decay (decomposition owing to oxidation and other chemical changes when compounds absorb light energy) rates, low detectability, and extremely variable background levels in natural rivers. Green dyes such as Lissamine *FF*, are highly visible but exhibit fairly high background concentrations. The ideal tracer would be nontoxic, usable in small quantities, cost-effective, invisible, easy to measure at very low concentrations, specific (no interference from other substances), and stable during the course of the study. Ideally the presence of a tracer would not be apparent to the casual observer.

An orange dye, Rhodamine WT was chosen because it meets most of these requirements and is probably the most commonly used tracer for field studies. Rhodamine WT does not have either the toxicity level or propensity to adsorption (tracer sticking to or coating fine sediment in suspension) that other orange dyes such as Rhodamine B exhibit. The detectable level of Rhodamine WT is as low as 0.01 parts per billion (ppb) with a fluorometer, which requires no special techniques or sample preparation. Its threshold of visibility is around 10 ppb, meaning that a dilution of 500:1 can be measured without being seen (Elhadi *et. al.* 1984). It is also a biodegradable material, tasteless, odorless and inoffensive to the environment and the public. This dye may cause staining if contacted, however the concentrations will be well below visible detection in all test locations beyond a couple 100 meters of the addition point.

4.1.4 Sampling

In a river, the tracer plume is usually sampled from a boat. During the early stages of a test, dye is visible to the naked eye, which facilitates sample collection. As the dye spreads out it becomes more difficult to assess the location of the plume by eye and a field fluorometer mounted in the boat can help enhance sampling. When sampling the tracer plume, accurate position fixing is essential. In the past, floats were usually located across the channel for horizontal positioning, but the use of GPS eliminates this need. Time to sample or sampling schedule is determined by time of travel estimates using basic streamflow characteristics and other river engineering parameters.

A number of transects at strategic distances downstream from the source are established in advance on the basis of preliminary calculations to ensure that:

(1) we add enough dye so it is detectable;
(2) there is adequate time to measure the concentration distribution at each transect; and
(3) there is a large enough change in concentration between sites to permit determination of the mixing coefficient.

For slug tests, the sampling period is scheduled to begin before the plume arrives and is continued until the extent of the plume has passed. A safety factor is introduced both before and after the estimated duration of the slug tests. For continuous tests, the sampling period begins when the plume concentration has attained steady state. Samples are then collected and stored in plastic bottles. Samples are usually collected at one depth. Occasionally samples are collected at different depths to verify that concentrations are consistent in the water column. Surface water samples are taken by sharply submerging the sample bottle below the water surface. Where subsurface sampling is required, sample bottles are secured in a pole-holder arranged to obtain the samples. Samples are usually kept out of light and sediments allowed to settle before analysis.

4.1.5 Recovery of Tracer

Various tracers are lost in transit due to adhesion on sediments and photochemical decay. Scott et al. (1969) found fluorescent dyes to be absorbed on fine sediments such as clay. Rhodamine WT dye has been shown both in the field and in laboratory to decay photochemically about 2-4% per day (Tai and Rathburn 1988). Kilpatrick (1993) noted decay rates tended to be higher in rivers, about 5% per day. To compare data and to have it simulate a conservative substance, it is necessary to remove the effects of tracer loss. The mass of tracer recovered can be expressed as

$$M_r = \frac{M}{M_{in}} \qquad .(4.1)$$

Where M_r is the mass recovery ratio, M is the mass of tracer to pass a cross section, and M_{in} is the mass of tracer injected.

If M_r is nearly equal to one throughout a study reach, it can be concluded that no significant losses occur. If on the other hand, M_r changes with x, it can be concluded that certain substance specific processes occur that cannot be ignored. Even though Rhodamine WT was found to be a conservative tracer, incomplete recovery of the tracer mass at each of the measured sections may have resulted due to:

a) Adsorption onto suspended solids,
b) Adsorption onto the stream boundaries,
c) Adsorption onto surfaces of the sampling container,
d) Photochemical decay, and
e) Chemical oxidation.

4.1.6 Concentration Measurements

The fluorometer measures the concentration of various analytes in the samples of interest via fluorescence. A fluorescent molecule has the ability to absorb light at one wavelength and almost instantly emit light at a new and longer wavelength. Light (exciting light) from a light source (the lamp) is passed through a color filter (excitation filter) that transmits light of the chosen wavelength range (color). The light passes through the sample, which emits light proportional to the concentration of the fluorescent material present and proportional to the intensity of the exciting light. Each fluorescent material has a "fingerprint", a wavelength of light (color) that causes it to fluoresce, and another wavelength at which it emits light. Rhodamine WT for example absorbs green light and emits red light.

4.1.7 Planning of Tracer Studies

Field testing to determine mixing coefficients requires detailed hydrometric surveys and generally at least two field crews. Manpower costs alone are extremely high per test, depending on the length of each and the flow rate during the test. Therefore, given the relatively high cost of field testing, it is important that such activities be properly planned and executed in order to maximize their effectiveness. Good planning is essential to get the most out of a field work program.

The design and successful execution of a tracer study requires advance planning. Planning requires some a priori estimate of stream flow and velocity. Also the volume of the dye required, the approximate time to peak concentration, and the spread and duration of the dye cloud are estimated before carrying out the study. Past surveys help provide background information necessary for selecting injection and sampling sites and for optimizing sampling procedures. Preparation of a comprehensive plan generally expedites the field work.

When investigating transverse mixing in rivers, it is sensible to start by making preliminary calculations aimed at getting familiar with the task. Such calculations are usually made with sparse data on channel bathymetry, slope, velocity and dispersion coefficients estimated from previously published works. As much information as possible regarding the survey area should be gathered. Valuable materials include location maps (outlining part of the watershed boundary and depicting the maximum river reach in which the study is to be conducted), topographic maps (1:250000 & 1:50000, scale showing the river reach, dye injection and sampling points), prior hydrographic surveys, aerial photographs (1: 30,000), streamflow records etc. Bathymetric requirements should be thoroughly examined and understood. The area being surveyed has to be clearly defined since it will be far too expensive and time-consuming to carry out surveys on what is not required.

Having decided where and when to collect samples, a survey schedule is drawn up specifying what each party should do. Each party is given a clear set of instructions detailing the exact location of each sampling site and the sampling procedure to be followed. Because people will have to work long hours in bad weather and under trying physical conditions it is worth spending time in planning to optimize their efforts. Good radio communication between field parties is also desirable. Careful book keeping is essential to label each gauging, echo sounding, dye sample and fluorometer trace with site, date, time, location etc.

Before starting any tests one has to apply for permission to conduct the dye tracer study on the river from an environmental protection agency or the proper regulatory authority. After the application is approved, a public notice of the issuance is put in the papers and in conspicuous and readily accessible locations around the proposed study area at least a month in advance of the proposed study so that there will be input from the public if they have any objections. Licensed water-withdrawal users are also notified of the impending study.

4.2 Athabasca River Field Tests

4.2.1 Introduction

The Advection Optimized Grid modelling method and other numerical procedures has been extensively studied in laboratory channels. However, only very limited assessment of the AOG model have been conducted with large-scale, two-dimensional, steady and unsteady input field tests. Additional field verification tests of this procedure were conducted in August 1997 on the Athabasca River. The Sustainable Forest Management Network of Centres of Excellence and Alberta Pacific Forest Industries Inc. supported this work, and so funding for the study dictated the location of the field tests.

In preparing for the tests, it was discovered two earlier tests had been conducted for Alberta Pacific Forest Industries Inc. but were never analyzed or modelled to determine the dimensionless mixing coefficient, β (Beak Consultants Ltd. 1995). This finding provided an opportunity to assess changes in the dimensionless mixing coefficient over a range of flow conditions. Determinations of β were based upon analysis of four tracer tests conducted on the river (three continuous input tests and one slug test). The tracer tests were conducted on different dates and covered a fairly wide range of flows and conditions (October 1994, 270 m^3/s; February 1995, 84 m^3/s, and August 1997, 960 m^3/s and 876 m^3/s). The February test was conducted under ice-covered conditions.

The transverse mixing in the river was determined for each tracer test using a model fit of predicted tracer concentrations compared to the concentrations of tracer samples collected in the field. By expressing the transverse mixing coefficient in a non-dimensional form the amount of the mixing which occurs at other flow conditions can be estimated by multiplying by an adjusted length and velocity scale. However, little field data is available to verify the reliability of this procedure.

Preliminary preparations and planning for the August 1997 survey were done on the basis of data from a study carried out by Beaks Consultants Limited for Alberta Pacific Forest Industries Inc. in October 1994 and February 1995. Flows for the Athabasca River spanning 77 years from 1913 through 1990 from Environment Canada Historical Streamflow Summary were also used. The background for these studies in 1994 and 1995 was in turn based on a 1989 study carried out by Sentar Consultants Limited for Alberta Pacific Forest Industries Inc.

4.2.2 Study Reach Description

The field tests were conducted on the Athabasca River near Boyle, Alberta. The study reach extends for approximately 32 km downstream of the effluent outfall structure of the Alberta Pacific Forest Industries Inc. pulp mill. The study reach is located in the Pinesands provincial natural area and between improvement district 17 & 18 of Athabasca county. The reach of the Athabasca River studied is intersected by the La Biche River and Calling River at approximately 17 km and 33 km, respectively, downstream from the pulp mill. The study reach was characterized by several cross sections downstream of the pulp mill. A plan view of the reach and the location of the transects is shown in Figure 4.1.

Using Environment Canada records for the gauging station at Athabasca, the discharge during the tracer tests was estimated. River flow data for 1913 to 1990 indicates that the open water high flow condition in the Athabasca River is typically observed in June. The average high flow rate (i.e., the maximum value of the daily average for each month) at the study site for this period of record is 1030 m^3/s. The one-in-ten-year low flow of 30 days duration (30Q10) is 58.6 m^3/s (Beaks Consultants Ltd., 1995). Average monthly flows for February, October and August based on Environment Canada Historical Streamflow Summary 1984 to 1994 are 80 m^3/s, 311 m^3/s and 698 m^3/s respectively. A summary of these characteristics is shown in Table 4.1. The river reach characteristics at different flows for the different tests are given in Appendix A.

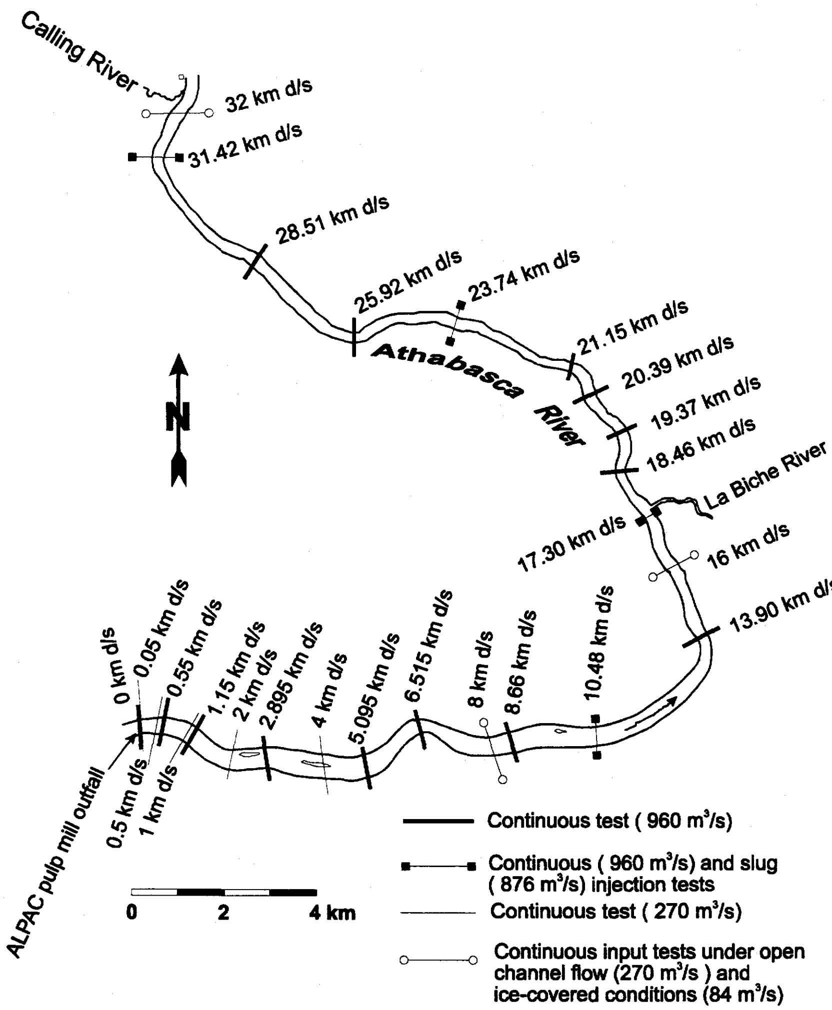

Figure 4.1 Athabasca River study reach downstream of the mill outfall.

The average slope of the water surface through the study reach was determined to be 0.000166 m/m using elevation measurements taken using GPS equipment. This is milder than the slope information presented by Kellerhals et al. (1972) along the same reach. Approximately 10 to 15 individual measurements of the water surface were recorded at each transect as the depth soundings were conducted. The average of these measurements at each transect was plotted versus distance and then the line of best fit through these points was used to approximate the slope of the water surface through the reach. This plot is shown in Figure 4.2.

Table 4.1 Summary of river reach characteristics.

Parameter	February, 1995	October, 1994	August, 1997
Flow (m^3/s)	84[a]	270[b]	960[b]
No. of sections surveyed	4	8	17
Avg. width (m)	250	283	302
range	187 to 326	203 to 350	209 to 467
Avg. depth (m)	1.1	1.5	2.9
range	1.0 to 1.3	1.2 to 2.0	2.1 to 3.4
Avg. velocity (m/s)	0.3	0.7	1.2
range	0.3 to 0.4	0.6 to 1.0	1.0 to 1.4

[a] ice-covered [b] open water

Note: the reach characteristics for the two August 1997 tests are very similar, therefore only the 960 m^3/s data are shown.

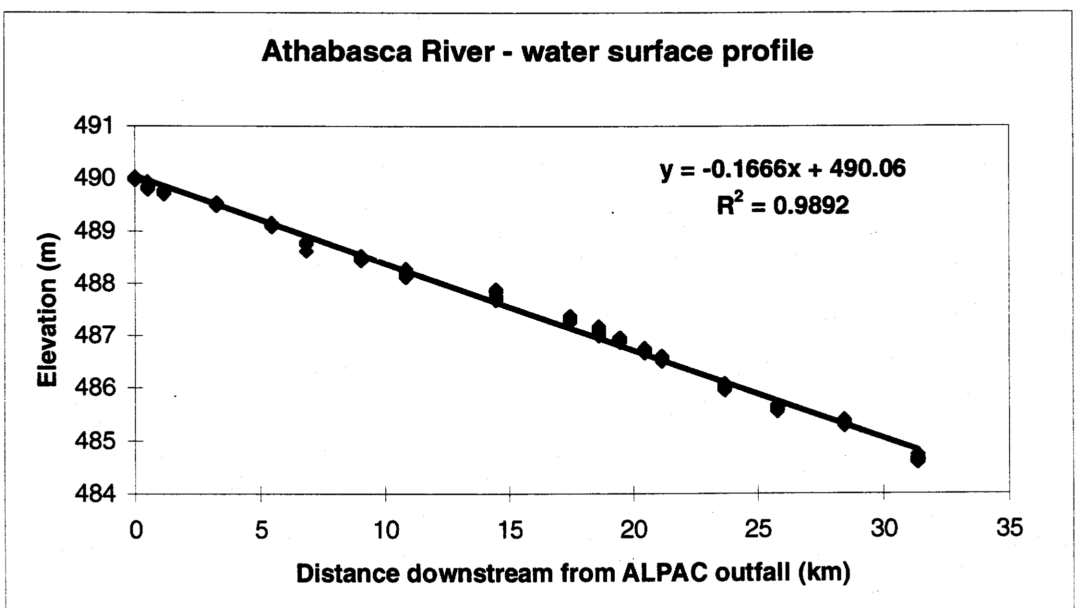

Figure 4.2 Athabasca River water surface profile.

4.2.3 Hydrographic Surveys

For both the slug tests and the continuous injection tests, hydrometric surveys are required at each sampling site, and preferably many additional cross sections. Accurate measurements of river width, depth and slope are needed to make reliable mixing calculations. One of the major difficulties with two-dimensional numerical flow models is obtaining an adequate representation of river bathymetry. Section markers are established at strategic points along the bank. Cross-sections need to be surveyed wherever there are major changes in channel shape.

Transects were marked at several locations downstream of the injection point as shown in Table 4.2. Positions and distances between sections was determined using Global Positioning System (GPS) equipment. Depths across each transect were measured using echo sounding equipment. Measurements of water surface were recorded at each transect as the depth soundings were conducted. Velocity measurements were done with a current meter and positions of the boat during velocity measurements were simultaneously determined by GPS measurements. Details of the survey method will be discussed in the following sections.

4.2.3.1 Position Measurements

Positions of sounding boats during the depth survey, positions of the seventeen transects and their location in relation to the mill outfall structure, sampling positions, velocity measurement positions and the exact positions during all other operations were measured using Global Positioning System (GPS) equipment. GPS is used to determine a position on the earth surface relative to bodies in space. It comprises of a constellation of satellites orbiting the Earth, broadcasting data that allows users on or near the Earth to determine their spatial positions. Position computations with GPS are done by ranging to the satellites. The satellite positions are known i.e., they are computed from the orbit parameters in the broadcast ephemeris. By intersecting the ranges from multiple satellites, the position of the receiver antenna can be calculated.

Table 4.2 Cross section distances downstream of the mill discharge structure (km).

February, 1995	October, 1994	August, 1997
0.05	0.05	0.55
8.00	0.50	1.15
16.00	1.00	2.90
32.00	2.00	5.10
	4.00	6.52
	8.00	8.66
	16.00	10.48
	32.00	13.90
		17.30
		18.46
		19.37
		20.39
		21.15
		23.74
		25.92
		28.51
		31.42

Any GPS survey project is simply a collection of three-dimensional (spatial) vectors. At least four satellites are required to compute a three-dimensional position. GPS is a three-dimensional system and requires a height of instrument (HI) to compute the position at the mark. Without reliable antenna height measurements, the system will not accurately compute final position and elevation at the station. Therefore in addition to providing latitude-longitude (or other "horizontal" information), a GPS receiver may also provide altitude information. GPS station sites are set up where they are free of significant obstructions and multipath conditions. It does not require station intervisibility, but does require line of sight to satellites. The GPS data were processed on a daily basis so as to spot possible areas of poor results or errors as the project progressed.

Hazards to successful data collection using GPS occurs when satellite signals are interrupted and this can be caused by a multitude of sources. Basically anything that passes between the antenna and satellite can interrupt the signal. Also data cannot be successfully collected inside buildings, underground, in severe precipitation, under heavy tree canopy, or anywhere else not having a direct view of a substantial portion of the sky. Since the GPS receiver system utilizes battery power it is subject to energy related problems since receivers have very high power consumption. Therefore receiver operators are provided with back up battery reserves. The selection of battery capacity is dependent on the power requirements of the unique receiver, which can vary from manufacturer to manufacturer. It is recommended that battery be charged to a full 100% level before data collection.

Base stations are first set up, then antennas are attached to the boats. The receiver/ datalogger is then turned on and set up for the rovers (roving receiver) who carry the equipment around. The height of the antenna from the water surface is measured and input into the receiver. One then waits for the receiver to lock onto enough satellites, to start recording data. Then at each position of interest one logs a data point into the receiver to register the required position and time.

4.2.3.2 Sampling

For the continuous test (1997), samples were collected at each transect from 10 points across the channel at two depths (at the surface & 1.4 m below the water surface). For the slug test (1997), each transect was traversed about 10 times and samples collected from the surface at 10 different points. So an average of 100 samples were collected at the surface for each transect. Samples collected in the field were temporarily stored at the Alberta Pacific Forest Industries Inc. storage facility. Samples were then transferred to the University of Alberta where they were held until being analyzed.

In the October 1994 test, each transect was traversed at least three times to ensure that steady conditions had been achieved in the plume and that a representative profile was obtained. During the ice covered condition test i.e. February 1995, the samples were withdrawn from holes drilled through the ice which had been used to measure the river depth and ice thickness (Beak Consultants Ltd., 1995).

4.2.3.3 Discharge Measurements

Accurate measurements of river discharge are essential for reliable mixing and mass balance calculations. River gaugings were done by one of the survey parties and also discharge measurements were obtained from Alberta Environment at a gauging station 40 km upstream of the study reach.

4.2.3.4 Velocity Measurements

Reliable estimates of velocity are very important for determining the time of travel of tracer. Velocity measurements were made using a Price current meter. The current meter is usually lowered from the boat, a heavy weight is attached directly below the meter and the meter is fixed so that the horizontal component of the current is measured. Each section of the river was divided into a number of vertical sections (in our case 10) to permit definition of the transverse variation of velocity in the river.

At each section the total depth of the water was measured by first zeroing the cups of the price meter to correspond with the water surface, and then lowering the sounding weight with the meter cable till it reaches the river bed. When the total depth was over 2m, measurements were taken at two depths (0.2D & 0.8D). In the shallow water near the shore and when the total depth was less than 2m a single velocity determination at 0.6 depth was used. The angle between the wet line and the true vertical was not large so it was not necessary to apply a correction to the measured depths. For the October 1994 and February 1995 tests, velocity was measured with a Valeport magnetic velocity meter (Beak Consultants Ltd. 1995).

4.2.3.5 Distance Measurements

Distances across transects to velocity measurement locations were measured with the aid of electronic distance measurement (EDM) equipment. The instrument is set up at a fixed point on the river bank. It then transmits a beam of the light that serves as a carrier for the waves used for measurement. The beam is received at the other end of the distance by a reflector that is held up by someone in the boat. Then the beam is returned to the transmitter, where the incoming light is converted to an electrical signal. An on-board computer deduces distance from the data by a phase comparison between transmitted and received signals. This method of distance measurement was used for the most part in conjunction with the GPS and occasionally when the GPS was unavailable. For the October 1994 and February 1995 field tests, river width at each transect was measured using a surveyors tape (Beak Consultants Ltd. 1995).

4.2.3.6 Depth Measurements

Depths by echo soundings were measured with a fathometer. This operates on the basic principle that sound produced near the water surface will travel to the bottom and be reflected back to the surface as an echo. Electromechanical means were used to produce the sound, receive and amplify the echo, and convert elapsed time into units of depths. The echo sounder (fathometer) then produced an analog graph from which the depths were computed. The position of the sounding boat during depth surveys was simultaneously determined by GPS measurements.

4.2.4 Tracer Test Methodologies

The type of information that is required from a tracer test can determine the technique to be used. Slug tests provide more information on mixing processes since steady state tests suppress temporal variations (Beltaos, 1980). The results obtainable from field-testing will vary depending on the level of effort expended on the operation. For example, it might be desired to determine if an effluent discharged at one bank would reach the opposite bank within a given distance downstream under certain flow conditions. Conducting a field test for this example would be relatively simple and inexpensive. On the other hand, field testing to determine the mixing coefficients requires detailed hydrometric surveys and at least two field crews during sampling.

4.2.4.1 960 m^3/s, Open Water, August 1997, Continuous Tracer Input

Effluent concentrations in the Athabasca River, downstream of the Alberta Pacific Forest Industries Inc. mill, were measured using a conservative tracer. The tracer, a 20% solution of Rhodamine WT fluorescent dye (specific gravity = 1.19), was continuously injected into the mill at a constant rate of 74 ml/min from 6:20 a.m. -1:30 p.m. on 21st August 1997. This sufficiently long period of continuous injection was maintained in order to establish steady-state conditions at each transect. The dye injection location selected was at the last point of access to the effluent on the mill site. This site was sufficiently upstream of the effluent diffuser that the dye would be completely mixed with the effluent and at the same temperature as the effluent before it reached the diffuser.

Treated effluent is discharged to the Athabasca River via an effluent diffuser, which is oriented perpendicular to the direction of flow, at a depth of less than 5m. The diffuser is 52m long, with 25 ports, 20 of which are currently used. The ends of the diffuser are approximately 192.91 m and 236.91 m from the left bank. The diffuser is designed to mix with approximately 50% of the river flow. The effluent plume measurements were carried out on 21 August 1997.

The dye plume was sampled at 11 transects located at 0.55km, 1.15km, 2.895km, 6.515km, 10.48km, 13.9km, 17.3km, 20.39km, 23.74km, 28.51km, 31.42km downstream of the effluent diffuser. Samples were collected at sampling times chosen within a steady-state 'window'. For the continuous test, the sampling window is the time after steady state has been achieved. The time to establishment of the sampling 'window' included a delay time i.e. the time of travel of the dye from the point of injection to the diffuser through the effluent pipeline. A sample calculation of the delay time is shown below:

Calculation of delay time:
Pipe diameter = 1050 mm,
Discharge = 74,013.8 m^3/d (0.86 m^3/s)
$A = \pi D^2/4 = 0.8659\ m^2$
$Q = UA \therefore U = Q/A = 0.86/0.8659 = 0.99$ m/s
$t = Distance/U = 5500m/0.99 = 5555$ sec $\Rightarrow$ 5555/3600 = 1.5 hrs = 90 minutes
If *distance* = 6000m then t = 1.68 hrs (100 minutes)
Therefore delay time ≈ 95 minutes
Sampling windows at various locations downstream are shown in Table 4.3.

4.2.4.2 270 m^3/s, Open Water, October 1994, Continuous Tracer Input

In the October 1994 field work, Rhodamine WT dye, was continuously injected into the mill effluent at a constant rate of 15 ml/min for 24 hours starting at 20:00 hours on 15 October 1994 (Beak Consultants Ltd. 1995). Effluent plume measurements were carried out on 16 and 17 October 1994. Transects were done at 50 m, 0.5 km, 1 km, 2 km, 4 km, 8 km, 16 km, and 32 km downstream of the effluent diffuser. At each transect, the dye concentration was determined using a flow-through field fluorometer (Turner Model 10) mounted on a survey vessel. To measure the dye concentrations in the plume, samples were pumped through the fluorometer using a positive displacement pump with an intake 0.5 m below the water surface.

Table 4.3 Sampling windows of various locations downstream – continuous input test.

Transects (km)	Sampling Windows
0.55	8:00 - 13.45
1.15	11:33 - 16:24
2.895	8:45 - 14:15
6.515	9:50 - 15:03
10.48	11:33 - 16:24
17.3	13:21 - 17:54
23.74	15:27 - 19:48
31.42	18:09 - 21:18

4.2.4.3 84 m^3/s, Ice Cover, February 1995, Continuous Tracer Input

For the February 1995 field work, a solution of Rhodamine WT dye was continuously input into the mill effluent at a constant rate of 17 ml/min for 48 hours starting at 17:00 hours on 26 February 1995. Effluent plume measurements were carried out on 27 and 28 February and 01 March 1995. Transects were marked at 50 m, 8 km, 16 km, and 32 km. More sections were not traversed due to concerns of safety of the field team. The dye concentration of samples taken through holes in the ice were determined using a field fluorometer with a cuvette system of measurement.

4.2.4.4 876 m^3/s, Open Water, August 1997, Slug Input of Tracer

Seventeen liters of 20% solution of Rhodamine WT dye, was instantaneously dumped into the river. This corresponds to a tracer mass of 4.05kg (i.e. 17 * 1.19 * 0.2). The injection location was about 5m west of a buoy, which is located approximately at the center of the diffuser. The dump time was 9:07 a.m. on 22 August 1997. The passage of the dye plume was sampled at 4 transects located 10.48km, 17.30km, 23.74km, and 31.42km downstream.

Samples were collected within the sampling window that was calculated using time of travel estimates. The sampling window for slug test is the period from the time the leading edge of the tracer plume arrives at a particular location (time of arrival, t_a) to the time it leaves (time of departure, t_d) a particular location. These times increase with distance downstream, as does the difference (t_d - t_a), which represents the residence time of the tracer at a given point. A rule of thumb for estimating the times of arrival and departure are:

$$t_a = 0.8 * t_p \qquad (4.2)$$

$$t_d = 1.5 * t_p \qquad (4.3)$$

Where, t_p is the travel time of the peak concentration.

The factors 0.8 and 1.5 are defined as the time when the concentration drops to the arbitrarily selected value of 2% of the peak concentration (Beltaos and Charnetski, 1980). No delay time was used in estimating the sampling windows since the dye was dumped directly into the river. Sampling windows for the slug test are shown in the Table 4.4 below:

Table 4.4 Sampling windows of various locations downstream – slug input test.

Transects (km)	**Sampling Window**	
	(est. sampling duration)	**(conservative est. used)**
10.48	11:49 - 12:58	11:30 - 1:00
17.30	13:20 - 14:46	13:00 - 15:00
23.74	14:48 - 16:52	14:30 - 17:00
31.42	16:43 - 19:34	16:00 - 19:30

5. ANALYSIS AND RESULTS

5.1 Hydrographic Data

Hydrographic data are necessary for modelling of mixing because they provide the principle characteristics of the river. Hydrographic data provide the cross section information required to adequately define the transverse and longitudinal variations in local depth and velocity. They also provide background information necessary for designing injection and sampling procedures. The hydraulic and geometric properties of the river to be modelled must be represented by a series of surveyed or synthesized cross sections. The series of cross sections is used to formulate a streamtube representation of the river.

The first preprocessing program STRMTUBE requires a compilation of hydrographic data as input. These are obtained through field measurement or simulation. Hydraulic and dimension characteristics for each cross section are required by the program. The computations for the hydraulic and dimension characteristics were done using a spreadsheet. The spreadsheet was used to compute a series of q/Q, average width, average depth, average velocity, and areas using established river engineering principles. A sample format of the spreadsheet is shown in Table 5.1 and an explanation of the terminology (column headings) used is given in Appendix B. The z locations were obtained from GPS readings using simple trigonometry calculations. The change in water level was monitored at the site, which allowed the mean depth and velocity to be determined for each tracer test. The local velocities and flow distributions were estimated using an exponential relationship (see Appendix C). An example tabulation and cross section plot for a section are shown in Table 5.1 and Figure 5.1 respectively.

Table 5.1 Sample cross-section tabulation.

X-section:	Athabasca River, 0.55 km d/s		
Date:	August 21, 1997		
Discharge (m^3/s) :	960.00	Estimated water surface elevation (m):	499.80
Width (m):	338.02	Left bank (LB) = 0.80	499.80
Mean depth (m):	2.46	Right bank (RB) = 338.81	499.80
Area (m^2):	832.42		
Mean velocity (m/s):	1.15		

Sta. (m)	Elev. (m)	h (m)	w/W	u (m/s)	DQ (m^3)	q/Q	Area (m^2)	adj. u (m/s)
0.80	499.80	0.00	0.000	0.000	0.00	0.000	0.00	0.000
4.06	498.98	0.82	0.010	0.553	0.37	0.000	1.33	0.544
35.10	496.78	3.02	0.101	1.322	55.85	0.058	60.92	1.302
41.98	497.04	2.76	0.122	1.245	25.54	0.084	80.82	1.226
58.67	497.21	2.59	0.171	1.192	54.38	0.140	125.45	1.174
80.22	497.49	2.31	0.235	1.105	60.55	0.202	178.19	1.088
111.46	497.56	2.24	0.327	1.084	77.81	0.282	249.30	1.067
142.01	497.49	2.31	0.418	1.105	76.07	0.360	318.83	1.088
173.56	497.04	2.76	0.511	1.245	93.97	0.456	398.82	1.226
196.83	497.32	2.48	0.580	1.160	73.37	0.531	459.84	1.142
204.37	496.97	2.83	0.602	1.264	24.28	0.556	479.87	1.245
211.27	496.56	3.24	0.623	1.383	27.67	0.585	500.77	1.363
240.82	497.43	2.37	0.710	1.125	103.95	0.691	583.65	1.108
259.59	496.99	2.81	0.766	1.259	57.93	0.751	632.25	1.240
273.40	497.43	2.37	0.806	1.125	42.63	0.794	668.03	1.108
276.84	497.30	2.50	0.817	1.166	9.60	0.804	676.40	1.148
288.08	496.62	3.18	0.850	1.369	40.51	0.846	708.37	1.348
299.32	496.83	2.97	0.883	1.307	46.25	0.893	742.95	1.287
303.87	496.65	3.15	0.897	1.359	18.55	0.912	756.86	1.339
307.75	496.18	3.62	0.908	1.490	18.72	0.932	770.00	1.468
330.23	498.40	1.40	0.975	0.792	64.36	0.998	826.40	0.780
338.81	499.80	0.00	1.000	0.000	2.38	1.000	832.42	0.000
			Est. total =		974.74			

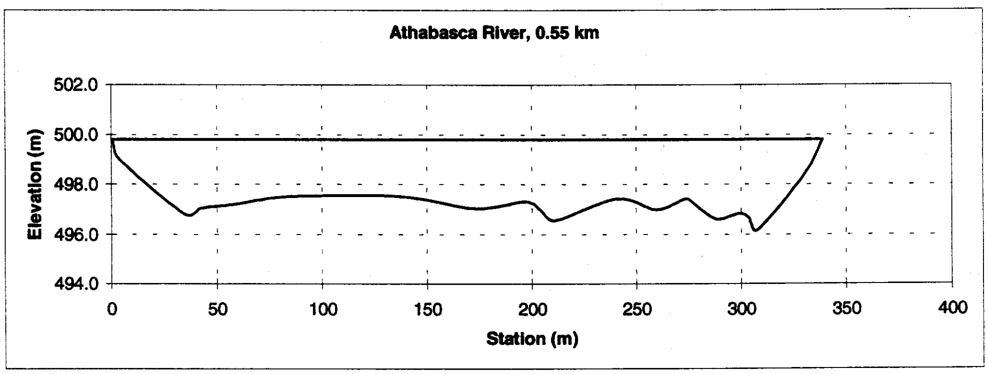

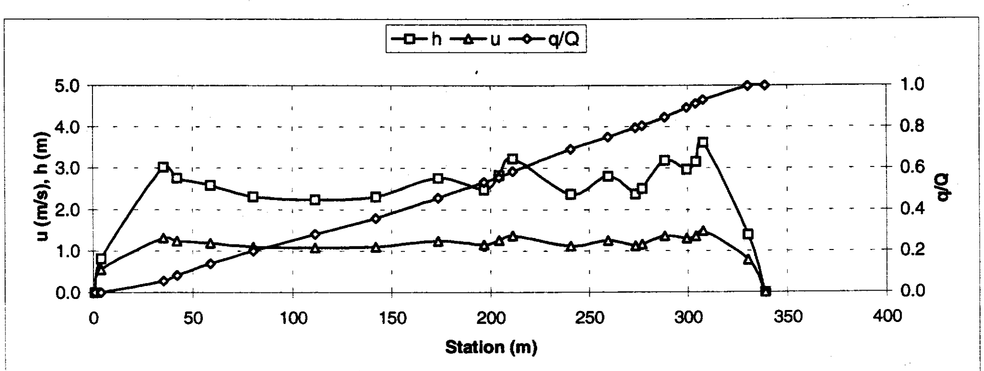

Figure 5.1 Example cross-section and flow distribution plot.

Cross section plots and tabulations for all sections used in the study are given in Appendix B. Explanation of the procedure is also in Appendix B. Local velocity was determined from measured depth data using an exponential relationship based upon Manning's formula. Velocity measurements were taken at a number of sections to provide a check of the synthesized local velocity and of the gauge flow. The synthesized velocities were very similar to the measured velocities, so the synthesized velocity data were used in the modelling. Tabulations and plots showing comparisons of measured and synthesized velocities are presented in Appendix C.

The measured velocity data were used to calculate the total discharge as a cross check against the discharge recorded at a gauging station. The discharge readings from the gauging station and the discharges calculated from the measured velocity readings are shown in Table 5.2. Total discharge was obtained from the Water Survey of Canada records of the gauging station located on Athabasca River at Athabasca (No. 07BE001). There was not much difference with the total stream flow obtained from the measured velocity readings and those from the gauging station (see Table 5.2). However, the discharge from the gauging station on the days of the different tests was used in the modelling. The depths were then adjusted to the water surface elevations measured on the day of the test. The simulated velocities were also adjusted to the gauge discharge reading. The data in Table 5.2 indicate the flow rate decreased with time (i.e., from day to day). However, the tracer tests are several hours in duration only, so the flow during an individual test was relatively steady.

5.2 Tracer Concentration Results

5.2.1 Tracer-Response Curves For Steady Input Tests

When the result of tracer studies for a continuous test is reported, the conventional method of presenting data is to plot tracer response curves. Forms of the tracer response curves for a steady input test include a plot of either concentration versus the transverse distance from one bank or concentration versus the cumulative discharge (q/Q).

Table 5.2 Discharge readings from a gauge station and discharges calculated from measured velocity readings.

Date	Transect (km)	Gauge discharge (m^3/s)	Measured discharge (m^3/s)
Aug. 19, 1997	11.50	1049.00	859.49
Aug. 19, 1997	28.95	1049.00	1027.19
Aug. 20, 1997	65.15	1083.00	1046.08
Aug. 20, 1997	10.48	1083.00	1034.69
Aug. 23, 1997	17.30	831.48	801.61
Aug. 24, 1997	23.74	780.12	826.35
Aug. 23, 1997	31.42	831.48	822.09

However plots of concentration versus the cumulative discharge are much more indicative of the actual mixing process (Yotsukura and Sayre, 1976). For C' versus q/Q plot, the horizontal axis on these plots represents the dimensionless cumulative flow, q/Q, where q is the flow accumulated from the left bank (looking downstream) and Q is the total stream flow. Thus q starts at zero at one bank and becomes equal to Q at the other bank.

The vertical axis represents non-dimensional concentration C', where C' = c/c_∞, c is a normalized measured concentration and c_∞ is the fully mixed concentration of the tracer mass within the river flow. These C' versus q/Q plots shows transverse variation in tracer concentration. Integration on the C' versus q/Q curve should result in a value of 1 for mass conservative substances, i.e. the mass flow rate represented by the area under the curve, should equal the mass flow into the river.

5.2.2 Tracer-Response Curves For Slug Tests

If a certain amount of tracer, M_{in}, has been injected in a river at a longitudinal position $x = 0$ over a finite time interval or more-or-less instantaneously, beginning at a time

$t = 0$, and sampling is carried out at several points within a cross section located x km downstream of the injection site during the anticipated time of passage of the tracer cloud, then analysis of the sample will result in a set of concentration-time curves (C-t). Hence, the conventional manner of displaying the response of a river to a slug injection of tracer is to plot the variation of concentration with time at a given number of cross sections downstream of the injection. These curves will generally be different for different points in the river.

The shape and magnitude of the observed tracer-response curves are determined by a number of factors: (1) the quantity of the tracer injected; (2) the degree to which the tracer is conservative; (3) the magnitude of the river discharge; and (4) transverse and longitudinal dispersion. The magnitude of tracer concentration in a river is in direct proportion to the mass of tracer injected (M_i). Increasing the amount of injected tracer for a given flow will increase the observed concentration in the same proportion, but the shape and duration of the tracer-response curve (C-t curve) will remain constant. For this reason most investigators normalize their data by dividing all observed tracer concentrations by the mass of tracer injected, (M_i) (Jobson 1997).

5.2.3. Steady Input Test

If injection of a tracer takes place at a constant rate over a finite period of time, a steady condition will be established for some time for locations within a certain distance downstream of the injection point. In the time interval for these locations, the concentration is independent of time and is generally referred to as the steady state 'window'. Concentrations will be steady at a section within the steady state 'window' established in the river.

As stated previously, there are always minor losses in the field due to adsorption, photo decay etc. Recovery of tracer for a continuous input test is determined by integrating the measured tracer concentration versus cumulative flow curves at each transect. The estimated dye recoveries based on measured concentration readings at each section for the continuous tests are shown in Table 5.3 (except for the column 876 m^3/s, which is for slug test). The results from the different tests that were conducted did not indicate much variation of the recovery ratio with distance downstream as seen in Figure 5.2. As seen from Table 5.3, relatively high recoveries were observed. This is not surprising since Rhodamine WT does not adsorb strongly to sediments. Table 5.3 shows some of the recovery ratios to be above one. This may be due to inaccurate definition of the flow distribution across a section, which can cause apparent recoveries to be in excess of 100 %.

The tracer concentrations were normalized to account for incomplete mass recovery at individual transects. The mass recovery ratio for each transects (designated M_r) is given in the upper left-hand corner of the individual plots for the three continuous input tests as can be seen from Figures 5.3, 5.4 and 5.5 for the 960 m^3/s, 270 m^3/s and 84 m^3/s flows, respectively. The mass recoveries for the 960 m^3/s, 270 m^3/s and 84 m^3/s was in the range of 90 to 100%, 80 to 100% and 80 to 92%, respectively. The range of the mass recovery for the 84 m^3/s test was observed to be lower than the other two continuous input tests.

As mentioned previously, the conventional manner of displaying the response of a river to continuous injection of tracer is to plot dimensionless concentration versus dimensionless cumulative flow. This form of tracer response curve is used in the presentation of results for this work.

Table 5.3 Tracer recoveries.

	Mass Recovery			
x-section (km)	**960 m^3/s**	**876 m^3/s**	**270 m^3/s**	**84 m^3/s**
0.5			0.80	
0.55	0.84			
1.0			0.86	
1.15	1.02			
2.0			0.87	
2.895	1.06			
4.0			1.11	
6.515	0.99			
8.0			0.93	0.91
10.48	1.28	0.84		
13.90	1.20			
16.00			0.92	0.91
17.30	1.03	0.75		
21.15	1.09			
23.74	0.92	0.63		
28.51	1.08			
31.42	1.03	0.67		
32.00			0.85	0.87

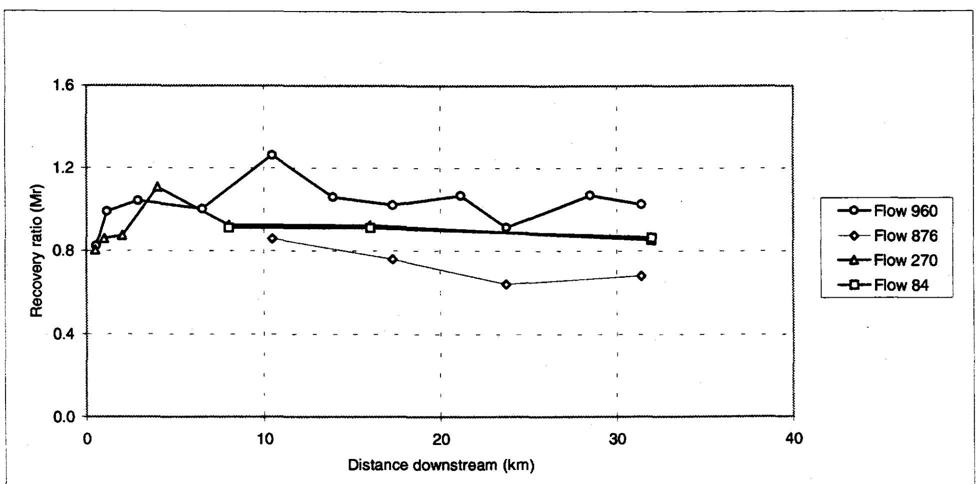

Figure 5.2 Recovery ratio (M_r) versus distance downstream (km).

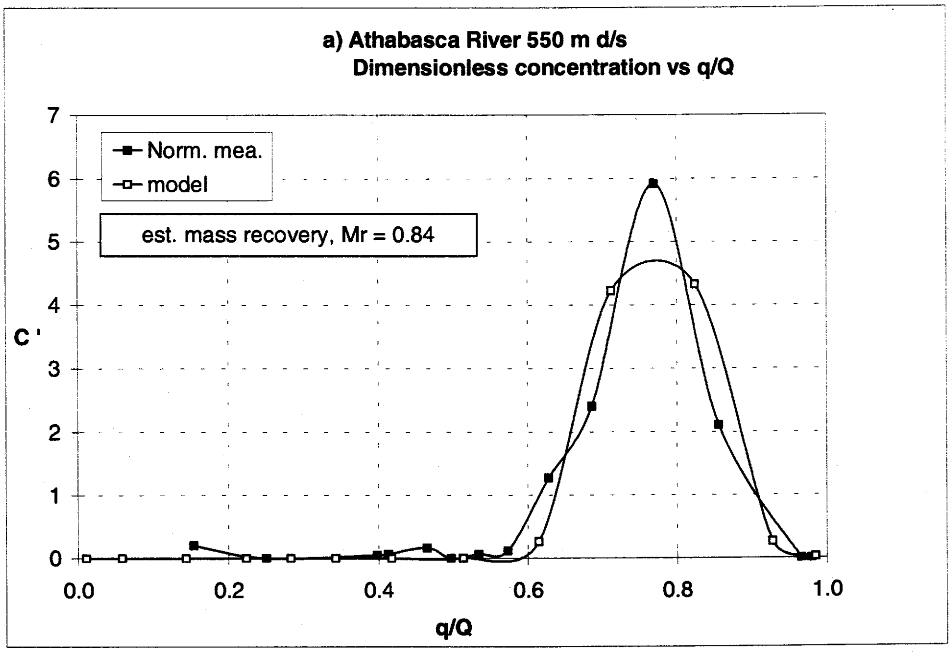

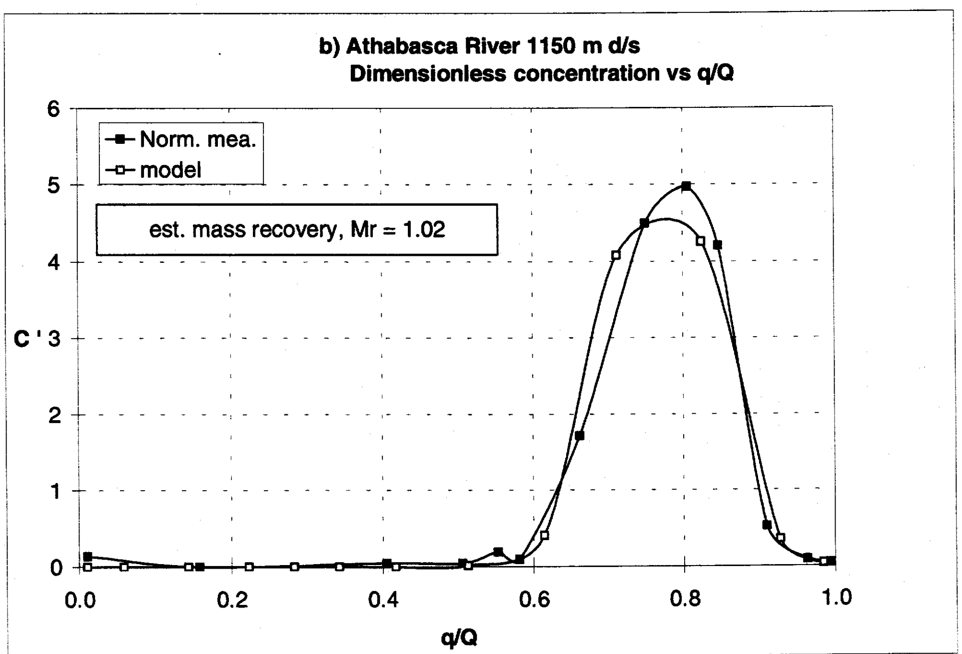

Figure 5.3 Tracer dimensionless concentrations and model results, 960 m^3/s, open water, continuous input.

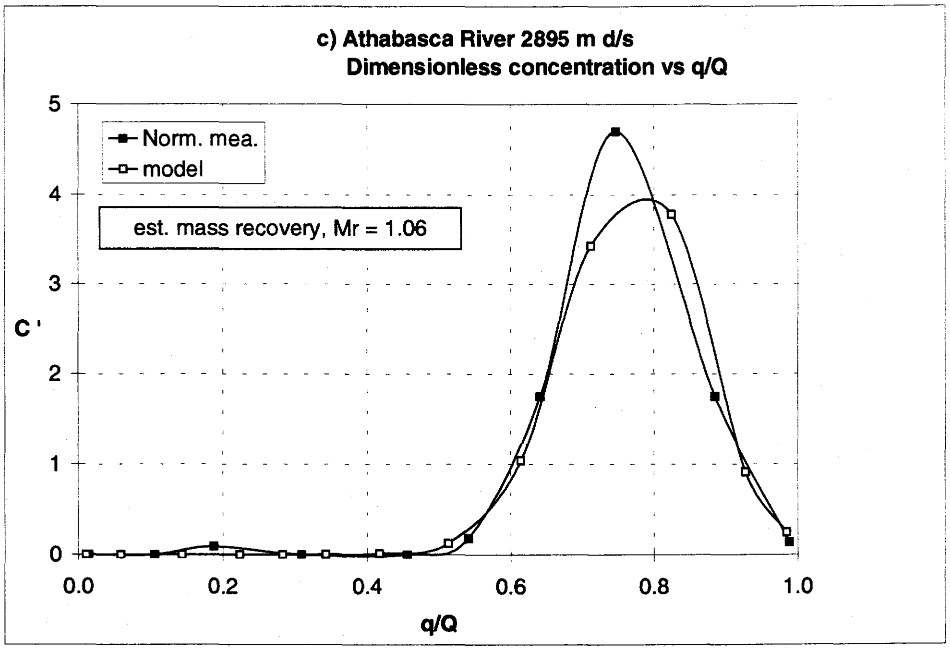

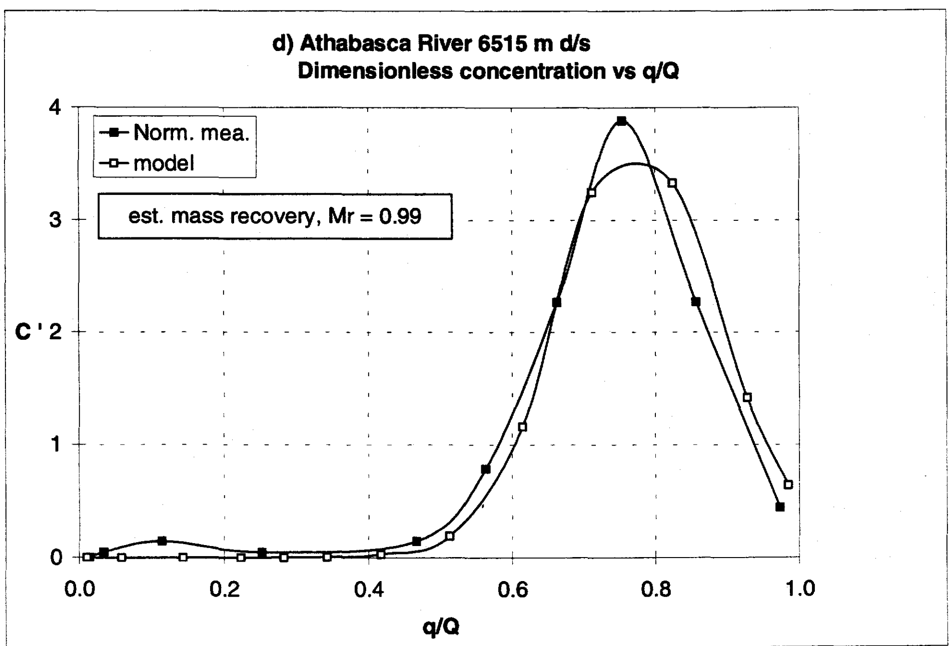

Figure 5.3 *Contd.*

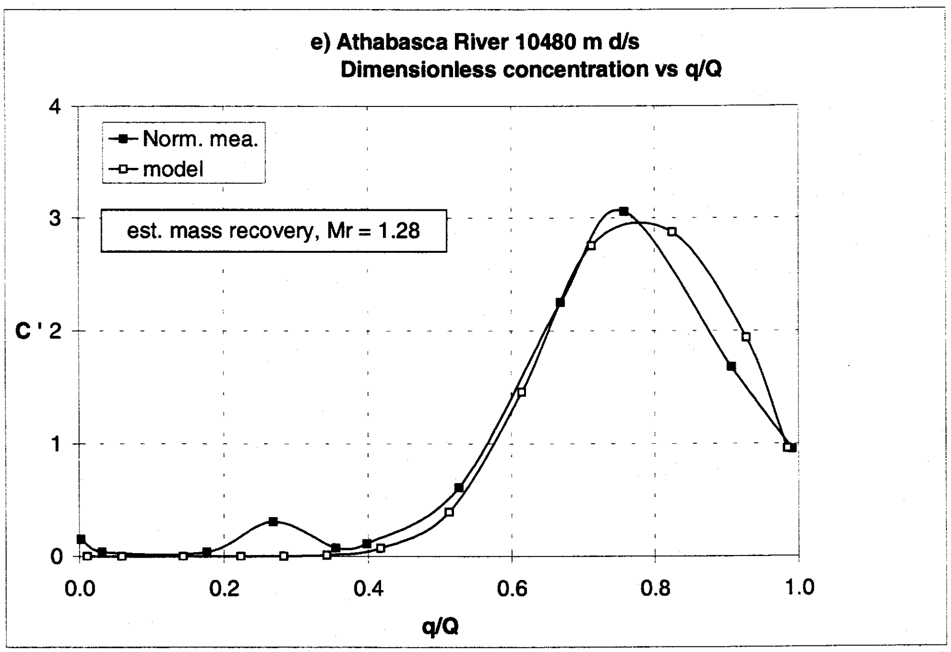

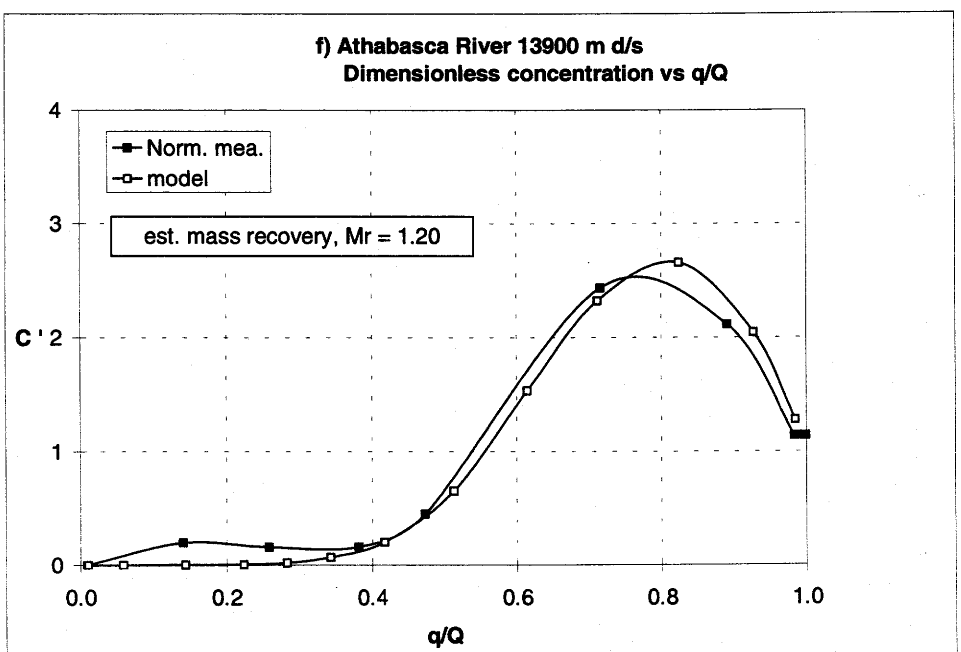

Figure 5.3 (*Contd.*)

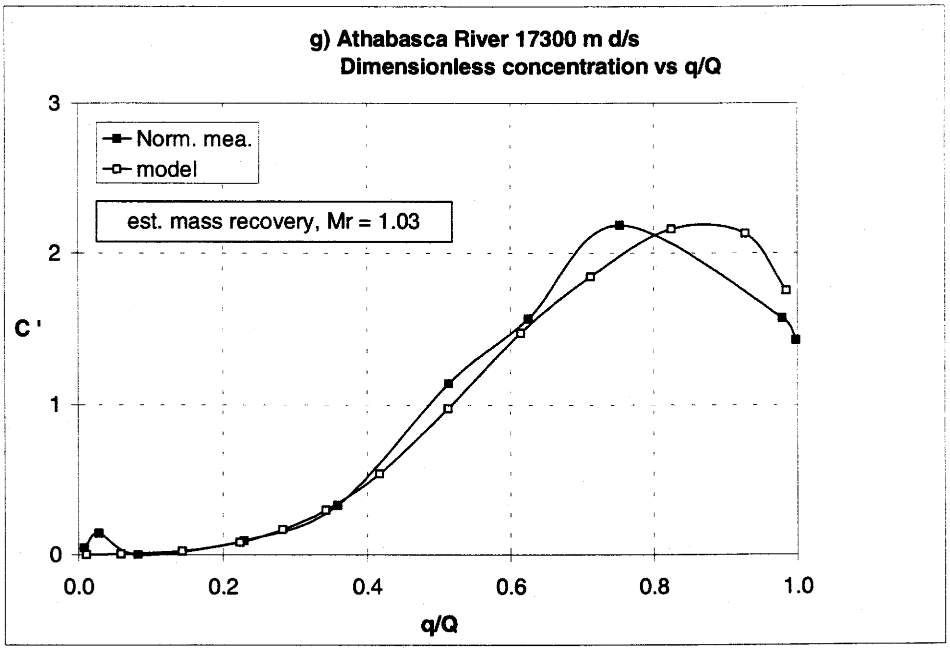

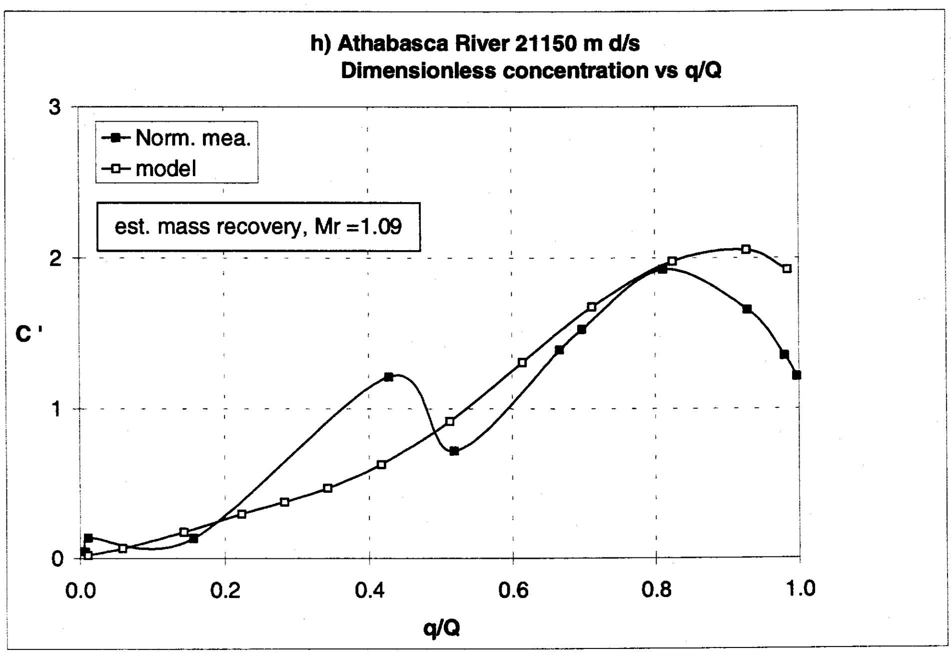

Figure 5.3 (*Contd.*).

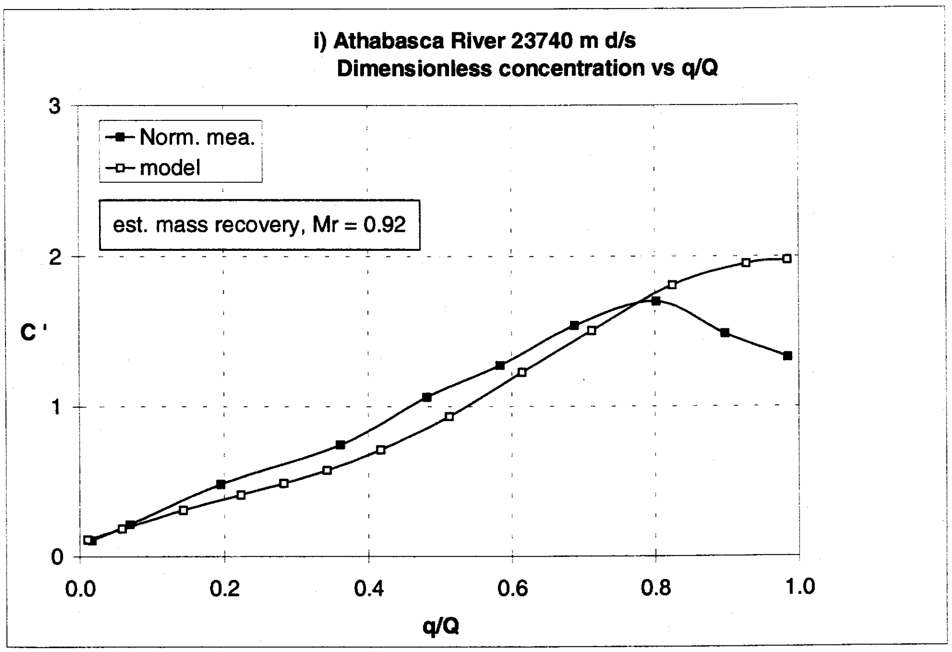

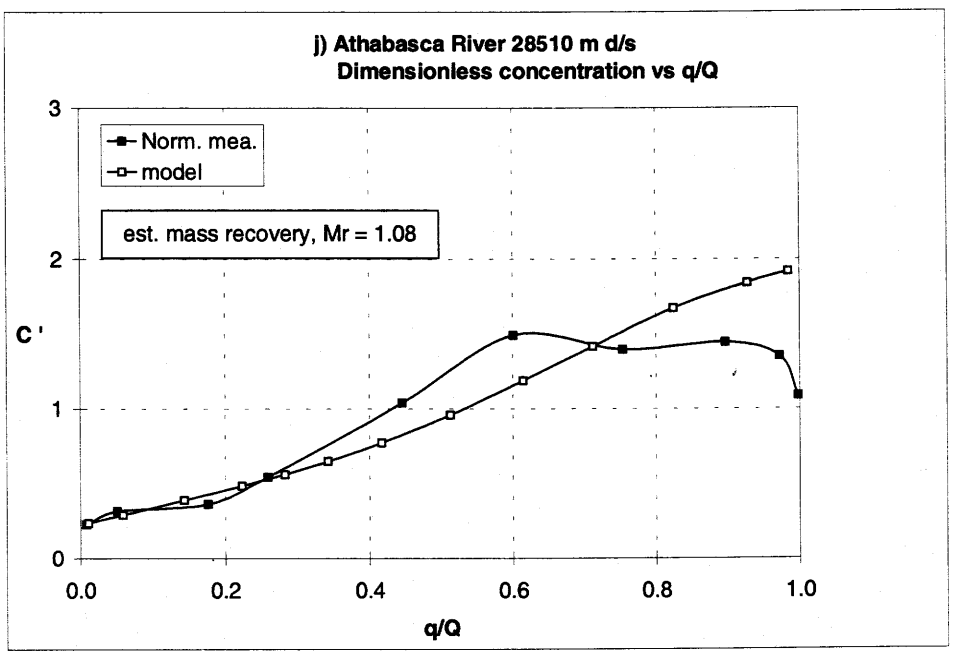

Figure 5.3 (*Contd.*).

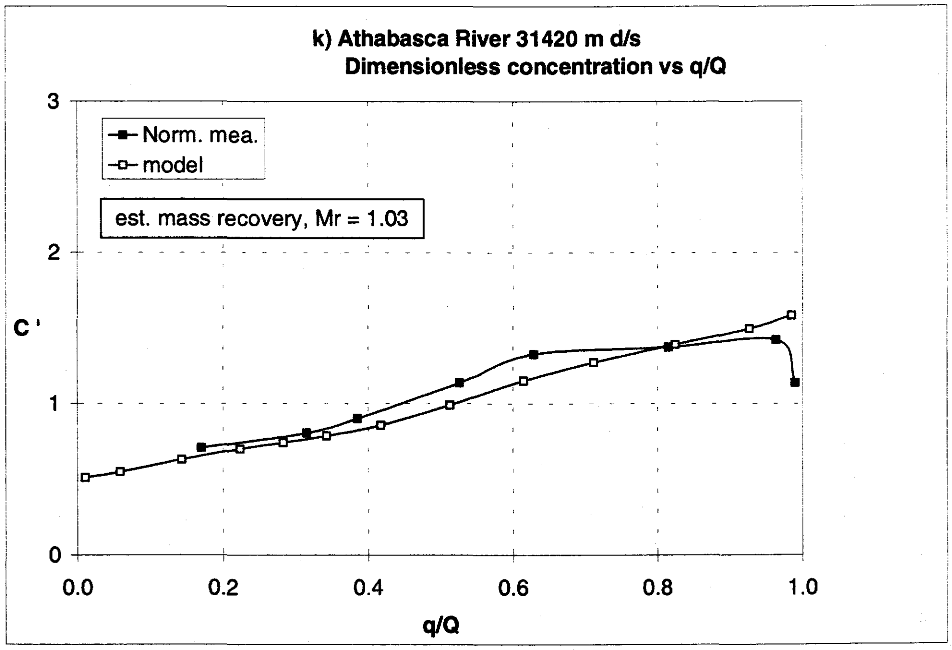

Figure 5.3 (*Contd.*)

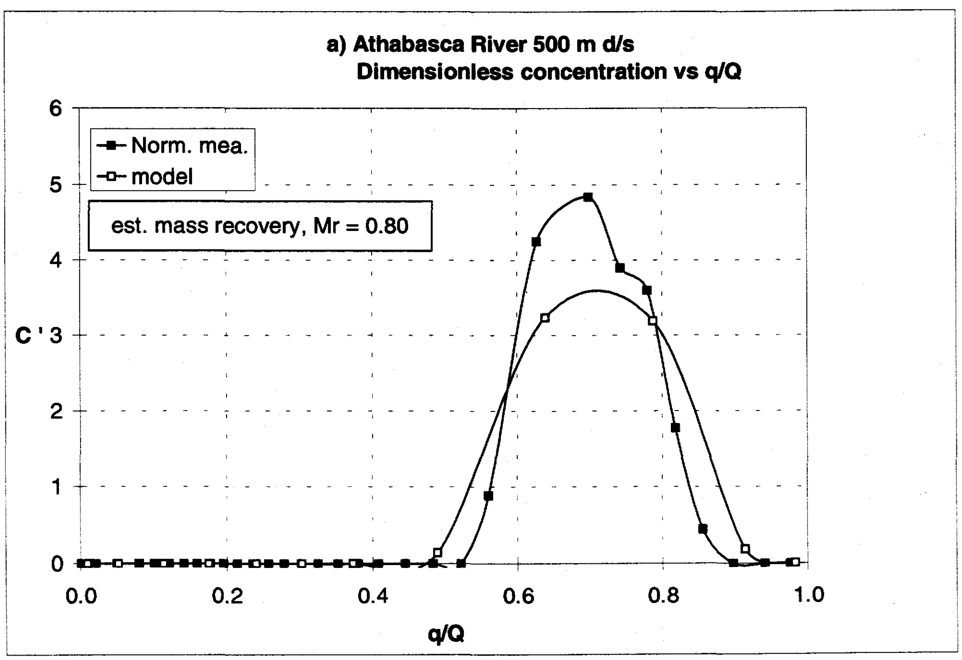

Figure 5.4 Tracer dimensionless concentrations and model results, 270 m^3/s, open water, continuous input.

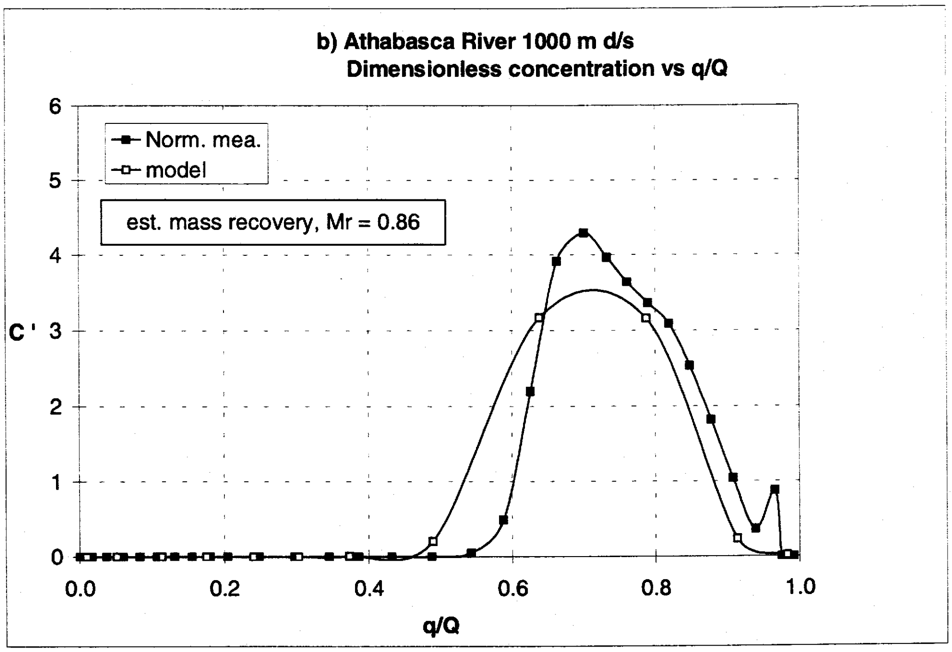

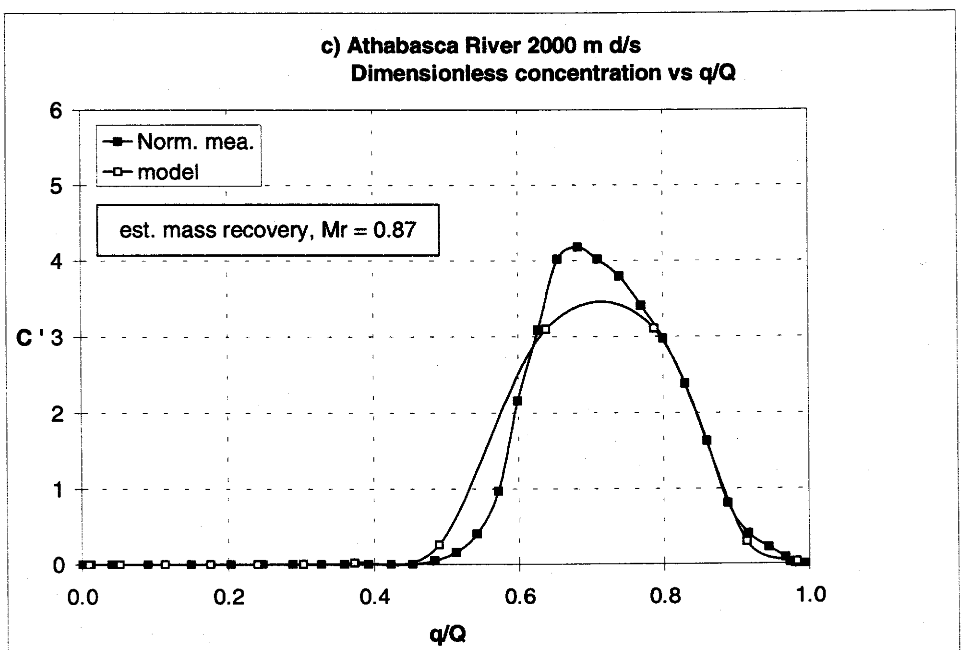

Figure 5.4 (*Contd.*)

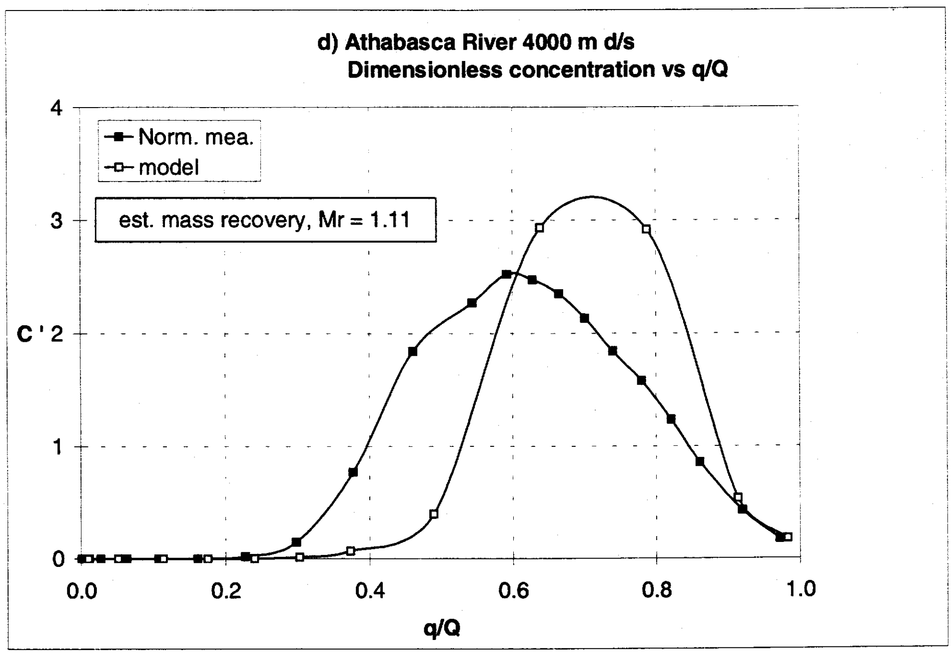

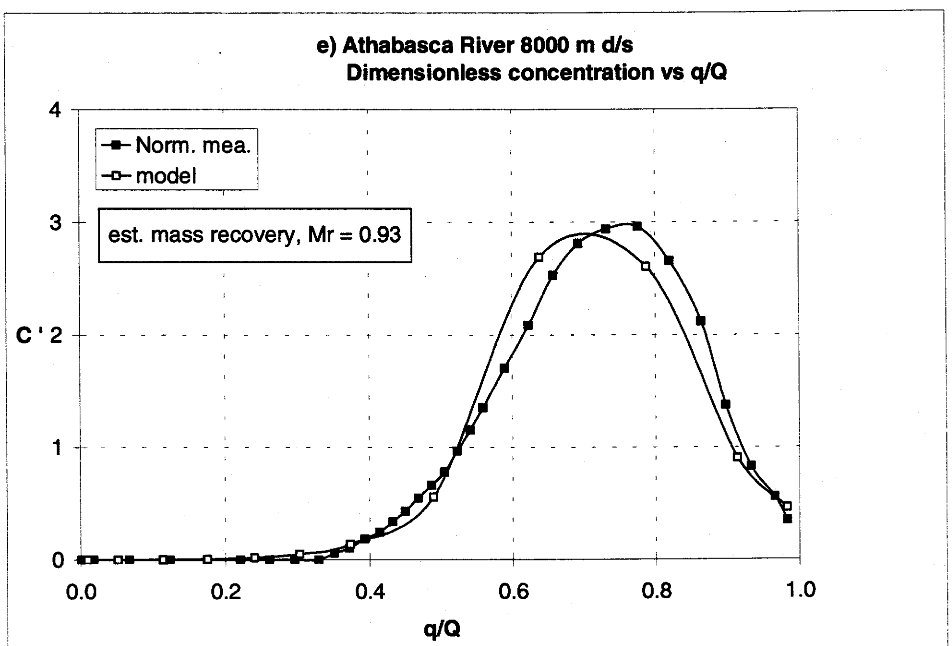

Figure 5.4 (*Contd.*)

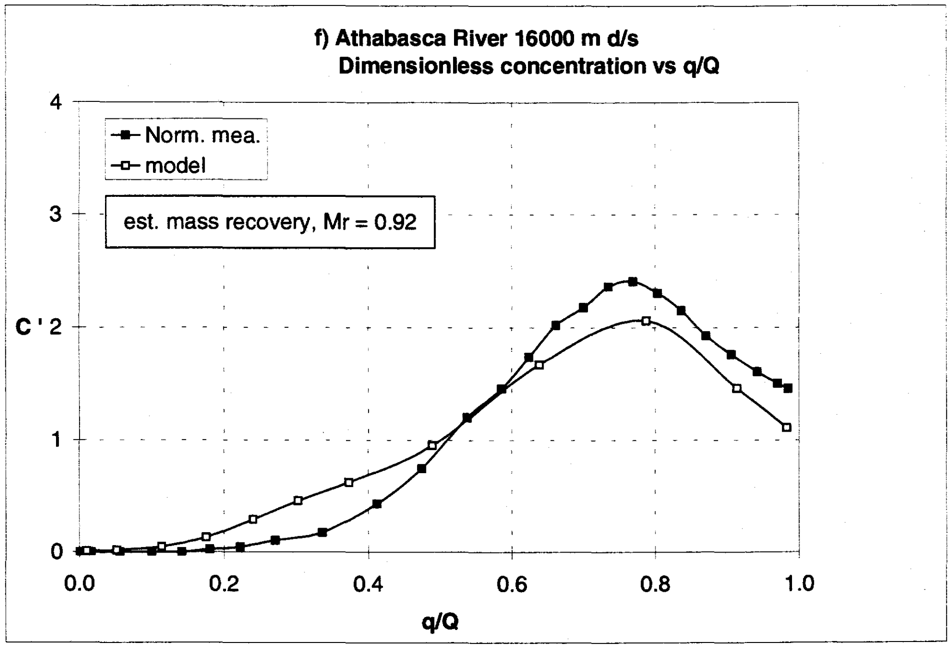

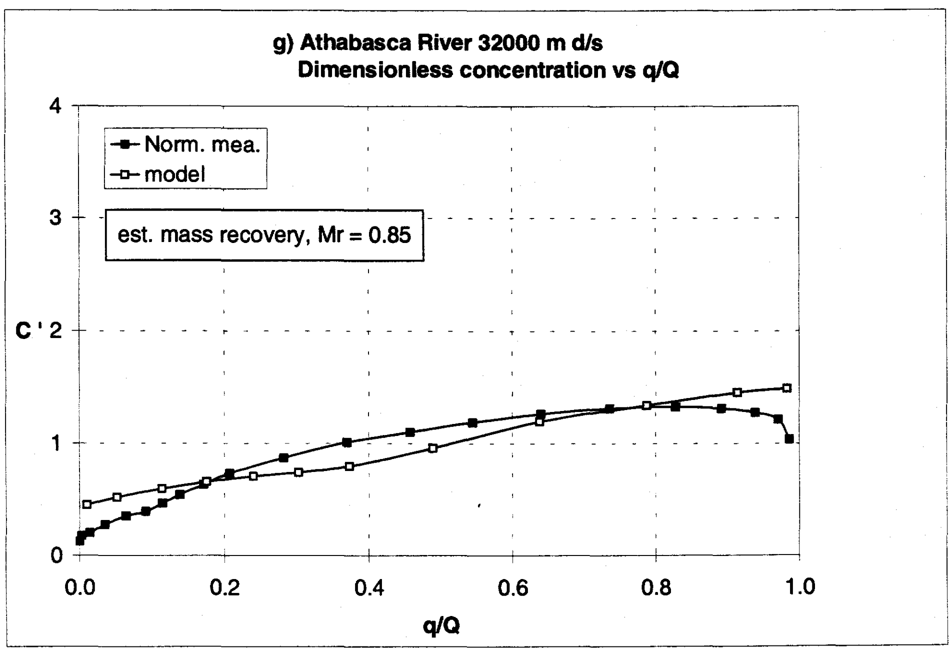

Figure 5.4 (*Contd.*)

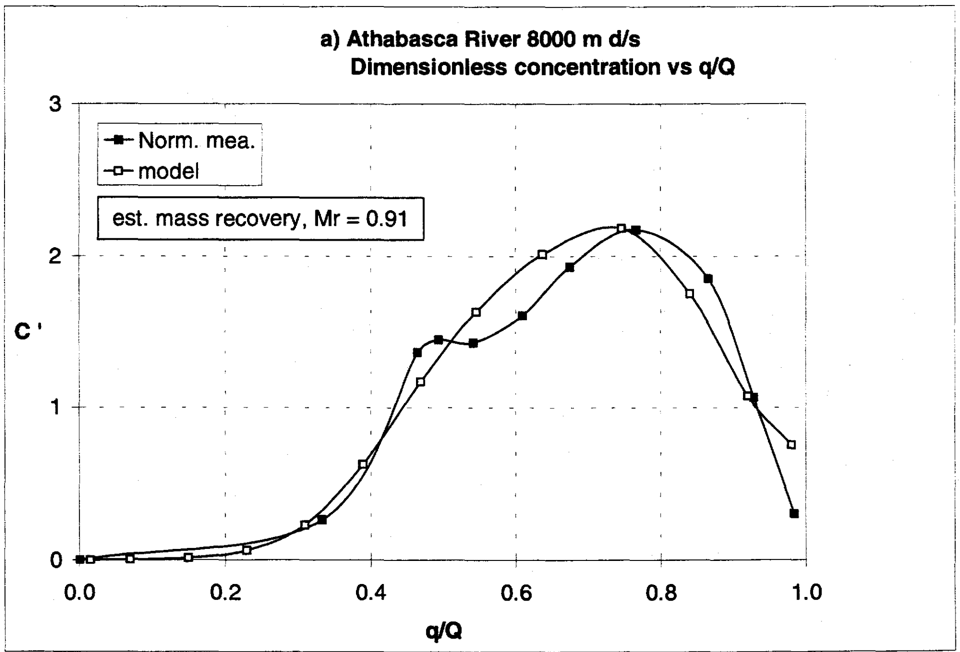

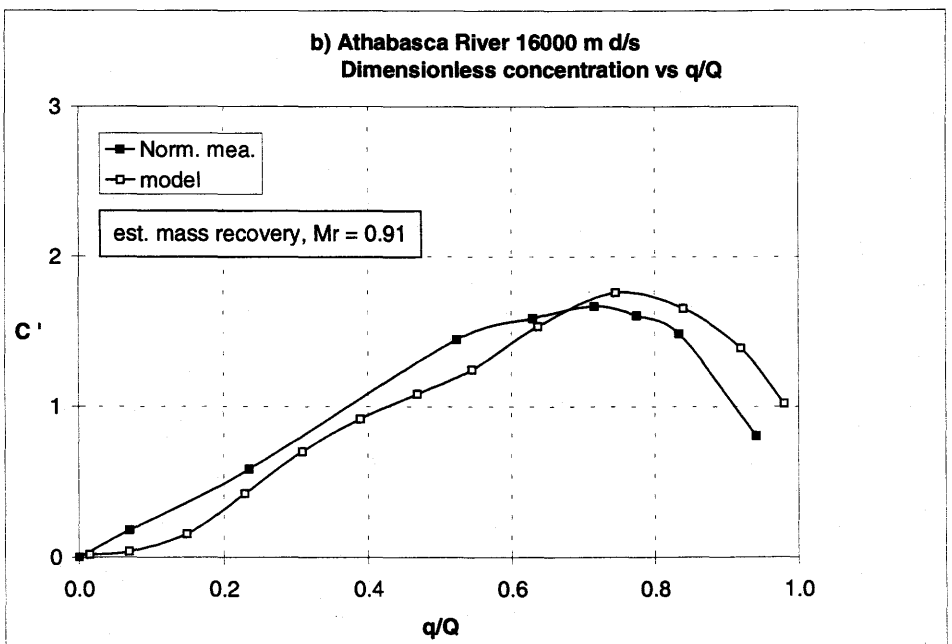

Figure 5.5 Tracer dimensionless concentrations and model results, 84 m^3/s, ice-covered, continuous input.

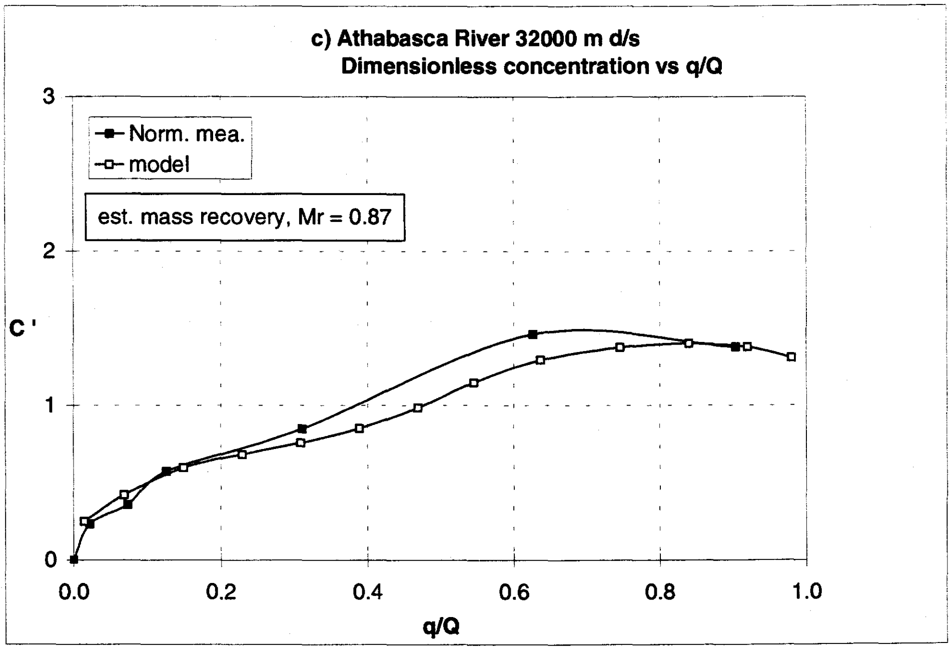

Figure 5.5 (*Contd.*)

5.2.4. Slug Input Test

When a tracer is injected at a point in a river, more-or-less instantaneously, the input concentration will vary with time and the concentration at any given point downstream will vary with time. Therefore such a situation is termed unsteady. Analysis of a slug input test results in the generation of a set of concentration-time curves (C-t). C-t curves will decrease in peak concentration and increase in duration with distance downstream of injection. Interpolation is done to obtain estimates of the tracer concentration at the centre of streamtubes to compare to the model. C-t plots for sections at 10.48 km, 17.3 km, 23.74 km and 31.42 km downstream are shown on Figures 5.6 through 5.9.

The concept of dosage was used to determine the transverse mixing coefficient from the slug injection test. Dosage is defined as the time integral of depth-average concentration at a given location downstream of a slug injection, i.e.,

$$D = \int_0^\infty c\,dt \quad . \quad . \quad . \quad . \quad . \quad . \quad . \quad . \quad . \qquad (5.1)$$

Where D is the dosage. The dosage is usually distributed across the channel. This distribution of dosage has been shown to be analogous to the distribution of concentration in the continuous test (Beltaos 1975). Hence, the resulting plots of dimensionless dosage versus cumulative flow are analogous to the plots of C' versus q/Q for the continuous input tests. The dosage versus q/Q plots shows the transverse distribution of mass passing a cross section. The normalized dosage distribution at each sampled section is shown in Figure 5.10. Comparison of the normalized and simulated dosage curves at each section indicates that there is very good agreement between normalized measurements and the model results.

Mass recovery of tracer for a slug input test is determined from the integration of dosage versus cumulative flow curves at each transect. The mass recovery ratio for each of the transects sampled during the slug test is given in the upper left-hand corner of the individual plots shown in Figures 5.10a to 5.10d. The mass recovery was found to be in the range 60 to 90%. Typically the mass recovery at the initial sections in a slug test is in the range of 80 to 100%. As can be seen from Figure 5.10a, it is about 84% at 10.48 km downstream, which is within the expected range. The mass recovery was however lower than those obtained for the continuous input tests.

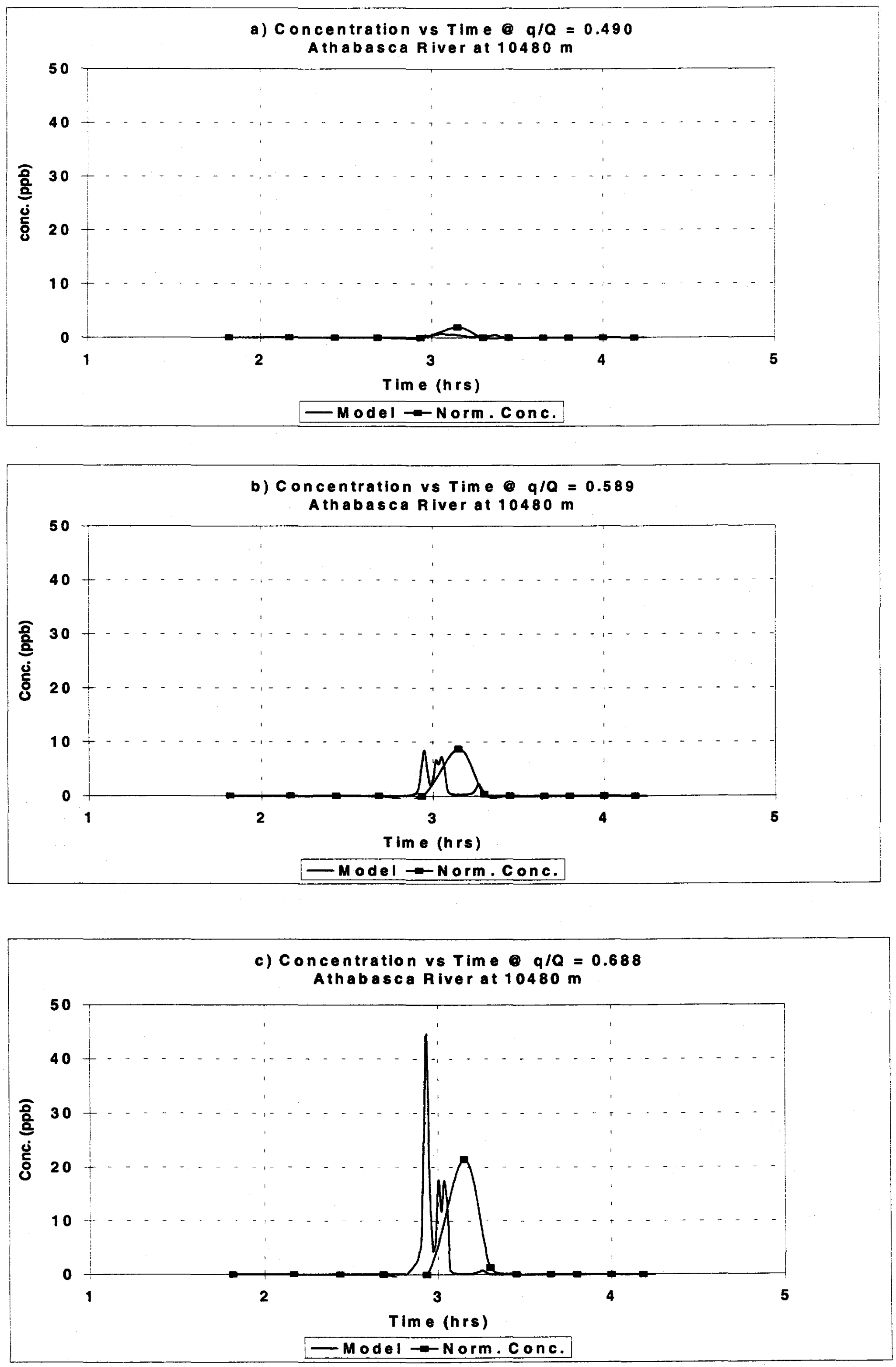

Figure 5.6 Athabasca River, C-t curves at 10480 m, extended slug input to the model.

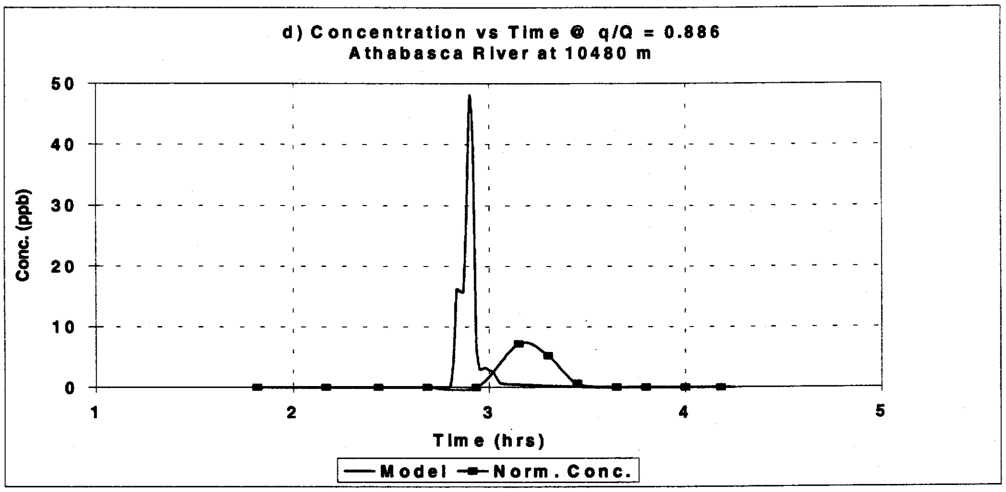

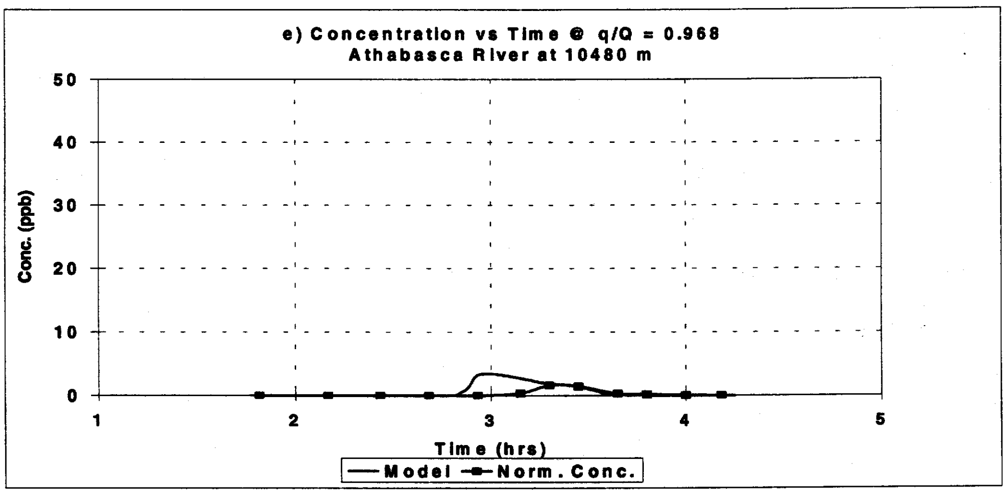

Figure 5.6 *Contd.*

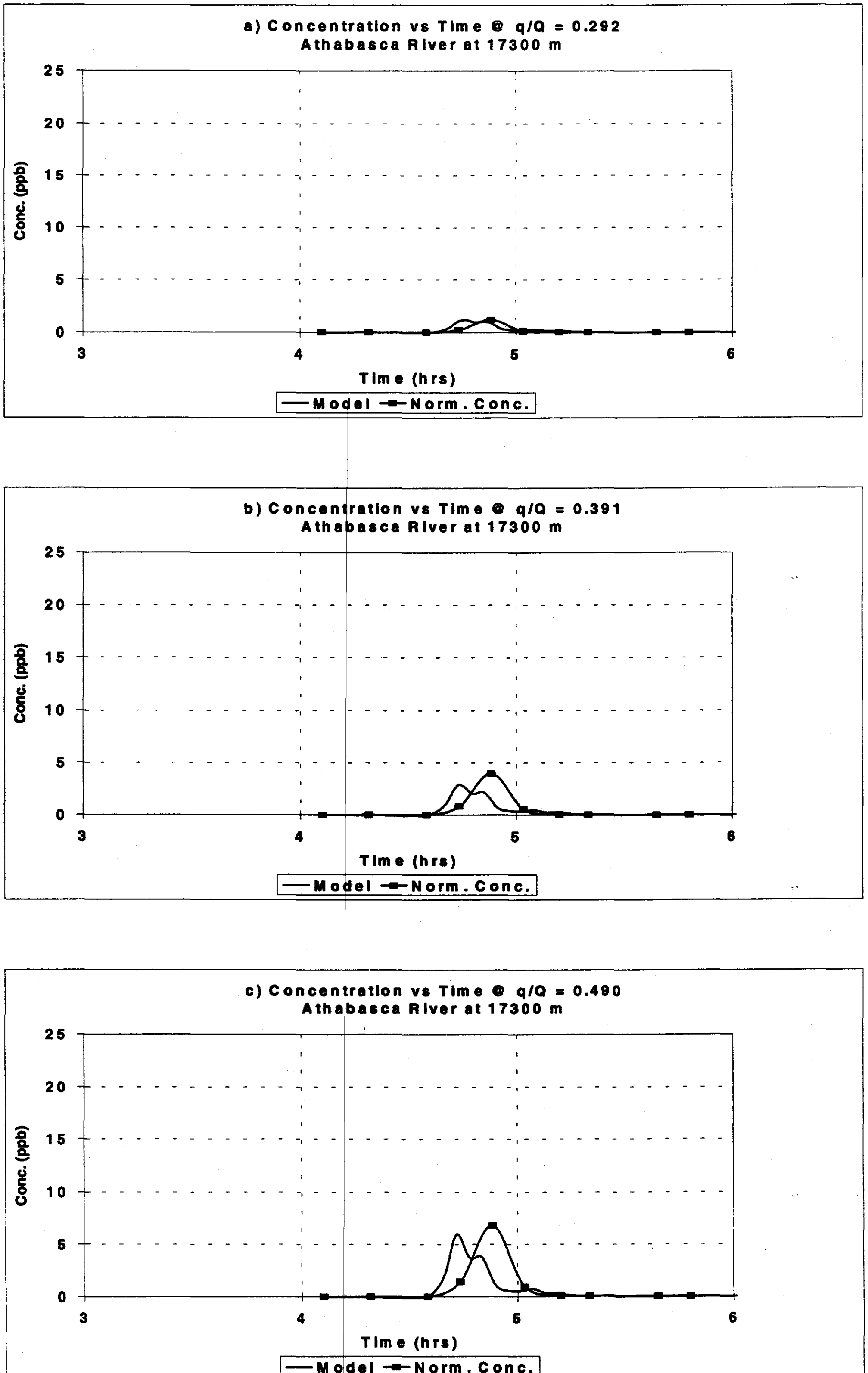

Figure 5.7 Athabasca River, C-t curves at 17300 m, extended slug input to the model.

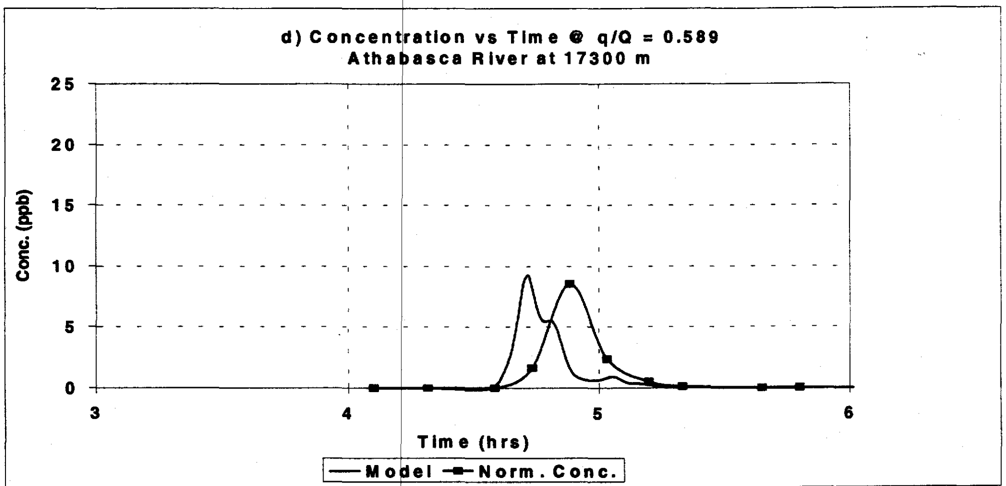

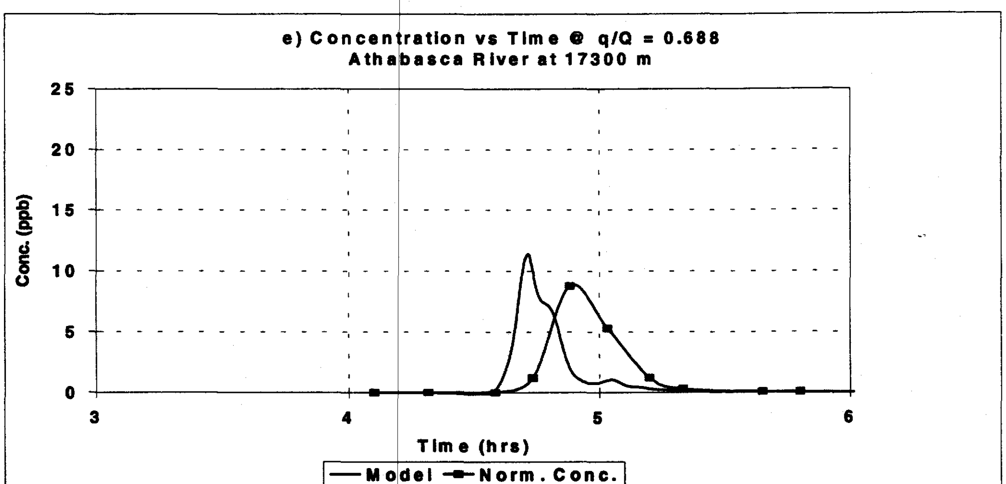

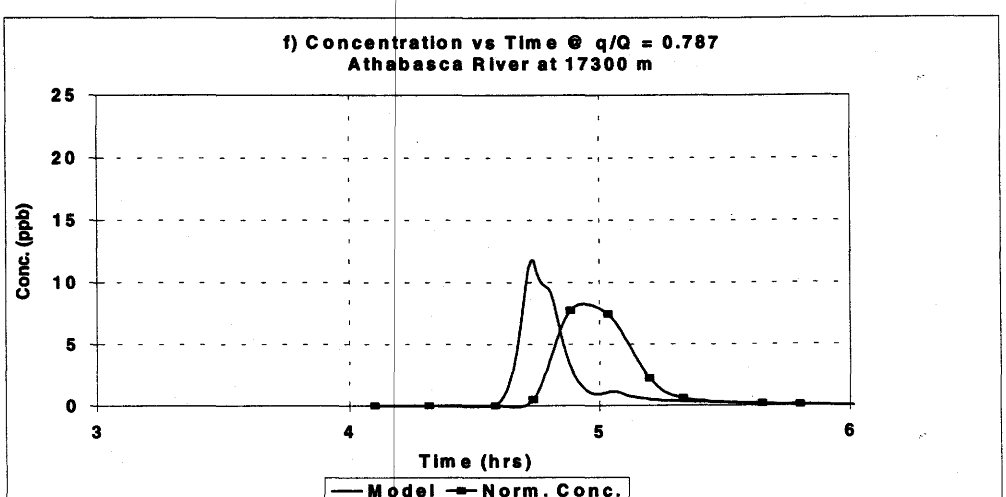

Figure 5.7 (*Contd.*)

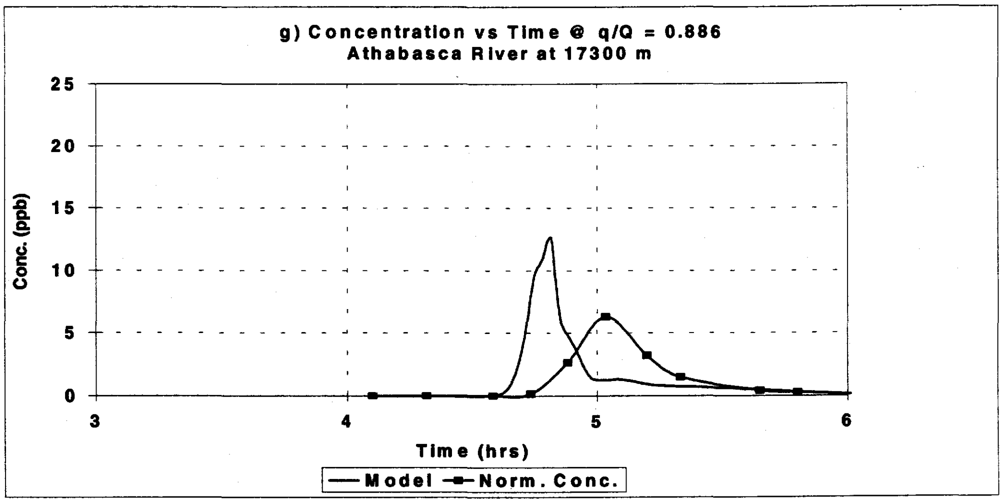

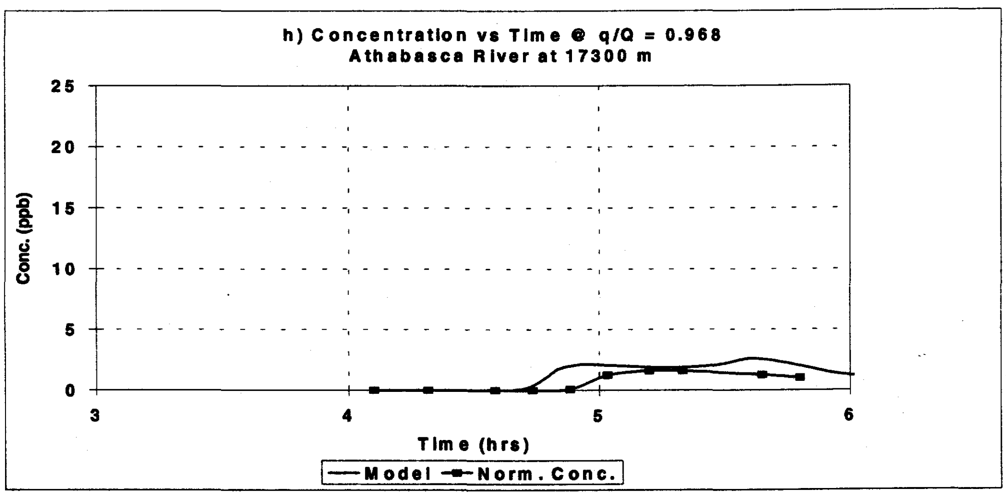

Figure 5.7 *Contd.*

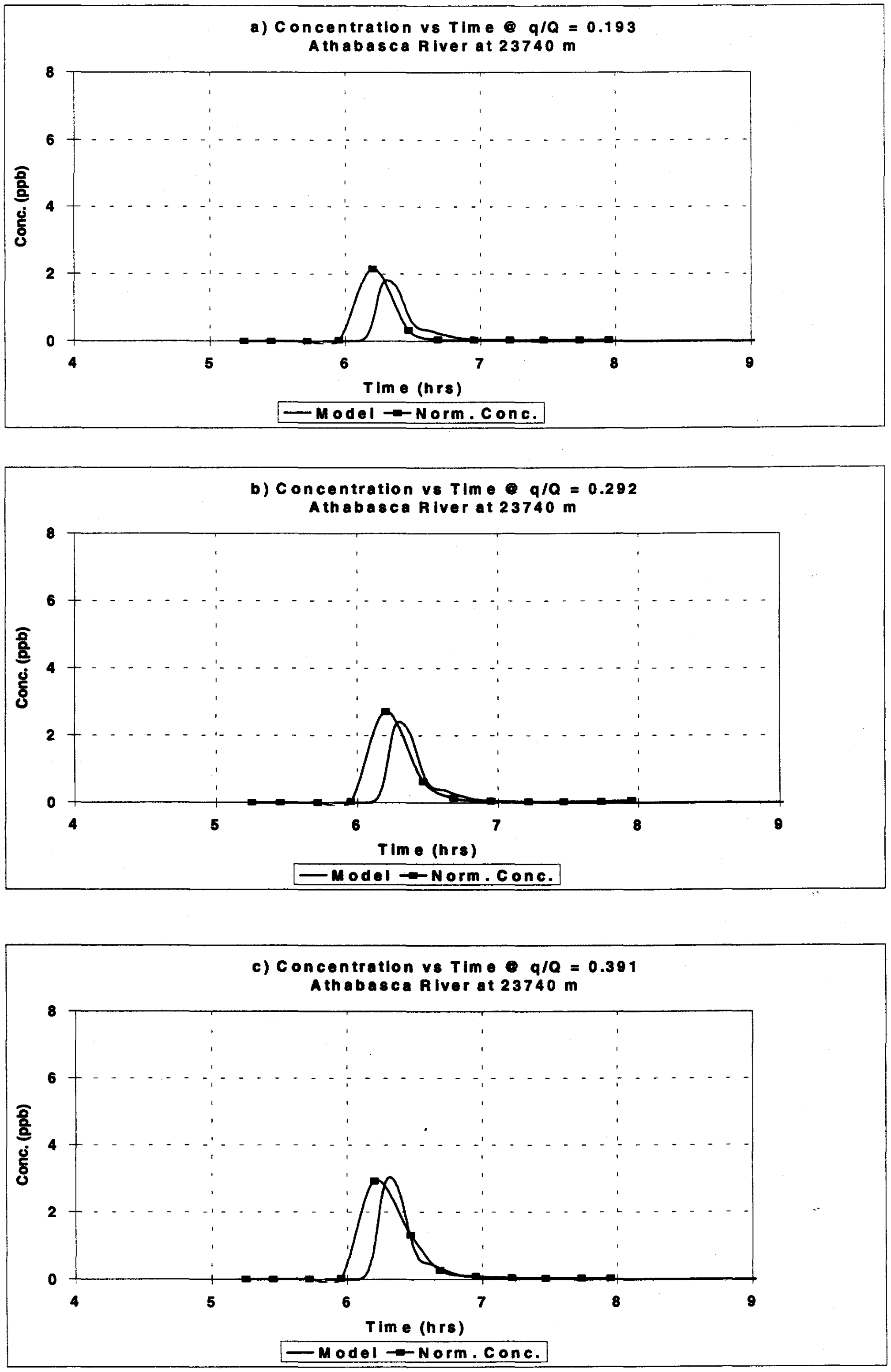

Figure 5.8 Athabasca River, C-t curves at 23740 m, extended slug input to the model.

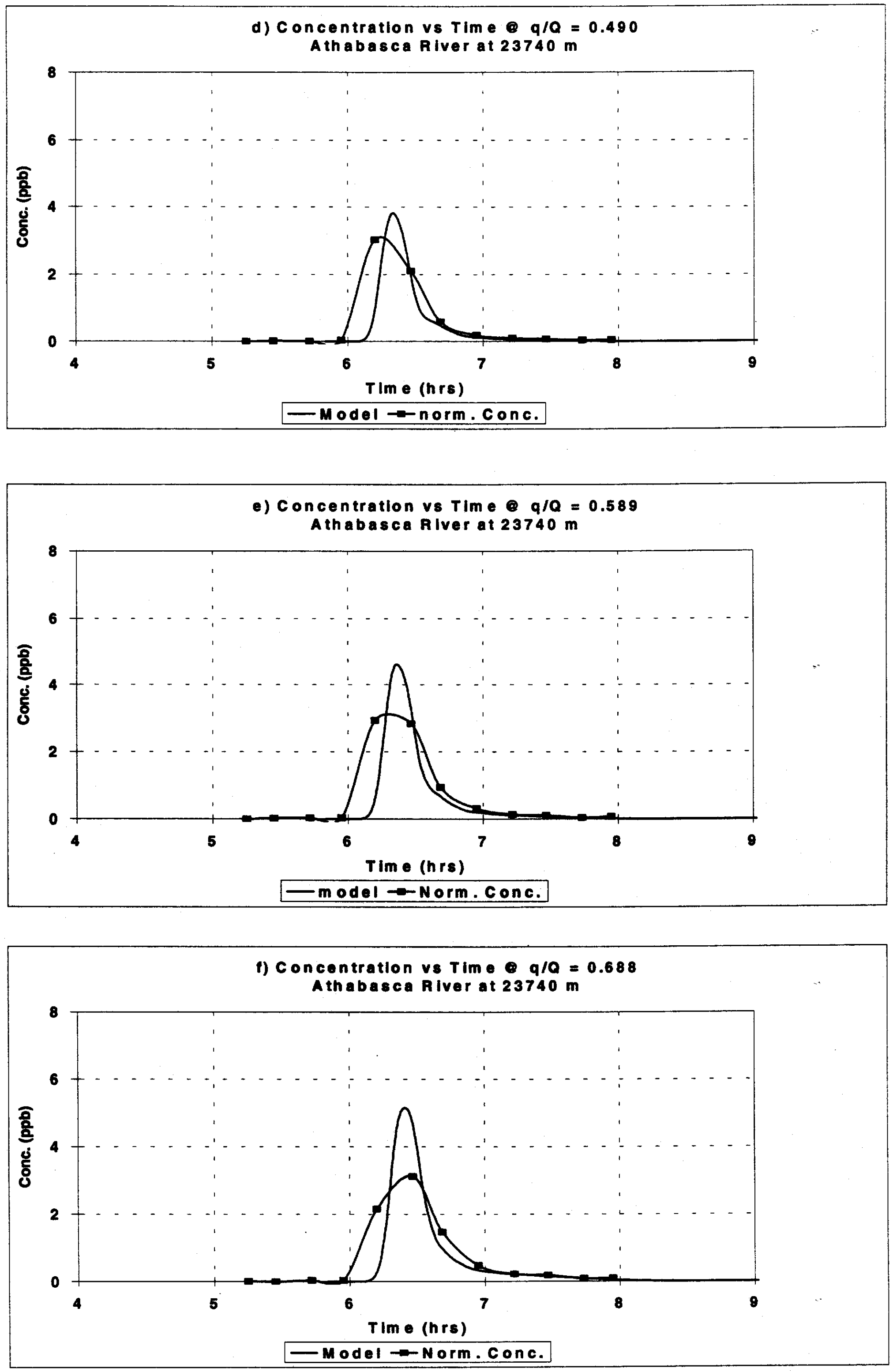

Figure 5.8 (*Contd.*)

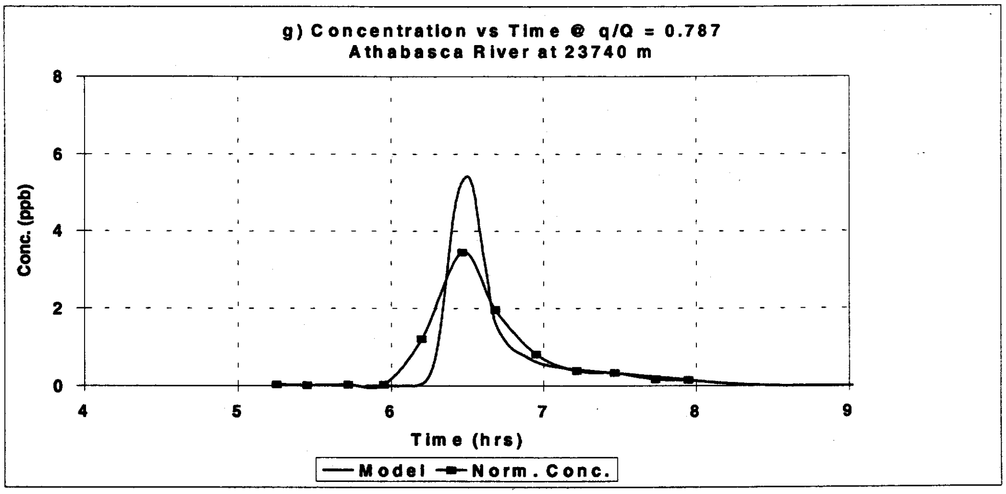

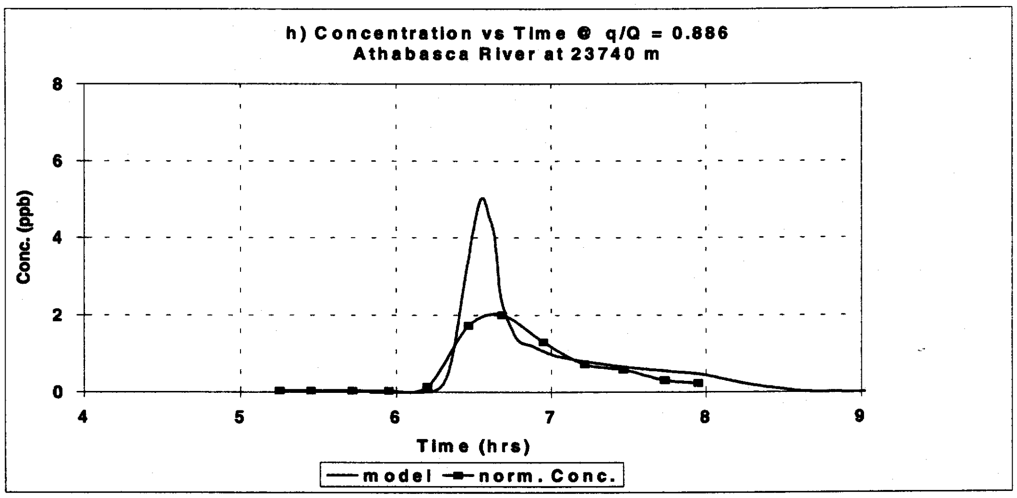

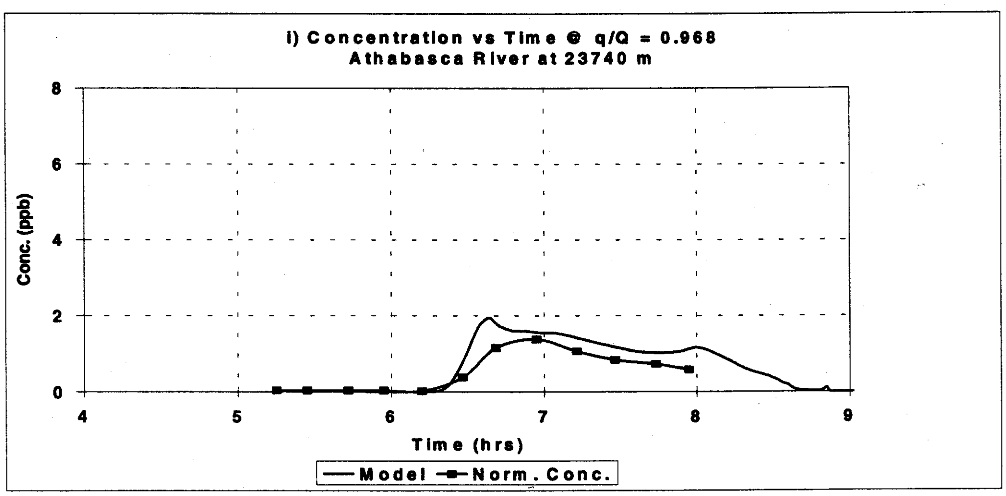

Figure 5.8 (*Contd.*)

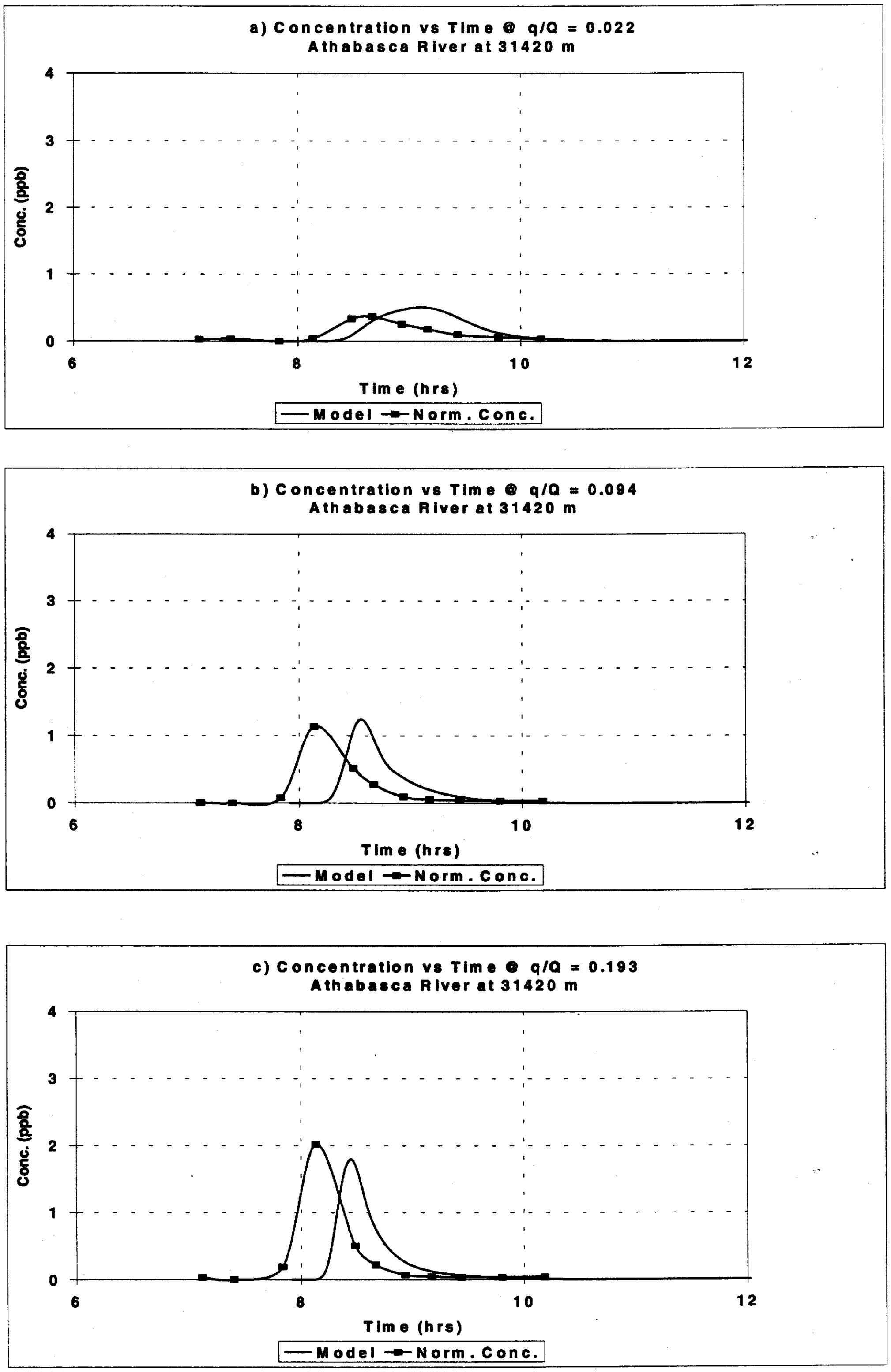

Figure 5.9 Athabasca River, C-t curves at 31420 m, extended slug input to the model.

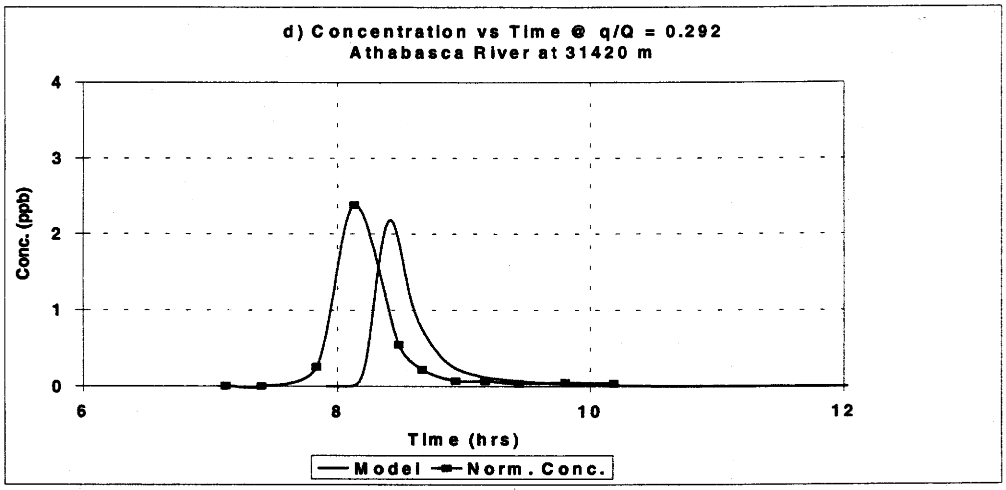

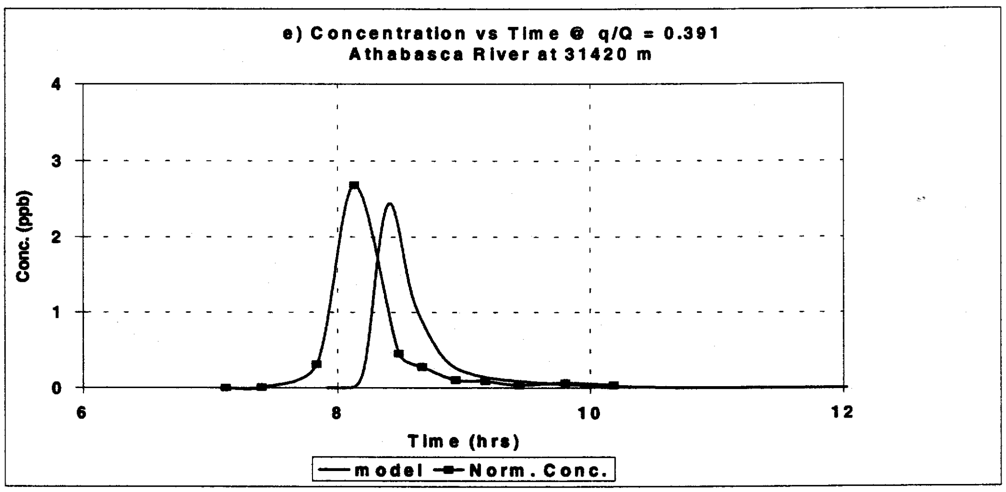

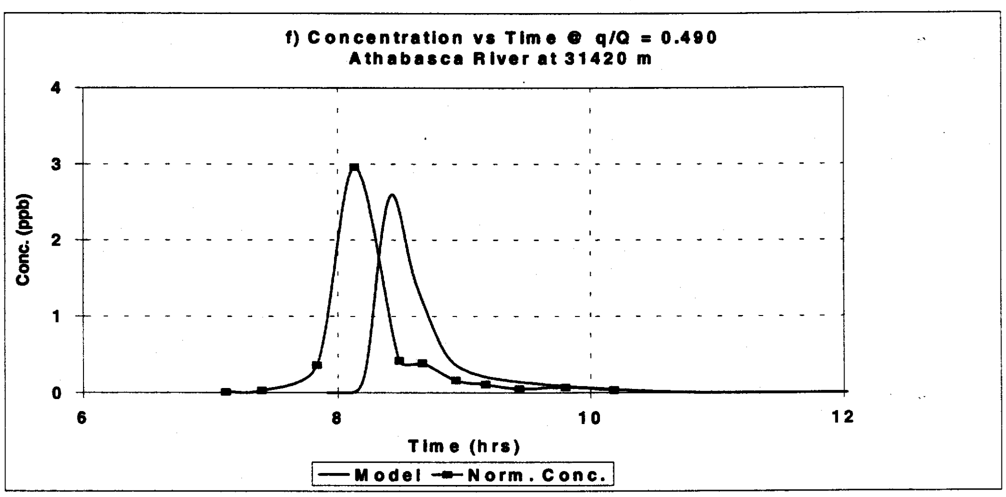

Figure 5.9 (*Contd.*)

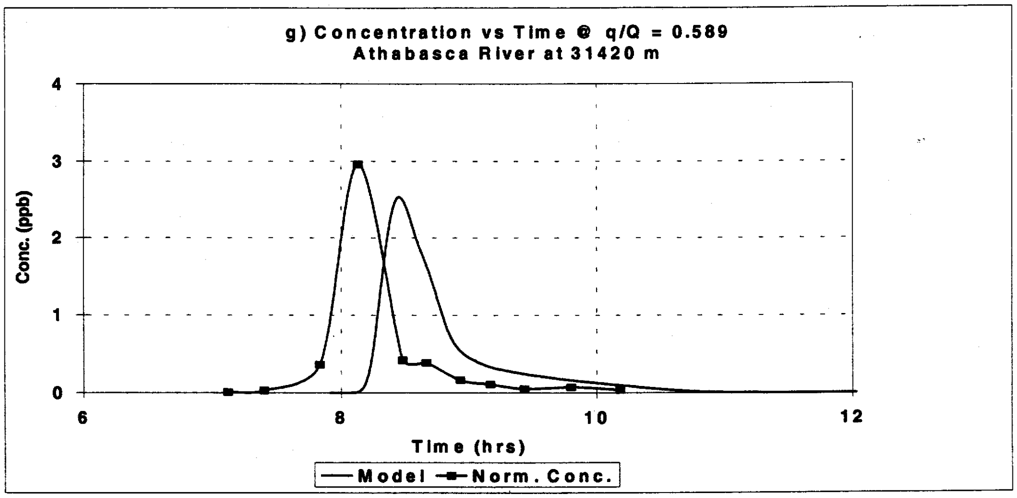

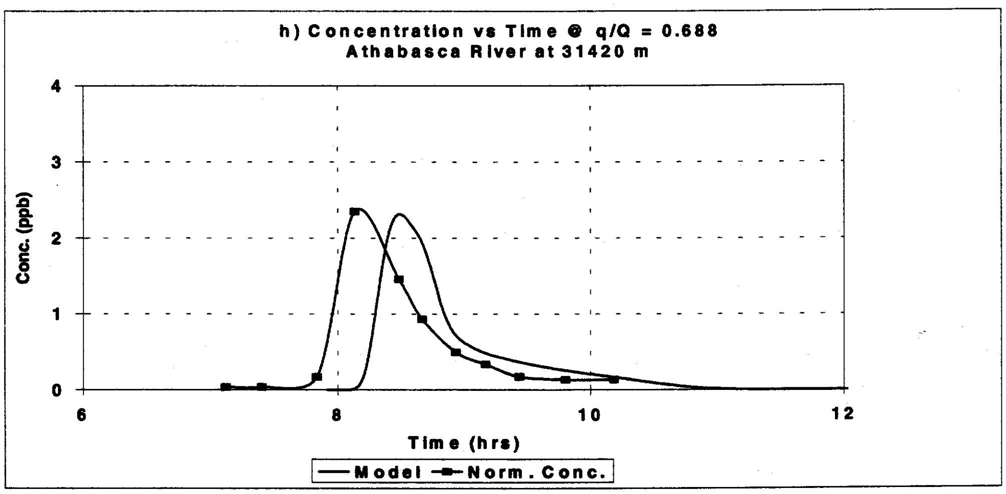

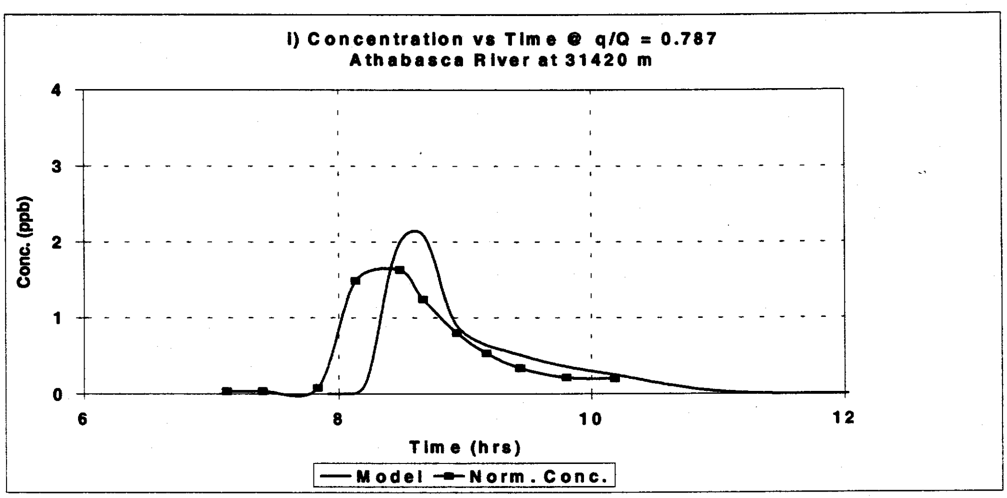

Figure 5.9 (*Contd.*)

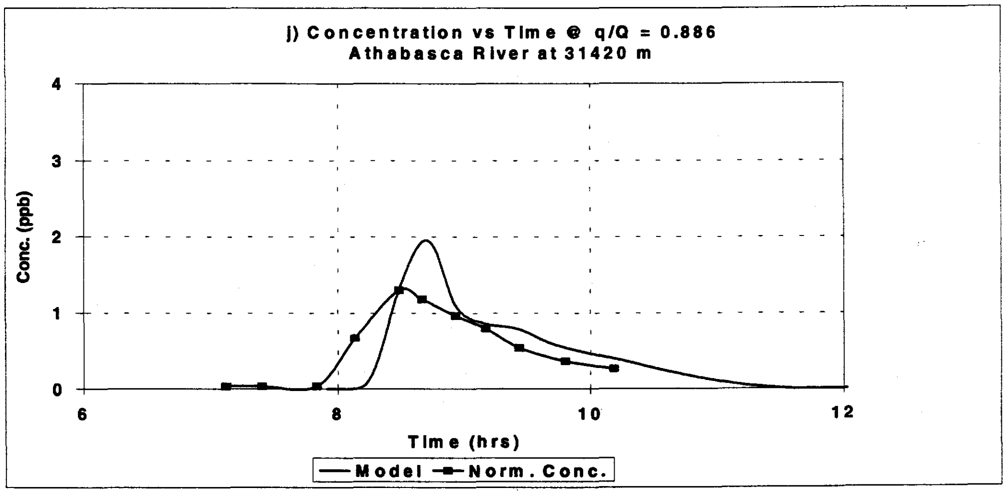

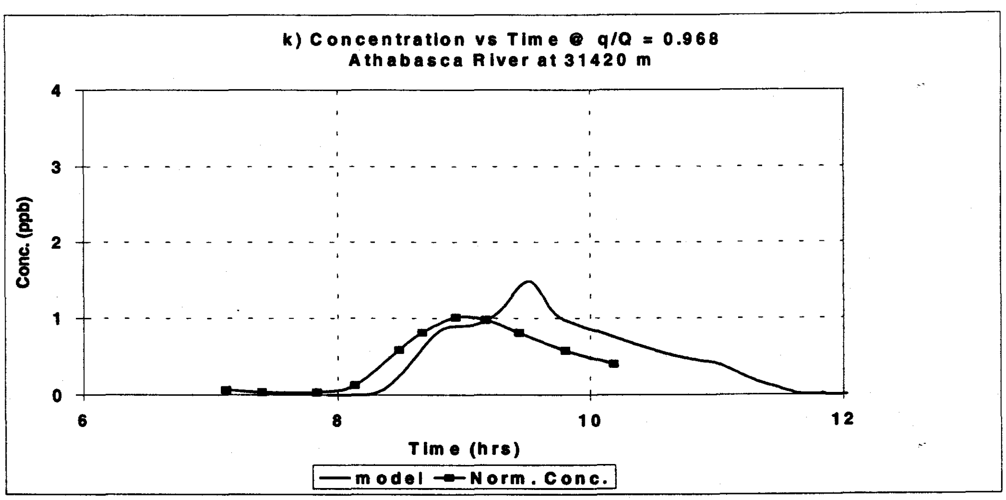

Figure 5.9 (*Contd.*)

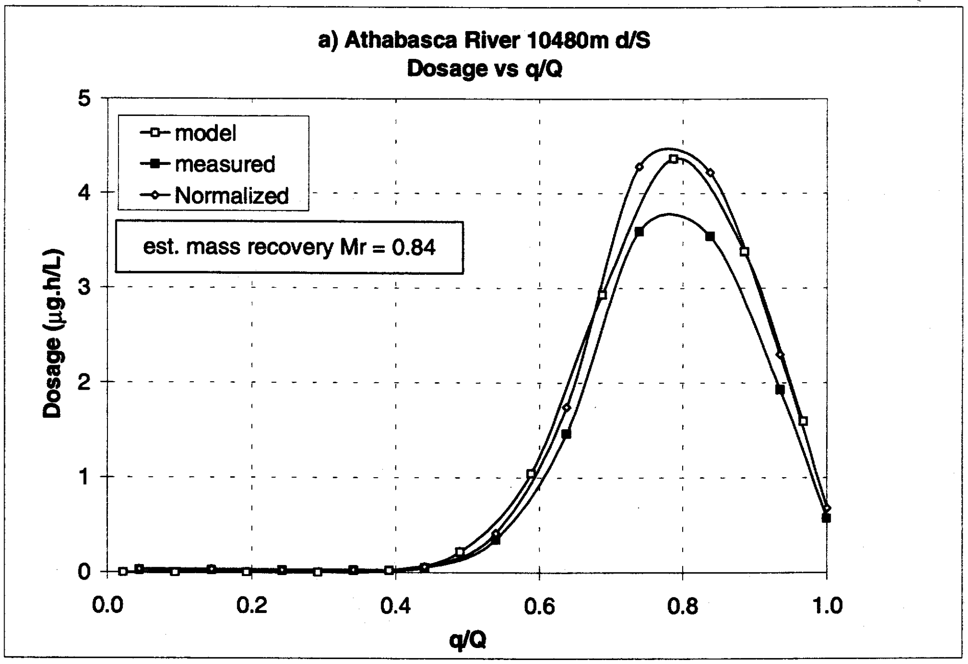

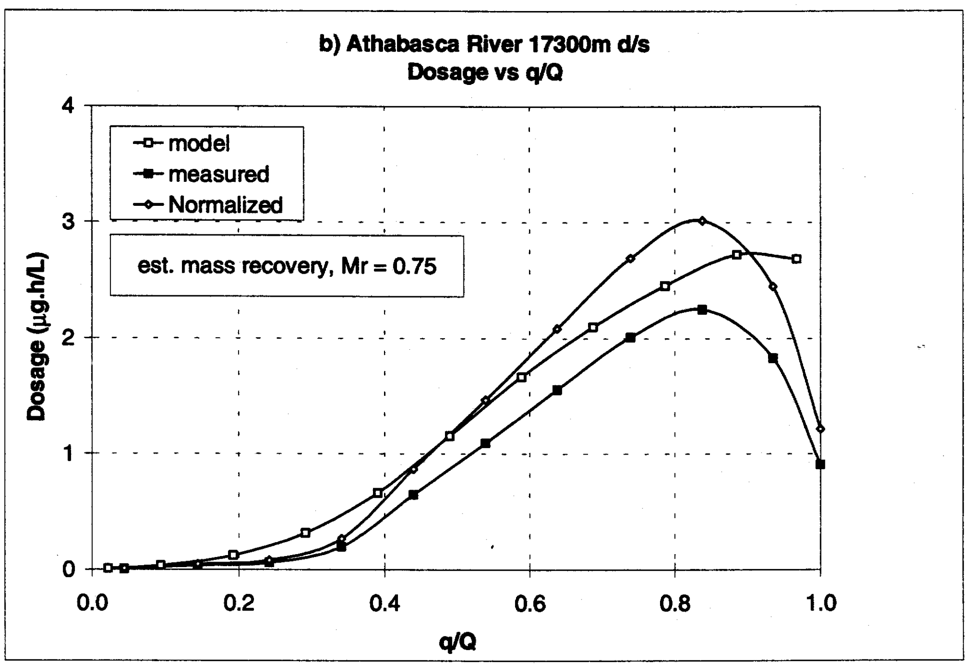

Figure 5.10 Tracer dimensionless dosage and model results, 876 m^3/s, open water slug input.

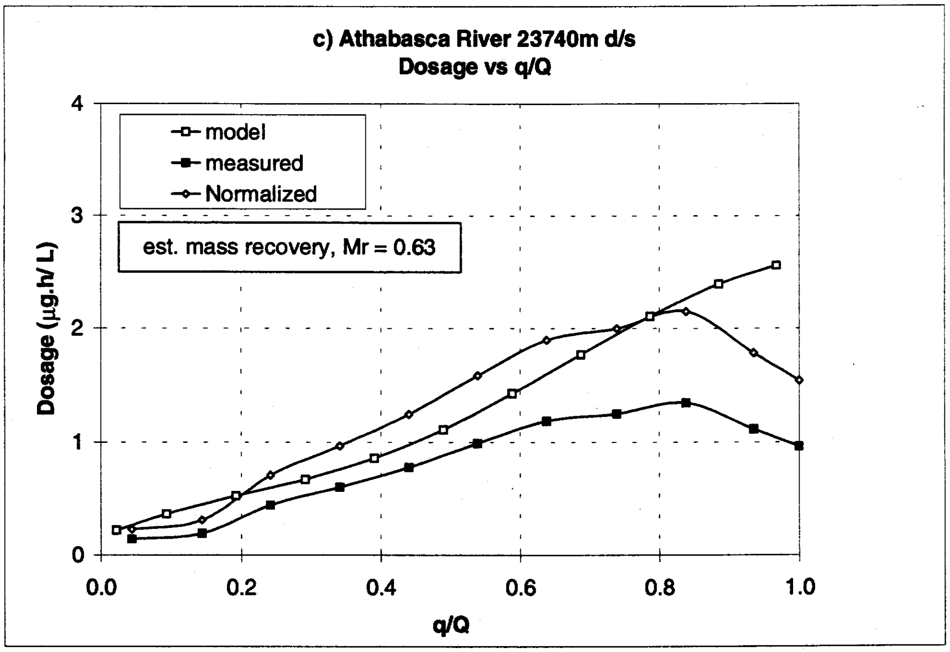

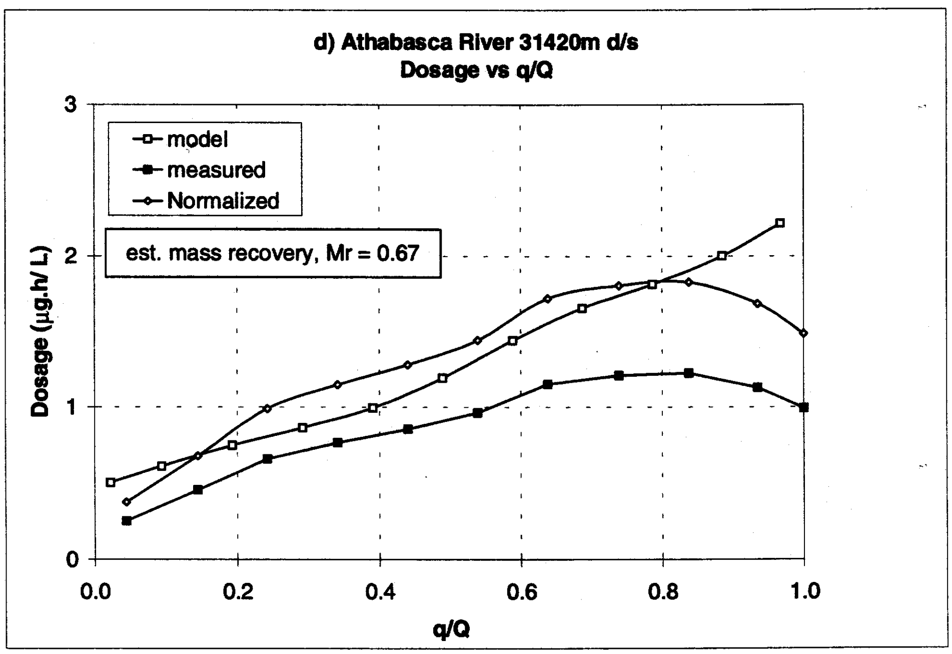

Figure 5.10 (*Contd.*)

5.3. Model Results

Values for the streamtube local depths, widths and slope and β, the local dimensionless mixing coefficients for each cross section were assembled into the GRIDGEN input file with the aid of the first preprocessing program STRMTUBE.

GRIDGEN was run making sure that PARM.DAT was located in the same directory. If the program runs properly, two output files RCHCHAR.OUT and SIMDIMS.OUT are created. The output files for GRIDGEN were then used as input files for 2DMIX after editing the RCHCHAR.OUT file. An additional file CONC.TXT used to simulate the discharge into the river is also needed to run 2DMIX.

After running 2DMIX, an output file named TIMECONC.DAT is be created. The output of the 2DMIX program is then used as input for XSLICE after editing RCHCHAR.OUT file once again. The output file LSLICE.DAT that is in text format is created after running XSLICE. These comprise of a series of concentration and time data pairs for each streamtube at the designated distance downstream. This is then imported into a spreadsheet. For the continuous tests, the data are reviewed to obtain the steady state concentrations. Steady state concentration in the spreadsheet is taken as the line in which the data does not change with time. These are then used to generate the various concentration or tracer-response curves. For the slug tests, the data are scanned and a range representing the passage of the slug is used to generate dosage or tracer response curves.

5.3.1. Continuous Input Modelling

5.3.1.1. 960 m^3/s Test

For the continuous test at 960 m^3/s, tracer samples were collected from 11 sections. The river channel was divided into 13 streamtubes with the following boundaries: q/Q= 0.021, 0.096, 0.190, 0.256, 0.309, 0.376, 0.458, 0.568, 0.661, 0.763, 0.886, 0.969 and 1.00, where q is the cumulative flow to a distance across the river channel and Q is the total river flow. Streamtube boundaries were chosen arbitrarily to obtain a good representation of the channel within the expected plume region. A time step of 60 seconds was chosen for the mixing calculations on the basis of stability criteria outlined by Putz (1996). The total injected mass was distributed within streamtubes no. 10 and 11 (i.e., q/Q= 0.661 to 0.886) over 430 time steps to simulate the length of time of the continuous injection. Mass was distributed in streamtubes no. 10 and 11 because they represent the length and location of the diffuser through which the dye mass was injected. Streamtube local depths, width, and slope at each cross section, and estimates of β, the local dimensionless mixing coefficient, were used for the generation of the numerical grid. Initial estimates of β were chosen arbitrarily based on the range of β values reported in the literature. In general, cross section coverage was sufficient to allow linear interpolation of depths and widths between surveyed sections.

Several computer simulations were conducted varying the magnitude of β along the river (i.e., longitudinal direction). The β value was held constant within each subreach (i.e. each sampled section) and transversely across the channel. Final values for β were selected by visual comparison of the model output to the normalized C'-q/Q curves. The mixing coefficient steadily increased as one moved further away from the injection point. The results of the model measurements are shown in Figures 5.3a to 5.3k. There was not much difference with the curves generated by the model over the first few sections close to the injection point. This might be because of their close proximity in the x-direction and therefore had limited time to mix. Comparison of the simulated and measured curves indicated that there is very good agreement except beyond 17.3 km downstream. This discrepancy might be due to the extra discharge from the La Biche River. Figures 5.3a to 5.3g shows that the maximum concentration occurs generally in the right bank region at $q/Q \approx 0.78$ as would have been expected from the fact that the injection source was located near $q/Q \approx 0.8$. However, Figures 5.3h to 5.3k show that the plume has crossed the river and encountered the left bank; the maximum has moved very close to the right bank (i.e. between $q/Q = 0.9$ to 1.0). This change begins around 21.15 km downstream.

5.3.1.2. 270 m^3/s Test

For the continuous test under a flow of 270 m^3/s, tracer samples were collected from 7 sections. The river channel was divided into 12 streamtubes with the following boundaries: q/Q = 0.019, 0.084, 0.143, 0.207, 0.273, 0.332, 0.414, 0.565, 0.712, 0.863, 0.965, and 1.00. A time step of 120 seconds was used. The injected mass was distributed in streamtubes 9 and 10 (i.e. q/Q = 0.712 to 0.863) over 720 time steps to simulate the length of time of the continuous injection. Mass was distributed in streamtubes no. 9 and 10 because they represent the length and location of the diffuser through which the dye was injected.

Additional sections were used in modelling the continuous test conducted at 270 m^3/s. The water level of sections from the 1997 surveys were adjusted to a flow of 270 m^3/s to obtain a better representation of the channel geometry. Also as in the 960 m^3/s test several computer simulations were conducted varying the magnitude of β along the river and final values for β were selected by visual comparison of the model output to the normalized C'-q/Q curves. The results of the tracer measurements are shown in Figures 5.4a to 5.4g.

Comparison of the simulated and measured curves indicated that there is very good agreement except at the section 4 km downstream. No concrete reason can be given since the test was conducted by Beak Consultants Ltd. Unlike in the 960 m^3/s flow continuous input test, the dilution effect due to the La Biche river inflow is not present in the analysis results. During this period the La Biche river flow was insignificant and had little or no dilution effect.

Figures 5.4a to 5.4f show that the maximum concentration occurs generally in the right bank region, as would have been expected from the fact that the injection source was located near q/Q $\approx$ 0.75.

5.3.1.3. 84 m^3/s Test

For the continuous test at a flow of 84 m^3/s, tracer samples were collected from 3 sections. The river channel was divided into 13 streamtubes with the following boundaries: q/Q = 0.029, 0.109, 0.189, 0.269, 0.349, 0.429, 0.509, 0.582, 0.692, 0.800, 0.880, 0.960 and 1.00. A time step of 360 seconds was used. The injected mass was distributed in streamtubes 8, 9, 10 and 11 (i.e. q/Q = 0.582 to 0.880) over 240 time steps to simulate the length of time of the continuous injection. Mass was distributed in streamtubes no. 8, 9, 10 and 11 because they represent the length and location of the diffuser through which the dye was injected. As in the 270 m^3/s flow, additional sections were used by water level adjustment of sections from the 1997 surveys to obtain better representation of the channel geometry.

As in the other simulations for the continuous test several computer runs were conducted varying the magnitude of β and final values for β were selected by visual comparison. The results of the tracer measurements are shown in Figures 5.5a to 5.5c. Comparison of the simulated and measured curves indicated that there is very good agreement. Similar to the 270 m^3/s flow continuous input test the La Biche River dilution effect was insignificant. Figure 5.5 shows that the maximum concentration occurs generally in the near right bank region, as in the 270 m^3/s test.

5.3.2. Slug Input Modelling (876 m^3/s Test)

For the slug test at a flow of 876 m^3/s, tracer samples were collected from 4 sections. The river channel was divided into ten streamtubes with the following boundaries: q/Q = 0.044, 0.143, 0.242, 0.341, 0.440, 0.539, 0.638, 0.737, 0.836, 0.935 and 1.00, where q is the cumulative flow to a distance across the river channel and Q is the total river flow. A time step of 60 seconds was chosen for the mixing calculations on the basis of stability criteria outlined by Beltaos and Arora (1988). The total injected mass was distributed within streamtube No. 8 (i.e., q/Q = 0.737 to 0.836) over the first time step to simulate a slug input.

5.3.2.1. Dosage Analysis

Computer simulations were conducted with different values of dimensionless mixing coefficient, β. Final values of the dimensionless mixing coefficient were chosen by visually comparing model and measured dosage plots. The dosage curves generated by the model for the selected β values are shown in Figure 5.10 together with the normalized measured dosage distribution at each sampling location. The vertical axis in the plots represents dimensionless dosage and the horizontal axis represents the dimensionless cumulative flow, q/Q. At 10.48 km there is a very good match between the model and the normalized dosage curve. In the other sections further downstream i.e. at 17.3 km, 23.74 km and 31.42 km the match is not as good as in the initial section. Figures 5.10a and 5.10b shows that the maximum concentration occurs generally in the near right bank region, as would have been expected from the fact that the dye was dumped near $q/Q \approx 0.8$.

5.3.2.2. C-t Analysis

The C-t curves generated by the model for the selected β values are shown in Figures 5.6 through 5.9 together with the normalized C-t distributions measured at each sampling location. At 10.48 km (Figure 5.7), it can be seen that model C-t curves have peak concentrations several times that of the normalized measurements. Figures 5.6a to 5.6e shows that the model peaks occur before the normalized measurements. This is a small translation in time, which is only approximately 10 minutes in approximately 3.25 hours, which is only a 5% error in travel time. The times of passage for the measured curves and the model curves are not that much different from one another. For instance time base of the curves at q/Q = 0.688 and 0.886 are almost identical.

At 17.3 km, the peak concentrations of the simulated and normalized measurement curves in the central portion of the river are close (see Figures 5.7a to 5.7d). The peak of the simulated curves still arrives before that of the normalized measurements. In the near right bank region at this same section, the peak concentrations of the simulated curves are higher than those of the normalized measurements and they also arrive earlier (see Figures 5.7e to 5.7g). As in the sections at 10.48 km, this is a small translation in time. In the central and near right bank regions, this translation is only approximately 10 and 20 minutes respectively in approximately 5 hours, which translates into a 3.3 to 6.7 % error in travel time.

In the near left bank region at 23.74km, there is very good agreement between the peaks and the time base of the simulated and measured waveforms (see Figures 5.8a to 5.8c). But towards the middle and near right bank region, the peaks of the simulated curves are higher than the measured and the time base of the simulated curves somewhat smaller (see Figures 5.8d to 5.8i). Despite these minor differences, the translation in time is about 10 to 15 minutes in 6.5 hours, which is only a 3 % error in travel time.

At 31.42km, there is very good agreement between the magnitude of the peaks and the time base of the concentration waveforms of both the simulated and normalized measurement curves. The peak of the normalized measurements tends to arrive before those of the simulated curves in the left and middle regions (see Figures 5.9a to 5.9h). This, as in most of the other sections represent a small translation in time, which is only approximately 25 minutes in approximately 8.5 hours, which translates into a 5 % error in travel time. In the near right bank region the peak of the normalized measurements are in good agreement with those of the simulated curves (see Figures 5.9i to 5.9k).

In general the match between the time bases of the modelled and measured waveforms is very good with no major differences. The time to peak and the time of passage are reasonable. The model appears to over estimate the peak at some of the sections. But this may be due to the fact that the actual peak may not have been captured in the sampling. There are minor discrepancies between the measured and simulated elapsed time to peak concentration. However, these discrepancies are small and generally less than 10%. This is well within the accuracy of streamflow measurements and the subsequent generation of the flow distribution at each cross section based upon these measurements.

Some of the discrepancy in the near right bank region might be as a result of dead zone effects. There are also a number of other factors that might have contributed to the discrepancies or poorer matches at some of the sections. Some of which might be:

a) Channel geometry and velocity distributions not being completely defined (i.e. poor streamtube characterization),

b) Interpolation of depths and velocities between measured sections not providing a completely accurate representation of the field conditions,

c) Minor time errors associated with designating an average sample time for all samples collected across a section during a particular sample run.

5.4 Dimensionless Mixing Coefficient (β)

The mixing model described earlier was used to determine appropriate values of the dimensionless mixing coefficient, β along the river reach for the prevailing flow conditions during the test. Values of β for each section along the study reach is selected on a trial and error basis. Several mixing simulations were conducted by varying the magnitude of β along the reach. The β value was held constant across the river channel. The β values input to the mixing model were adjusted to obtain what was considered to be the best fit to the normalized tracer concentrations (or dosage) at each transect. The best fit was assessed by visual comparison of the model output with the normalized measured dosage curve, the normalized C'-q/Q curves and the normalized C-t curves. E_z for open water condition is calculated by the model using β and local flow characteristics (i.e. h and u*). Whereas E_z for ice covered condition is calculated by the model using β and local flow characteristics (i.e. h for depth, h/2 for hydraulic radius in the expression for u*).

A plot of final β values used in each mixing simulation versus distance is shown in Figure 5.11. The dimensionless mixing coefficients used in the model are given in Table 5.4. The reach average β values for the 960 m^3/s, 876 m^3/s, 270 m^3/s and 84 m^3/s

flows are 0.34, 0.36, 0.48 and 0.48, respectively. These reach averages were calculated using a weighting approach based upon sub-reach lengths.

The trend of the model results for each of the flows suggests a step function increase in values of β with distance from the injection point (see Figure 5.11). However, values of β for the 960 m^3/s flow at about 5 km downstream deviated from this trend. There was also a very steep increase in β values for each of the flows at about 17 km downstream. This might be due to the influence of the La Biche River. Also an inverse linear relationship is observed between the different range of flows and the weighted average β values i.e. the higher the flow the lower the weighted average β value. The plot in Figure 5.12 shows this trend. The analysis indicates an overall reach-averaged value of 0.41.

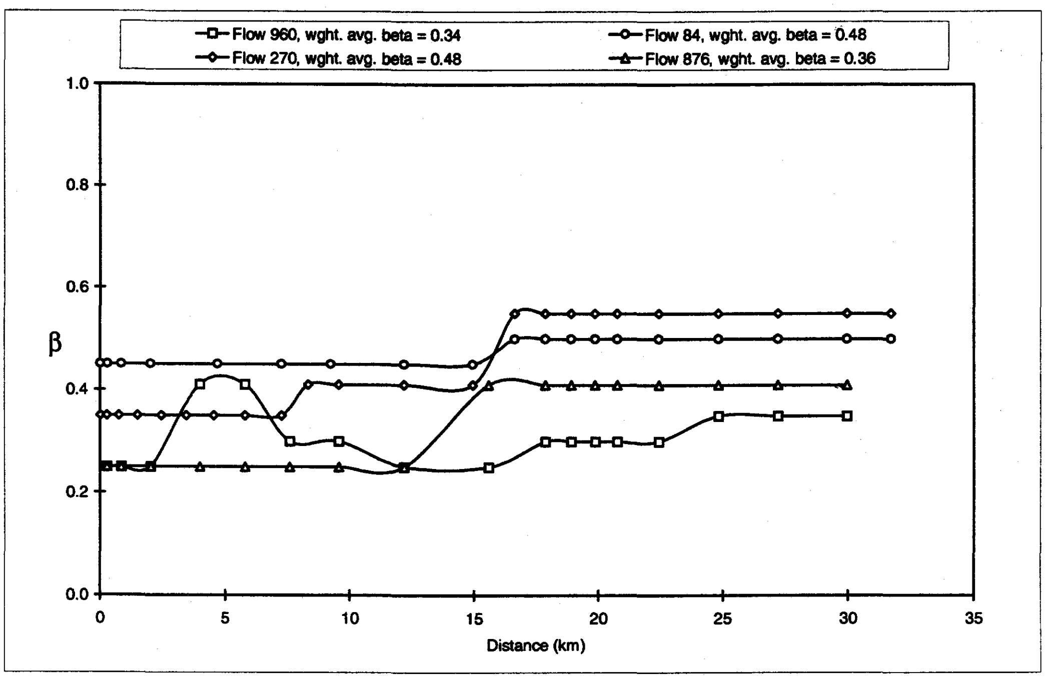

Figure 5.11 Dimensionless transverse mixing coefficient, β versus distance downstream, km.

Table 5.4 Dimensionless transverse mixing coefficients used in the model.

Flow (m^3/s)	Sub-reach (km)	β used
960	0 to 1.15	0.25
	2.895 to 5.095	0.41
	6.515 to 8.66	0.30
	10.48 to 13.9	0.25
	17.3 to 21.15	0.30
	23.74 to 28.51	0.35
	31.42	0.55
876	0 to 10.48	0.25
	13.9 to 28.51	0.41
	31.42	0.45
270	0 to 6.515	0.35
	6.515 to 16	0.41
	16 to 32	0.55
84	0 to 16	0.45
	16 to 32	0.50
	32	0.41

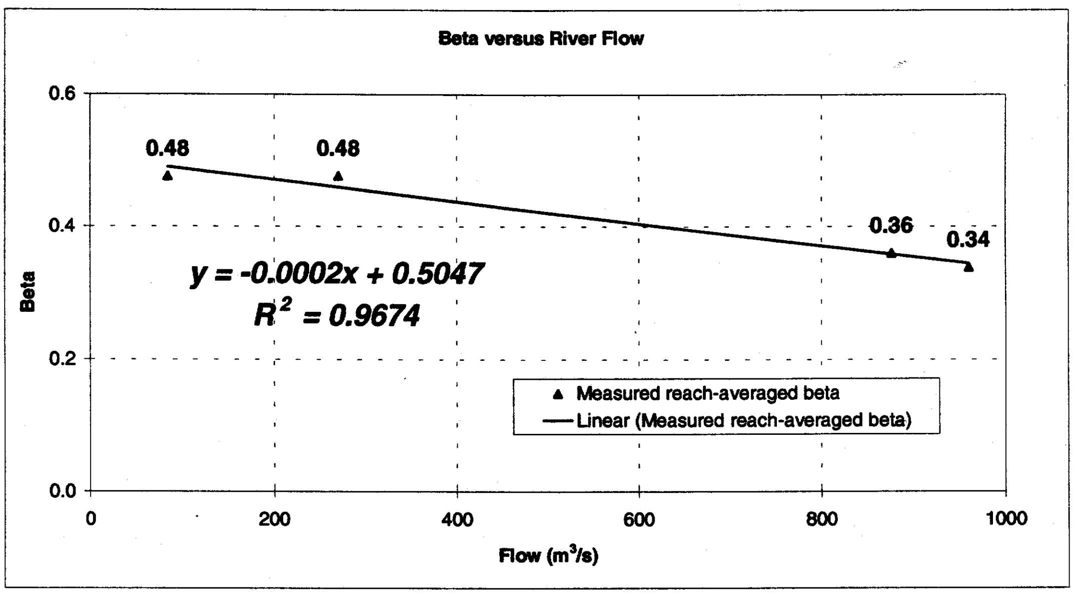

Figure 5.12 Plot showing the inverse relationship between β and different flows.

5.5 Discussion of Results

5.5.1 β Versus X and Q

The mixing model described in this thesis was used to determine appropriate values of β along the river reach for the prevailing flow conditions during each field test. E_z is calculated by the model using β and local flow characteristics. The final values of β used in the model were selected by visual comparison of the model output with the normalized concentration and dosage curves.

The plots of β versus distance shown in Figure 5.11 indicate there is some minor variation in the dimensionless mixing coefficient along the study reach. Values of β tended to increase with distance downstream. However reach-averaged β is fairly consistent (in the range of 0.34 to 0.48) for the range of flow conditions represented by the four tests. The overall weighted average of the different ranges of flow was found to be 0.41.

Figure 5.13 shows sample model plots of C' versus q/Q for maximum, minimum and overall average values of dimensionless mixing coefficients for the 960 m^3/s flow. From these plots it can be seen that there is not much difference in the model results for the range of β. These results demonstrate that β measured at one flow condition may be used with the appropriate flow parameters to estimate E_z for other flow conditions without causing significant errors.

The reach-averaged values of β for the two August 1997 tests are the same. The results show that β decreases as flow increases. This trend can be seen in Figure 5.12. Figure 5.12 also shows that there is a linear trend and that if several tests were available at a reach then this type of relationship could be used to predict β.

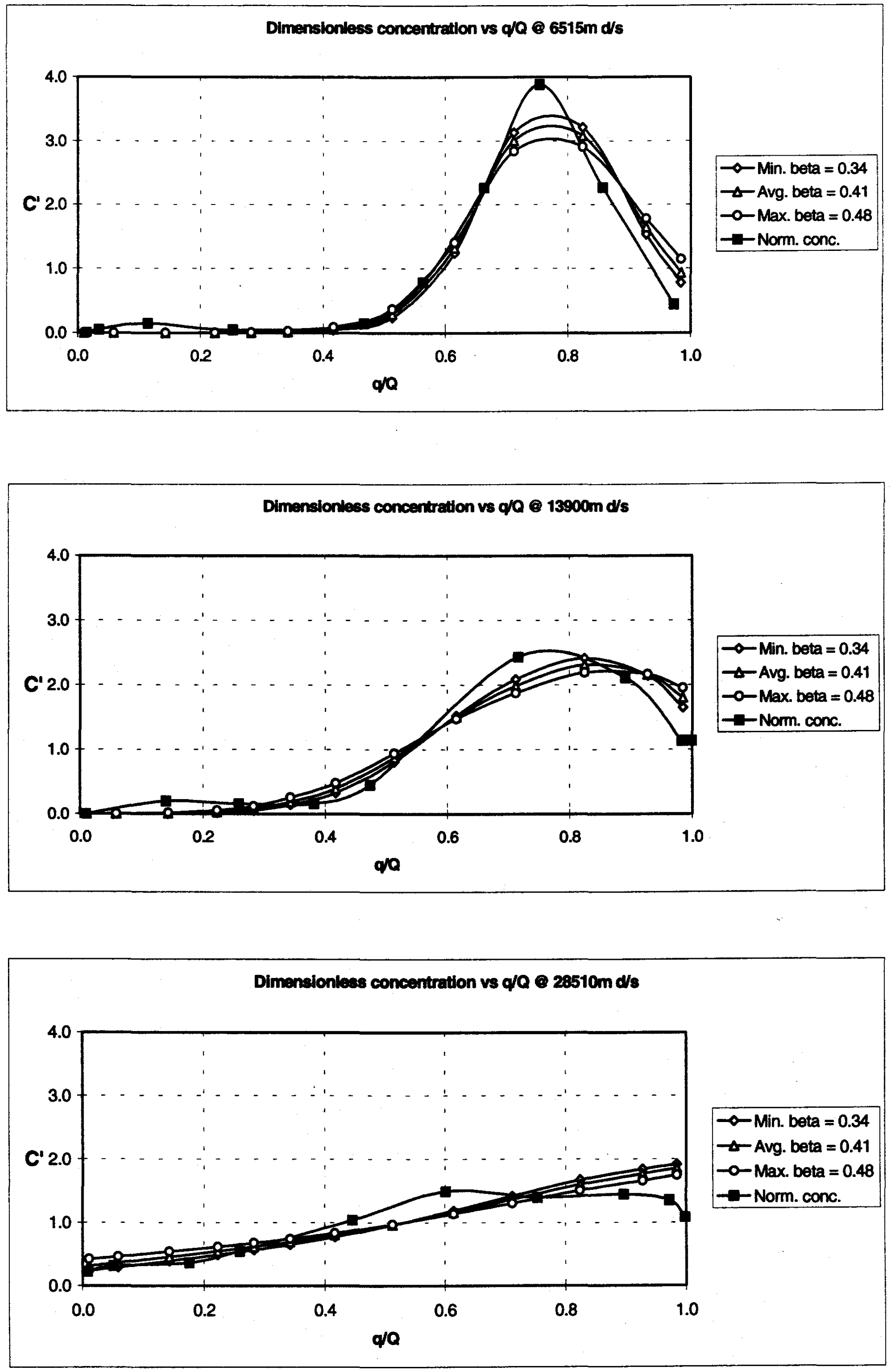

Figure 5.13 Plots comparing the effect of different β used for the 960 m^3/s test.

The values of β, which characterize the transverse mixing in this reach of the Athabasca River, fall well within the range of reported values of β from other studies. For example, compilations prepared by Elhadi et al. (1984) and Rutherford (1994) report a range of 0.22 to 3.3 and 0.12 to 3.4, respectively. In particular the values of β obtained in this study agree very closely with a reported reach-averaged value of $\beta = 0.41$ for the 40 km stretch of the Athabasca River immediately downstream of the town of Athabasca (Beltaos, 1978). This portion of the river is immediately upstream of the reach investigated in this study. Beltaos conducted this test on September 16th 1974 and the flow during the test was 566 m^3/s. Putting this flow into the linear equation in Figure 5.13 gives $\beta = 0.40$ which is a very good fit.

5.5.2 Effect of Tributary Inflow

Stream discharge is a factor that decreases the peak concentration of the tracer response curves. The diluting effect of tributary inflows, as well as that of natural ground water accretion, differs from river to river and with location on the same river. Figure 4.2 shows that two tributary streams enter the Athabasca River within the study reach. These are the La Biche River and Calling River at about 17.5 and 32 km downstream of the Alberta Pacific Forest Industries Inc. outfall respectively. This results in an increase in the main channel discharge. The relative contributions of these tributaries to the main channel flow are subject to fluctuations, depending upon the size, type, and meterologic conditions associated with the respective drainage basins. Because these tributaries are not gauged, accurately predicting tributary inflows is difficult.

The La Biche River in particular may have had an influence on the analysis results, especially during the August 1997 tests. Comparison of the simulated and measured curves for the August 1997 tests indicated that there is very good agreement except downstream of the confluence of the La Biche River in the near right region. Unlike in the August 1997 tests, the dilution effect due to the La Biche River inflow was found to have had little effect during the fall and winter tests. During this period the La Biche River flow was insignificant.

5.5.3 Effect of Ice Cover

Almost all of Canada's rivers and streams becomes ice covered in winter. The presence of an ice cover can cause substantial changes in the flow and mixing properties of a river. When an ice cover forms on a river, it almost doubles the wetted perimeter and invariably increases the total boundary shear. For a given discharge, the depth of flow will be larger than when the river had a free surface. The velocity, shear stress, and diffusivity distributions within the flow may all change. Therefore, the mixing characteristics of the river may also change.

Lau and Krishnappan (1981) found from their turbulence model calculations that the presence of an ice cover reduces the turbulent diffusive transport. Direct comparison of E_z values for open water and ice-covered conditions is not often possible because discharge values are quite different. However, Beltaos (1978) reported that the values of E_z/U_*H under ice cover are about the same as that for open water conditions.

Engmann and Kellerhals (1974) suggested that an ice cover reduces the mixing capacity of a stream in a way that the dimensionless coefficient $\beta = (E_z/R_hU_*)$ is about the same for both ice covered and open water conditions. However, Beltoas (1980) shows that values of β are smaller under ice cover than with open water flow by as much as two and one-half times. Lau and Krishnappan suggest the reduced mixing capacity is the result of increased aspect ratio under ice cover which, among other things, could be expected to reduce the transverse velocities at bends as suggested by Beltaos. However with present knowledge, conclusions on the effect of an ice cover on the value of dimensionless E_z cannot be drawn with any confidence.

The results of the analysis for this reach show little difference between values for dimensionless mixing coefficient, β, (non-dimensionalized using E_z/U^*h, where h is the local depth) obtained for the February 1995, ice-covered test and the October 1994, open water test.

5.5.4 Slug Input Modelling

There were some minor discrepancies in the elapsed time to peak concentration predicted by the model and that observed in the field. These discrepancies could easily be the result of gauging station error in reporting total flow or due to errors in representing the channel shape and the flow distribution.

The results shown in Figures 5.7 to 5.10 indicate the mixing model also does a reasonable job of predicting the time of passage of mass conservative parameters at a given location following an instantaneous discharge. It appears however that more spreading occurs in the downstream direction than is predicted by the model. This may be the result of inaccurate simulation of the input condition. For example, the tracer was dumped on the surface and may have initially spread very rapidly in the downstream direction as it was carried along by high velocities near the water surface. This would cause an initial spreading of the effluent mass in the downstream direction that is unaccounted for by the model. Further work is required to determine if this inaccuracy is the result of poor representation of the input conditions or if the model requires the incorporation of a downstream direction diffusion component.

6. CONCLUSIONS AND RECOMMENDATIONS

The values of the dimensionless mixing coefficient, β, indicates some variation along the study reach. However reach-averaged β is fairly consistent for the four tracer tests. These results demonstrate that β measured at one flow condition can be used with the appropriate flow parameters to estimate E_z for other flow conditions for the same reach. The values of β which, characterize the transverse mixing in the 32 km study reach of the Athabasca River, fall within the range of β values reported from other studies. The analysis also demonstrate a small linear decrease in β with discharge. The presence of ice cover did not seem to significantly affect the value of the dimensionless mixing coefficient, β when non-dimensionalized using E_z/U^*h (where h is the local depth).

The mixing simulations provide a very good representation of the measured concentration distributions and the mixing model utilized in this study, once calibrated, accurately simulates the distribution of mass conservative parameters resulting from a continuous input to a river (Figures 5.3 to 5.5).

The four field studies demonstrate that the AOG method can be applied to two-dimensional, steady and unsteady source mixing problems in the natural streams satisfactorily. Poor prediction of C-t distributions are mostly attributed to the influence of dead zones or backwater areas and so is not a drawback specific to the AOG method. It should be noted that the Advection Optimized Grid (AOG) method does not completely eliminate numerical errors. The method is still subject to numerical dispersion errors caused by transverse diffusion between nonaligned elements and the apparent forward movement of the mass by the concentration averaging within the elements.

However, this error can be controlled by limiting element dimensions to $\Delta x/ \Delta z < 10$ (Beltaos and Arora 1988). The field studies that have been described in this thesis further establish the validity of the use of the AOG method for two-dimensional modelling in natural channels. These studies also reinforced the point that there is a very large and necessary requirement for representative hydrometric data for two-dimensional modelling.

At present, the prediction of transverse mixing coefficients for natural streams using empirical equations is only satisfactory for preliminary calculations. The actual value of the transverse mixing coefficient at any location and flow condition should be accompanied with a tracer test to reduce this uncertainty. Additional research is therefore required to reliably and accurately predict the transverse mixing coefficient on the basis of easily measured channel geometry and flow parameters.

Despite the success in modelling the transverse mixing of a conservative tracer in this study caution must be employed when attempting to extrapolate results to other locations. The current uncertainty in estimating transverse mixing coefficients and the requirement of stream geometry and velocity data for both analytical and numerical solutions of effluent mixing often limit their utility to preliminary studies. It is believed that field mixing tests will continue to be desirable for the identification of plume regions for receiving water monitoring programs, assessment of effluent plume environmental impact and to aid in the establishment of site specific regulations regarding receiving and effluent water quality.

From this thesis it is apparent that the ability to deal with mixing problems is still hampered by inadequate knowledge of certain aspects of the mixing process. For field studies there are still uncertainties regarding the appropriate scales for non-dimensionalizing the transverse mixing coefficient, E_z. And questions as to which length scale (i.e., vertical or a horizontal length scale) that is more representative of the eddies involved in the mixing process still need to be addressed.

More research should be done toward improving the estimation of β. It is recommended that emphasis be laid on finding what parameters could be included in β to help characterize secondary flow and also to include a velocity measurement in the transverse direction. This should improve the efficacy of E_z as a 'catch all' parameter for describing the transverse mixing in a channel.

REFERENCES

Beak Consultants Ltd. 1995. Effluent plume delineation study for Alberta Pacific Forest Industries Inc. Beak Consultants Ltd., Reference 7.10610.1, Brampton, Ontario.

Beltaos, S. 1975. Evaluation of transverse mixing coefficients from slug tests. Journal of hydraulic Research, 13(4):351-360.

Beltaos, S. 1978. Transverse mixing in natural streams. Alberta Research Council, report SWE 78-1, Edmonton, Alberta.

Beltaos, S. 1979. Transverse mixing in natural streams. Canadian Journal of Civil Engineering, CSCE, Vol. 6, No. 4, pp. 575-591.

Beltoas, S. 1980. Mixing and effects of insecticides: a working hypothesis for an analytical model. in: Control of blackflies in the Athabasca River. Haufe, W.O. and Croome, G.C.R (ed.), Alberta Environment, Edmonton, Alberta, pp. 97-122.

Beltaos, S. and Charnetski, W. A. 1980. Mixing of insecticide: One-dimensional analysis of methoxychlor concentration data. In: Control of blackflies in the Athabasca River. Haufe, W.O. and Croome, G.C.R (ed.), Alberta Environment, Edmonton, Alberta, pp. 123-130.

Beltaos, S., and Arora, V.K. 1988. An explicit algorithm to simulate transient transverse mixing in rivers. Canadian Journal of Civil Engineering, 15(6):964-976.

Elder, J. W. 1959. The dispersion of marked fluid in turbulent shear flow. Journal of Fluid mechanics, 5(4), pp. 554-560.

Elhadi, N., Harrington, A., Hill, I., Lau, Y.L., and Krishnappan, B.G. 1984. River mixing - A state of the art report. Canadian Journal of Civil Engineering, 11(3):585-609.

Engmann, J. E. O., and Kellerhals, R. 1974. Transverse mixing in an ice covered river. Water Resources Research, 10(4), pp. 775-784.

Fischer, H. B. 1967. The mechanics of dispersion in natural streams. Journal of the Hydraulics Division, ASCE, 93, HY6, pp. 187-216.

Fischer, H. B. 1968. Methods for predicting dispersion coefficients in natural streams with applications to the lower reaches of the Green and Duwamish Rivers, Washington. United States Geological Survey, Professional paper, 582-A, Washington, D.C.

Fischer, H. B. 1972. A lagrangian method for predicting pollutant dispersion in Bolinas lagoon, Marin County, California. United States Geological Survey, Professional paper, 582-B, pp. b1-b32.

Fischer, H.B., 1973. Longitudinal dispersion and turbulent mixing in open channel flow, Annual review of fluid mechanics, Vol. 5, pp. 59-78.

Fischer, H.B., List, E. J., Koh, R. C. Y., Imberger, J., Brooks, N. H., 1979. Mixing in Inland and Coastal Waters, Academic Press, San Diego.

Glover, R.E. 1964. Dispersion of dissolved or suspended materials in flowing streams. United States geological Survey, professional paper 433-B.

Heslop, S. E., and Allen, C. M. 1989. Turbulence and dispersion in larger UK rivers. Proceedings international association for hydraulic research. Vol. 4 pp. D39-D44.

Holley, E. R., Abraham, G. 1973. Laboratory studies on transverse mixing in rivers. Journal of Hydraulic research, Vol. 11, pp. 219-253.

Holley, E. R., Siemons, J. and Abraham, G. 1972. Some aspects of analyzing transverse diffusion in rivers. Journal of Hydraulic research, Vol. 10. No. 1, pp. 27-57.

Holly, F.M. 1975. Two-dimensional mass dispersion in rivers. Hydrology papers, No. 78 Colorado State University, Fort Collins, Colorado.

Holley, F.M., and Nerat, G. 1984. Field calibration of stream-tube dispersion model. Journal of Hydraulic Engineering, 109 (11), pp. 1455-1470.

Jobson, H. E., 1997. Predicting travel time and dispersion in rivers and streams. Journal of Hydraulic Engineering. Vol. 123, No. 11, pp. 971-978.

Kellerhals, R., Neill, C. R. and Bray, D. I 1972. Hydraulic and geomorphic characteristics of rivers in Alberta. Alberta Research Council, River Engineering and Surface Hydrology Division, Report No. 72-1.

Larsson, R. 1989. Lateral mixing in open channels - the important processes. Proceedings International Association for Hydraulic Research. Vol. 4 pp. D39-D44.

Lau, Y. L. and Krishnappan, B.G. 1977. Transverse dispersion in rectangular channels. ASCE Journal of the Hydraulics Division, Vol. 103, HY10, pp. 1173-1189.

Lau, Y. L. and Krishnappan, B.G. 1981. Modelling transverse mixing in natural streams. ASCE Journal of the Hydraulics Division, Vol. 107, HY2, pp. 209-226.

Lau, Y. L. and Krishnappan, B.G. 1983. Users manual for model RIVMIX. National Water Research Institute, Environment Canada, Burlington, Ontario.

Luk, G.Y.K., Lau, Y.L., and Watt, W.E. 1990. Two-dimensional mixing in rivers with unsteady pollutant source. Journal of Environmental Engineering, 116(1):125-143.

Nokes, R. I. and Wood, I. R. 1988. Vertical and lateral turbulent dispersion in open channels. journal of Fluid Mechanics, Vol. 187, pp. 373-394.

Putz, G. 1983. Mixing and microorganism survival, Slave River, N.W.T. M.Sc. thesis, Department of Civil Engineering, University of Alberta, Edmonton, Alberta.

Putz, G. 1996. Dynamic two-dimensional river quality modeling, Ph.D. thesis, Department of Civil Engineering, University of Alberta, Edmonton, Alberta.

Putz, G., and Smith, D. W. 1998. Verification of a transient input, two-dimensional, river mixing model. Canadian journal of Civil Engineering, 25(1) pp. 51-66.

Rutherford, J.C. 1994. River Mixing. John Wiley and Sons, New York, New York.

Sayre, W. W., and Yeh, T. P. 1973. Transverse mixing characteristics of the Missouri river downstream of the cooper Nuclear station. Iowa Institute of Hydraulic Research, University of Iowa, Iowa city, IA, Report No. 145.

Smart, P. L., and Laidlaw, I. M. S. 1977. An evaluation of some fluorescent dyes for water tracing. Water Resources research, 13 (1), 15-33.

Smith, D. W. and Gerald, R. 1981. Mixing and microorganism survival in the Slave River N.W.T. Proceedings, American Society of Civil Engineers, New York, N. Y. pp. 555-569.

Snoeyink, V. L. and Jenkins, D. 1980. Water Chemistry. John Wiley and Sons, New York, New York.

Somlyody, L. 1982. An approach to the study of transverse mixing in streams. Journal of Hydraulic Research, 20, pp. 203-220.

Taylor, G. I. 1954. The dispersion of matter in turbulent flow through a pipe. Proceedings, Royal Society of London, Series A, Vol. 223, pp. 446-468.

Yotsukura, N., Fischer, H. B. and Sayre, W. W. 1970. Mixing characteristics of the Missouri River between Sioux City, Iowa and Platmouth, Nebraska. US geological survey, Water supply Paper, No. 1899-G.

Yotsukura, N., and Cobb, E.D. 1972. Transverse diffusion of solutes in natural streams. United States Geological Survey, Professional Paper, 582-C, pp. c1-c19.

Yotsukura, N., and Sayre, W. W. 1976. Transverse mixing in natural channels. Water Resources Research, 12(4), pp. 695-704.

Webel, G. and Schatzmann, M. 1984. Transverse mixing in open channel flow. Journal of hydraulic Engineering, ASCE, Vol. 110, No. 4, pp. 423-435.

APPENDIX A. Athabasca River Reach Characteristics at Different Flows

Appendix A.1 Athabasca River reach characteristics at 960 m^3/s and 876 m^3/s (characteristics for 876 m^3/s are shown in brackets)

Station (km)	Average width (m)	Average depth (m)	Average velocity (m/s)
0.00	273 (272)	2.89 (2.77)	1.21 (1.16)
0.55	338 (336)	2.46 (2.34)	1.15 (1.11)
1.15	395 (392)	2.27 (2.16)	1.07 (1.04)
2.895	426 (424)	2.12 (1.99)	1.06 (1.03)
5.095	467 (465)	2.15 (2.03)	0.96 (0.93)
6.515	248 (245)	2.69 (2.59)	1.44 (1.38)
8.660	465 (463)	2.16 (2.03)	0.96 (0.93)
10.48	415 (413)	2.38 (2.26)	0.97 (0.94)
13.90	240 (236)	2.99 (2.90)	1.33 (1.27)
17.30	253 (251)	3.22 (3.11)	1.18 (1.12)
18.46	212 (211)	3.23 (3.12)	1.40 (1.33)
19.37	233 (232)	3.36 (3.25)	1.23 (1.16)
20.39	267 (266)	3.16 (3.04)	1.14 (1.08)
21.15	209 (205)	3.31 (3.23)	1.39 (1.32)
23.74	251 (250)	3.27 (3.15)	1.17 (1.11)
25.92	221 (220)	3.39 (3.27)	1.28 (1.22)
28.51	291 (289)	3.29 (3.18)	1.00 (0.95)
31.42	227 (226)	3.11 (3.00)	1.36 (1.29)

Appendix A.2 Athabasca River reach characteristics at 270 m^3/s

Station (km)	Average width (m)	Average depth (m)	Average velocity (m/s)
0.05	257	1.72	0.61
0.5	325	1.20	0.69
1	337	1.31	0.61
2	350	1.29	0.6
4	212	1.23	1.03
8	334	1.48	0.55
16	251	1.42	0.76
32	203	1.95	0.68

Appendix A.3 Athabasca River reach characteristics at 84 m^3/s.

Station (km)	Average width (m)	Average depth (m)	Average velocity (m/s)
0.05	246.08	1.15	0.3
8	326.57	0.98	0.26
16	240.92	0.95	0.37
32	187.36	1.34	0.34

APPENDIX B. Cross Sections

Appendix B.1	**Athabasca River, 960 m^3/s, Open water, August 1997. Differences between 876 m^3/s and 960 m^3/s cross section characteristics are minor (see Appendix A.1), therefore only the 960 m^3/s cross sections are presented.**
Appendix B.2	**Athabasca River, 270 m^3/s, Open water, October 1994**
Appendix B.3	**Athabasca River, 84 m^3/s, Ice cover, February 1995**

Explanation of column headings

Sta. (m)	distance from the left bank.
Elev. (m)	estimated water surface elevation at the corresponding distance from the left bank.
h (m)	local flow depth.
w/W	width. This is the ratio of the distance from the left bank to the width of the river.
u (m/s)	local flow velocity in longitudinal direction. These velocities are estimated using an exponential relationship based on Manning's resistance equation.
DQ (m^3)	est. u * dA
Est. total	Σ DQ
q/Q	dimensionless cumulative flow
Area (m^2)	cumulative area
Adj. u (m/s)	adjusted velocity. When Σ *DQ* is different from the measured or gauge discharge, Q, the velocity is adjusted to account for the difference. (adj. u = (Q/Σ *DQ*) * est.u)

Appendix B.1 - Athabasca River, 960 m^3/s @ 0.0 km d/s

X-section:	Athabasca River, 0.0 km d/s (approx. 10 m d/s of diffuser)			
Date:	August 21, 1997			
Discharge (m^3/s) :	960.00	Estimated water surface elevation (m):		499.80
Width (m):	273.90	Left bank (LB) =	0.96	499.80
Mean depth (m):	2.89	Right bank (RB) =	274.87	499.80
Area (m^2):	790.78			
Mean velocity (m/s):	1.21			

Sta. (m)	Elev. (m)	h (m)	w/W	u (m/s)	DQ (m^3)	q/Q	Area (m^2)	adj. u (m/s)
0.96	499.80	0.00	0.000	0.000	0.00	0.000	0.00	0.000
7.23	498.46	1.33	0.023	0.724	1.51	0.002	4.17	0.707
20.09	497.62	2.17	0.070	1.005	19.48	0.021	26.70	0.980
30.80	497.10	2.69	0.109	1.159	28.19	0.050	52.76	1.130
43.67	496.73	3.07	0.156	1.264	44.90	0.096	89.83	1.233
53.54	496.97	2.82	0.192	1.196	35.75	0.132	118.89	1.166
70.63	496.99	2.80	0.254	1.190	57.33	0.190	166.95	1.161
88.81	496.78	3.02	0.321	1.250	64.55	0.256	219.86	1.219
103.26	496.89	2.91	0.373	1.219	52.81	0.309	262.63	1.189
123.33	497.17	2.63	0.447	1.140	65.51	0.376	318.16	1.112
131.35	497.15	2.64	0.476	1.144	24.13	0.400	339.29	1.116
147.17	496.58	3.21	0.534	1.303	56.63	0.458	385.58	1.271
160.24	496.29	3.50	0.582	1.381	58.87	0.518	429.44	1.347
171.47	496.65	3.15	0.623	1.286	49.77	0.568	466.77	1.254
192.91	496.45	3.35	0.701	1.339	91.32	0.661	536.35	1.306
199.37	496.39	3.41	0.724	1.355	29.37	0.691	558.15	1.322
208.26	495.92	3.88	0.757	1.478	45.87	0.738	590.53	1.442
212.75	496.02	3.78	0.773	1.452	25.17	0.763	607.71	1.416
226.65	496.33	3.47	0.824	1.372	71.09	0.835	658.05	1.339
236.91	496.25	3.55	0.861	1.392	49.76	0.886	694.05	1.358
238.21	496.24	3.55	0.866	1.395	6.43	0.893	698.66	1.360
240.94	496.47	3.32	0.876	1.334	12.81	0.906	708.05	1.301
248.41	497.10	2.69	0.903	1.159	28.00	0.934	730.52	1.130
258.90	496.89	2.91	0.942	1.219	34.93	0.969	759.89	1.189
269.64	497.88	1.91	0.981	0.923	27.72	0.998	785.76	0.900
274.87	499.80	0.00	1.000	0.000	2.31	1.000	790.78	0.000
			Est. total =		984.19			

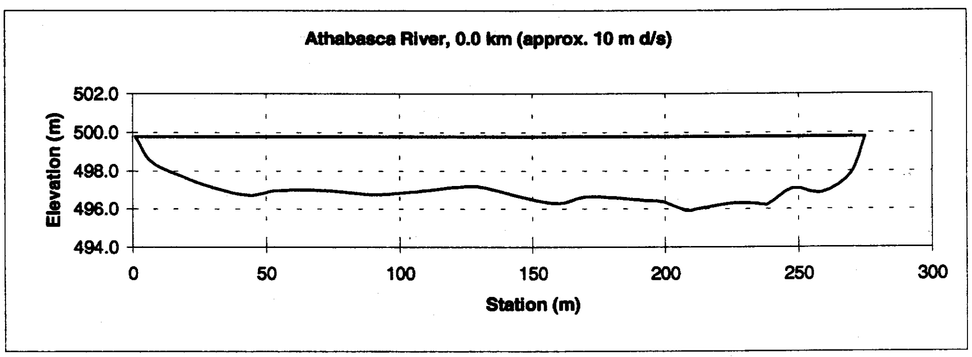

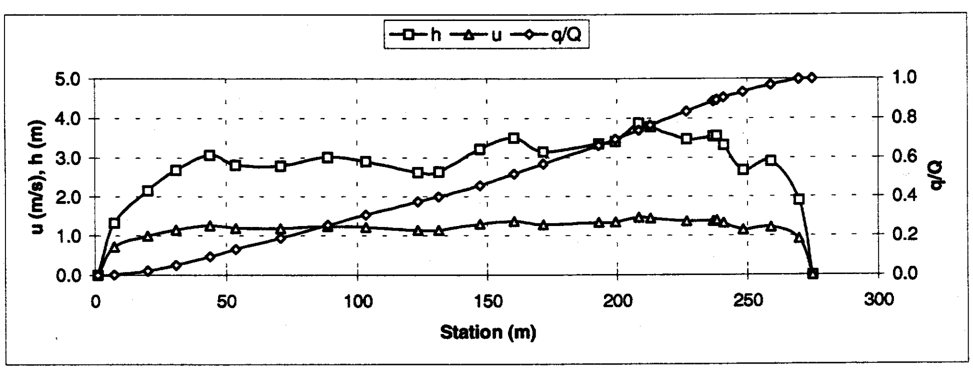

Appendix B.1 - Athabasca River, 960 m^3/s @ 0.55 km d/s

X-section:	Athabasca River, 0.55 km d/s				
Date:	August 21, 1997				
Discharge (m^3/s) :	960.00	Estimated water surface elevation (m):		499.80
Width (m):	338.02	Left bank (LB) =	0.80	499.80
Mean depth (m):	2.46	Right bank (RB) =	338.81	499.80
Area (m^2):	832.42			
Mean velocity (m/s):	1.15			

Sta. (m)	Elev. (m)	h (m)	w/W	u (m/s)	DQ (m^3)	q/Q	Area (m^2)	adj. u (m/s)
0.80	499.80	0.00	0.000	0.000	0.00	0.000	0.00	0.000
4.06	498.98	0.82	0.010	0.553	0.37	0.000	1.33	0.544
35.10	496.78	3.02	0.101	1.322	55.85	0.058	60.92	1.302
41.98	497.04	2.76	0.122	1.245	25.54	0.084	80.82	1.226
58.67	497.21	2.59	0.171	1.192	54.38	0.140	125.45	1.174
80.22	497.49	2.31	0.235	1.105	60.55	0.202	178.19	1.088
111.46	497.56	2.24	0.327	1.084	77.81	0.282	249.30	1.067
142.01	497.49	2.31	0.418	1.105	76.07	0.360	318.83	1.088
173.56	497.04	2.76	0.511	1.245	93.97	0.456	398.82	1.226
196.83	497.32	2.48	0.580	1.160	73.37	0.531	459.84	1.142
204.37	496.97	2.83	0.602	1.264	24.28	0.556	479.87	1.245
211.27	496.56	3.24	0.623	1.383	27.67	0.585	500.77	1.363
240.82	497.43	2.37	0.710	1.125	103.95	0.691	583.65	1.108
259.59	496.99	2.81	0.766	1.259	57.93	0.751	632.25	1.240
273.40	497.43	2.37	0.806	1.125	42.63	0.794	668.03	1.108
276.84	497.30	2.50	0.817	1.166	9.60	0.804	676.40	1.148
288.08	496.62	3.18	0.850	1.369	40.51	0.846	708.37	1.348
299.32	496.83	2.97	0.883	1.307	46.25	0.893	742.95	1.287
303.87	496.65	3.15	0.897	1.359	18.55	0.912	756.86	1.339
307.75	496.18	3.62	0.908	1.490	18.72	0.932	770.00	1.468
330.23	498.40	1.40	0.975	0.792	64.36	0.998	826.40	0.780
338.81	499.80	0.00	1.000	0.000	2.38	1.000	832.42	0.000
			Est. total =		974.74			

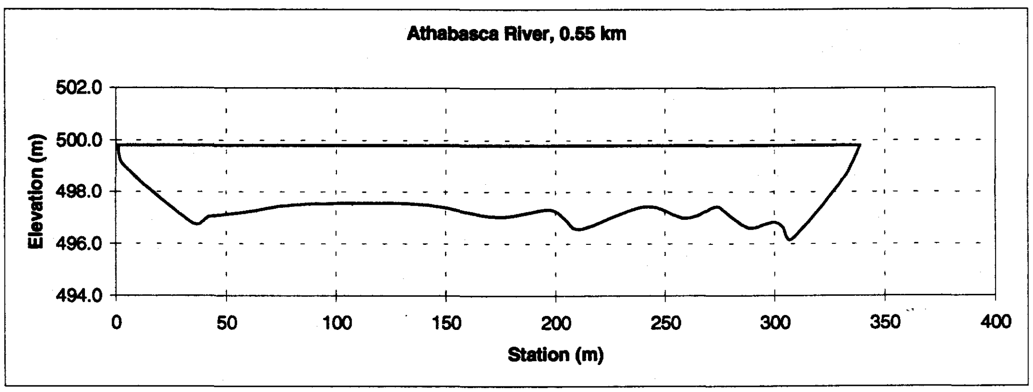

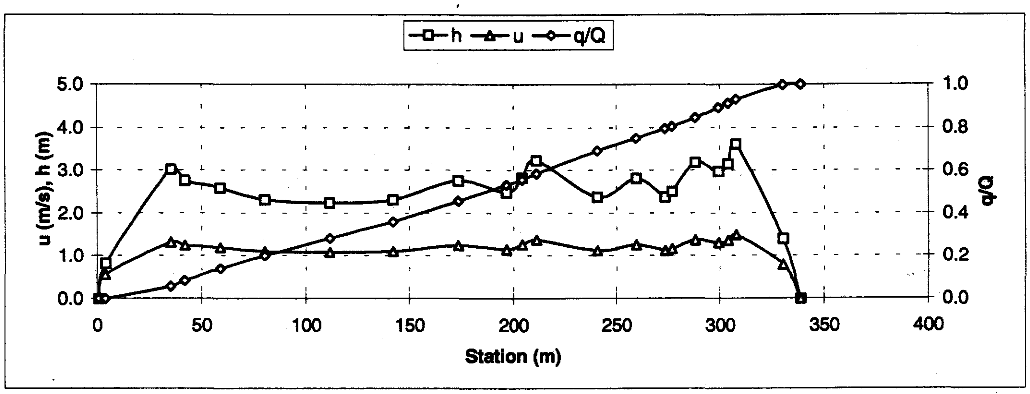

Appendix B.1 - Athabasca River, 960 m^3/s @ 1.15 km d/s

X-section:	Athabasca River, 1.15 km d/s			
Date:	August 21, 1997			
Discharge (m^3/s) :	960.00	Estimated water surface elevation (m):		499.80
Width (m):	395.91	Left bank (LB) =	1.43	499.80
Mean depth (m):	2.27	Right bank (RB) =	397.34	499.80
Area (m^2):	897.51			
Mean velocity (m/s):	1.07			

Sta. (m)	Elev. (m)	h (m)	w/W	u (m/s)	DQ (m^3)	q/Q	Area (m^2)	adj. u (m/s)
1.43	499.80	0.00	0.000	0.000	0.00	0.000	0.00	0.000
7.73	498.92	0.88	0.016	0.570	0.79	0.001	2.78	0.534
20.57	498.29	1.51	0.048	0.816	10.66	0.011	18.15	0.765
37.54	497.36	2.44	0.091	1.123	32.48	0.043	51.66	1.052
50.65	497.54	2.26	0.124	1.068	33.76	0.076	82.48	1.001
66.42	497.36	2.44	0.164	1.123	40.61	0.115	119.55	1.052
80.50	496.34	3.46	0.200	1.417	52.68	0.167	161.03	1.328
102.41	496.45	3.35	0.255	1.387	104.44	0.269	235.54	1.299
117.60	496.24	3.56	0.293	1.445	74.24	0.341	287.97	1.354
138.93	496.78	3.02	0.347	1.295	96.18	0.435	358.16	1.214
173.98	497.17	2.63	0.436	1.182	122.73	0.555	457.25	1.108
188.08	497.32	2.48	0.471	1.137	41.79	0.596	493.30	1.065
208.52	496.91	2.89	0.523	1.258	65.78	0.660	548.24	1.179
235.76	497.23	2.57	0.592	1.162	89.98	0.748	622.59	1.089
263.09	497.62	2.18	0.661	1.042	71.48	0.818	687.46	0.976
295.92	497.62	2.18	0.744	1.042	74.50	0.890	758.97	0.976
328.68	498.27	1.53	0.827	0.823	56.64	0.946	819.72	0.771
355.57	498.33	1.47	0.895	0.800	32.70	0.978	860.03	0.749
381.58	498.92	0.88	0.960	0.570	20.91	0.998	890.56	0.534
397.34	499.80	0.00	1.000	0.000	1.98	1.000	897.51	0.000
			Est. total =		1024.34			

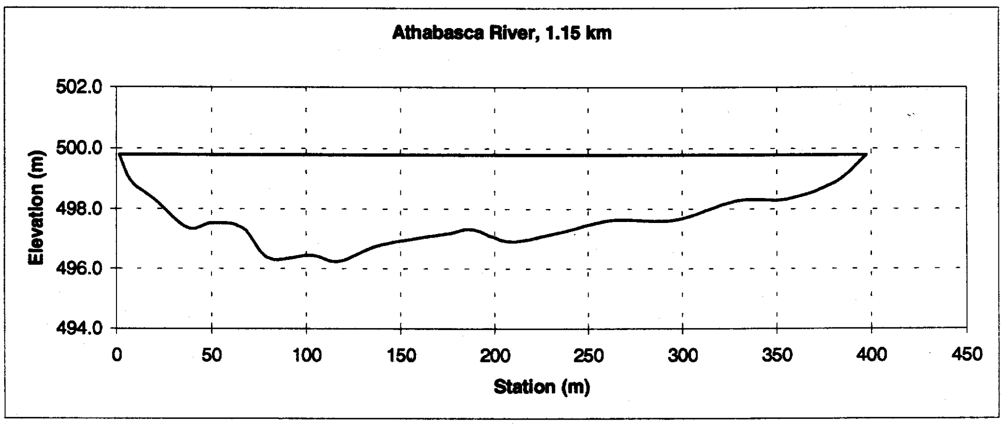

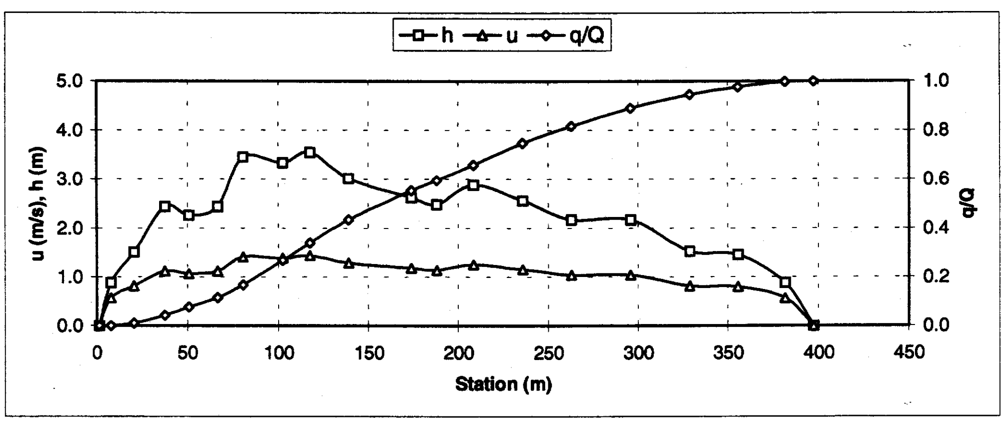

Appendix B.1 - Athabasca River, 960 m^3/s @ 2.895 km d/s

X-section:	Athabasca River, 2.895 km d/s		
Date:	August 21, 1997		
Discharge (m^3/s) :	960.00	Estimated water surface elevation (m):	499.80
Width (m):	426.00	Left bank (LB) = 0.59	499.80
Mean depth (m):	2.12	Right bank (RB) = 426.59	499.80
Area (m^2):	902.39		
Mean velocity (m/s):	1.06		

Sta. (m)	Elev. (m)	h (m)	w/W	u (m/s)	DQ (m^3)	q/Q	Area (m^2)	adj. U (m/s)
0.59	499.80	0.00	0.000	0.000	0.00	0.000	0.00	0.000
3.55	498.79	1.01	0.007	0.650	0.49	0.000	1.50	0.623
26.44	498.20	1.60	0.061	0.881	22.84	0.023	31.35	0.844
48.63	498.27	1.53	0.113	0.857	30.12	0.053	66.03	0.821
75.94	498.40	1.40	0.177	0.807	33.30	0.087	106.06	0.774
102.70	498.27	1.53	0.240	0.857	32.64	0.119	145.29	0.821
121.03	498.24	1.56	0.283	0.869	24.45	0.144	173.64	0.833
139.86	498.20	1.60	0.327	0.881	26.01	0.170	203.38	0.844
177.76	497.75	2.05	0.416	1.041	66.34	0.236	272.44	0.997
201.46	497.75	2.05	0.472	1.041	50.53	0.286	321.00	0.997
208.45	497.49	2.31	0.488	1.127	16.50	0.303	336.23	1.080
225.17	497.43	2.37	0.527	1.148	44.51	0.347	375.37	1.100
239.39	497.17	2.63	0.561	1.230	42.30	0.389	410.95	1.179
258.17	497.43	2.37	0.605	1.148	55.88	0.445	457.96	1.100
280.15	497.30	2.50	0.656	1.189	62.60	0.508	511.54	1.140
321.55	497.10	2.70	0.753	1.250	131.25	0.639	619.17	1.198
351.97	496.67	3.13	0.825	1.381	116.62	0.755	707.84	1.323
368.11	496.91	2.89	0.863	1.309	65.39	0.820	756.46	1.255
401.49	496.78	3.02	0.941	1.348	131.11	0.951	855.13	1.292
414.68	497.62	2.18	0.972	1.084	41.69	0.993	889.42	1.039
426.59	499.80	0.00	1.000	0.000	7.03	1.000	902.39	0.000
			Est. total =		1001.60			

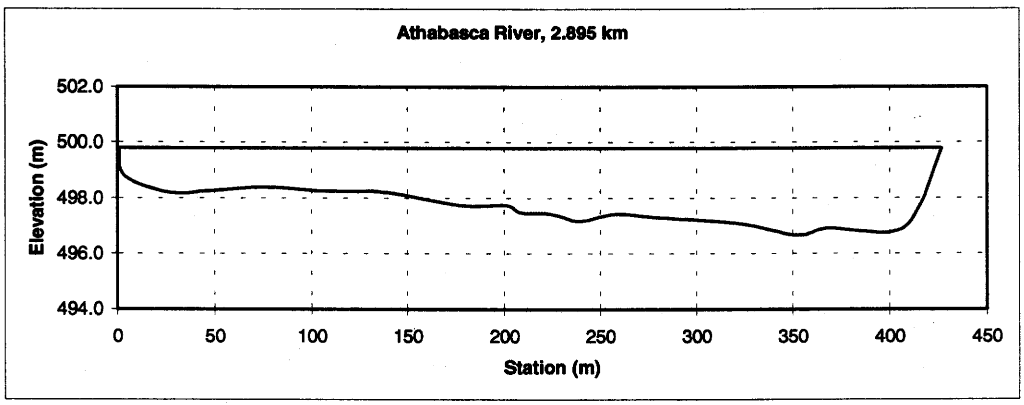

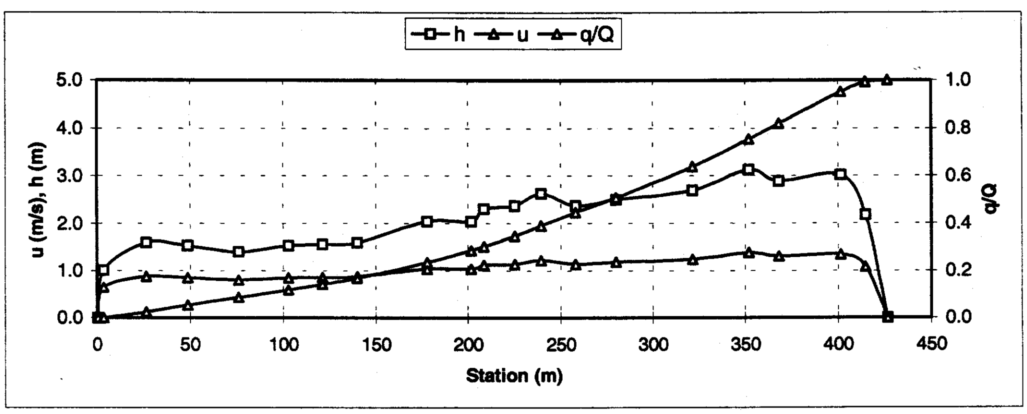

Appendix B.1 - Athabasca River, 960 m^3/s @ 5.095 km d/s

X-section:	Athabasca River, 5.095 km d/s			
Date:	August 21, 1997			
Discharge (m^3/s) :	960.00	Estimated water surface elevation (m):		499.80
Width (m):	467.54	Left bank (LB) =	2.02	499.80
Mean depth (m):	2.15	Right bank (RB) =	469.57	499.80
Area (m^2):	1003.29			
Mean velocity (m/s):	0.96			

Sta. (m)	Elev. (m)	h (m)	w/W	u (m/s)	DQ (m^3)	q/Q	Area (m^2)	adj. U (m/s)
2.02	499.80	0.00	0.000	0.000	0.00	0.000	0.00	0.000
13.57	498.66	1.14	0.025	0.628	2.07	0.002	6.59	0.609
24.91	497.32	2.48	0.049	1.055	17.29	0.020	27.15	1.022
42.34	498.14	1.66	0.086	0.806	33.61	0.053	63.26	0.781
48.41	498.19	1.61	0.099	0.792	7.94	0.061	73.20	0.767
71.64	497.43	2.37	0.149	1.023	42.04	0.104	119.52	0.992
107.83	497.10	2.70	0.226	1.115	98.08	0.203	211.28	1.080
125.88	496.99	2.81	0.265	1.145	56.10	0.260	260.94	1.109
143.96	496.84	2.96	0.304	1.185	60.69	0.321	313.05	1.148
177.69	497.04	2.76	0.376	1.132	111.74	0.434	409.49	1.097
211.73	498.01	1.79	0.449	0.848	76.70	0.511	486.96	0.822
239.20	498.33	1.47	0.507	0.742	35.55	0.547	531.68	0.719
266.11	498.27	1.53	0.565	0.764	30.35	0.578	571.99	0.740
306.16	498.14	1.66	0.650	0.806	50.17	0.628	635.89	0.781
345.76	497.95	1.85	0.735	0.868	58.27	0.687	705.49	0.841
398.95	496.91	2.89	0.849	1.167	128.47	0.817	831.71	1.131
410.58	496.99	2.81	0.874	1.145	38.33	0.855	864.86	1.109
452.53	497.10	2.70	0.964	1.115	130.41	0.987	980.31	1.080
469.57	499.80	0.00	1.000	0.000	12.81	1.000	1003.29	0.000
			Est. total =		990.60			

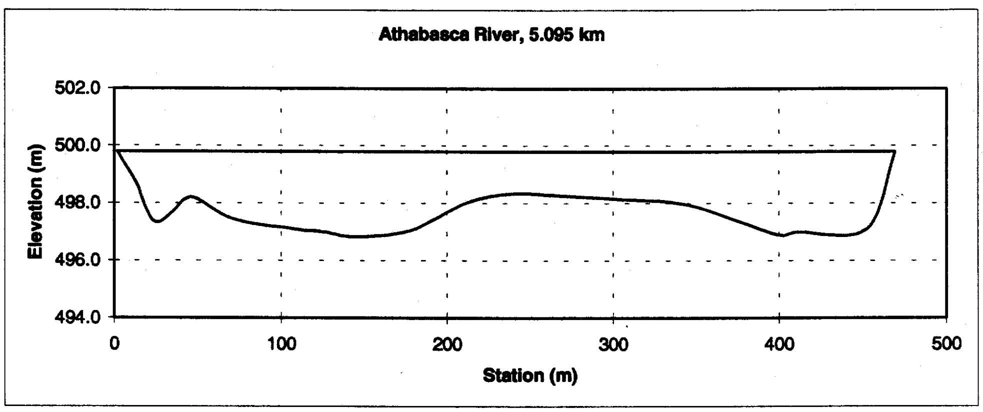

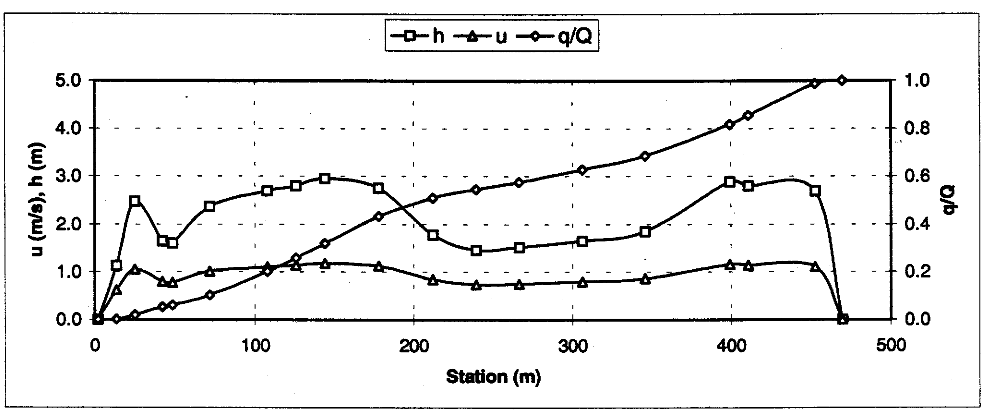

Appendix B.1 - Athabasca River, 960 m^3/s @ 6.515 km d/s

X-section:	Athabasca River, 6.515 km d/s			
Date:	August 21, 1997			
Discharge (m^3/s) :	960.00	Estimated water surface elevation (m):		499.80
Width (m):	248.44	Left bank (LB) =	1.95	499.80
Mean depth (m):	2.69	Right bank (RB) =	250.39	499.80
Area (m^2):	667.82			
Mean velocity (m/s):	1.44			

Sta. (m)	Elev. (m)	h (m)	w/W	u (m/s)	DQ (m^3)	q/Q	Area (m^2)	adj. U (m/s)
1.95	499.80	0.00	0.000	0.000	0.00	0.000	0.00	0.000
16.25	498.33	1.47	0.058	0.959	5.03	0.005	10.48	0.901
36.06	497.36	2.44	0.137	1.347	44.58	0.049	49.14	1.264
45.71	497.38	2.42	0.176	1.342	31.56	0.079	72.61	1.260
56.69	496.91	2.89	0.220	1.509	41.60	0.120	101.79	1.417
69.30	496.34	3.46	0.271	1.700	64.23	0.183	141.82	1.596
79.29	496.65	3.15	0.311	1.598	54.41	0.236	174.82	1.500
101.14	496.52	3.28	0.399	1.642	113.81	0.347	245.08	1.541
121.86	496.26	3.54	0.483	1.727	119.05	0.464	315.75	1.621
142.65	496.13	3.67	0.566	1.769	131.00	0.592	390.69	1.661
154.76	496.67	3.13	0.615	1.592	69.18	0.660	431.86	1.494
166.91	496.52	3.28	0.664	1.642	62.98	0.721	470.82	1.541
180.72	496.94	2.86	0.720	1.498	66.55	0.786	513.21	1.406
191.10	496.78	3.02	0.761	1.554	46.59	0.832	543.73	1.459
201.13	496.13	3.67	0.802	1.769	55.74	0.886	577.28	1.661
212.78	496.91	2.89	0.849	1.509	62.67	0.948	615.51	1.417
234.96	498.72	1.08	0.938	0.781	50.39	0.997	659.51	0.733
250.39	499.80	0.00	1.000	0.000	3.25	1.000	667.82	0.000
			Est. total =		1022.60			

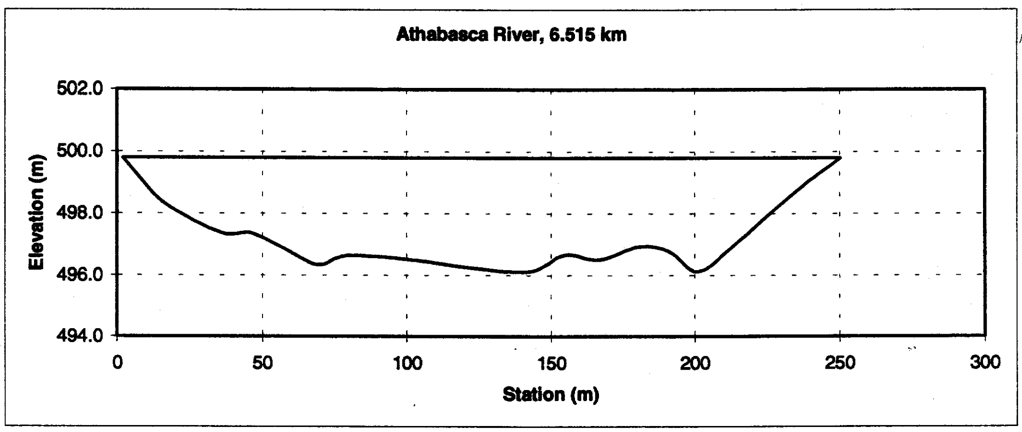

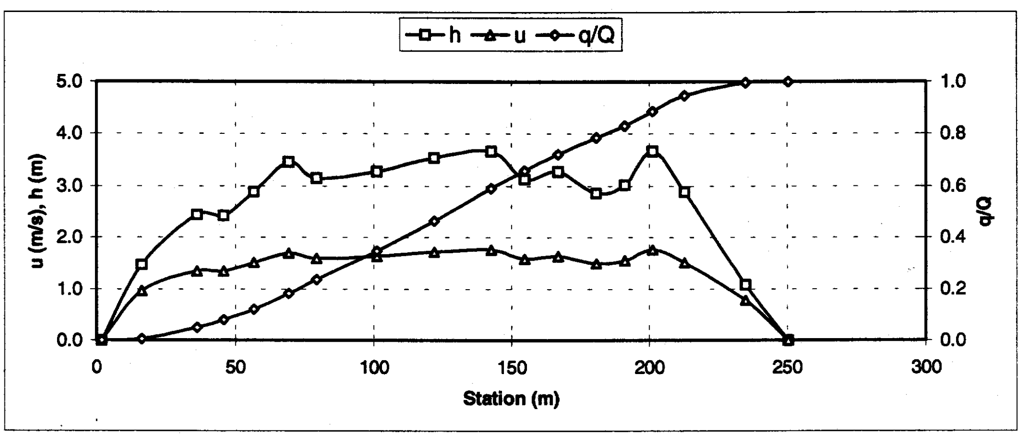

Appendix B.1 – Athabasca River, 960 m^3/s @ 8.66 km d/s

X-section:	Athabasca River, 8.66 km d/s			
Date:	August 21, 1997			
Discharge (m^3/s) :	960.00	Estimated water surface elevation (m):		499.80
Width (m):	465.82	Left bank (LB) =	1.11	499.80
Mean depth (m):	2.16	Right bank (RB) =	466.93	499.80
Area (m^2):	1004.00			
Mean velocity (m/s):	0.96			

Sta. (m)	Elev. (m)	h (m)	w/W	u (m/s)	DQ (m^3)	q/Q	Area (m^2)	adj. U (m/s)
1.11	499.80	0.00	0.000	0.000	0.00	0.000	0.00	0.000
7.77	498.59	1.21	0.014	0.649	1.31	0.001	4.02	0.608
30.92	498.07	1.73	0.064	0.824	25.00	0.026	37.95	0.771
33.49	497.75	2.05	0.070	0.924	4.24	0.030	42.80	0.865
44.56	497.82	1.98	0.093	0.905	20.42	0.050	65.13	0.847
63.39	497.54	2.26	0.134	0.988	37.84	0.087	105.11	0.924
81.71	497.88	1.92	0.173	0.885	35.87	0.122	143.42	0.828
126.92	497.88	1.92	0.270	0.885	76.80	0.196	230.20	0.828
150.27	498.29	1.51	0.320	0.755	32.84	0.228	270.26	0.706
173.12	498.27	1.53	0.369	0.761	26.33	0.254	305.01	0.712
200.60	498.14	1.66	0.428	0.803	34.29	0.287	348.84	0.752
227.52	498.07	1.73	0.486	0.824	37.08	0.324	394.41	0.771
261.55	497.95	1.85	0.559	0.865	51.45	0.374	455.33	0.809
295.69	497.69	2.11	0.632	0.944	61.27	0.434	523.08	0.883
334.94	497.04	2.76	0.717	1.128	99.13	0.530	618.76	1.056
374.55	496.33	3.47	0.802	1.315	150.89	0.677	742.28	1.230
395.26	496.07	3.73	0.846	1.380	100.56	0.775	816.93	1.291
416.28	495.74	4.06	0.891	1.458	116.19	0.888	898.81	1.365
424.63	495.48	4.32	0.909	1.520	52.09	0.939	933.80	1.422
435.57	498.40	1.40	0.933	0.717	35.00	0.973	965.08	0.671
443.17	497.86	1.94	0.949	0.891	10.20	0.983	977.77	0.834
455.44	498.59	1.21	0.975	0.649	14.87	0.998	997.07	0.608
466.93	499.80	0.00	1.000	0.000	2.25	1.000	1004.00	0.000
			Est. total =		1025.92			

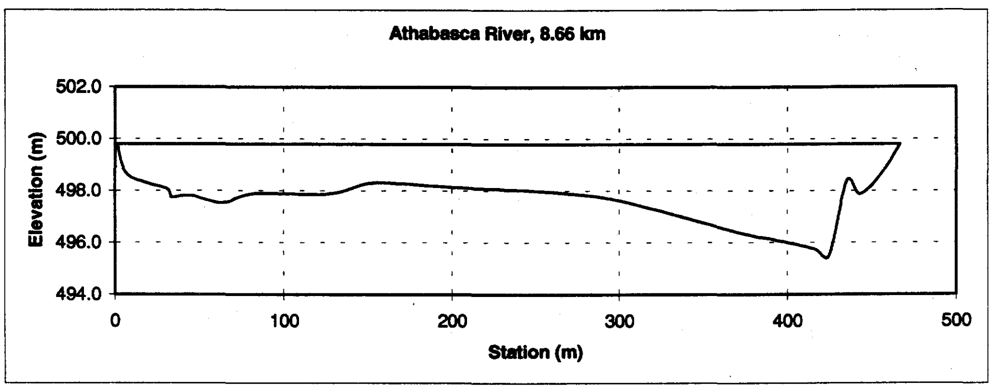

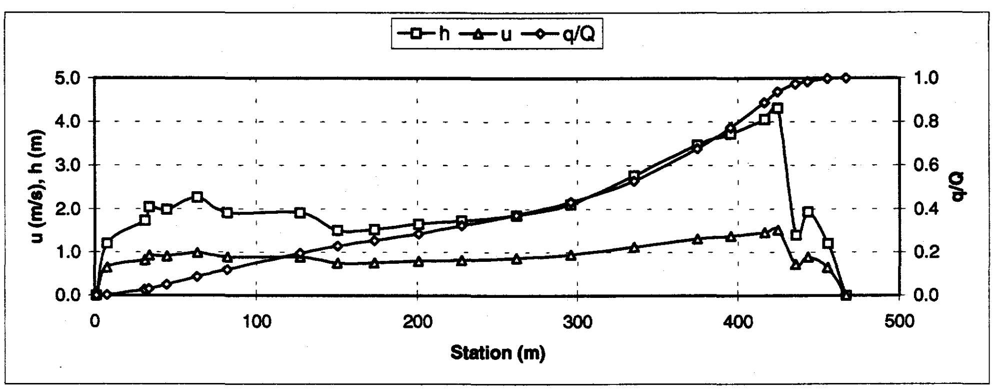

Appendix B.1 – Athabasca River, 960 m³/s @ 10.48 km d/s

X-section:	Athabasca River, 10.48 km d/s			
Date:	August 21, 1997			
Discharge (m^3/s) :	960.00	Estimated water surface elevation (m):		499.80
Width (m):	415.64	Left bank (LB) =	1.35	499.80
Mean depth (m):	2.38	Right bank (RB) =	416.99	499.80
Area (m^2):	987.63			
Mean velocity (m/s):	0.97			

Sta. (m)	Elev. (m)	h (m)	w/W	u (m/s)	DQ (m^3)	q/Q	Area (m^2)	adj. U (m/s)
1.35	499.80	0.00	0.000	0.000	0.00	0.000	0.00	0.000
9.50	498.59	1.21	0.020	0.619	1.52	0.002	4.92	0.608
28.52	498.14	1.66	0.065	0.765	18.86	0.021	32.18	0.752
48.05	497.62	2.18	0.112	0.917	31.54	0.053	69.67	0.901
67.44	497.30	2.50	0.159	1.006	43.65	0.098	115.06	0.989
86.35	497.30	2.50	0.205	1.006	47.62	0.147	162.38	0.989
115.83	497.30	2.50	0.275	1.006	74.23	0.223	236.15	0.989
145.83	497.30	2.50	0.348	1.006	75.56	0.300	311.24	0.989
176.25	497.36	2.44	0.421	0.989	74.98	0.377	386.40	0.971
206.14	497.23	2.57	0.493	1.024	75.27	0.454	461.20	1.006
242.88	497.23	2.57	0.581	1.024	96.56	0.552	555.54	1.006
280.31	497.23	2.57	0.671	1.024	98.37	0.653	651.64	1.006
311.47	497.10	2.70	0.746	1.058	85.37	0.740	733.68	1.039
342.29	497.17	2.63	0.820	1.041	86.17	0.829	815.80	1.022
370.88	497.04	2.76	0.889	1.075	81.54	0.912	892.89	1.056
399.86	497.43	2.37	0.959	0.971	76.11	0.990	967.30	0.954
416.99	499.80	0.00	1.000	0.000	9.87	1.000	987.63	0.000
			Est. total =		977.22			

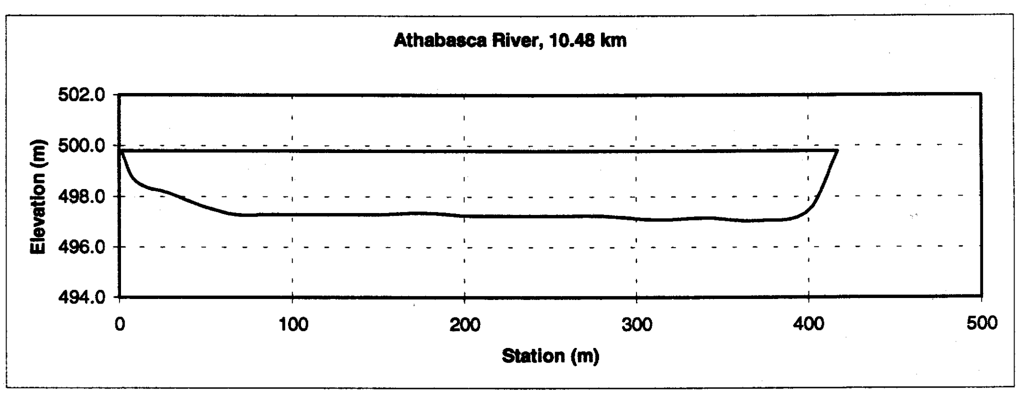

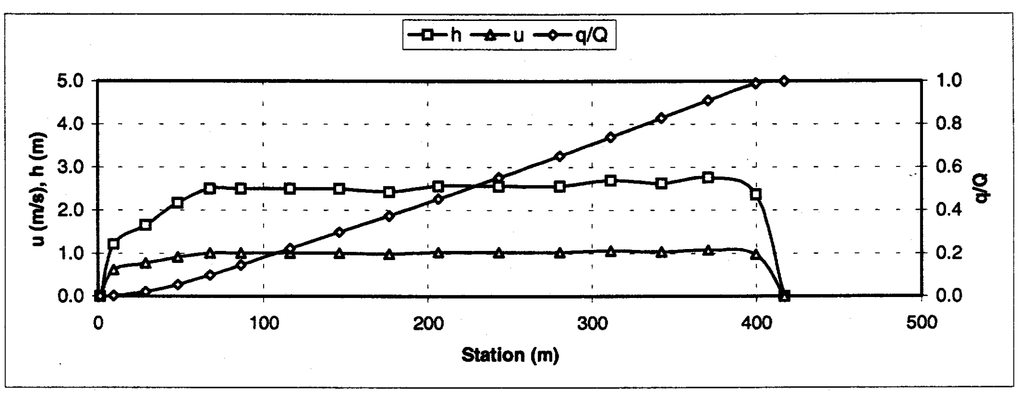

Appendix B.1 – Athabasca River, 960 m^3/s @ 13.9 km d/s

X-section:	Athabasca River, 13.9 km d/s		
Date:	August 21, 1997		
Discharge (m^3/s) :	960.00	Estimated water surface elevation (m):	499.80
Width (m):	240.31	Left bank (LB) = 1.55	499.80
Mean depth (m):	2.99	Right bank (RB) = 241.87	499.80
Area (m^2):	719.16		
Mean velocity (m/s):	1.33		

Sta. (m)	Elev. (m)	h (m)	w/W	u (m/s)	DQ (m^3)	q/Q	Area (m^2)	adj. U (m/s)
1.55	499.80	0.00	0.000	0.000	0.00	0.000	0.00	0.000
14.46	498.14	1.66	0.054	0.901	4.83	0.005	10.71	0.818
42.90	496.58	3.22	0.172	1.400	79.79	0.080	80.04	1.272
71.04	495.29	4.51	0.289	1.755	171.60	0.242	188.79	1.594
83.45	495.32	4.48	0.341	1.747	97.69	0.335	244.58	1.587
91.17	495.29	4.51	0.373	1.755	60.81	0.392	279.30	1.594
102.24	494.83	4.97	0.419	1.871	95.09	0.482	331.74	1.700
111.81	495.55	4.25	0.459	1.687	78.50	0.557	375.86	1.533
130.54	495.87	3.93	0.537	1.601	125.96	0.676	452.47	1.454
142.85	496.34	3.46	0.588	1.469	69.75	0.742	497.92	1.335
149.06	496.58	3.22	0.614	1.400	29.71	0.770	518.62	1.272
156.69	496.67	3.13	0.646	1.376	33.62	0.802	542.84	1.250
170.35	496.65	3.15	0.702	1.382	59.16	0.858	585.75	1.255
192.16	496.84	2.96	0.793	1.324	90.10	0.943	652.36	1.203
209.25	498.20	1.60	0.864	0.877	42.83	0.983	691.26	0.797
226.19	498.92	0.88	0.935	0.591	15.41	0.998	712.24	0.537
241.87	499.80	0.00	1.000	0.000	2.04	1.000	719.16	0.000
			Est. total =		1056.89			

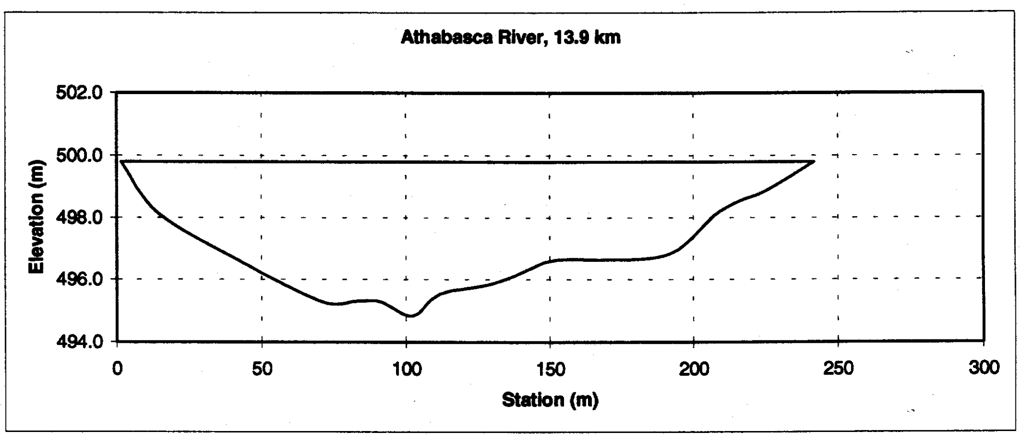

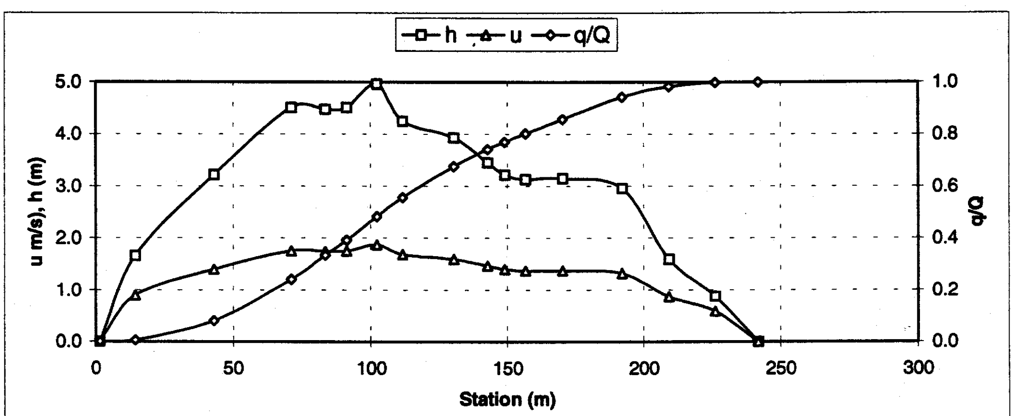

Appendix B.1 – Athabasca River, 960 m³/s @ 17.3 km d/s

X-section:	Athabasca River, 17.3 km d/s			
Date:	August 21, 1997			
Discharge (m^3/s) :	960.00	Estimated water surface elevation (m):		499.8
Width (m):	253.44	Left bank (LB) =	0.88	499.8
Mean depth (m):	3.22	Right bank (RB) =	254.32	499.8
Area (m^2):	814.96			
Mean velocity (m/s):	1.18			

Sta. (m)	Elev. (m)	h (m)	w/W	u (m/s)	DQ (m^3)	q/Q	Area (m^2)	adj. U (m/s)
0.88	499.80	0.00	0.000	0.000	0.00	0.000	0.00	0.000
4.76	498.92	0.88	0.015	0.497	0.43	0.000	1.71	0.463
26.34	497.49	2.31	0.100	0.944	24.81	0.024	36.14	0.879
34.70	496.45	3.35	0.133	1.209	25.46	0.049	59.78	1.126
36.48	496.78	3.02	0.140	1.130	6.63	0.056	65.44	1.052
43.33	496.02	3.78	0.168	1.312	28.44	0.083	88.74	1.221
48.40	496.58	3.22	0.188	1.178	22.08	0.105	106.47	1.096
74.60	496.13	3.67	0.291	1.286	111.12	0.212	196.65	1.197
100.78	495.87	3.93	0.394	1.346	130.92	0.339	296.11	1.253
129.68	495.94	3.86	0.508	1.331	150.77	0.485	408.72	1.239
159.17	495.29	4.51	0.625	1.477	173.38	0.653	532.20	1.374
169.32	495.05	4.75	0.665	1.528	70.67	0.722	579.24	1.423
184.49	495.68	4.12	0.725	1.390	98.27	0.817	646.57	1.294
209.94	496.52	3.28	0.825	1.194	121.69	0.935	740.75	1.111
225.79	497.36	2.44	0.887	0.979	49.25	0.983	786.08	0.911
231.77	498.51	1.29	0.911	0.641	9.03	0.992	797.23	0.596
242.69	498.85	0.95	0.954	0.521	7.10	0.999	809.45	0.485
254.32	499.80	0.00	1.000	0.000	1.44	1.000	814.96	0.000
			Est. total =		1031.48			

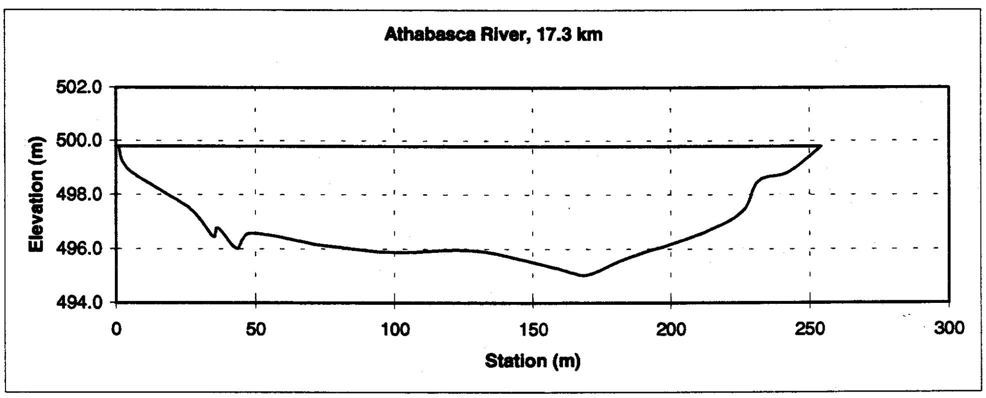

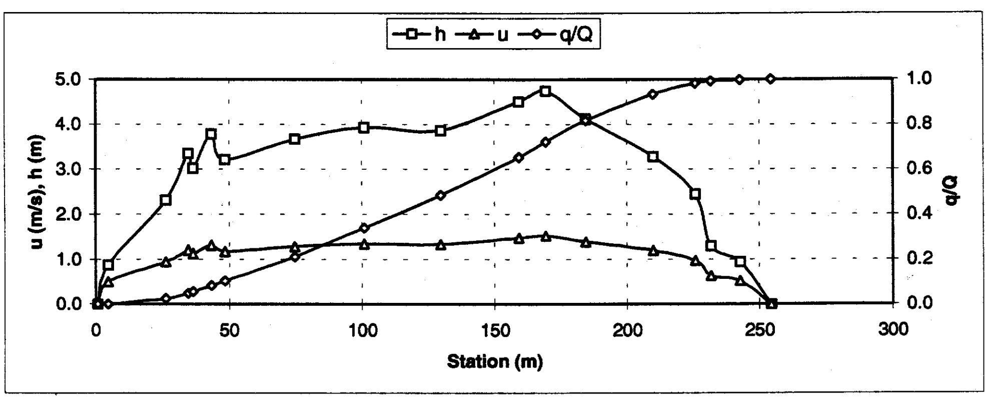

Appendix B.1 – Athabasca River, 960 m³/s @ 18.46 km d/s

X-section:	Athabasca River, 18.46 km d/s			
Date:	August 21, 1997			
Discharge (m^3/s) :	960.00	Estimated water surface elevation (m):		499.80
Width (m):	212.28	Left bank (LB) =	1.20	499.80
Mean depth (m):	3.23	Right bank (RB) =	213.48	499.80
Area (m^2):	685.83			
Mean velocity (m/s):	1.40			

Sta. (m)	Elev. (m)	h (m)	w/W	u (m/s)	DQ (m^3)	q/Q	Area (m^2)	adj. U (m/s)
1.20	499.80	0.00	0.000	0.000	0.00	0.000	0.00	0.000
5.71	499.05	0.75	0.021	0.530	0.45	0.000	1.70	0.489
18.89	498.53	1.27	0.083	0.751	8.54	0.009	15.03	0.694
31.26	496.00	3.80	0.142	1.559	36.26	0.044	46.41	1.440
49.76	495.22	4.58	0.229	1.766	128.80	0.167	123.88	1.630
68.66	495.09	4.71	0.318	1.799	156.38	0.318	211.62	1.661
87.45	495.09	4.71	0.406	1.799	159.07	0.471	300.04	1.661
106.81	495.81	3.99	0.498	1.612	143.61	0.609	384.24	1.488
127.03	496.39	3.41	0.593	1.451	114.63	0.719	459.08	1.340
147.35	496.71	3.09	0.688	1.358	92.70	0.808	525.09	1.253
156.22	496.56	3.24	0.730	1.401	38.67	0.845	553.13	1.293
161.03	496.33	3.47	0.753	1.469	23.16	0.868	569.26	1.357
175.22	496.71	3.09	0.820	1.358	65.77	0.931	615.80	1.253
184.03	497.43	2.37	0.861	1.139	30.04	0.960	639.86	1.052
187.85	497.32	2.48	0.879	1.174	10.73	0.970	649.13	1.084
192.80	497.95	1.85	0.903	0.967	11.49	0.981	659.86	0.892
200.18	498.83	0.97	0.937	0.626	8.29	0.989	670.28	0.578
204.59	498.29	1.51	0.958	0.843	4.01	0.993	675.74	0.778
210.46	498.53	1.27	0.986	0.751	6.52	0.999	683.92	0.694
213.48	499.80	0.00	1.000	0.000	0.72	1.000	685.83	0.000
			Est. total =		1039.85			

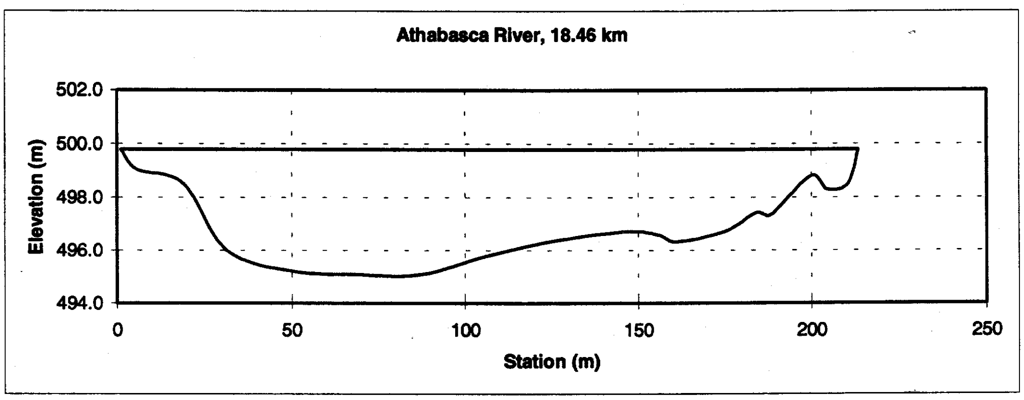

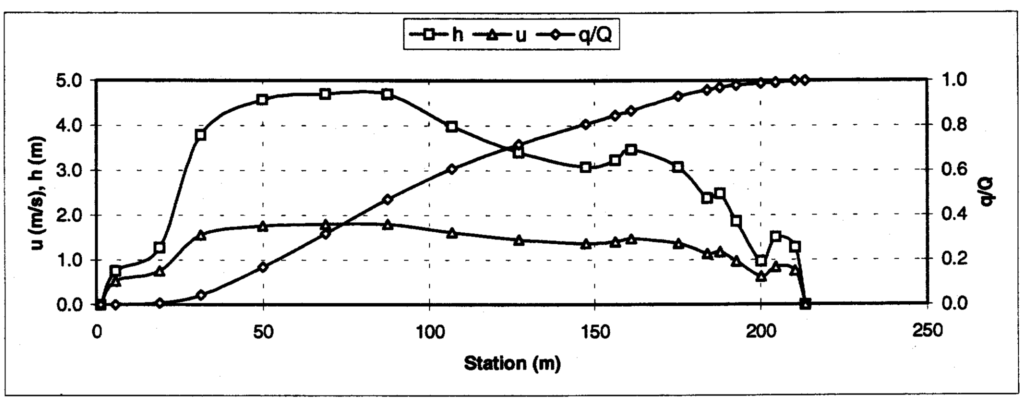

Appendix B.1 – Athabasca River, 960 m^3/s @ 19.37 km d/s

X-section:	Athabasca River, 19.37 km d/s		
Date:	August 21, 1997		
Discharge (m^3/s) :	960.00	Estimated water surface elevation (m):	499.80
Width (m):	233.17	Left bank (LB) = 0.97	499.80
Mean depth (m):	3.36	Right bank (RB) = 234.14	499.80
Area (m^2):	783.64		
Mean velocity (m/s):	1.23		

Sta. (m)	Elev. (m)	h (m)	w/W	u (m/s)	DQ (m^3)	q/Q	Area (m^2)	adj. U (m/s)
0.97	499.80	0.00	0.000	0.000	0.00	0.000	0.00	0.000
4.00	499.18	0.62	0.013	0.398	0.19	0.000	0.94	0.372
15.77	498.40	1.40	0.063	0.683	6.44	0.006	12.85	0.638
28.39	497.10	2.70	0.118	1.058	22.52	0.028	38.71	0.987
44.40	495.81	3.99	0.186	1.374	65.15	0.092	92.28	1.283
59.92	495.09	4.71	0.253	1.534	98.15	0.187	159.79	1.431
79.49	494.64	5.16	0.337	1.631	152.70	0.336	256.31	1.522
98.89	495.22	4.58	0.420	1.505	148.09	0.480	350.75	1.405
109.84	495.92	3.88	0.467	1.349	66.12	0.544	397.09	1.259
121.94	496.13	3.67	0.519	1.299	60.50	0.603	442.78	1.213
145.42	496.13	3.67	0.619	1.299	111.90	0.712	528.93	1.213
154.85	496.02	3.78	0.660	1.325	46.08	0.756	564.06	1.237
166.88	496.07	3.73	0.712	1.314	59.66	0.814	609.27	1.227
188.16	496.71	3.09	0.803	1.157	89.65	0.901	681.81	1.080
194.54	496.45	3.35	0.830	1.221	24.41	0.925	702.34	1.140
208.68	497.23	2.57	0.891	1.024	46.93	0.971	744.15	0.956
216.99	498.40	1.40	0.926	0.683	14.07	0.985	760.63	0.638
221.71	497.86	1.94	0.947	0.849	6.04	0.990	768.52	0.792
228.33	498.40	1.40	0.975	0.683	8.46	0.999	779.56	0.638
234.14	499.80	0.00	1.000	0.000	1.39	1.000	783.64	0.000
			Est. total =		1028.45			

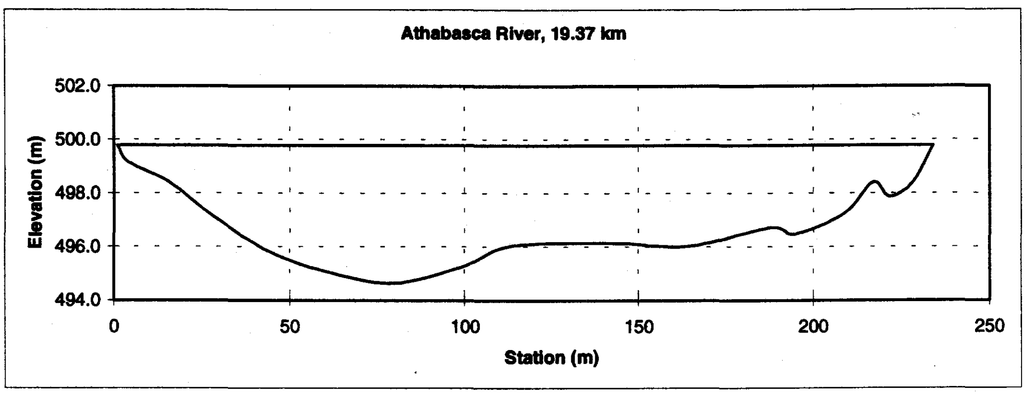

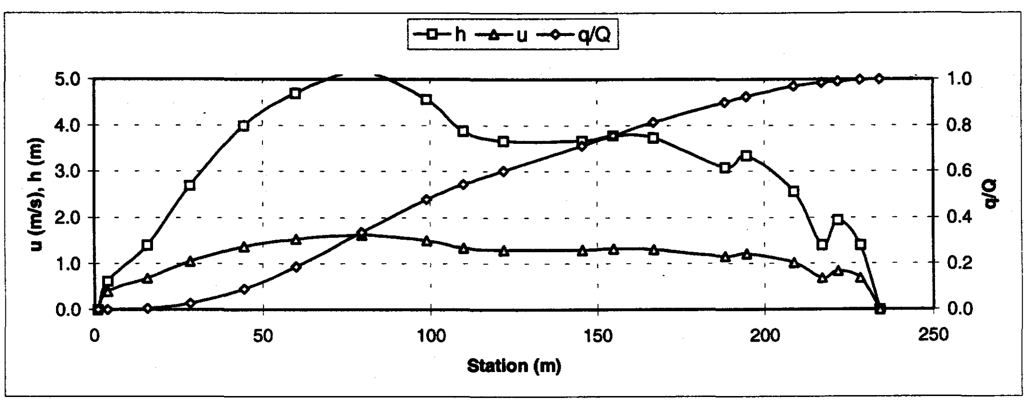

Appendix B.1 – Athabasca River, 960 m³/s @ 20.39 km d/s

X-section:	Athabasca River, 20.39 km d/s			
Date:	August 21, 1997			
Discharge (m^3/s) :	960.00	Estimated water surface elevation (m):		499.80
Width (m):	267.23	Left bank (LB) =	0.62	499.80
Mean depth (m):	3.16	Right bank (RB) =	267.85	499.80
Area (m^2):	843.93			
Mean velocity (m/s):	1.14			

Sta. (m)	Elev. (m)	h (m)	w/W	u (m/s)	DQ (m^3)	q/Q	Area (m^2)	adj. U (m/s)
0.62	499.80	0.00	0.000	0.000	0.00	0.000	0.00	0.000
5.34	498.27	1.53	0.018	0.702	1.27	0.001	3.62	0.663
15.34	498.72	1.08	0.055	0.555	8.19	0.009	16.65	0.525
23.52	498.46	1.34	0.086	0.641	5.90	0.015	26.51	0.606
26.08	497.86	1.94	0.095	0.822	3.07	0.018	30.71	0.777
29.83	498.07	1.73	0.109	0.760	5.43	0.023	37.58	0.718
41.08	496.71	3.09	0.151	1.120	25.44	0.049	64.65	1.059
53.56	496.67	3.13	0.198	1.131	43.67	0.092	103.44	1.069
63.97	496.33	3.47	0.237	1.212	40.31	0.131	137.84	1.146
80.26	496.24	3.56	0.298	1.232	70.01	0.200	195.12	1.165
87.52	495.94	3.86	0.325	1.301	34.15	0.234	222.08	1.230
97.29	495.16	4.64	0.362	1.471	57.56	0.290	263.61	1.390
108.21	495.42	4.38	0.403	1.415	71.09	0.360	312.87	1.338
129.87	496.07	3.73	0.484	1.272	118.12	0.477	400.78	1.202
141.87	495.70	4.10	0.529	1.355	61.76	0.538	447.81	1.280
156.13	495.94	3.86	0.582	1.301	75.45	0.612	504.63	1.230
165.63	495.92	3.88	0.617	1.306	47.95	0.659	541.41	1.234
181.89	495.74	4.06	0.678	1.345	85.56	0.743	605.98	1.271
201.11	496.24	3.56	0.750	1.232	94.31	0.836	679.18	1.165
220.60	496.65	3.15	0.823	1.136	77.40	0.912	744.56	1.074
258.77	498.14	1.66	0.966	0.741	86.17	0.997	836.40	0.700
267.85	499.80	0.00	1.000	0.000	2.79	1.000	843.93	0.000
			Est. total =		1015.61			

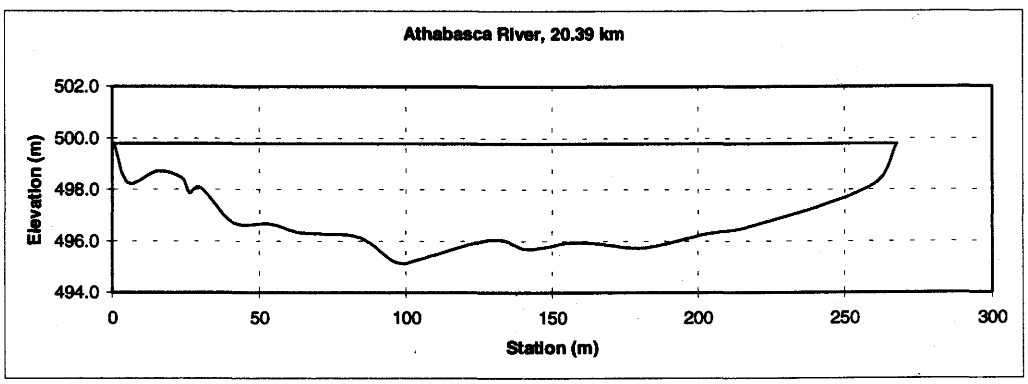

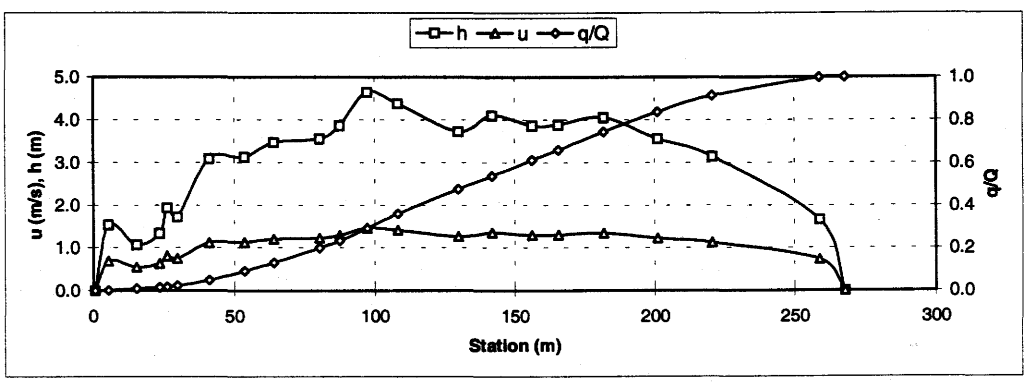

Appendix B.1 – Athabasca River, 960 m^3/s @ 21.15 km d/s

X-section:	Athabasca River, 21.15 km d/s				
Date:	August 21, 1997				
Discharge (m^3/s) :	960.00	Estimated water surface elevation (m):		499.80
Width (m):	209.10	Left bank (LB) =	1.58	499.80
Mean depth (m):	3.31	Right bank (RB) =	210.69	499.80
Area (m^2):	691.42			
Mean velocity (m/s):	1.39			

Sta. (m)	Elev. (m)	h (m)	w/W	u (m/s)	DQ (m^3)	q/Q	Area (m^2)	adj. U (m/s)
1.58	499.80	0.00	0.000	0.000	0.00	0.000	0.00	0.000
6.52	499.18	0.62	0.024	0.456	0.35	0.000	1.54	0.405
27.35	497.49	2.31	0.123	1.093	23.64	0.022	32.06	0.970
47.99	495.61	4.19	0.222	1.625	91.13	0.106	99.12	1.443
61.89	493.86	5.94	0.288	2.052	129.37	0.226	169.48	1.822
68.73	494.32	5.48	0.321	1.946	78.06	0.298	208.54	1.728
79.98	494.62	5.18	0.375	1.873	114.54	0.404	268.53	1.663
89.94	494.77	5.03	0.423	1.837	94.28	0.491	319.36	1.631
108.52	495.61	4.19	0.511	1.625	148.26	0.629	405.00	1.443
118.76	495.70	4.10	0.560	1.604	68.55	0.692	447.46	1.424
126.99	495.68	4.12	0.600	1.609	54.37	0.742	481.31	1.428
135.76	496.13	3.67	0.642	1.488	52.91	0.791	515.48	1.322
141.73	496.07	3.73	0.670	1.506	33.10	0.822	537.59	1.337
155.82	496.07	3.73	0.738	1.506	79.18	0.895	590.18	1.337
175.00	497.17	2.63	0.829	1.193	82.38	0.971	651.24	1.059
193.56	498.92	0.88	0.918	0.575	28.84	0.998	683.86	0.511
210.69	499.80	0.00	1.000	0.000	2.17	1.000	691.42	0.000
			Est. total =		1081.13			

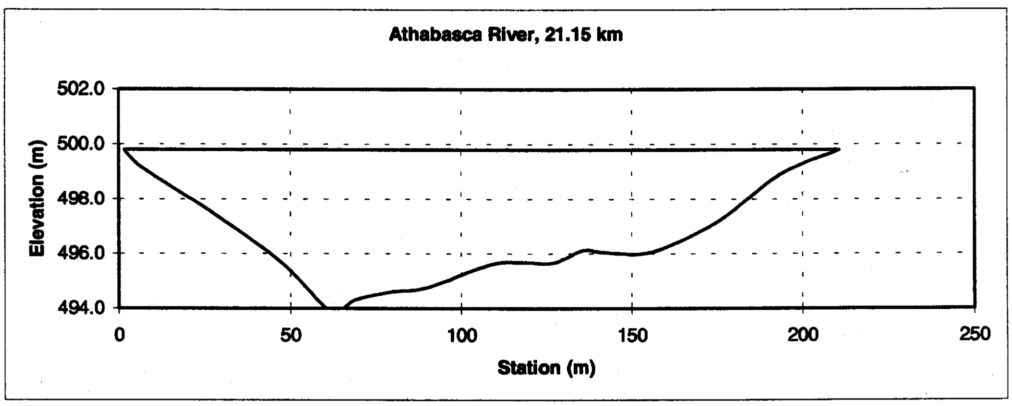

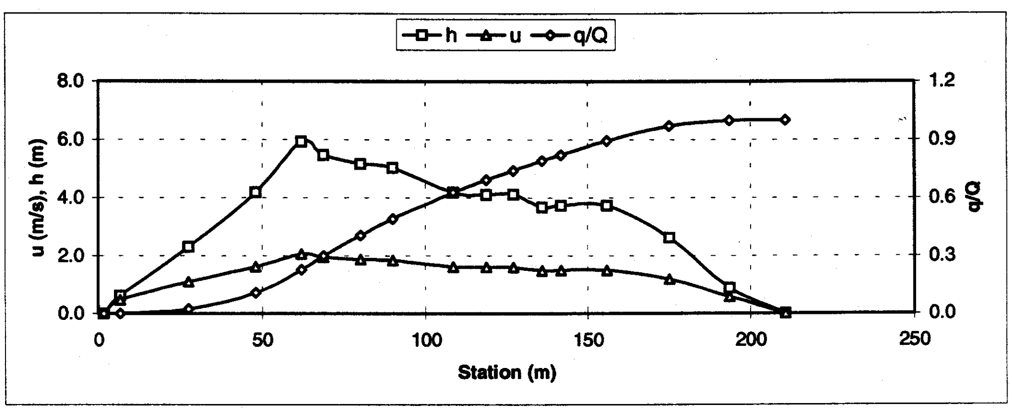

Appendix B.1 – Athabasca River, 960 m³/s @ 23.74 km d/s

X-section:	Athabasca River, 23.74 km d/s			
Date:	August 21, 1997			
Discharge (m^3/s) :	960.00	Estimated water surface elevation (m):		499.80
Width (m):	251.43	Left bank (LB) =	0.77	499.80
Mean depth (m):	3.27	Right bank (RB) =	252.20	499.80
Area (m^2):	821.55			
Mean velocity (m/s):	1.17			

Sta. (m)	Elev. (m)	h (m)	w/W	u (m/s)	DQ (m^3)	q/Q	Area (m^2)	adj. U (m/s)
0.77	499.80	0.00	0.000	0.000	0.00	0.000	0.00	0.000
5.65	498.53	1.27	0.019	0.623	0.97	0.001	3.10	0.610
22.52	496.65	3.15	0.087	1.141	32.89	0.035	40.41	1.117
38.91	496.71	3.09	0.152	1.125	57.89	0.094	91.52	1.102
60.72	496.33	3.47	0.238	1.217	83.80	0.179	163.07	1.192
82.34	496.00	3.80	0.324	1.292	98.63	0.280	241.68	1.265
100.18	496.00	3.80	0.395	1.292	87.60	0.369	309.48	1.265
117.93	496.00	3.80	0.466	1.292	87.13	0.458	376.91	1.265
139.42	496.20	3.60	0.551	1.248	100.98	0.561	456.43	1.222
159.82	496.00	3.80	0.633	1.292	95.92	0.659	531.97	1.265
181.22	496.33	3.47	0.718	1.217	97.66	0.758	609.80	1.192
223.03	497.23	2.57	0.884	0.995	139.72	0.901	736.10	0.974
224.63	496.45	3.35	0.890	1.187	5.17	0.906	740.84	1.163
244.57	496.45	3.35	0.970	1.187	79.18	0.987	807.55	1.163
245.35	496.56	3.24	0.973	1.161	3.01	0.990	810.11	1.137
245.95	496.34	3.46	0.975	1.213	2.38	0.993	812.12	1.188
250.05	499.05	0.75	0.991	0.439	7.12	1.000	820.74	0.430
252.20	499.80	0.00	1.000	0.000	0.18	1.000	821.55	0.000
			Est. total =		980.23			

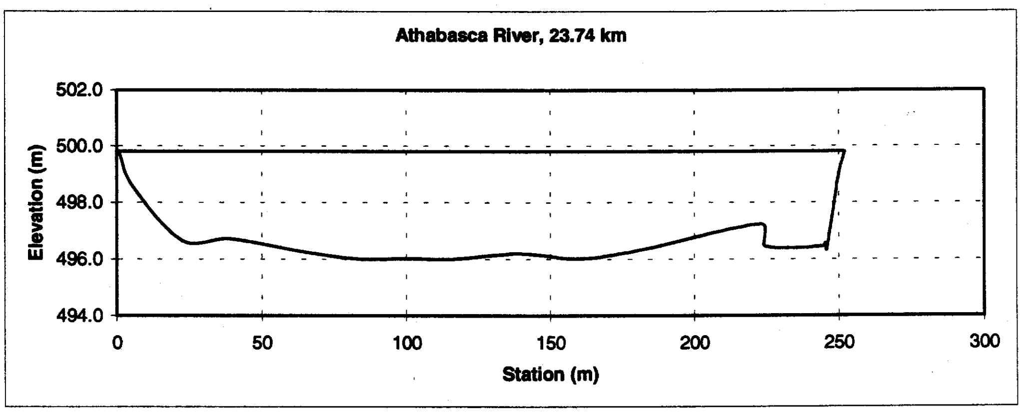

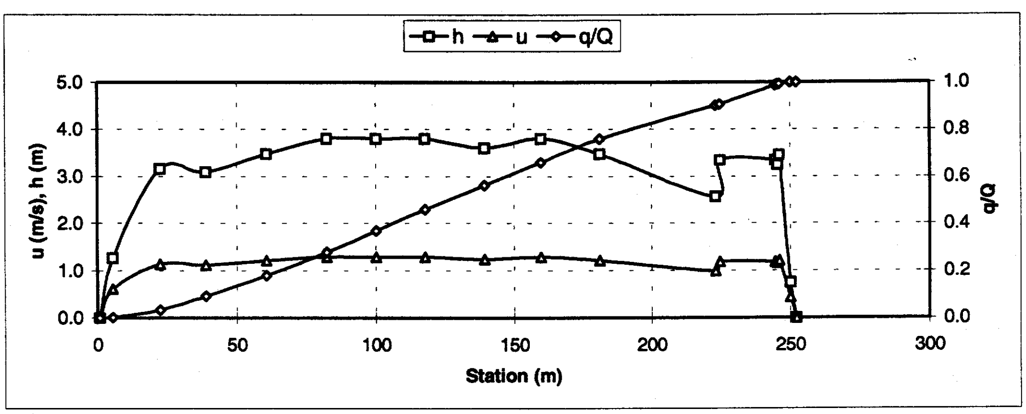

Appendix B.1 – Athabasca River, 960 m³/s @ 25.92 km d/s

X-section:	Athabasca River, 25.92 km d/s			
Date:	August 21, 1997			
Discharge (m^3/s) :	960.00	Estimated water surface elevation (m):		499.80
Width (m):	220.85	Left bank (LB) =	0.55	499.80
Mean depth (m):	3.39	Right bank (RB) =	221.40	499.80
Area (m^2):	748.46			
Mean velocity (m/s):	1.28			

Sta. (m)	Elev. (m)	h (m)	w/W	u (m/s)	DQ (m^3)	q/Q	Area (m^2)	adj. U (m/s)
0.55	499.80	0.00	0.000	0.000	0.00	0.000	0.00	0.000
5.11	498.14	1.66	0.021	0.797	1.51	0.002	3.79	0.762
23.33	496.71	3.09	0.103	1.205	43.26	0.045	47.01	1.152
40.93	495.55	4.25	0.183	1.492	87.09	0.131	111.59	1.427
59.49	495.22	4.58	0.267	1.567	125.40	0.256	193.56	1.499
77.31	495.29	4.51	0.348	1.552	126.29	0.382	274.53	1.485
96.83	495.55	4.25	0.436	1.492	130.21	0.512	360.06	1.427
116.52	496.07	3.73	0.525	1.368	112.45	0.624	438.68	1.309
132.88	496.07	3.73	0.599	1.368	83.64	0.707	499.80	1.309
149.17	496.45	3.35	0.673	1.272	76.07	0.783	557.43	1.216
166.83	496.71	3.09	0.753	1.205	70.34	0.853	614.24	1.152
184.67	496.45	3.35	0.834	1.272	71.03	0.924	671.60	1.216
190.63	496.78	3.02	0.861	1.188	23.34	0.947	690.58	1.136
200.61	497.49	2.31	0.906	0.993	28.99	0.976	717.17	0.950
217.44	498.66	1.14	0.982	0.621	23.43	0.999	746.20	0.594
221.40	499.80	0.00	1.000	0.000	0.70	1.000	748.46	0.000
		Est. total =			1003.75			

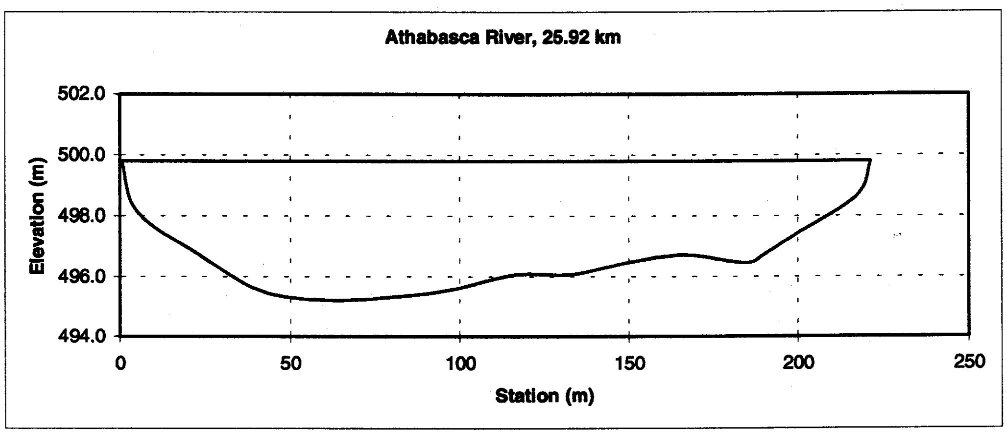

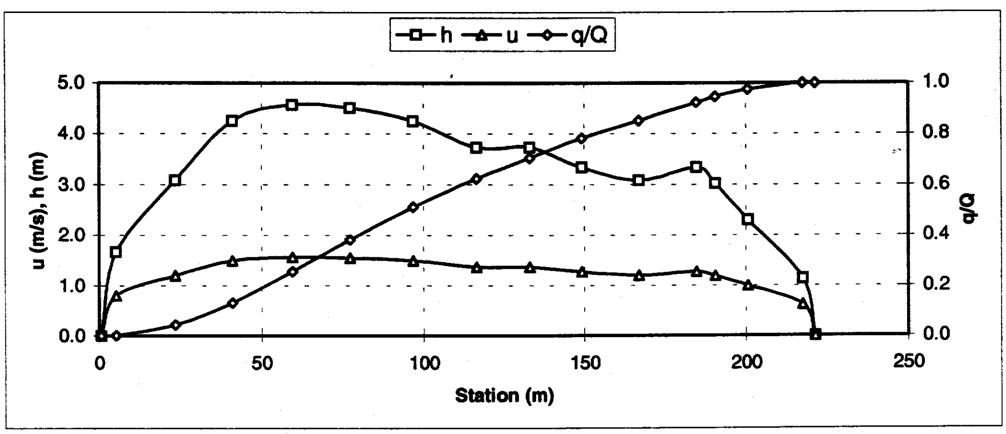

Appendix B.1 – Athabasca River, 960 m³/s @ 28.51 km d/s

X-section:	Athabasca River, 28.51 km d/s			
Date:	August 21, 1997			
Discharge (m^3/s) :	960.00	Estimated water surface elevation (m):		499.80
Width (m):	291.04	Left bank (LB) =	0.87	499.80
Mean depth (m):	3.29	Right bank (RB) =	291.91	499.80
Area (m^2):	958.96			
Mean velocity (m/s):	1.00			

Sta. (m)	Elev. (m)	h (m)	w/W	u (m/s)	DQ (m^3)	q/Q	Area (m^2)	adj. U (m/s)
0.87	499.80	0.00	0.000	0.000	0.00	0.000	0.00	0.000
5.52	498.72	1.08	0.016	0.475	0.60	0.001	2.51	0.448
25.88	497.30	2.50	0.086	0.833	23.83	0.024	38.94	0.786
46.29	496.33	3.47	0.156	1.037	57.05	0.080	99.94	0.979
72.36	496.13	3.67	0.246	1.076	98.39	0.177	193.07	1.015
98.29	496.00	3.80	0.335	1.101	105.38	0.280	289.91	1.039
120.51	495.81	3.99	0.411	1.138	96.87	0.376	376.45	1.074
142.33	495.68	4.12	0.486	1.163	101.90	0.476	465.04	1.097
162.69	495.55	4.25	0.556	1.187	100.15	0.574	550.30	1.120
183.22	495.55	4.25	0.627	1.187	103.60	0.676	637.59	1.120
200.85	495.61	4.19	0.687	1.175	87.84	0.762	711.98	1.108
217.59	495.68	4.12	0.745	1.163	81.30	0.842	781.55	1.097
234.97	496.39	3.41	0.804	1.024	71.58	0.913	847.01	0.966
251.32	496.91	2.89	0.861	0.918	50.02	0.962	898.53	0.866
269.70	498.33	1.47	0.924	0.583	30.06	0.991	938.58	0.550
288.06	499.18	0.62	0.987	0.330	8.75	1.000	957.76	0.311
291.91	499.80	0.00	1.000	0.000	0.20	1.000	958.96	0.000
			Est. total =		1017.52			

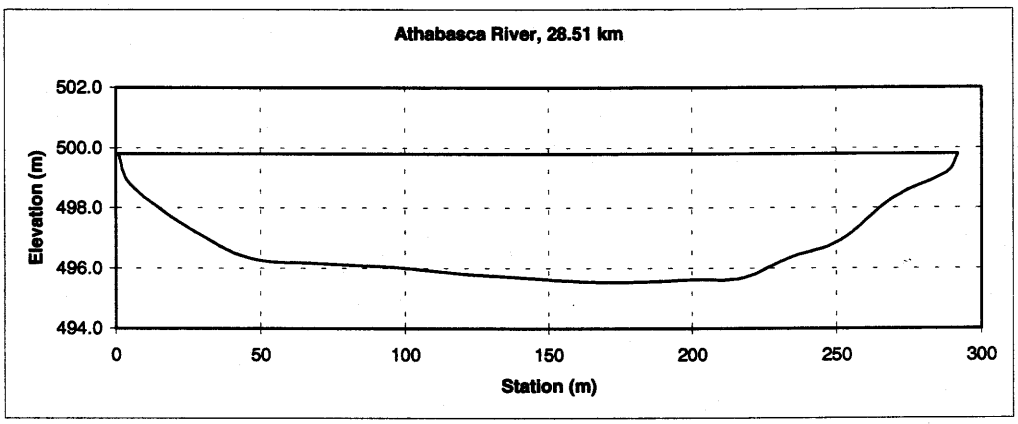

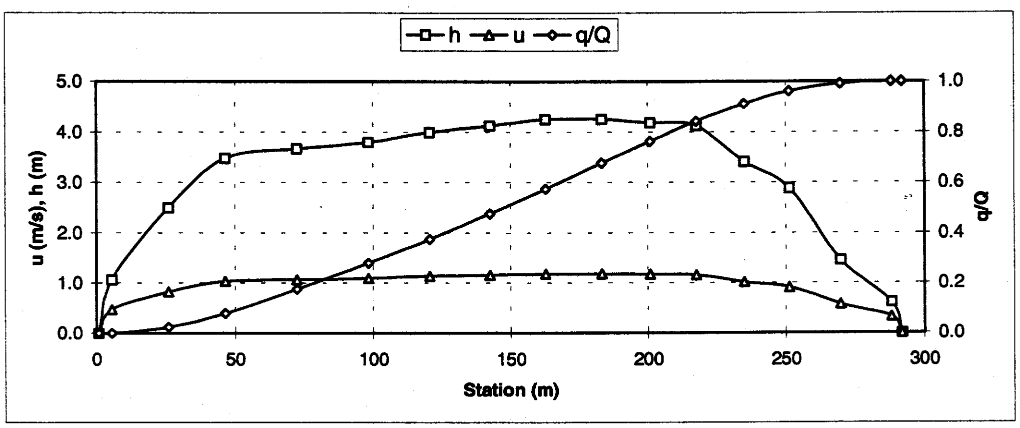

Appendix B.1 – Athabasca River, 960 m^3/s @ 31.42 km d/s

X-section:	Athabasca River, 31.42 km d/s			
Date:	August 21, 1997			
Discharge (m^3/s) :	960.00	Estimated water surface elevation (m):		499.80
Width (m):	227.50	Left bank (LB) =	0.88	499.80
Mean depth (m):	3.11	Right bank (RB) =	228.37	499.80
Area (m^2):	707.65			
Mean velocity (m/s):	1.36			

Sta. (m)	Elev. (m)	h (m)	w/W	u (m/s)	DQ (m^3)	q/Q	Area (m^2)	adj. U (m/s)
0.88	499.80	0.00	0.000	0.000	0.00	0.000	0.00	0.000
5.88	498.66	1.14	0.022	0.695	0.99	0.001	2.86	0.655
21.33	497.32	2.48	0.090	1.167	26.08	0.027	30.86	1.099
23.87	498.66	1.14	0.101	0.695	4.28	0.031	35.46	0.655
41.19	497.17	2.63	0.177	1.214	31.21	0.061	68.16	1.143
66.76	496.07	3.73	0.290	1.532	111.76	0.171	149.55	1.443
83.63	495.11	4.69	0.364	1.785	117.88	0.287	220.63	1.681
93.01	495.48	4.32	0.405	1.688	73.40	0.359	262.89	1.590
109.59	496.33	3.47	0.478	1.461	101.67	0.458	327.47	1.375
125.90	496.58	3.22	0.550	1.387	77.71	0.535	382.05	1.306
145.64	496.20	3.60	0.636	1.497	97.03	0.630	449.35	1.409
161.45	495.05	4.75	0.706	1.800	108.90	0.736	515.42	1.694
165.00	495.55	4.25	0.721	1.671	27.73	0.764	531.40	1.574
177.01	496.78	3.02	0.774	1.330	65.56	0.828	575.08	1.253
181.91	496.07	3.73	0.796	1.532	23.67	0.851	591.62	1.443
188.02	495.37	4.43	0.823	1.717	40.53	0.891	616.57	1.616
199.03	497.04	2.76	0.871	1.253	58.76	0.949	656.14	1.180
205.85	496.94	2.86	0.901	1.282	24.31	0.972	675.31	1.207
212.11	498.33	1.47	0.928	0.821	14.23	0.986	688.84	0.773
216.08	498.07	1.73	0.946	0.916	5.51	0.992	695.18	0.862
225.63	499.11	0.69	0.988	0.496	8.13	1.000	706.71	0.467
228.37	499.80	0.00	1.000	0.000	0.23	1.000	707.65	0.000
		Est. total =			1019.60			

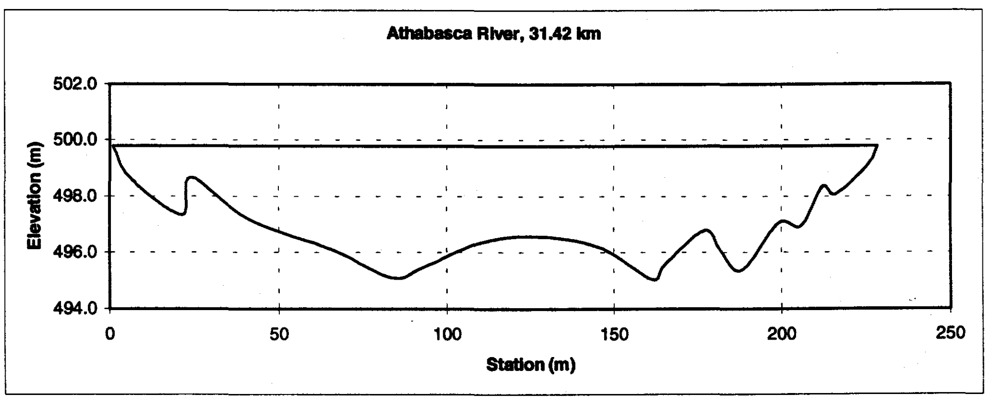

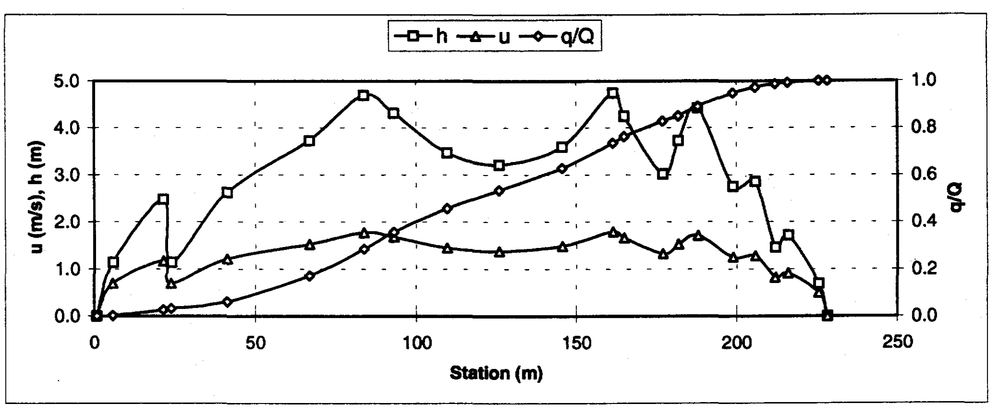

Appendix B.2 – Athabasca River, 270 m³/s @ 0.05 km d/s

X-section:	Athabasca River, 0.05 km d/s			
Date:	October 15, 1994			
Discharge (m^3/s) :	270.00	Estimated water surface elevation (m):		500.00
Width (m):	257.00	Left bank (LB) =	0.00	500.00
Mean depth (m):	1.72	Right bank (RB) =	257.00	500.00
Area (m^2):	442.43			
Mean velocity (m/s):	0.61			

Sta. (m)	Elev. (m)	h (m)	w/W	u (m/s)	DQ (m^3)	q/Q	Area (m^2)	adj. U (m/s)
0.00	500.00	0.00	0.000	0.000	0.00	0.000	0.00	0.000
7.00	499.15	0.85	0.027	0.381	0.57	0.002	2.98	0.361
17.00	498.70	1.30	0.066	0.506	4.77	0.019	13.73	0.479
27.00	498.30	1.70	0.105	0.605	8.33	0.048	28.73	0.573
37.00	498.30	1.70	0.144	0.605	10.29	0.084	45.73	0.573
47.00	498.58	1.42	0.183	0.537	8.91	0.115	61.33	0.508
57.00	498.54	1.46	0.222	0.547	7.80	0.143	75.73	0.517
67.00	498.36	1.64	0.261	0.591	8.82	0.173	91.23	0.559
77.00	498.38	1.62	0.300	0.586	9.59	0.207	107.53	0.554
87.00	498.34	1.66	0.339	0.596	9.69	0.241	123.93	0.564
97.00	498.49	1.51	0.377	0.559	9.15	0.273	139.78	0.529
107.00	498.45	1.55	0.416	0.569	8.63	0.303	155.08	0.538
117.00	498.57	1.43	0.455	0.539	8.26	0.332	169.98	0.510
127.00	498.21	1.79	0.494	0.626	9.38	0.365	186.08	0.593
137.00	497.72	2.28	0.533	0.736	13.86	0.414	206.43	0.696
147.00	498.03	1.97	0.572	0.668	14.92	0.466	227.68	0.632
157.00	497.94	2.06	0.611	0.688	13.66	0.514	247.83	0.651
167.00	497.88	2.12	0.650	0.701	14.52	0.565	268.73	0.663
177.00	497.40	2.60	0.689	0.803	17.75	0.627	292.33	0.760
187.00	496.90	3.10	0.728	0.903	24.32	0.712	320.83	0.855
197.00	497.45	2.55	0.767	0.793	23.96	0.796	349.08	0.750
207.00	497.63	2.37	0.805	0.755	19.05	0.863	373.68	0.715
217.00	497.81	2.19	0.844	0.717	16.78	0.922	396.48	0.678
227.00	498.90	1.10	0.883	0.453	9.62	0.955	412.93	0.428
237.00	498.70	1.30	0.922	0.506	5.75	0.975	424.93	0.479
247.00	498.90	1.10	0.961	0.453	5.75	0.996	436.93	0.428
257.00	500.00	0.00	1.000	0.000	1.24	1.000	442.43	0.000
		Est. total =			285.37			

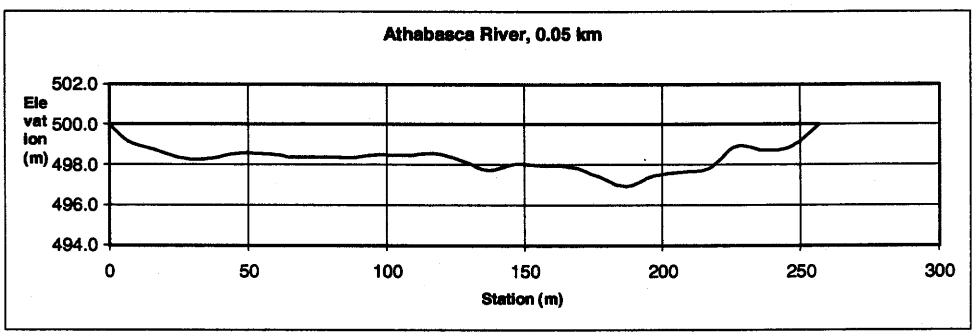

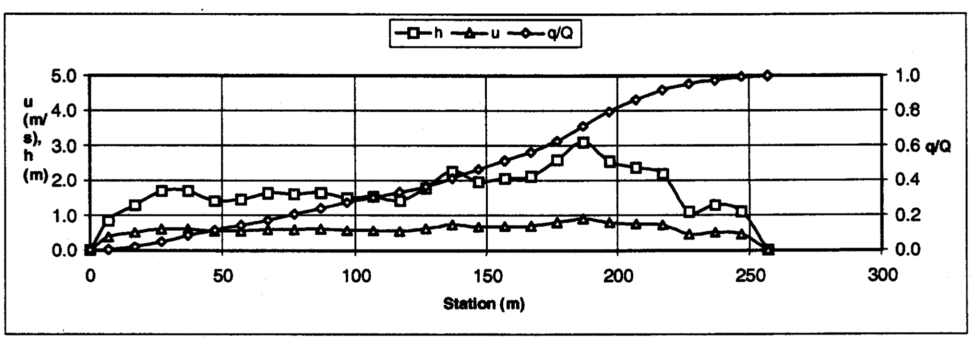

Appendix B.2 – Athabasca River, 270 m^3/s @ 0.5 km d/s

X-section:	Athabasca River, 0.5 km d/s			
Date:	October 15, 1994			
Discharge (m^3/s) :	270.00	Estimated water surface elevation (m):		500.00
Width (m):	325.00	Left bank (LB) =	0.00	500.00
Mean depth (m):	1.20	Right bank (RB) =	325.00	500.00
Area (m^2):	389.40			
Mean velocity (m/s):	0.69			

Sta. (m)	Elev. (m)	h (m)	w/W	u (m/s)	DQ (m^3)	q/Q	Area (m^2)	adj. U (m/s)
0.00	500.00	0.00	0.000	0.000	0.00	0.000	0.00	0.000
5.00	499.60	0.40	0.015	0.334	0.17	0.001	1.00	0.320
15.00	498.50	1.50	0.046	0.805	5.41	0.020	10.50	0.773
25.00	498.80	1.20	0.077	0.694	10.12	0.056	24.00	0.666
35.00	499.03	0.97	0.108	0.602	7.03	0.081	34.85	0.578
45.00	499.00	1.00	0.138	0.615	5.99	0.102	44.70	0.590
55.00	499.08	0.92	0.169	0.581	5.74	0.123	54.30	0.558
65.00	499.13	0.87	0.200	0.560	5.11	0.141	63.25	0.538
75.00	499.13	0.87	0.231	0.560	4.87	0.158	71.95	0.538
85.00	499.09	0.91	0.262	0.577	5.06	0.176	80.85	0.554
95.00	499.09	0.91	0.292	0.577	5.25	0.195	89.95	0.554
105.00	499.09	0.91	0.323	0.577	5.25	0.213	99.05	0.554
115.00	499.00	1.00	0.354	0.615	5.69	0.234	108.60	0.590
125.00	498.96	1.04	0.385	0.631	6.35	0.256	118.80	0.606
135.00	499.03	0.97	0.415	0.602	6.20	0.278	128.85	0.578
145.00	499.08	0.92	0.446	0.581	5.59	0.298	138.30	0.558
155.00	498.77	1.23	0.477	0.706	6.92	0.323	149.05	0.678
165.00	498.81	1.19	0.508	0.690	8.44	0.353	161.15	0.663
175.00	499.03	0.97	0.538	0.602	6.98	0.378	171.95	0.578
185.00	498.55	1.45	0.569	0.787	8.41	0.408	184.05	0.756
195.00	499.03	0.97	0.600	0.602	8.41	0.437	196.15	0.578
205.00	498.42	1.58	0.631	0.834	9.16	0.470	208.90	0.801
215.00	498.90	1.10	0.662	0.655	9.98	0.505	222.30	0.629
225.00	497.80	2.20	0.692	1.040	13.98	0.555	238.80	0.999
235.00	497.89	2.11	0.723	1.011	22.10	0.634	260.35	0.971
245.00	498.15	1.85	0.754	0.926	19.18	0.702	280.15	0.890
255.00	498.46	1.54	0.785	0.820	14.80	0.755	297.10	0.787
265.00	499.03	0.97	0.815	0.602	8.92	0.786	309.65	0.578
275.00	498.99	1.01	0.846	0.619	6.04	0.808	319.55	0.594
285.00	497.80	2.20	0.877	1.040	13.31	0.855	335.60	0.999
295.00	499.12	0.88	0.908	0.564	12.35	0.899	351.00	0.542
305.00	498.10	1.90	0.938	0.943	10.48	0.936	364.90	0.906
315.00	498.50	1.50	0.969	0.805	14.86	0.989	381.90	0.773
325.00	500.00	0.00	1.000	0.000	3.02	1.000	389.40	0.000
			Est. total =		281.19			

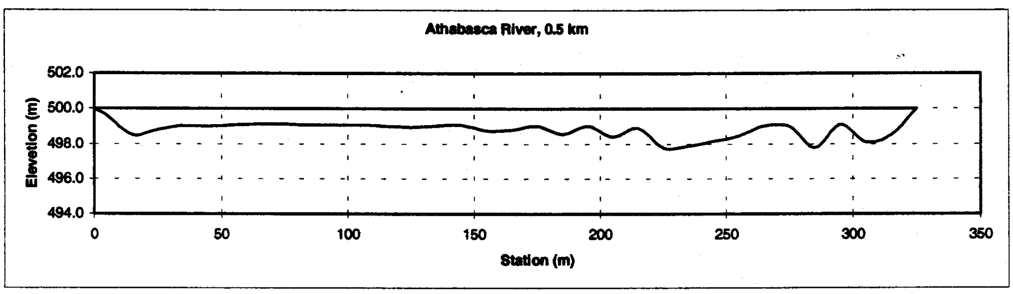

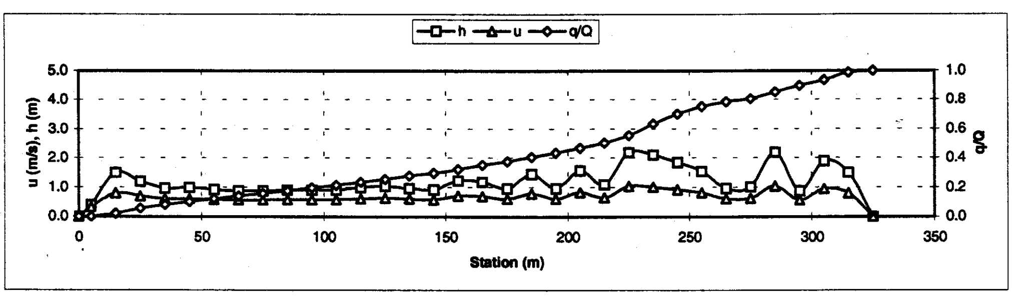

Appendix B.2 – Athabasca River, 270 m^3/s @ 1 km d/s

X-section:	Athabasca River, 1 km d/s				
Date:	October 15, 1994				
Discharge (m^3/s) :	270.00	Estimated water surface elevation (m):			500.00
Width (m):	337.00	Left bank (LB) =		0.00	500.00
Mean depth (m):	1.31	Right bank (RB) =		337.00	500.00
Area (m^2):	439.83				
Mean velocity (m/s):	0.61				

Sta. (m)	Elev. (m)	h (m)	w/W	u (m/s)	DQ (m^3)	q/Q	Area (m^2)	adj. U (m/s)
0.00	500.00	0.00	0.000	0.000	0.00	0.000	0.00	0.000
7.00	499.55	0.45	0.021	0.302	0.24	0.001	1.57	0.284
17.00	498.73	1.27	0.050	0.603	3.89	0.014	10.17	0.568
27.00	498.86	1.14	0.080	0.561	7.01	0.039	22.22	0.529
37.00	498.90	1.10	0.110	0.548	6.21	0.061	33.42	0.516
47.00	498.81	1.19	0.139	0.577	6.44	0.083	44.87	0.544
57.00	498.73	1.27	0.169	0.603	7.26	0.108	57.17	0.568
67.00	498.86	1.14	0.199	0.561	7.01	0.133	69.22	0.529
77.00	498.97	1.03	0.228	0.524	5.89	0.153	80.07	0.494
87.00	498.92	1.08	0.258	0.541	5.62	0.173	90.62	0.510
97.00	498.40	1.60	0.288	0.703	8.34	0.202	104.02	0.663
107.00	498.20	1.80	0.318	0.761	12.44	0.246	121.02	0.717
117.00	498.02	1.98	0.347	0.811	14.85	0.297	139.92	0.764
127.00	498.24	1.76	0.377	0.749	14.59	0.348	158.63	0.706
137.00	498.02	1.98	0.407	0.811	14.59	0.399	177.33	0.764
147.00	498.18	1.82	0.436	0.766	14.98	0.451	196.33	0.722
157.00	498.11	1.89	0.466	0.786	14.40	0.502	214.88	0.741
167.00	498.31	1.69	0.496	0.729	13.56	0.549	232.77	0.687
177.00	498.42	1.58	0.525	0.697	11.66	0.590	249.12	0.657
187.00	498.53	1.47	0.555	0.665	10.38	0.626	264.37	0.626
197.00	498.42	1.58	0.585	0.697	10.38	0.662	279.62	0.657
207.00	498.42	1.58	0.614	0.697	11.02	0.701	295.42	0.657
217.00	498.42	1.58	0.644	0.697	11.02	0.739	311.22	0.657
227.00	498.62	1.38	0.674	0.637	9.88	0.774	326.02	0.600
237.00	498.59	1.41	0.703	0.646	8.95	0.805	339.97	0.609
247.00	498.95	1.05	0.733	0.531	7.24	0.830	352.27	0.500
257.00	498.95	1.05	0.763	0.531	5.58	0.850	362.77	0.500
267.00	498.59	1.41	0.792	0.646	7.24	0.875	375.08	0.609
277.00	498.53	1.47	0.822	0.665	9.44	0.908	389.48	0.626
287.00	498.59	1.41	0.852	0.646	9.44	0.941	403.88	0.609
297.00	498.81	1.19	0.881	0.577	7.95	0.969	416.88	0.544
307.00	499.25	0.75	0.911	0.424	4.86	0.985	426.58	0.400
317.00	499.50	0.50	0.941	0.324	2.34	0.994	432.83	0.305
327.00	499.55	0.45	0.970	0.302	1.49	0.999	437.58	0.284
337.00	500.00	0.00	1.000	0.000	0.34	1.000	439.83	0.000
			Est. total =		286.51			

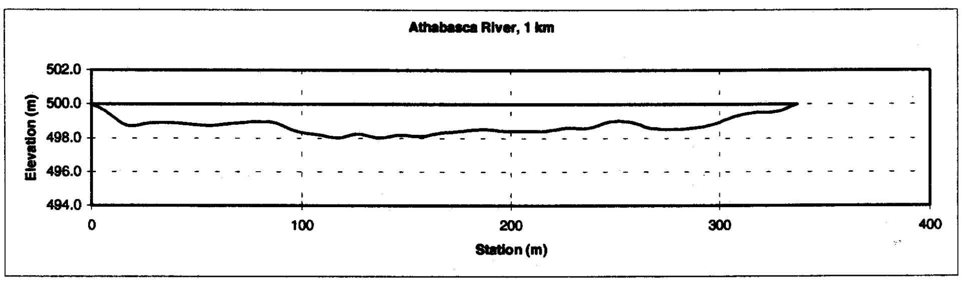

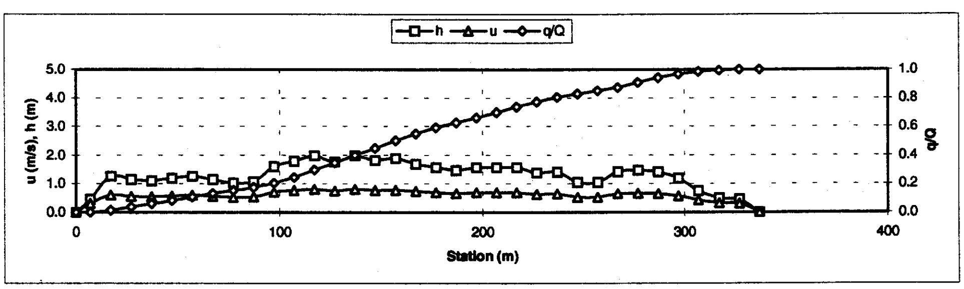

Appendix B.2 – Athabasca River, 270 m^3/s @ 2 km d/s

X-section:	Athabasca River, 2 km d/s				
Date:	October 15, 1994				
Discharge (m^3/s) :	270.00	Estimated water surface elevation (m):			500.00
Width (m):	350.00	Left bank (LB) =		0.00	500.00
Mean depth (m):	1.29	Right bank (RB) =		350.00	500.00
Area (m^2):	452.00				
Mean velocity (m/s):	0.60				

Sta. (m)	Elev. (m)	h (m)	w/W	u (m/s)	DQ (m^3)	q/Q	Area (m^2)	adj. U (m/s)
0.00	500.00	0.00	0.000	0.000	0.00	0.000	0.00	0.000
10.00	499.09	0.91	0.029	0.473	1.08	0.004	4.55	0.441
20.00	498.21	1.79	0.057	0.743	8.21	0.032	18.05	0.693
30.00	497.82	2.18	0.086	0.847	15.78	0.087	37.90	0.790
40.00	498.01	1.99	0.114	0.797	17.14	0.146	58.75	0.743
50.00	497.88	2.12	0.143	0.831	16.73	0.204	79.30	0.776
60.00	498.50	1.50	0.171	0.660	13.50	0.250	97.40	0.616
70.00	498.27	1.73	0.200	0.726	11.19	0.289	113.55	0.677
80.00	498.53	1.47	0.229	0.651	11.02	0.327	129.55	0.607
90.00	498.63	1.37	0.257	0.621	9.04	0.358	143.75	0.580
100.00	498.47	1.53	0.286	0.669	9.35	0.390	158.25	0.624
110.00	498.50	1.50	0.314	0.660	10.07	0.425	173.40	0.616
120.00	498.30	1.70	0.343	0.718	11.02	0.463	189.40	0.669
130.00	498.70	1.30	0.371	0.600	9.88	0.497	204.40	0.560
140.00	498.84	1.16	0.400	0.556	7.11	0.522	216.70	0.519
150.00	498.73	1.27	0.429	0.591	6.97	0.546	228.85	0.551
160.00	498.79	1.21	0.457	0.572	7.21	0.571	241.25	0.534
170.00	498.86	1.14	0.486	0.550	6.59	0.594	253.00	0.513
180.00	498.63	1.37	0.514	0.621	7.35	0.619	265.55	0.580
190.00	498.58	1.42	0.543	0.636	8.77	0.649	279.50	0.594
200.00	498.66	1.34	0.571	0.612	8.62	0.679	293.30	0.571
210.00	498.53	1.47	0.600	0.651	8.88	0.710	307.35	0.607
220.00	498.40	1.60	0.629	0.689	10.29	0.745	322.70	0.643
230.00	498.50	1.50	0.657	0.660	10.46	0.782	338.20	0.616
240.00	498.89	1.11	0.686	0.540	7.83	0.809	351.25	0.504
250.00	498.66	1.34	0.714	0.612	7.06	0.833	363.50	0.571
260.00	498.73	1.27	0.743	0.591	7.85	0.860	376.55	0.551
270.00	498.66	1.34	0.771	0.612	7.85	0.887	389.60	0.571
280.00	498.63	1.37	0.800	0.621	8.36	0.916	403.15	0.580
290.00	498.60	1.40	0.829	0.630	8.67	0.946	417.00	0.588
300.00	498.90	1.10	0.857	0.537	7.29	0.971	429.50	0.501
310.00	499.10	0.90	0.886	0.469	5.03	0.989	439.50	0.438
320.00	499.70	0.30	0.914	0.226	2.09	0.996	445.50	0.210
330.00	499.75	0.25	0.943	0.200	0.58	0.998	448.25	0.186
340.00	499.75	0.25	0.971	0.200	0.50	1.000	450.75	0.186
350.00	500.00	0.00	1.000	0.000	0.12	1.000	452.00	0.000
		Est. total =			289.46			

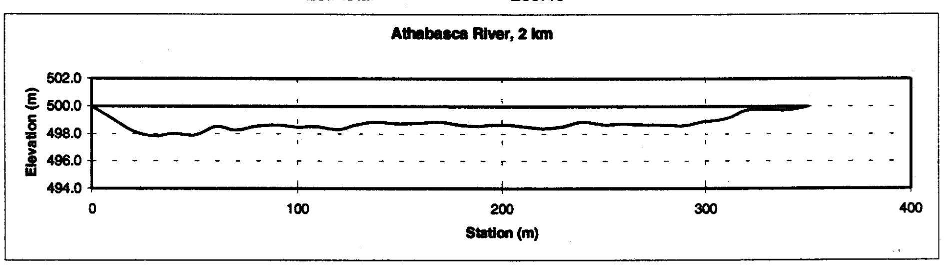

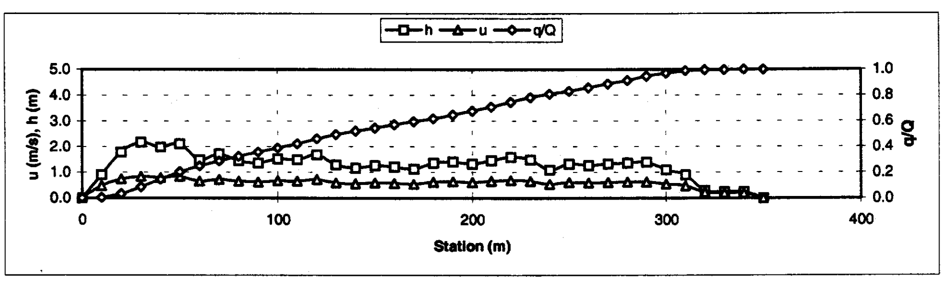

Appendix B.2 – Athabasca River, 270 m^3/s @ 4 km d/s

X-section:	Athabasca River, 4 km d/s			
Date:	October 15, 1994			
Discharge (m^3/s) :	270.00	Estimated water surface elevation (m):		500.00
Width (m):	212.00	Left bank (LB) =	0.00	500.00
Mean depth (m):	1.23	Right bank (RB) =	212.00	500.00
Area (m^2):	261.20			
Mean velocity (m/s):	1.03			

Sta. (m)	Elev. (m)	h (m)	w/W	u (m/s)	DQ (m^3)	q/Q	Area (m^2)	adj. U (m/s)
0.00	500.00	0.00	0.000	0.000	0.00	0.000	0.00	0.000
12.00	499.40	0.60	0.057	0.640	1.15	0.004	3.60	0.609
22.00	499.13	0.87	0.104	0.820	5.36	0.023	10.95	0.780
32.00	498.85	1.15	0.151	0.987	9.12	0.055	21.05	0.939
42.00	498.57	1.43	0.198	1.142	13.73	0.103	33.95	1.086
52.00	498.63	1.37	0.245	1.110	15.76	0.159	47.95	1.056
62.00	498.24	1.76	0.292	1.311	18.94	0.226	63.60	1.248
72.00	498.52	1.48	0.340	1.168	20.08	0.297	79.80	1.111
82.00	498.09	1.91	0.387	1.385	21.64	0.373	96.75	1.318
92.00	498.07	1.93	0.434	1.394	26.68	0.467	115.95	1.327
102.00	498.33	1.67	0.481	1.266	23.95	0.551	133.95	1.205
112.00	498.91	1.09	0.528	0.953	15.31	0.605	147.75	0.906
122.00	499.02	0.98	0.575	0.887	9.52	0.639	158.10	0.844
132.00	499.09	0.91	0.623	0.845	8.18	0.668	167.55	0.804
142.00	498.87	1.13	0.670	0.976	9.28	0.700	177.75	0.928
152.00	498.79	1.21	0.717	1.021	11.68	0.741	189.45	0.972
162.00	498.50	1.50	0.764	1.179	14.90	0.794	203.00	1.121
172.00	499.24	0.76	0.811	0.749	10.89	0.832	214.30	0.713
182.00	498.91	1.09	0.858	0.953	7.87	0.860	223.55	0.906
192.00	498.37	1.63	0.906	1.246	14.95	0.913	237.15	1.185
202.00	498.41	1.59	0.953	1.225	19.89	0.983	253.25	1.166
212.00	500.00	0.00	1.000	0.000	4.87	1.000	261.20	0.000
			Est. total =		283.78			

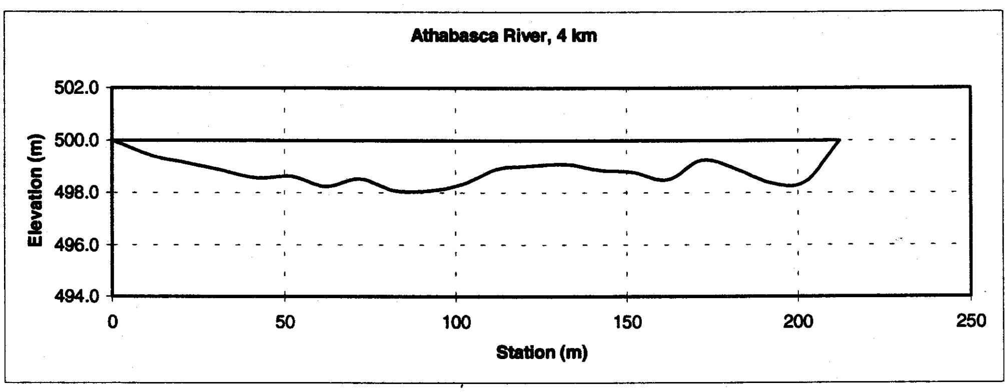

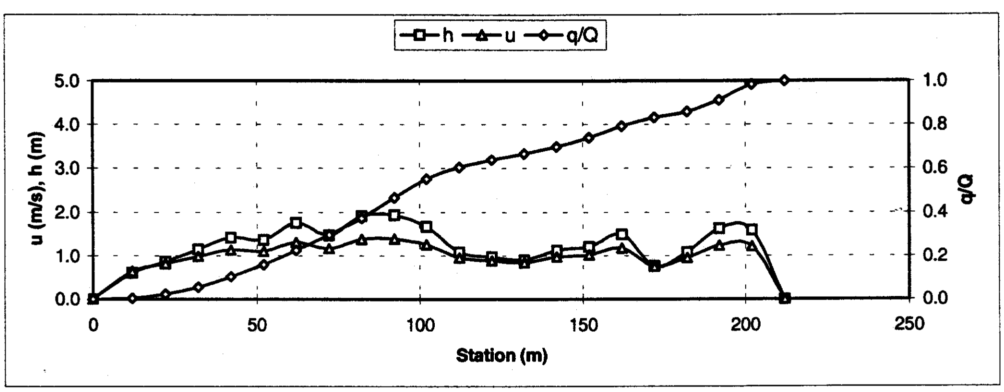

Appendix B.2 – Athabasca River, 270 m³/s @ 8 km d/s

X-section:	Athabasca River, 8 km d/s			
Date:	October 15, 1994			
Discharge (m^3/s) :	270.00	Estimated water surface elevation (m):		500.00
Width (m):	334.00	Left bank (LB) =	0.00	500.00
Mean depth (m):	1.48	Right bank (RB) =	334.00	500.00
Area (m^2):	494.75			
Mean velocity (m/s):	0.55			

Sta. (m)	Elev. (m)	h (m)	w/W	u (m/s)	DQ (m^3)	q/Q	Area (m^2)	adj. U (m/s)
0.00	500.00	0.00	0.000	0.000	0.00	0.000	0.00	0.000
4.00	499.35	0.65	0.012	0.315	0.20	0.001	1.30	0.302
14.00	498.53	1.47	0.042	0.543	4.55	0.017	11.90	0.521
24.00	497.52	2.48	0.072	0.770	12.96	0.063	31.65	0.738
34.00	497.78	2.22	0.102	0.715	17.44	0.125	55.15	0.685
44.00	497.98	2.02	0.132	0.671	14.69	0.177	76.35	0.644
54.00	498.20	1.80	0.162	0.621	12.34	0.221	95.45	0.596
64.00	498.11	1.89	0.192	0.642	11.66	0.262	113.90	0.616
74.00	498.43	1.57	0.222	0.567	10.46	0.299	131.20	0.544
84.00	498.53	1.47	0.251	0.543	8.44	0.329	146.40	0.521
94.00	498.60	1.40	0.281	0.526	7.67	0.357	160.75	0.504
104.00	498.77	1.23	0.311	0.482	6.63	0.380	173.90	0.462
114.00	498.95	1.05	0.341	0.434	5.22	0.399	185.30	0.416
124.00	499.00	1.00	0.371	0.420	4.38	0.414	195.55	0.403
134.00	499.05	0.95	0.401	0.406	4.03	0.429	205.30	0.389
144.00	499.09	0.91	0.431	0.394	3.72	0.442	214.60	0.378
154.00	498.99	1.01	0.461	0.423	3.92	0.456	224.20	0.405
164.00	498.89	1.11	0.491	0.450	4.63	0.472	234.80	0.432
174.00	498.95	1.05	0.521	0.434	4.77	0.489	245.60	0.416
184.00	498.79	1.21	0.551	0.477	5.15	0.507	256.90	0.457
194.00	498.63	1.37	0.581	0.518	6.42	0.530	269.80	0.497
204.00	498.56	1.44	0.611	0.536	7.40	0.556	283.85	0.514
214.00	498.53	1.47	0.641	0.543	7.85	0.584	298.40	0.521
224.00	498.34	1.66	0.671	0.589	8.86	0.616	314.05	0.565
234.00	498.17	1.83	0.701	0.628	10.62	0.653	331.50	0.603
244.00	498.27	1.73	0.731	0.605	10.98	0.692	349.30	0.580
254.00	498.30	1.70	0.760	0.598	10.32	0.729	366.45	0.574
264.00	497.91	2.09	0.790	0.687	12.17	0.772	385.40	0.658
274.00	498.11	1.89	0.820	0.642	13.22	0.819	405.30	0.616
284.00	498.04	1.96	0.850	0.658	12.51	0.864	424.55	0.631
294.00	498.17	1.83	0.880	0.628	12.19	0.907	443.50	0.603
304.00	498.69	1.31	0.910	0.503	8.88	0.938	459.20	0.482
314.00	498.37	1.63	0.940	0.582	7.97	0.967	473.90	0.558
324.00	498.73	1.27	0.970	0.492	7.79	0.994	488.40	0.472
334.00	500.00	0.00	1.000	0.000	1.56	1.000	494.75	0.000
		Est. total =			281.58			

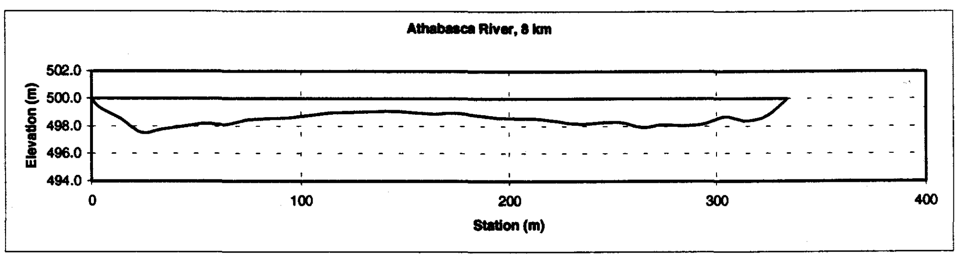

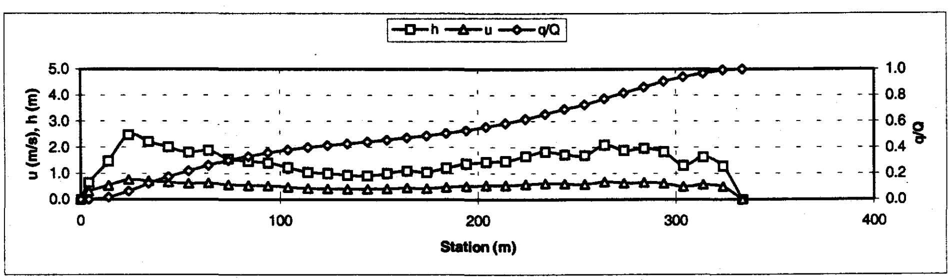

Appendix B.2 – Athabasca River, 270 m^3/s @ 16 km d/s

X-section:	Athabasca River, 16 km d/s			
Date:	October 15, 1994			
Discharge (m^3/s) :	270.00	Estimated water surface elevation (m):		500.00
Width (m):	251.00	Left bank (LB) =	0.00	500.00
Mean depth (m):	1.42	Right bank (RB) =	251.00	500.00
Area (m^2):	357.48			
Mean velocity (m/s):	0.76			

Sta. (m)	Elev. (m)	h (m)	w/W	u (m/s)	DQ (m^3)	q/Q	Area (m^2)	adj. U (m/s)
0.00	500.00	0.00	0.000	0.000	0.00	0.000	0.00	0.000
11.00	498.63	1.37	0.044	0.736	2.77	0.010	7.54	0.711
21.00	498.17	1.83	0.084	0.893	13.03	0.057	23.54	0.862
31.00	498.66	1.34	0.124	0.725	12.82	0.102	39.38	0.701
41.00	498.50	1.50	0.163	0.782	10.70	0.141	53.58	0.755
51.00	498.66	1.34	0.203	0.725	10.70	0.179	67.78	0.701
61.00	498.43	1.57	0.243	0.806	11.14	0.219	82.33	0.779
71.00	498.17	1.83	0.283	0.893	14.44	0.270	99.33	0.862
81.00	497.94	2.06	0.323	0.966	18.08	0.335	118.78	0.933
91.00	497.75	2.25	0.363	1.025	21.45	0.412	140.33	0.990
101.00	497.94	2.06	0.402	0.966	21.45	0.489	161.88	0.933
111.00	498.43	1.57	0.442	0.806	16.08	0.546	180.03	0.779
121.00	498.50	1.50	0.482	0.782	12.19	0.590	195.38	0.755
131.00	498.53	1.47	0.522	0.771	11.53	0.631	210.23	0.745
141.00	498.66	1.34	0.562	0.725	10.51	0.669	224.28	0.701
151.00	498.73	1.27	0.602	0.700	9.30	0.702	237.33	0.676
161.00	498.76	1.24	0.641	0.689	8.71	0.733	249.88	0.665
171.00	498.69	1.31	0.681	0.714	8.94	0.765	262.63	0.690
181.00	498.69	1.31	0.721	0.714	9.36	0.799	275.73	0.690
191.00	498.63	1.37	0.761	0.736	9.72	0.833	289.13	0.711
201.00	498.56	1.44	0.801	0.761	10.52	0.871	303.18	0.735
211.00	498.59	1.41	0.841	0.750	10.77	0.909	317.43	0.725
221.00	498.66	1.34	0.880	0.725	10.14	0.946	331.18	0.701
231.00	498.92	1.08	0.920	0.628	8.19	0.975	343.28	0.607
241.00	499.12	0.88	0.960	0.548	5.76	0.996	353.08	0.529
251.00	500.00	0.00	1.000	0.000	1.21	1.000	357.48	0.000
			Est. total =		279.50			

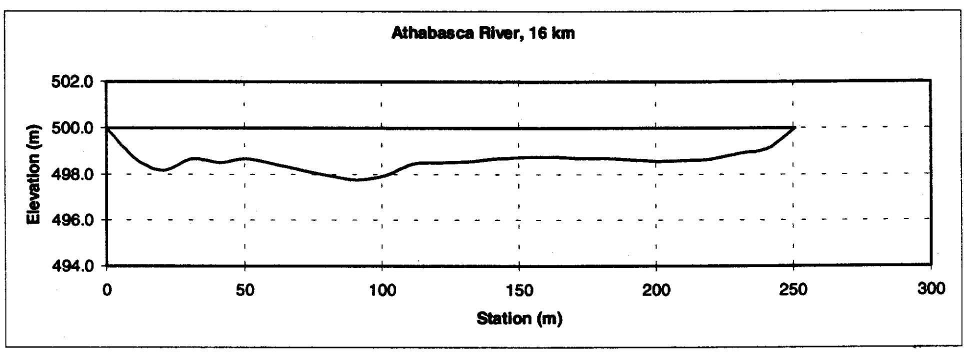

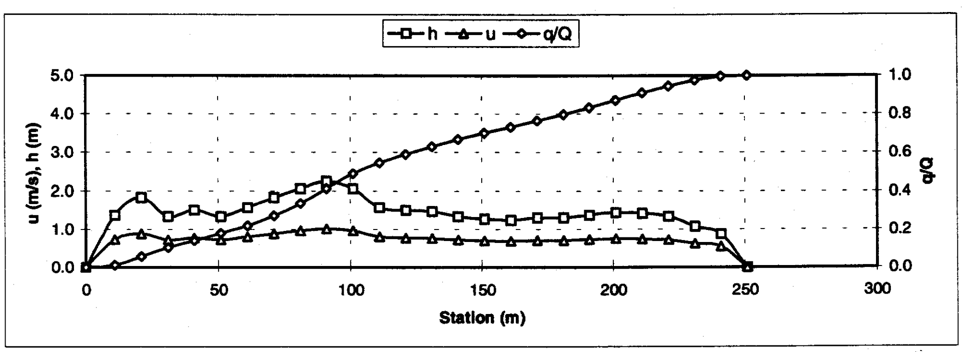

Appendix B.2 – Athabasca River, 270 m^3/s @ 32 km d/s

X-section:	Athabasca River, 32 km d/s			
Date:	October 15, 1994			
Discharge (m^3/s) :	270.00	Estimated water surface elevation (m):		500.00
Width (m):	203.00	Left bank (LB) =	0.00	500.00
Mean depth (m):	1.95	Right bank (RB) =	203.00	500.00
Area (m^2):	395.10			
Mean velocity (m/s):	0.68			

Sta. (m)	Elev. (m)	h (m)	w/W	u (m/s)	DQ (m^3)	q/Q	Area (m^2)	adj. U (m/s)
0.00	500.00	0.00	0.000	0.000	0.00	0.000	0.00	0.000
3.00	499.60	0.40	0.015	0.238	0.07	0.000	0.60	0.215
13.00	498.91	1.09	0.064	0.464	2.62	0.009	8.05	0.419
23.00	498.43	1.57	0.113	0.592	7.02	0.032	21.35	0.534
33.00	498.38	1.62	0.163	0.605	9.54	0.064	37.30	0.545
43.00	498.60	1.40	0.212	0.549	8.71	0.093	52.40	0.495
53.00	498.73	1.27	0.261	0.514	7.09	0.117	65.75	0.464
63.00	498.86	1.14	0.310	0.478	5.98	0.137	77.80	0.431
73.00	498.34	1.66	0.360	0.615	7.65	0.163	91.80	0.554
83.00	497.77	2.23	0.409	0.748	13.25	0.207	111.25	0.675
93.00	496.95	3.05	0.458	0.922	22.05	0.281	137.65	0.832
103.00	497.07	2.93	0.507	0.898	27.21	0.371	167.55	0.810
113.00	497.16	2.84	0.557	0.879	25.63	0.457	196.40	0.793
123.00	497.07	2.93	0.606	0.898	25.63	0.543	225.25	0.810
133.00	496.81	3.19	0.655	0.950	28.27	0.637	255.85	0.857
143.00	496.77	3.23	0.704	0.958	30.63	0.739	287.95	0.864
153.00	497.03	2.97	0.754	0.906	28.89	0.836	318.95	0.817
163.00	497.81	2.19	0.803	0.739	21.22	0.907	344.75	0.667
173.00	498.38	1.62	0.852	0.605	12.80	0.949	363.80	0.545
183.00	498.64	1.36	0.901	0.538	8.51	0.978	378.70	0.485
193.00	499.04	0.96	0.951	0.427	5.59	0.997	390.30	0.385
203.00	500.00	0.00	1.000	0.000	1.02	1.000	395.10	0.000
			Est. total =		299.41			

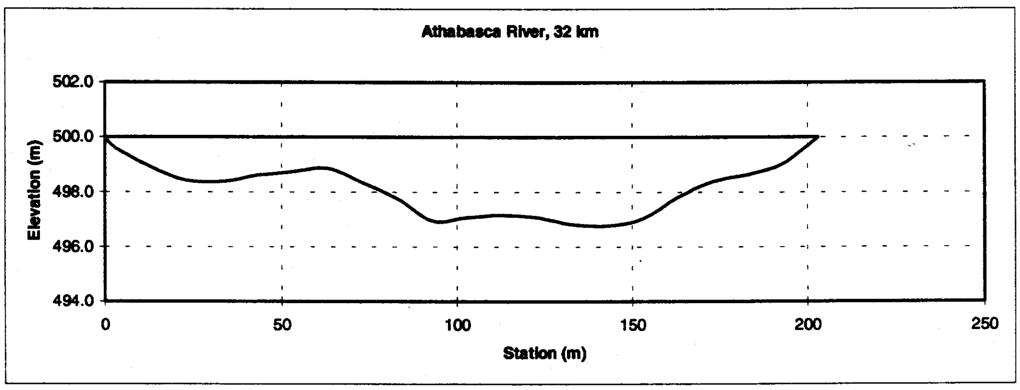

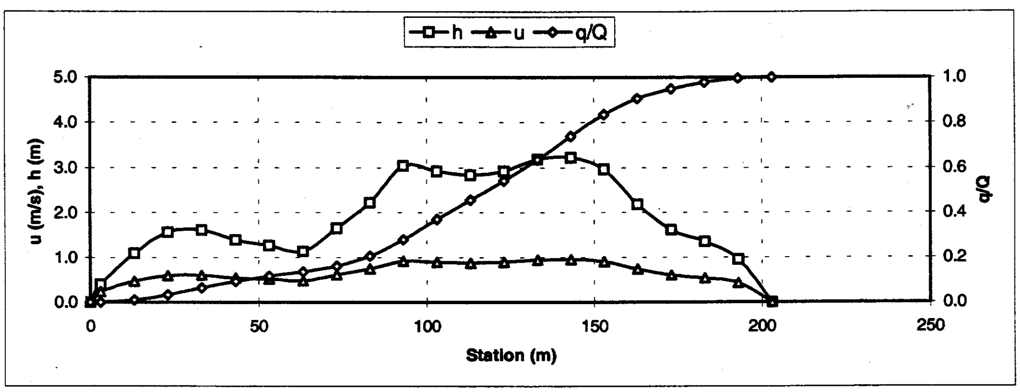

Appendix B.3 – Athabasca River, 84 m^3/s @ 0.05 km d/s

X-section:	Athabasca River, 0.05 km d/s			
Date:	February 26, 1995			
Discharge (m^3/s) :	84.00	Estimated water surface elevation		499.37
Width (m):	246.08	Left bank (LB) =	5.19	499.37
Mean depth (m):	1.15	Right bank (RB) =	251.27	499.37
Area (m^2):	283.95			
Mean velocity (m/s):	0.30			

Sta. (m)	Elev. (m)	h (m)	w/W	u (m/s)	DQ (m^3)	q/Q	Area (m^2)	adj. U (m/s)
5.19	499.37	0.00	0.000	0.000	0.00	0.000	0.00	0.000
7.00	499.15	0.22	0.007	0.098	0.01	0.000	0.20	0.089
17.00	498.70	0.67	0.048	0.206	0.68	0.007	4.65	0.188
27.00	498.30	1.07	0.089	0.281	2.12	0.030	13.35	0.257
37.00	498.30	1.07	0.129	0.281	3.01	0.063	24.05	0.257
47.00	498.58	0.79	0.170	0.230	2.38	0.089	33.35	0.210
57.00	498.54	0.83	0.211	0.237	1.89	0.109	41.45	0.217
67.00	498.36	1.01	0.251	0.271	2.34	0.135	50.65	0.247
77.00	498.38	0.99	0.292	0.267	2.69	0.164	60.65	0.244
87.00	498.34	1.03	0.332	0.274	2.73	0.194	70.75	0.250
97.00	498.49	0.88	0.373	0.247	2.49	0.221	80.30	0.225
107.00	498.45	0.92	0.414	0.254	2.26	0.245	89.30	0.232
117.00	498.57	0.80	0.454	0.232	2.09	0.268	97.90	0.211
127.00	498.21	1.16	0.495	0.297	2.59	0.296	107.70	0.271
137.00	497.72	1.65	0.536	0.376	4.72	0.347	121.75	0.342
147.00	498.03	1.34	0.576	0.327	5.25	0.404	136.70	0.298
157.00	497.94	1.43	0.617	0.341	4.63	0.455	150.55	0.311
167.00	497.88	1.49	0.658	0.351	5.05	0.509	165.15	0.320
177.00	497.40	1.97	0.698	0.423	6.69	0.582	182.45	0.385
187.00	496.90	2.47	0.739	0.491	10.15	0.692	204.65	0.448
197.00	497.45	1.92	0.779	0.415	9.95	0.800	226.60	0.379
207.00	497.63	1.74	0.820	0.389	7.36	0.880	244.90	0.355
217.00	497.81	1.56	0.861	0.362	6.19	0.947	261.40	0.330
227.00	498.90	0.47	0.901	0.163	2.66	0.976	271.55	0.148
237.00	498.70	0.67	0.942	0.206	1.05	0.988	277.25	0.188
247.00	498.90	0.47	0.983	0.163	1.05	0.999	282.95	0.148
251.27	499.37	0.00	1.000	0.000	0.08	1.000	283.95	0.000
			Est. total =		92.11			

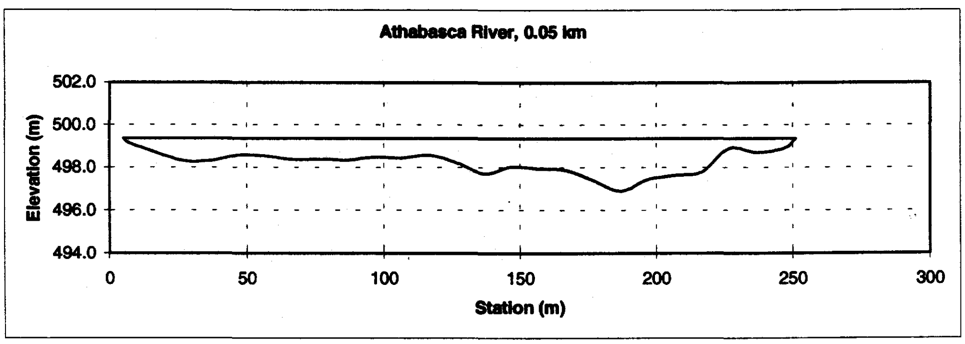

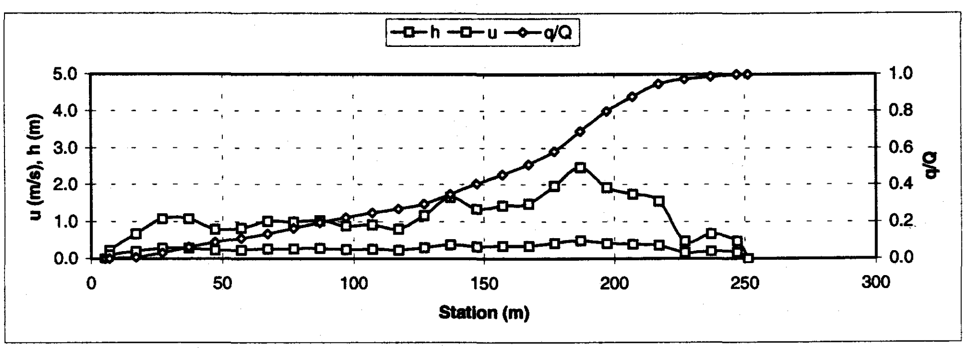

Appendix B.3 – Athabasca River, 84 m^3/s @ 8 km d/s

X-section:	Athabasca River, 8 km d/s			
Date:	February 26, 1995			
Discharge (m^3/s) :	84.00	Estimated water surface elevation		499.47
Width (m):	326.57	Left bank (LB) =	3.26	499.47
Mean depth (m):	0.98	Right bank (RB) =	329.83	499.47
Area (m^2):	319.70			
Mean velocity (m/s):	0.26			

Sta. (m)	Elev. (m)	h (m)	w/W	u (m/s)	DQ (m^3)	q/Q	Area (m^2)	adj. U (m/s)
3.26	499.47	0.00	0.000	0.000	0.00	0.000	0.00	0.000
4.00	499.35	0.12	0.002	0.065	0.00	0.000	0.04	0.060
14.00	498.53	0.94	0.033	0.256	0.85	0.009	5.34	0.236
24.00	497.52	1.95	0.064	0.416	4.85	0.063	19.79	0.384
34.00	497.78	1.69	0.094	0.378	7.23	0.142	37.99	0.349
44.00	497.98	1.49	0.125	0.348	5.77	0.205	53.89	0.321
54.00	498.20	1.27	0.155	0.313	4.56	0.255	67.69	0.288
64.00	498.11	1.36	0.186	0.327	4.21	0.301	80.84	0.302
74.00	498.43	1.04	0.217	0.274	3.60	0.341	92.84	0.252
84.00	498.53	0.94	0.247	0.256	2.62	0.370	102.74	0.236
94.00	498.60	0.87	0.278	0.243	2.26	0.395	111.79	0.224
104.00	498.77	0.70	0.308	0.210	1.78	0.414	119.64	0.194
114.00	498.95	0.52	0.339	0.172	1.17	0.427	125.74	0.159
124.00	499.00	0.47	0.370	0.161	0.83	0.436	130.69	0.149
134.00	499.05	0.42	0.400	0.149	0.69	0.444	135.14	0.138
144.00	499.09	0.38	0.431	0.140	0.58	0.450	139.14	0.129
154.00	498.99	0.48	0.462	0.163	0.65	0.457	143.44	0.151
164.00	498.89	0.58	0.492	0.185	0.92	0.467	148.74	0.171
174.00	498.95	0.52	0.523	0.172	0.98	0.478	154.24	0.159
184.00	498.79	0.68	0.553	0.206	1.14	0.490	160.24	0.190
194.00	498.63	0.84	0.584	0.237	1.68	0.509	167.84	0.219
204.00	498.56	0.91	0.615	0.250	2.13	0.532	176.59	0.231
214.00	498.53	0.94	0.645	0.256	2.34	0.558	185.84	0.236
224.00	498.34	1.13	0.676	0.289	2.82	0.589	196.19	0.267
234.00	498.17	1.30	0.707	0.317	3.69	0.629	208.34	0.293
244.00	498.27	1.20	0.737	0.301	3.87	0.672	220.84	0.278
254.00	498.30	1.17	0.768	0.296	3.54	0.711	232.69	0.273
264.00	497.91	1.56	0.798	0.359	4.47	0.760	246.34	0.331
274.00	498.11	1.36	0.829	0.327	5.01	0.815	260.94	0.302
284.00	498.04	1.43	0.860	0.338	4.64	0.866	274.89	0.312
294.00	498.17	1.30	0.890	0.317	4.48	0.915	288.54	0.293
304.00	498.69	0.78	0.921	0.226	2.82	0.946	298.94	0.208
314.00	498.37	1.10	0.952	0.284	2.40	0.972	308.34	0.262
324.00	498.73	0.74	0.982	0.218	2.31	0.997	317.54	0.201
329.83	499.47	0.00	1.000	0.000	0.24	1.000	319.70	0.000
			Est. total =		91.09			

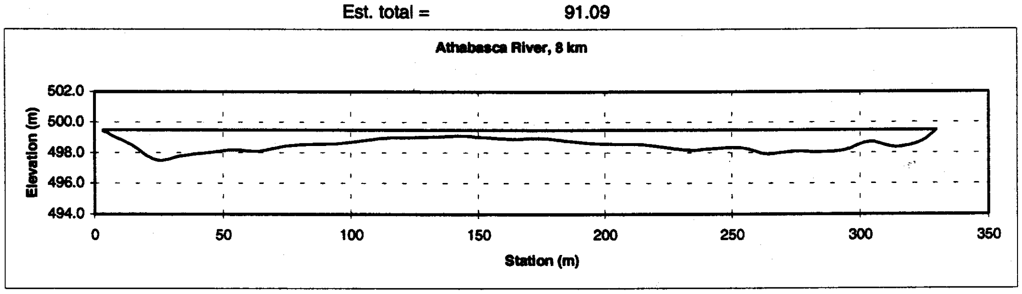

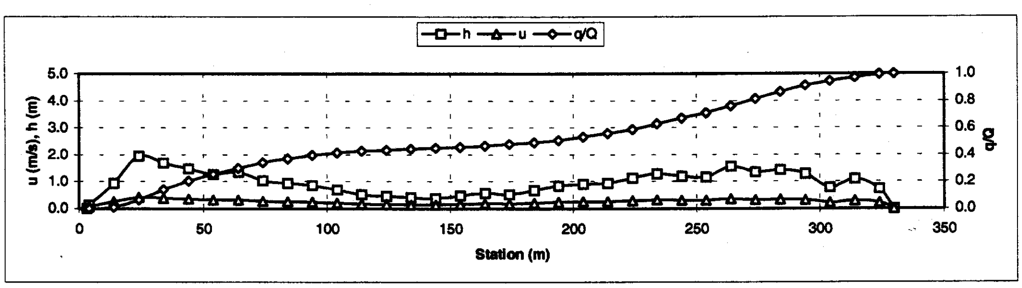

Appendix B.3 – Athabasca River, 84 m³/s @ 16 km d/s

X-section:	Athabasca River, 16 km d/s			
Date:	February 26, 1995			
Discharge (m^3/s) :	84.00	Estimated water surface elevation		499.48
Width (m):	240.92	Left bank (LB) =	4.18	499.48
Mean depth (m):	0.95	Right bank (RB) =	245.09	499.48
Area (m^2):	229.59			
Mean velocity (m/s):	0.37			

Sta. (m)	Elev. (m)	h (m)	w/W	u (m/s)	DQ (m^3)	q/Q	Area (m^2)	adj. U (m/s)
4.18	499.48	0.00	0.000	0.000	0.00	0.000	0.00	0.000
11.00	498.63	0.85	0.028	0.339	0.49	0.006	2.90	0.321
21.00	498.17	1.31	0.070	0.452	4.27	0.054	13.70	0.429
31.00	498.66	0.82	0.111	0.331	4.17	0.101	24.35	0.314
41.00	498.50	0.98	0.153	0.373	3.17	0.137	33.35	0.353
51.00	498.66	0.82	0.194	0.331	3.17	0.172	42.35	0.314
61.00	498.43	1.05	0.236	0.390	3.37	0.210	51.70	0.370
71.00	498.17	1.31	0.277	0.452	4.97	0.267	63.50	0.429
81.00	497.94	1.54	0.319	0.504	6.81	0.343	77.75	0.478
91.00	497.75	1.73	0.360	0.545	8.57	0.440	94.10	0.516
101.00	497.94	1.54	0.402	0.504	8.57	0.537	110.45	0.478
111.00	498.43	1.05	0.443	0.390	5.79	0.602	123.40	0.370
121.00	498.50	0.98	0.485	0.373	3.87	0.646	133.55	0.353
131.00	498.53	0.95	0.526	0.365	3.56	0.686	143.20	0.346
141.00	498.66	0.82	0.568	0.331	3.08	0.721	152.05	0.314
151.00	498.73	0.75	0.609	0.312	2.52	0.749	159.90	0.296
161.00	498.76	0.72	0.651	0.303	2.26	0.775	167.25	0.288
171.00	498.69	0.79	0.692	0.323	2.36	0.802	174.80	0.306
181.00	498.69	0.79	0.734	0.323	2.55	0.830	182.70	0.306
191.00	498.63	0.85	0.775	0.339	2.71	0.861	190.90	0.321
201.00	498.56	0.92	0.817	0.357	3.08	0.896	199.75	0.339
211.00	498.59	0.89	0.858	0.350	3.20	0.932	208.80	0.331
221.00	498.66	0.82	0.900	0.331	2.91	0.965	217.35	0.314
231.00	498.92	0.56	0.942	0.257	2.03	0.988	224.25	0.243
241.00	499.12	0.36	0.983	0.191	1.03	0.999	228.85	0.181
245.09	499.48	0.00	1.000	0.000	0.07	1.000	229.59	0.000
			Est. total =		88.60			

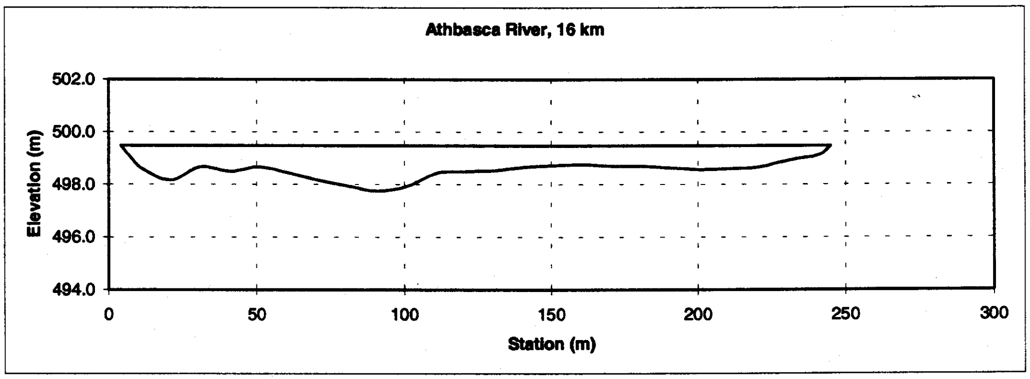

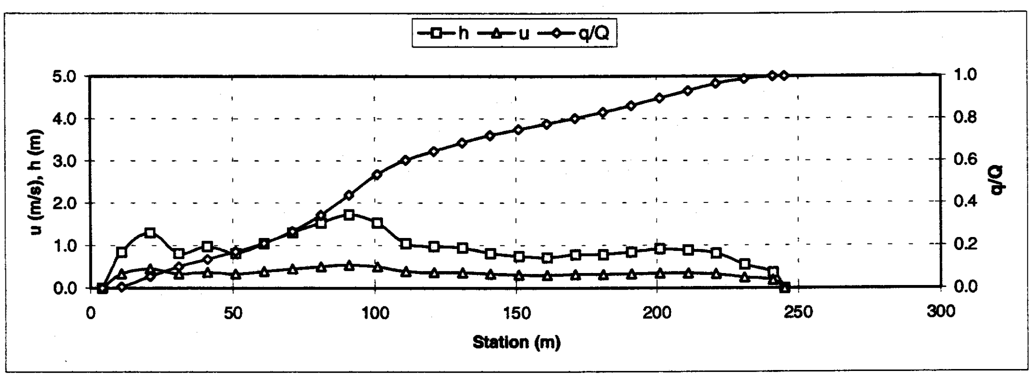

Appendix E.B – Athabasca River, 84 m³/s @ 32 km d/s

X-section:	Athabasca River, 32 km d/s			
Date:	February 26, 1995			
Discharge (m^3/s) :	84.00	Estimated water surface elevation		499.26
Width (m):	187.36	Left bank (LB) =	7.93	499.26
Mean depth (m):	1.34	Right bank (RB) =	195.29	499.26
Area (m^2):	250.19			
Mean velocity (m/s):	0.34			

Sta. (m)	Elev. (m)	h (m)	w/W	u (m/s)	DQ (m^3)	q/Q	Area (m^2)	adj. U (m/s)
7.93	499.26	0.00	0.000	0.000	0.00	0.000	0.00	0.000
13.00	498.91	0.35	0.027	0.137	0.06	0.001	0.89	0.116
23.00	498.43	0.83	0.080	0.244	1.13	0.012	6.79	0.206
33.00	498.38	0.88	0.134	0.254	2.13	0.033	15.34	0.215
43.00	498.60	0.66	0.187	0.210	1.79	0.051	23.04	0.177
53.00	498.73	0.53	0.241	0.181	1.16	0.063	28.99	0.153
63.00	498.86	0.40	0.294	0.150	0.77	0.071	33.64	0.127
73.00	498.34	0.92	0.347	0.262	1.36	0.084	40.24	0.221
83.00	497.77	1.49	0.401	0.361	3.75	0.122	52.29	0.305
93.00	496.95	2.31	0.454	0.484	8.03	0.203	71.29	0.409
103.00	497.07	2.19	0.507	0.467	10.70	0.310	93.79	0.394
113.00	497.16	2.10	0.561	0.454	9.88	0.410	115.24	0.383
123.00	497.07	2.19	0.614	0.467	9.88	0.509	136.69	0.394
133.00	496.81	2.45	0.668	0.503	11.26	0.622	159.89	0.425
143.00	496.77	2.49	0.721	0.509	12.50	0.748	184.59	0.430
153.00	497.03	2.23	0.774	0.473	11.58	0.864	208.19	0.399
163.00	497.81	1.45	0.828	0.355	7.61	0.941	226.59	0.299
173.00	498.38	0.88	0.881	0.254	3.55	0.976	238.24	0.215
183.00	498.64	0.62	0.934	0.201	1.71	0.993	245.74	0.170
193.00	499.04	0.22	0.988	0.101	0.63	1.000	249.94	0.085
195.29	499.26	0.00	1.000	0.000	0.01	1.000	250.19	0.000
			Est. total =		99.49			

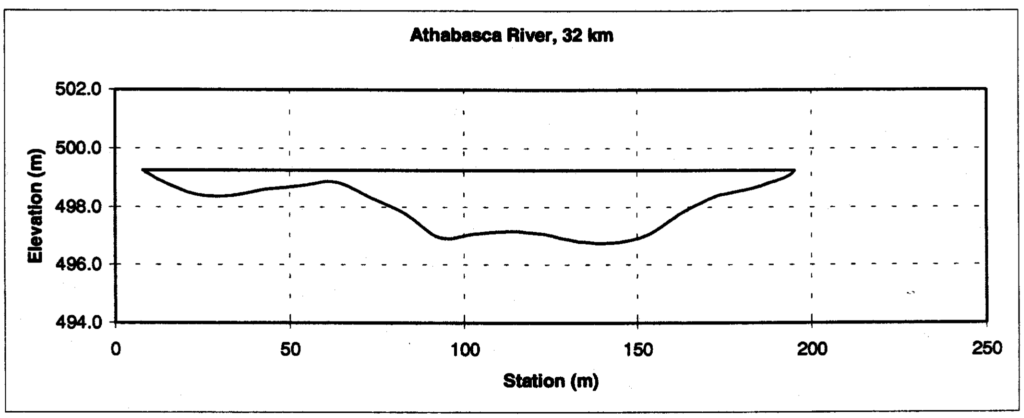

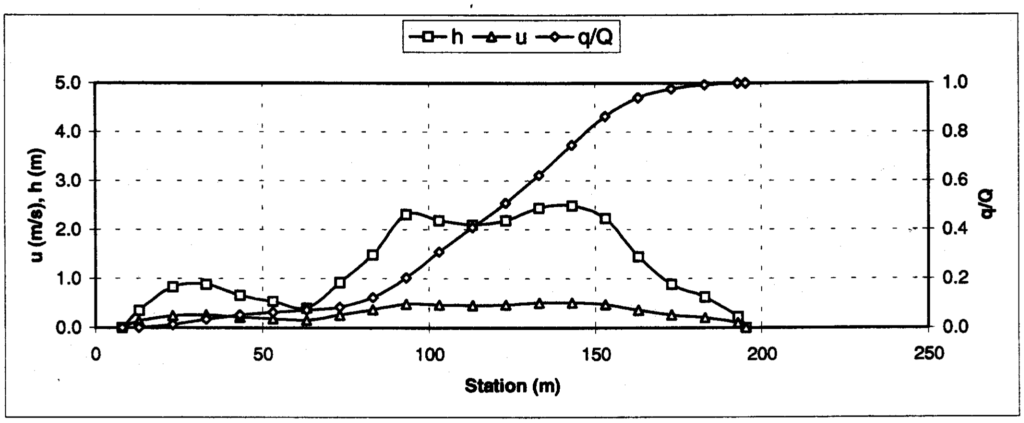

APPENDIX C Velocity Measurement, Estimates and Flow Distributions

Appendix C.1 Method for Estimating Velocity and Flow Distribution

Depth-averaged velocity at any vertical was estimated using a resistance equation since the cross section geometry was known. The expression used was suggested by Sayre and Yeh (Beltaos 1979), and is given by the following equation

$$\frac{u}{V} = \left(\frac{h}{H}\right)^{a} \qquad \text{(B-1)}$$

where u is the depth averaged streamwise velocity at a vertical, V is the mean section velocity, h is the total depth or depth below ice at a vertical, H is the mean section depth or depth below ice, and a is an exponent which depends upon a resistance equation from which equation (B-1) is derived. For this study equation (B-1) was derived from the Manning's resistance equation:

$$V = \frac{1}{n} R^{\frac{2}{3}} S^{\frac{1}{2}} \qquad \text{(B-2)}$$

where R is the section hydraulic radius, S is the slope of the water surface, n is the friction factor or roughness coefficient. In a channel the local depth-averaged velocity for a unit with of the stream is also given by

$$u = \frac{1}{n} r^{\frac{2}{3}} S^{\frac{1}{2}} \qquad \text{(B-3)}$$

where r is the hydraulic radius of the stream. For open water conditions r ≈ h at a vertical and $R \approx H$, whereas under ice cover $r \approx h/2$ and $R \approx H/2$. Dividing equation (B-3) by (B-2) and expressing r and R in terms of h and H gives

$$\frac{u}{V} = \left(\frac{h}{H}\right)^{0.67} \quad . \quad . \quad . \quad . \quad . \quad . \quad . \quad . \quad . \qquad \text{(B-4)}$$

or $a = 0.67$ for the Manning equation. This equation gave very good estimates of the measured velocity.

Flow Distributions:

Cumulative flow distributions for the sampled sections were estimated using the measured stream geometry. The flow was accumulated from the right bank to the left bank. The dimensionless cumulative flow distribution was calculated using

$$\left({q}/{Q} \right)_i = \frac{1}{Q} \sum_{i=0}^{i=m} \frac{(h_{i-1} + h_i)(z_i - z_{i-1})}{2} \frac{(u_{i-1} + u_i)}{2} \quad . \quad . \quad . \quad . \qquad \text{(B-5)}$$

where i =0 designates the right bank position and $i = m$ designates the left bank position.

Appendix C.2 Plot of comparison of measured and calculated velocity readings

Appendix C.2 Plot of comparison of measured and calculated velocity readings @ 1.15 km d/s

X-section: Athabasca River, 1.15 km d/s
Date: August 19, 1997

Measured velocity readings

Sta. (m)	vel. (m/s)
33.98	0.57
34.17	0.57
62.23	0.55
84.47	0.97
134.37	1.07
147.26	1.05
171.85	0.99
205.91	1.10
249.80	1.11
249.70	1.11
249.90	1.11
306.30	0.99
Average =	0.93

Velocity readings calculated from exponential relationship based upon Manning's formula

Sta. (m)	vel. (m/s)
37.54	1.01
50.65	0.96
66.42	1.01
80.50	1.29
102.41	1.26
117.60	1.32
138.93	1.18
173.98	1.07
188.08	1.03
208.52	1.14
235.76	1.05
263.09	0.94
295.92	0.94
328.68	0.73
Average =	1.07

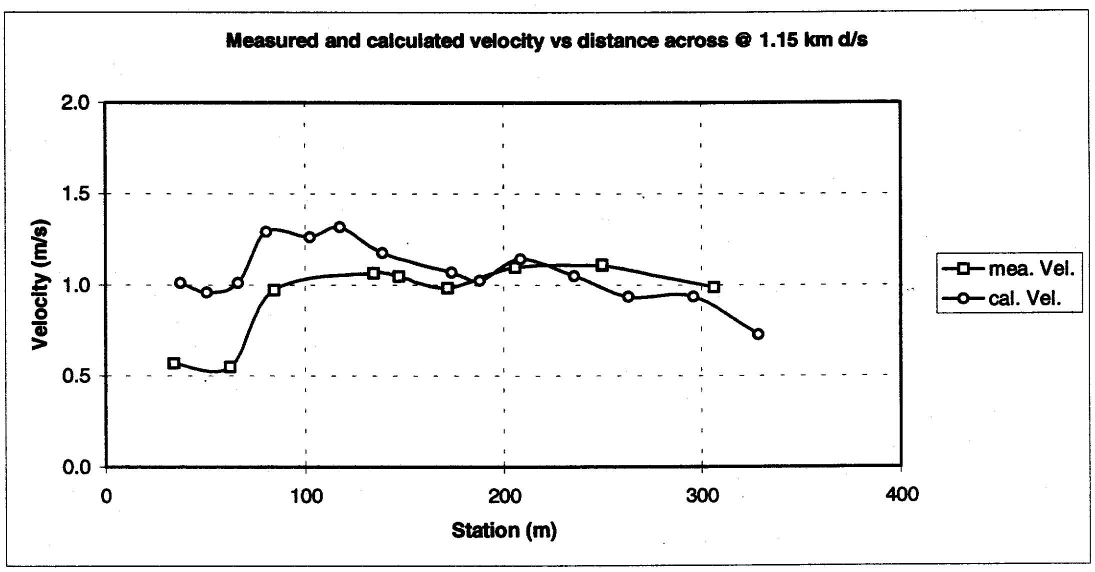

Appendix C.2 Plot of comparison of measured and calculated velocity readings @ 2.895 km d/s

X-section: Athabasca River, 2.895 km d/s
Date: August 19, 1997

Measured velocity readings

Sta. (m)	vel. (m/s)
54.87	0.81
109.20	0.80
143.20	0.88
194.20	0.95
253.73	1.08
318.56	1.09
344.56	1.13
379.37	1.18
405.81	1.15
409.77	1.02
Average =	1.01

Velocity readings calculated from exponential relationship based upon Manning's formula

Sta. (m)	vel. (m/s)
48.63	0.780
75.94	0.731
102.70	0.780
121.03	0.792
139.86	0.804
177.76	0.962
201.46	0.962
208.45	1.047
225.17	1.067
239.39	1.148
258.17	1.067
280.15	1.108
321.55	1.168
351.97	1.296
368.11	1.226
401.49	1.264
414.68	1.005
Average =	1.01

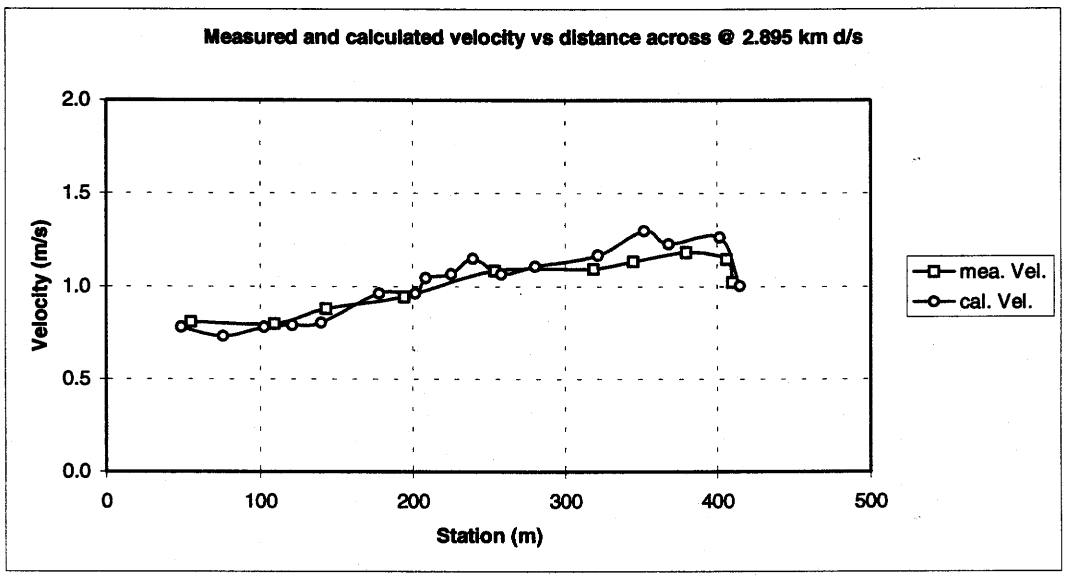

Appendix C.2 Plot of comparison of measured and calculated velocity readings @ 6.515 km d/s

X-section: Athabasca River, 6.515 km d/s
Date: August 20, 1997

Measured velocity readings

Sta. (m)	vel. (m/s)
39.84	1.33
59.80	1.12
74.70	1.38
128.34	1.49
165.21	1.39
203.82	1.44
229.49	1.01
Average =	1.31

Velocity readings calculated from exponential relationship based upon Manning's formula

Sta. (m)	vel. (m/s)
36.06	1.199
45.71	1.194
56.69	1.351
69.30	1.529
79.29	1.434
101.14	1.475
121.86	1.555
142.65	1.594
154.76	1.428
166.91	1.475
180.72	1.340
191.10	1.393
201.13	1.594
212.78	1.351
234.96	0.662
Average =	1.37

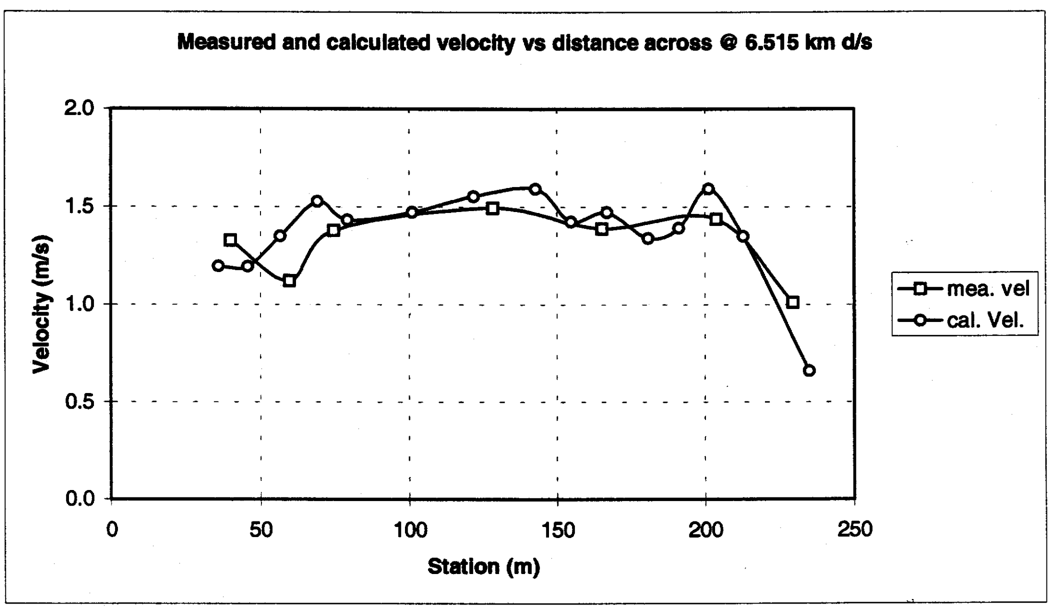

Appendix C.2 Plot of comparison of measured and calculated velocity readings @ 10.48 km d/s

X-section: Athabasca River, 10.48 km d/s
Date: August 20, 1997

Measured velocity readings

Sta. (m)	vel. (m/s)
32.69	0.96
65.32	1.01
97.32	0.94
142.62	0.87
183.82	0.87
228.63	0.92
255.14	0.89
305.68	0.96
354.88	0.97
387.40	0.80
Average =	0.92

Velocity readings calculated from exponential relationship based upon Manning's formula

Sta. (m)	vel. (m/s)
28.52	0.711
48.05	0.864
67.44	0.953
86.35	0.953
115.83	0.953
145.83	0.953
176.25	0.935
206.14	0.970
242.88	0.970
280.31	0.970
311.47	1.004
342.29	0.987
370.88	1.021
399.86	0.918
Average =	0.94

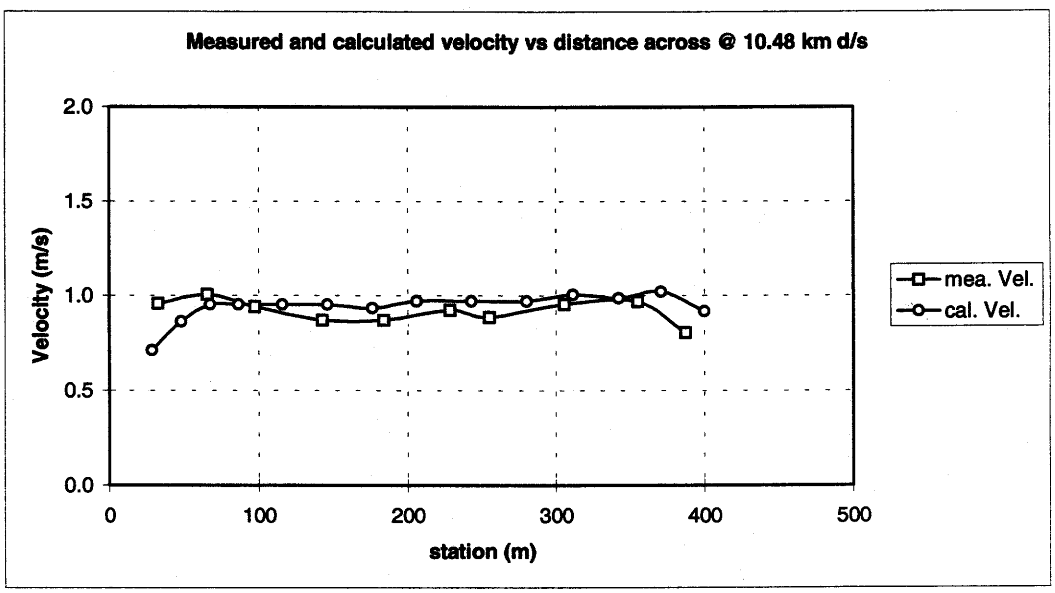

Appendix C.2 Plot of comparison of measured and calculated velocity readings @ 17.3 km d/s

X-section: Athabasca River, 17.3 km d/s
Date: August 23, 1997

Measured velocity readings

Sta. (m)	vel. (m/s)
22.17	0.74
34.05	0.83
56.10	0.88
78.53	1.03
107.66	1.10
135.00	1.09
165.16	1.14
191.66	1.14
197.01	1.05
226.09	0.76
Average =	0.97

Velocity readings calculated from exponential relationship based upon Manning's formula

Sta. (m)	vel. (m/s)
26.34	0.821
34.70	1.064
36.48	0.992
43.33	1.158
48.40	1.036
74.60	1.135
100.78	1.190
129.68	1.176
159.17	1.309
169.32	1.356
184.49	1.230
209.94	1.050
225.79	0.853
231.77	0.540
Average =	1.06

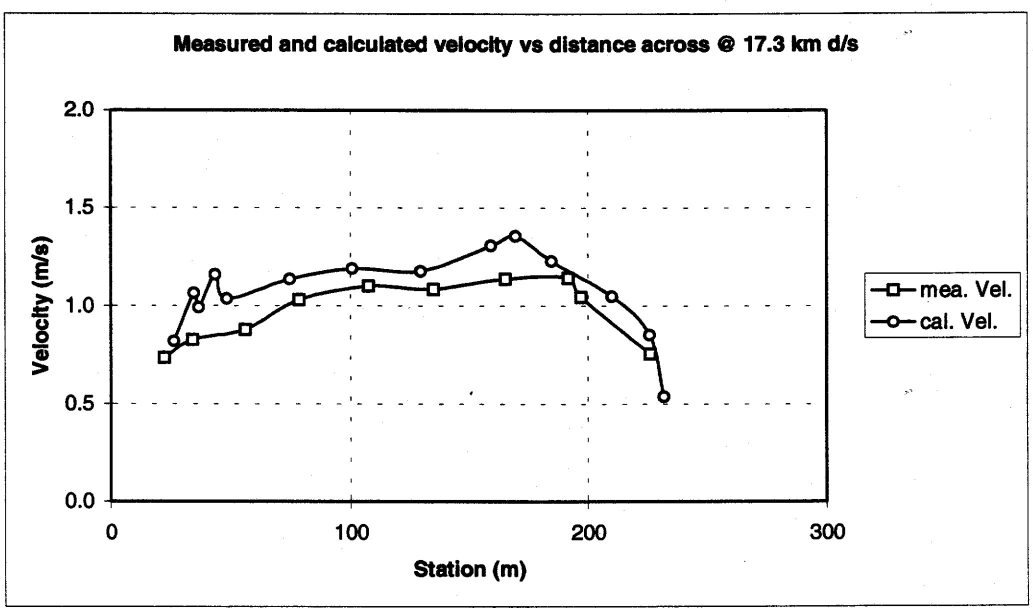

Appendix C.2 Plot of comparison of measured and calculated velocity readings @ 23.74 km d/s

X-section: Athabasca River, 23.74 km d/s
Date: August 24, 1997

Measured velocity readings		Velocity readings calculated from exponential relationship based upon Manning's formula	
Sta. (m)	vel. (m/s)	Sta. (m)	vel. (m/s)
21.45	0.68	22.52	1.058
31.10	0.91	38.91	1.043
50.83	1.04	60.72	1.133
68.98	1.09	82.34	1.205
82.87	1.21	100.18	1.205
113.70	1.19	117.93	1.205
141.13	1.14	139.42	1.162
164.23	1.13	159.82	1.205
184.63	1.08	181.22	1.133
202.17	1.14	223.03	0.917
223.14	1.00	224.63	1.103
Average =	1.06	Average =	1.12

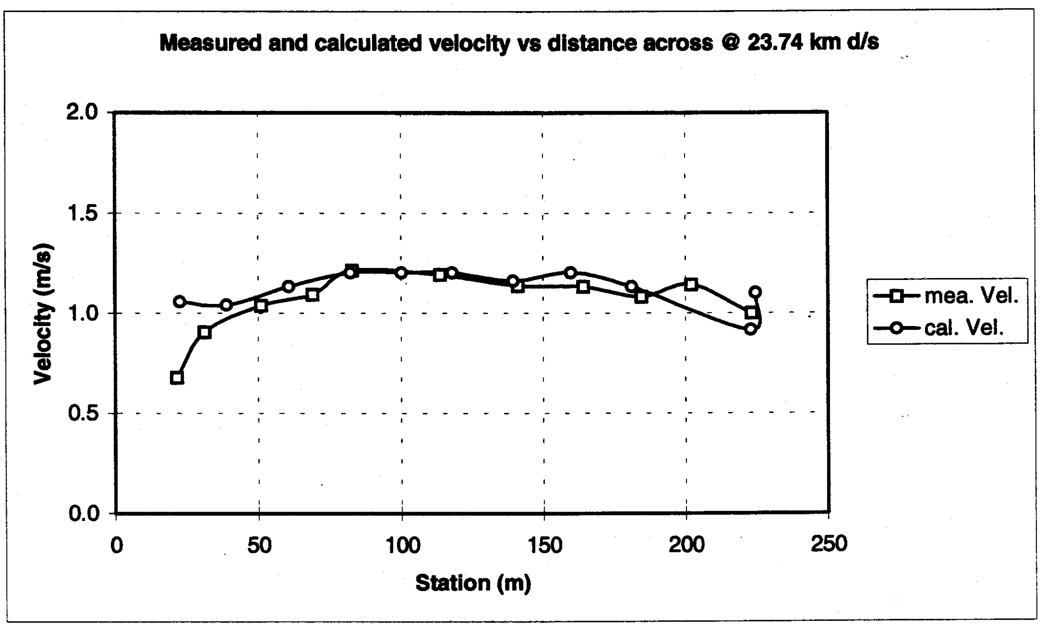

Appendix C.2 Plot of comparison of measured and calculated velocity readings @ 31.42 km d/s

X-section: Athabasca River, 31.42 km d/s
Date: August 23, 1997

Measured velocity readings

Sta. (m)	vel. (m/s)
18.68	0.76
29.51	1.20
54.88	1.32
61.24	1.27
87.28	1.28
96.37	1.30
119.66	1.45
136.40	1.17
170.18	1.35
211.27	0.71
Average =	1.18

Velocity readings calculated from exponential relationship based upon Manning's formula

Sta. (m)	vel. (m/s)
21.33	1.033
23.87	0.588
41.19	1.076
66.76	1.373
83.63	1.607
93.01	1.517
109.59	1.306
125.90	1.238
145.64	1.340
161.45	1.621
165.00	1.502
177.01	1.185
181.91	1.373
188.02	1.544
199.03	1.113
205.85	1.141
212.11	0.708
Average =	1.25

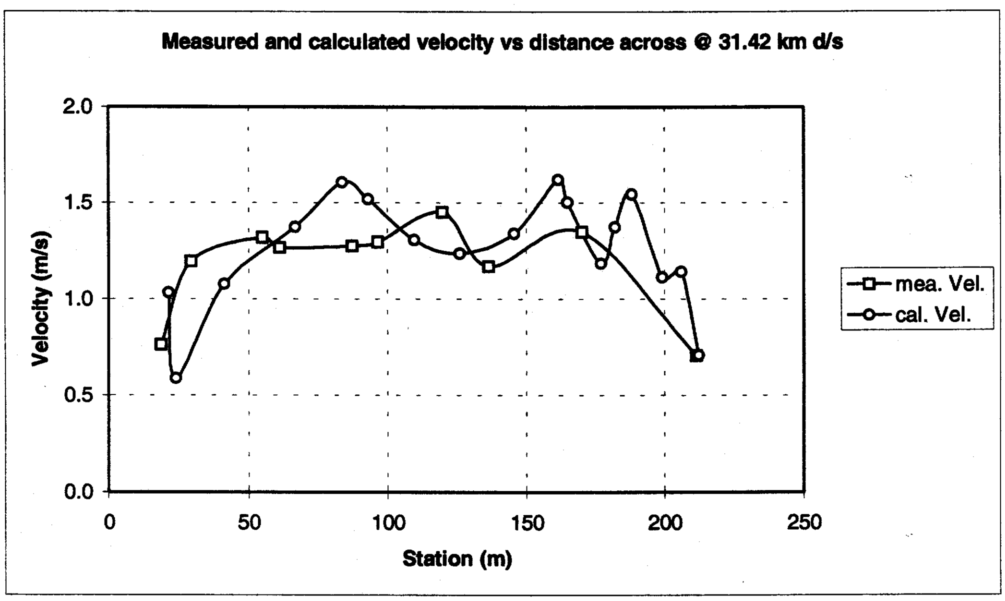

APPENDIX D. Input/ Output Summary of AOG Programs

Appendix D.1 STRMTUBE Input/ output summary.

Input	Output
for each reach:	**for each section:**
total flow, Q	streamtube average depths
time step, Δt	streamtube widths
q/Q streamtube boundaries	streamtube right boundary depths
for each section:	dimensionless mixing coefficient, β
downstream location, x	channel slope, S
series of h, z, q/Q coordinates	
dimensionless mixing coefficient, β	
channel slope, S	

Appendix D.2 GRIDGEN Input/ output summary.

Input	Output
for each reach:	**to SIMDIMS.DAT for each element:**
no. of sections	average depth
no. of streamtubes	width
time step, Δt	right boundary depth
total flow, Q	dimensional mixing coefficient, E_z
q/Q streamtube boundaries	downstream boundary position, x
for each section:	**to RCHCHAR>OUT for the reach:**
STRMTUBE output	no. of sections
	no. of streamtubes
	no. of elements in each streamtube
	vol. of elements in each streamtube

Appendix D.3 2DMIX Input/ output summary.

Input	**output**
for each reach:	**for each element and time step:**
total flow, Q	output concentrations, c
time step, Δt	elaspsed time, t
q/Q streamtube boundaries	
input concentration at each time step, c	
for each section:	
downstream location, x	
series of h, z, q/Q coordinates	
dimensionless mixing coefficient, β	
channel slope, S	

Appendix D.4 XSLICE Input/ output summary.

Input	**Output**
for each section:	**for each element and time step:**
downstream location, x	output concentrations, c
	elaspsed time, t

A listing of the Advection optimized Grid Program (STRMTUBE, GRIDGEN, 2DMIX and XSLICE) can be can be found in Putz (1996).

APPENDIX E. Samples of Data Files

Appendix E.1 Filename 1.txt file

ns	**Δt**
14	25

Specified q/Q boundaries
0.000,0.021,0.096,0.190,0.256,0.309,0.376,0.458,0.568,0.661,0.763,0.886,0.969,1.000

x	**Flow**	**NT**	**β**	**S**
0	960	26	0.25	0.0001666

z	**h**	**defined q/Q**
0.96	0	0
7.23	1.33	0.002
20.09	2.17	0.021
30.80	2.69	0.050
43.67	3.07	0.096
53.54	2.82	0.132
70.63	2.80	0.190
88.81	3.02	0.256
103.26	2.91	0.309
131.35	2.64	0.400
147.17	3.21	0.458
171.47	3.15	0.568
192.91	3.35	0.661
199.37	3.41	0.691
212.75	3.78	0.763
238.21	3.55	0.893
269.64	1.91	0.998
274.87	0.00	1.000

This file goes into the STRMTUBE program. Any filename with extension txt is given when prompted for by the STRMTUBE program. This file contains channel geometry and flow information compiled from cross section surveys or simulated data using established river engineering principles.

Appendix E.2 Filename 2.txt file

Specified q/Q boundaries
.02100 .09600 .19000 .25600 .30900 .37600 .45800 .56800
.66100 .76300 .88600 .96900 1.00000

h	sw	rbd
0.0	0.0	0.0
1.39	19.1	2.17
2.68	23.6	3.07
2.86	27.0	2.80
2.91	18.2	3.02
2.97	14.5	2.91
2.77	20.1	2.63
2.83	23.8	3.21
3.34	24.3	3.15
3.25	21.4	3.35
3.60	19.8	3.78
3.58	24.2	3.55
2.99	22.0	2.91
1.93	16.0	.00

x	β	S
.0	.250	.000167
.0	.250	.000167
.0	.250	.000167
.0	.250	.000167
.0	.250	.000167
.0	.250	.000167
.0	.250	.000167

This is one of the output files from the STRMTUBE program. It contains information on streamtube characteristics. This data goes directly into the PARM.DAT file.

Appendix E.3 Filename 3.txt file

NO. OF STREAMTUBES = 14

q/Q

0.000000E+00 2.100000E-02 1.900000E-01 2.560000E-01 3.760000E-01
5.680000E-01 6.610000E-01 8.860000E-01 9.690000E-01 1.000000

x	**flow**	**NT**
.00	960.0	26

z	**h**	**q/Q**	**A**
1.0	.00	.000000	.0
7.2	1.33	.002000	4.2
20.1	2.17	.021000	26.7
30.8	2.69	.050000	52.7
43.7	3.07	.096000	89.8
53.5	2.82	.132000	118.8
88.8	3.02	.256000	219.8
123.3	2.63	.376000	318.2
160.2	3.50	.518000	429.5
192.9	3.35	.661000	536.5
212.8	3.78	.763000	607.9
274.9	.00	1.000000	791.0

mean v.	**rbd**	**sw**	**q/Q**	**Δx/Δz**	**A**	**x**
.756	2.17	19.1	.021000	1.0	26.67	20.09
1.141	3.07	23.6	.096000	1.2	89.77	43.67
1.171	2.80	27.0	.190000	1.1	166.86	70.63
1.198	3.02	18.2	.256000	1.6	219.76	88.81
1.188	2.91	14.5	.309000	2.1	262.60	103.26
1.157	2.63	20.1	.376000	1.4	318.20	123.33
1.168	3.21	23.8	.458000	1.2	385.60	147.17
1.301	3.15	24.3	.568000	1.3	466.79	171.47
1.281	3.35	21.4	.661000	1.5	536.47	192.91
1.371	3.78	19.8	.763000	1.7	607.91	212.75
1.367	3.55	24.2	.886000	1.4	694.31	236.91
1.211	2.91	22.0	.969000	1.4	760.12	258.90
.964	.00	16.0	1.000000	1.5	791.00	274.87

This file contains a summary of the STRMTUBE output information and also a check of the proposed streamtube widths (i.e. the transverse grid spacing) and the time step against $\Delta x/\Delta z < 10$ and $E_z\Delta t/\Delta z^2 < 0.5$ criteria.

Appendix E.4 PARM.DAT file

NS	ns	Δt	flow
18,	13,	60.0,	960.0

Specified q/Q boundaries

.02100 .09600 .19000 .25600 .30900 .37600 .45800 .56800
.66100 .76300 .88600 .96900 1.00000

h	sw	rbd
0.0	0.0	0.0
1.39	19.1	2.17
2.68	23.6	3.07
2.86	27.0	2.80
2.91	18.2	3.02
2.97	14.5	2.91
2.77	20.1	2.63
2.83	23.8	3.21
3.34	24.3	3.15
3.25	21.4	3.35
3.60	19.8	3.78
3.58	24.2	3.55
2.99	22.0	2.91
1.93	16.0	.00

x	β	S
.0	.250	.000167
.0	.250	.000167
.0	.250	.000167
.0	.250	.000167
.0	.250	.000167
.0	.250	.000167

This file is a direct input from FILENAME2.TXT. An extra cross section is always added to extend the calculations beyond the last section to prevent interpolation and truncation errors.

Appendix E.5 RCHCHAR.OUT file

NS	ns	max. Δt	min Δt	Δt	no. of Δt's	initial x	to
18	13	763	439	60.000	900	0.0	0.0

Volume of dye

763 .1209600E+04

541 .4320000E+04

482 .5414400E+04

468 .3801600E+04

458 .3052800E+04

448 .3859200E+04

442 .4723200E+04

449 .6336000E+04

456 .5356800E+04

439 .5875200E+04

453 .7084800E+04

485 .4780800E+04

732 .1785600E+04

This file is generated from the GRIDGEN program (except for the last three entries on the first line) and is used as input for 2DMIX and XSLICE programs. Before it is used as input for the 2DMIX and XSLICE programs, it is edited. For the 2DMIX, two numbers, the number of time step and the initial x are added. And for the XSLICE program, an additional parameter, the time offset (this is required to correct the elaspsed time if the initial input does occur at time zero) is added.

Appendix E.6 SIMDIMS.OUT file

1	1	.4577293E+02	.1890406E+02	.1397906E+01	.1672457E-01
2	1	.9199245E+02	.1851099E+02	.1413796E+01	.1701054E-01
3	1	.1386949E+03	.1811395E+02	.1429846E+01	.1730102E-01
4	1	.1859196E+03	.1771264E+02	.1446070E+01	.1759632E-01
5	1	.2337097E+03	.1730665E+02	.1462481E+01	.1789672E-01
6	1	.2821125E+03	.1689564E+02	.1479097E+01	.1820257E-01
7	1	.3311801E+03	.1647917E+02	.1495932E+01	.1851424E-01
8	1	.3809701E+03	.1605678E+02	.1513008E+01	.1883214E-01
9	1	.4315469E+03	.1562792E+02	.1530344E+01	.1915674E-01
10	1	.4829826E+03	.1519204E+02	.1547964E+01	.1948855E-01
11	1	.5353585E+03	.1474848E+02	.1565895E+01	.1982815E-01
12	1	.5879696E+03	.1464479E+02	.1569934E+01	.1990466E-01
13	1	.6389002E+03	.1545565E+02	.1536653E+01	.1927602E-01

This file is an output file from the GRIDGEN program. It contains the i, j designation of each element and the list of element parameters. The information is organized so that there is one element per line beginning at position (1,1) and proceeding down each streamtube in succession.

Appendix E.7 CONC.TXT file

Δt	**Concentration values (continuous input)**								
60	0.0	0.0	0.0	0.0	0.0	0.0	1.13557	1.14898	0.0
120	0.0	0.0	0.0	0.0	0.0	0.0	1.13557	1.14898	0.0
180	0.0	0.0	0.0	0.0	0.0	0.0	1.13557	1.14898	0.0
240	0.0	0.0	0.0	0.0	0.0	0.0	1.13557	1.14898	0.0
300	0.0	0.0	0.0	0.0	0.0	0.0	1.13557	1.14898	0.0

Δt	**Concentration values (slug input)**								
60	0.0	0.0	0.0	0.0	0.0	0.0	1.13557	1.14898	0.0
120	0.0	0.0	0.0	0.0	0.0	0.0	0.0	0.0	0.0
180	0.0	0.0	0.0	0.0	0.0	0.0	0.0	0.0	0.0
240	0.0	0.0	0.0	0.0	0.0	0.0	0.0	0.0	0.0
300	0.0	0.0	0.0	0.0	0.0	0.0	0.0	0.0	0.0

This file is one of the input files for the 2DMIX program. It contains concentration values for the grid element in each streamtube for a series of time steps. It specifies the manner in which mass is input into the model. For continuous input, concentration values are put in the steamtubes where the dye was injected for the duration of the dye injection. Whereas for the slug test, the concentration values are put only in the first line to simulate instantaneous injection.

Appendix E.8 LSLICE.DAT file

elapsed time, *t*			**Concentration values**		
60	0.00E+00	0.00E+00	0.00E+00	0.00E+00	0.00E+00
120	0.00E+00	0.00E+00	0.00E+00	0.00E+00	0.00E+00
180	0.00E+00	0.00E+00	0.00E+00	0.00E+00	0.00E+00
9780	0.00E+00	0.00E+00	0.00E+00	0.00E+00	0.00E+00
9840	2.20E-08	1.79E-07	2.51E-07	1.06E-08	0.00E+00
9900	4.12E-08	7.12E-07	1.69E-06	1.58E-06	5.99E-07
9960	5.22E-07	4.75E-06	1.03E-05	1.02E-05	5.73E-06

This is the output file from the XSLICE program. It contains concentration versus time data for specified longitudinal position in the river reach. This file is in text format and can be imported into a spreadsheet.